Middle Rio Grande
Isleta Reach:
Isleta Diversion Dam to Rio Puerco
Hydraulic Modeling and
Silvery Minnow Habitat Analysis
1918-2016

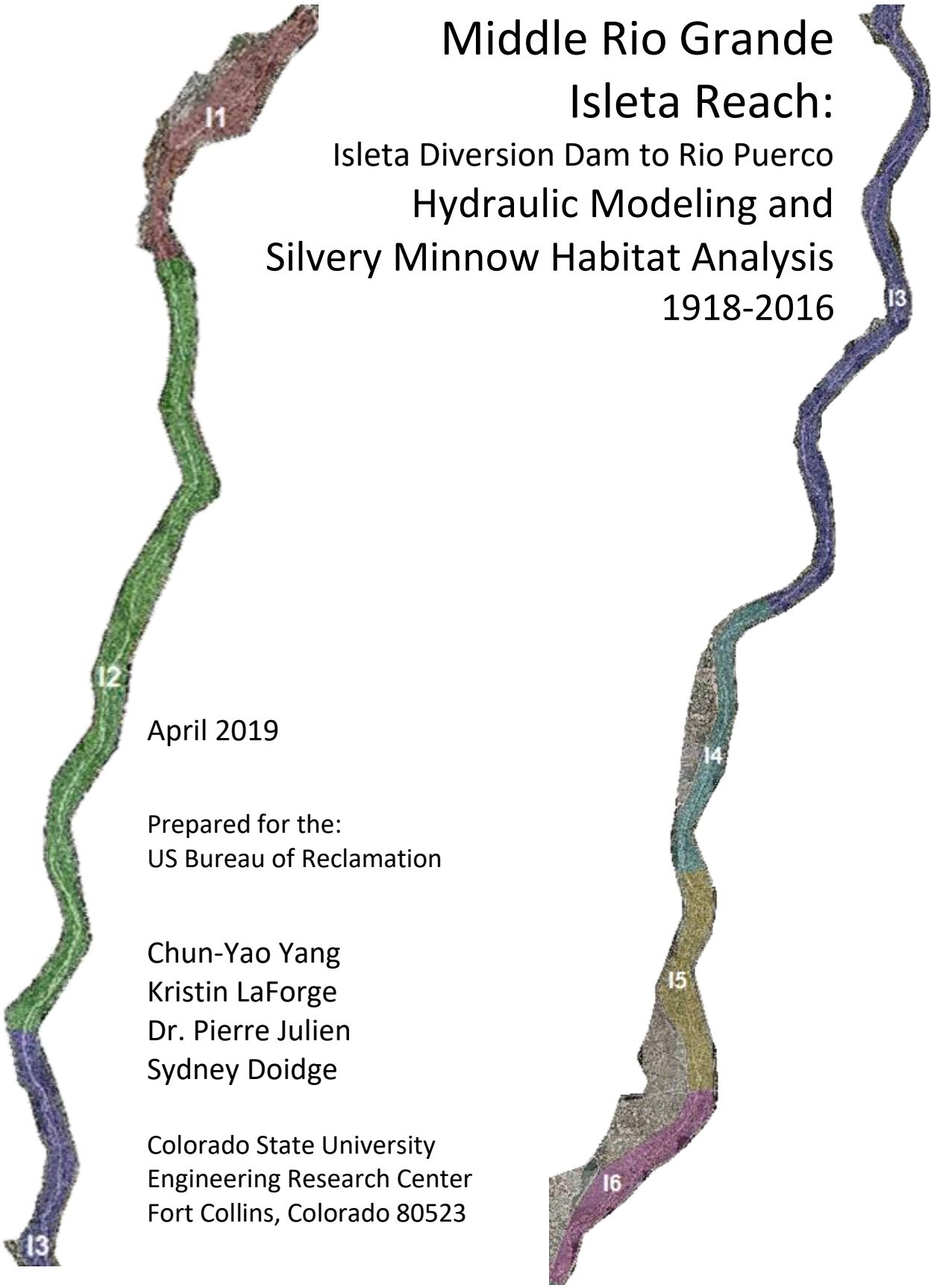

April 2019

Prepared for the:
US Bureau of Reclamation

Chun-Yao Yang
Kristin LaForge
Dr. Pierre Julien
Sydney Doidge

Colorado State University
Engineering Research Center
Fort Collins, Colorado 80523

Abstract

The Isleta Reach spans about 42 miles from the Isleta Diversion Dam to the confluence with the Rio Puerco on the Middle Rio Grande (MRG), in New Mexico. This reach report for the United States Bureau of Reclamation (USBR) aims at better understanding the morphodynamic processes of the reach. The reach is divided into six subreaches (I1, I2, I3, I4, I5 and I6) to facilitate the analysis of spatial and temporal trends in channel geometry and morphology.

The hydrology and hydraulics have been in flux over the past century. The mean annual discharge decreased since the 2000s and the suspended sediment discharge has been declining since the 1970s, resulting in channel degradation.

The GIS analysis of aerial photographs as far back as 1918 show geomorphic changes for each of the subreaches. The current channel width is less than one-fifth of what it was in 1918. This pattern is consistent throughout all subreaches. There is also a slight increase in depth, velocity, median grain size and sinuosity (the highest sinuosity occurs in I3), while the slope decreased from 1972-2012. To further understand the channel evolution, a geomorphic conceptual model based on Massong et al. (2010) and Klein et al. (2018a) was considered.

In the Appendix of this report, a novel approach is proposed. It combines a 1-D HEC-RAS analysis in combination with visual observations from aerial photographs in GIS to assess habitat conditions for the endangered Rio Grande Silvery Minnow (RGSM). This initial step should be pursued and likely integrated into a comprehensive linkage report to tie hydraulic processes with RGSM habitat quality.

Table of Contents

List of Figures

List of Tables

1. Introduction

The Middle Rio Grande (MRG) in New Mexico spans about 170 miles from the Cochiti Dam to Elephant Butte Reservoir (Tetra Tech 2002). It has been heavily impacted over the past few centuries due to settlements along the river (Scurlock 1998). Levees, jetty jacks, and dams were put in place throughout the 1900s to control the flow and mitigate extreme floods and droughts. These measures caused the river to become narrower and more incised than its previous shallow braided planform (Larsen 2007). In response to these changes, there has been a shift towards more sustainable management of the river in the past few decades (Scurlock 1998; Tetra Tech 2014). Current maintenance goals include habitat improvements for species listed by the Endangered Species Act and support of channel sustainability while continuing to provide effective water delivery (U.S. Bureau of Reclamation 2012).

The purpose of this reach report is to evaluate the morpho-dynamic conditions on the MRG with focus on the Rio Grande Silvery Minnows (RGSM). It is part of a series of reports commissioned by Reclamation to include morpho-dynamic reach reports (from CSU), reports on the biological-habitat conditions for the RGSM (from UNM), and process linkage reports (from CSU and UNM). The process linkage reports will connect morpho-dynamic conditions with the required biological-habitat conditions. This report focuses on the physical habitat and it is a first step towards that larger goal. The specific objectives of this reach report are to:

- Delineate the reach into meaningful subreaches;
- Summarize the flow and sediment discharge history;
- Analyze the geomorphologic drivers at a subreach level (sinuosity, width, braiding, bed elevation, bed material, volume change, and hydraulic parameters); and
- Examine a conceptual geomorphic model to help predict future river changes.

Many studies have been done to understand the geomorphology of the Rio Grande (Happ 1948; Crawford et al. 1993; Berry and Lewis 1997; Bauer 2000; Richard 2001; MEI 2002; Richard et al. 2005; Larsen 2007; Bovee et al. 2008; Makar 2010; Swanson et al. 2010; Massong 2010; Tetra Tech 2014; Baird 2014 and 2016; Easterling 2015; Horner 2016; Varyu 2016; Posner 2017; Julien 2018; Klein et al. 2018a). This report will build upon the recent work from Klein et al. (2018a), “Isleta to San Acacia Geomorphic Analysis”.

This report extends the analysis from the Klein et al. (2018a) report (which processed data through 2014), to include data through 2017 whenever possible. Klein’s report also did not analyze trends on a subreach level, which is a specific objective and contribution of this report.

Since a fair amount of work had been previously completed by Klein et al. (2018a), it was suggested by the Bureau of Reclamation that we extend our analysis beyond the original scope of work to start linking biological trends with morphologic ones (Ari Posner, email, May 29, 2018). Therefore, initial attempts were made by CSU to start linking silvery minnow habitat as described in the literature with hydraulic/morpho-dynamic conditions in the river.

The overarching objectives for this additional work aim at:

- Developing a framework for the analysis of silvery minnow habitat based on morpho-dynamic characteristics (including visual information such as bars, vegetation and side channels… from aerial photos at different times and discharges); and
- Carrying out a complementary hydraulic analysis of flow depths and velocities with models like HEC-RAS at comparative discharges for the determination of suitable habitat conditions for the RGSM under different phases of their life cycle.

Since this effort has been presented in preliminary form and requires more discussion with the UNM team and with Reclamation, the results that we developed so far are hereby presented as a brief summary in Section 4 of this report with plenty of relevant material in Appendices.

1.1. Site Description and Background

The Middle Rio Grande has historically been characterized by occasional large spring floods from snowmelt, with periods of droughts, sometimes lasting years. These floods often caused large scale shifts of the course of the river and rapid aggradation (Massong et al. 2010). Floods, while sometimes resulting in loss of life or land along the Rio Grande, also provided benefits. The floods leached out salts and supplied rich alluvium to the farm land, and helped maintain aquatic ecosystems by connecting the main channel flow to the floodplains (Scurlock 1998). Starting in the 1900s, levees, dams and channelization techniques were used to control the river. While these efforts enabled development of agriculture and large settlements along the MRG, they have also fundamentally changed the river, reducing peak flows and sediment supply, and altering channel geometry and vegetation (Posner 2017). This has created an environment with considerable ecological stress, as seen in the decline of species such as the Rio Grande Silvery Minnow (Mortensen et al. 2019).

The lsleta Reach of the MRG begins at the Isleta Diversion Dam to the confluence of Rio Puerco (Figure 1). The reach is about 42 miles and is relatively straight. The Isleta Diversion Dam was constructed in 1934 to divert water for irrigation into the Belen Highline and Peralta Main canals (U.S. Bureau of Reclamation n.d.). The reach is relatively stable because of channelization efforts during 1950s and 1960s. The floodplain is confined by a comprehensive levee system to protect the agricultural and municipal land on its perimeter (Posner 2017). To prevent levee erosion, kellner jetties were placed on the banks of the river. Sediment has subsequently filled most of the areas between the jack lines and levees, and the channel has become narrower (Varyu 2016). Narrowing continues with channel degradation due to lower sediment supply and the formation of vegetated bars which encroach into the channel (Varyu 2013; Massong et al. 2010). The river is continuing to adjust to anthropomorphic effects (Posner 2017).

1.1.1. Subreach Delineation

To analyze hydraulic trends along the Isleta Reach, the reach was segmented into six subreaches. These subreaches were determined first by geomorphic characteristics such as confluences or bridges, and then where no such features were available, by cumulative plots of hydraulic variables including flow depth, velocity, slope and width (Figure 2). The location breaks of subreach are designated when there is noticeable change in slope in the cumulative plots. 3000 cfs was selected for this analysis based on guidance from the USBR that this flow is contained within the main channel and does not require levee designations within HEC-RAS (Drew Baird, personal communication, June 19, 2018). The variables were obtained by using HEC-RAS with the geometry files provided by the USBR. The geometry files of 1992, 2002, and 2012 were used. Table 1 shows the subreach definition that is used in this study. These subreaches are used in analyses throughout this report.

Subreaches are identified by aggradation/degradation lines (agg/deg line) which are "spaced approximately 500-feet apart and are used to estimate sedimentation and morphological changes in the river channel and floodplain for the entire MRG" (Posner 2017). The agg/deg line that fell closest to a change in slope of a cumulative plot or other feature was used to delineate a subreach.

Subreach I1 (Isleta-1) begins at the Isleta Diversion Dam and continues to a right bank drain outfall. Subreach I2 continues from there to a sharp bend at agg/deg line 815. This is a location where the slope of the cumulative width changes. Subreach I3 stops at the confluence with Abo Arroyo, which flows in from the east. Subreach I4 stops at agg/deg line 1015. Although there are no visible distinctive characteristics, there is a dip in cumulative cross section volume. Subreach I5 continues until the Highway 60 bridge. Finally, I6, the last subreach, ends at the confluence with the Rio Puerco and is the conclusion of the entire Isleta reach. See Appendix A for all cumulative mass plots used in making these determinations.

Table 1: Isleta Reach subreach delineation.

Subreach Number	Agg-Deg Rangeline Numbers	Notable Geomorphic Controls and Comments
I1	657-700	Isleta Diversion Dam (657)-Right Bank Drain Outfall (700)
I2	700-815	Bend (815)
I3	815-964	Straight reach, Abo Arroyo Confluence (964)
I4	964-1015	No geomorphic control visible on aerial photograph
I5	1015-1053	Highway 60 Bridge (1053)
I6	1053-1097	Rio Puerco Confluence (1097)

Figure 1: Map of Isleta Reach and locations of breaks of each subreach and the USGS gage

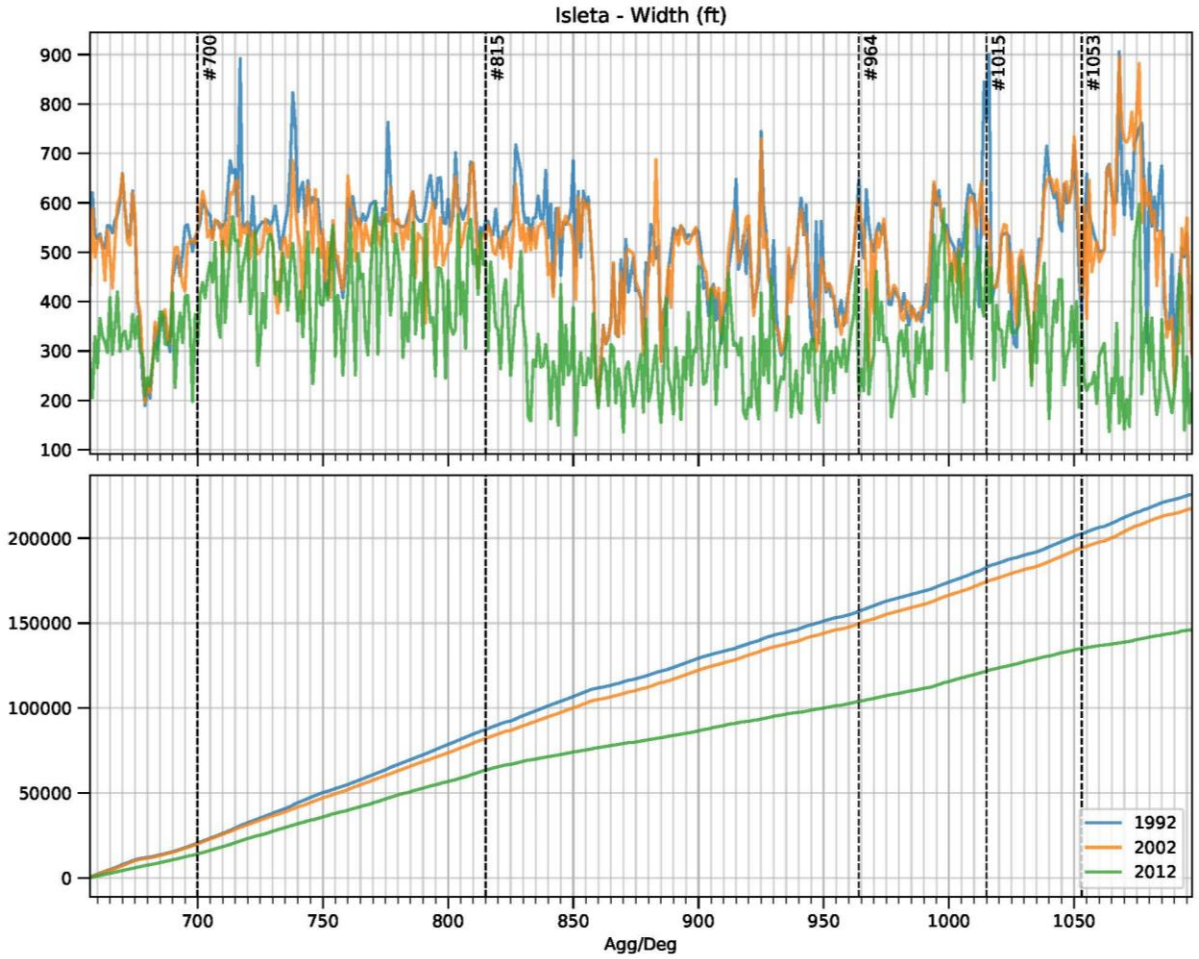

Figure 2: Width (up) and cumulative width (down) at agg/deg line 657 to 1097

2. Precipitation, Flow and Sediment Discharge Analysis

2.1 Precipitation

Precipitation data is collected from areas in between Los Lunas and Sevilleta by the Bosque Ecosystem Monitoring Program from University of New Mexico (BEMP Data 2017). The locations of data collection are shown in Figure 3.

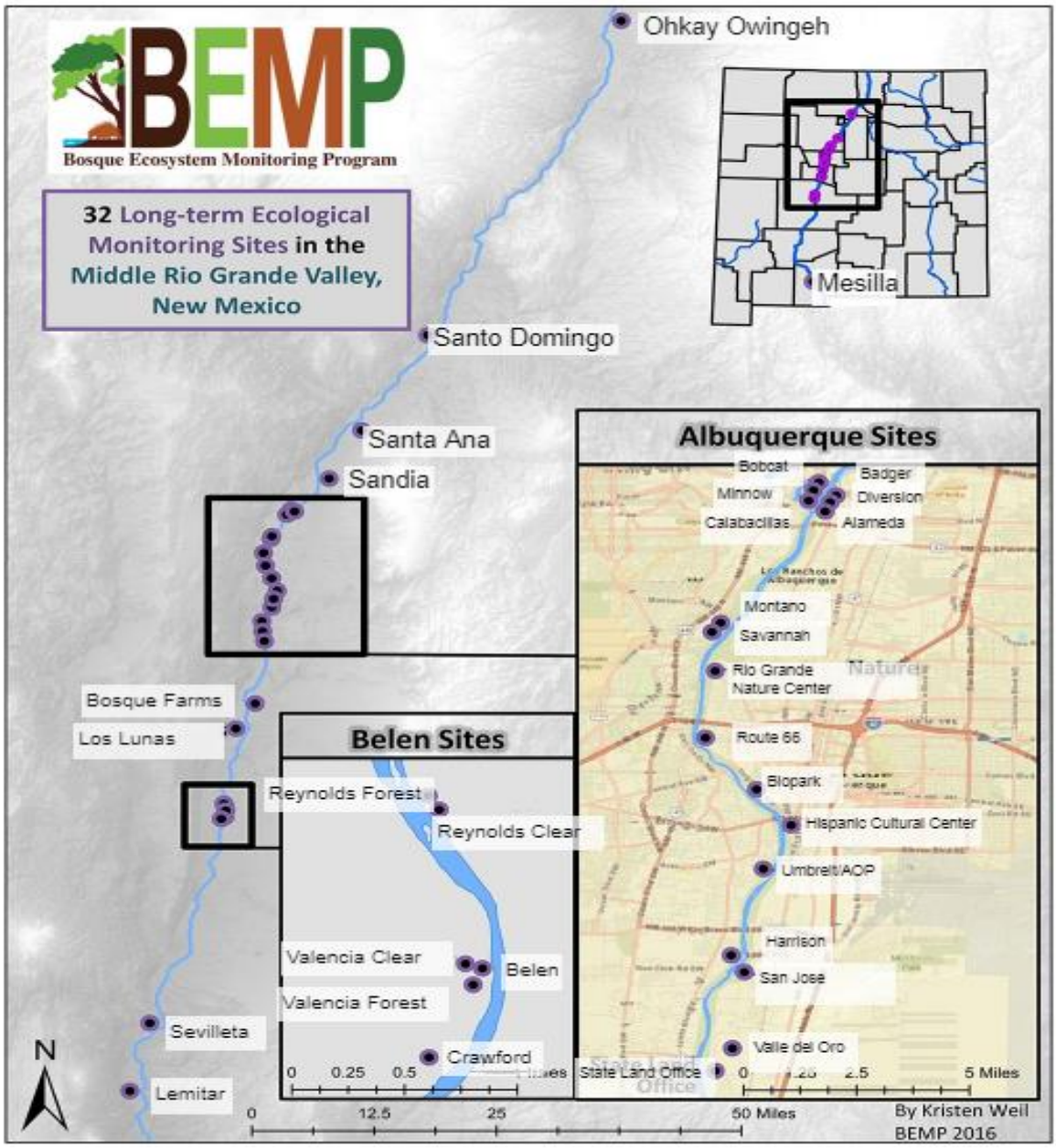

Figure 3: BEMP data collection sites (figure source: http://bemp.org/).

The Los Lunas site is just downstream of the start of the Isleta reach and the Sevilleta site is in the Sevilleta National Wildlife Refuge near the confluence of the Rio Puerco and the end of the Isleta reach. The average annual and monthly precipitation data accounts for both open and vegetated areas. The annual precipitation data between Los Lunas and Sevilleta are shown in Figure 4, with all station averages in Figure 5.

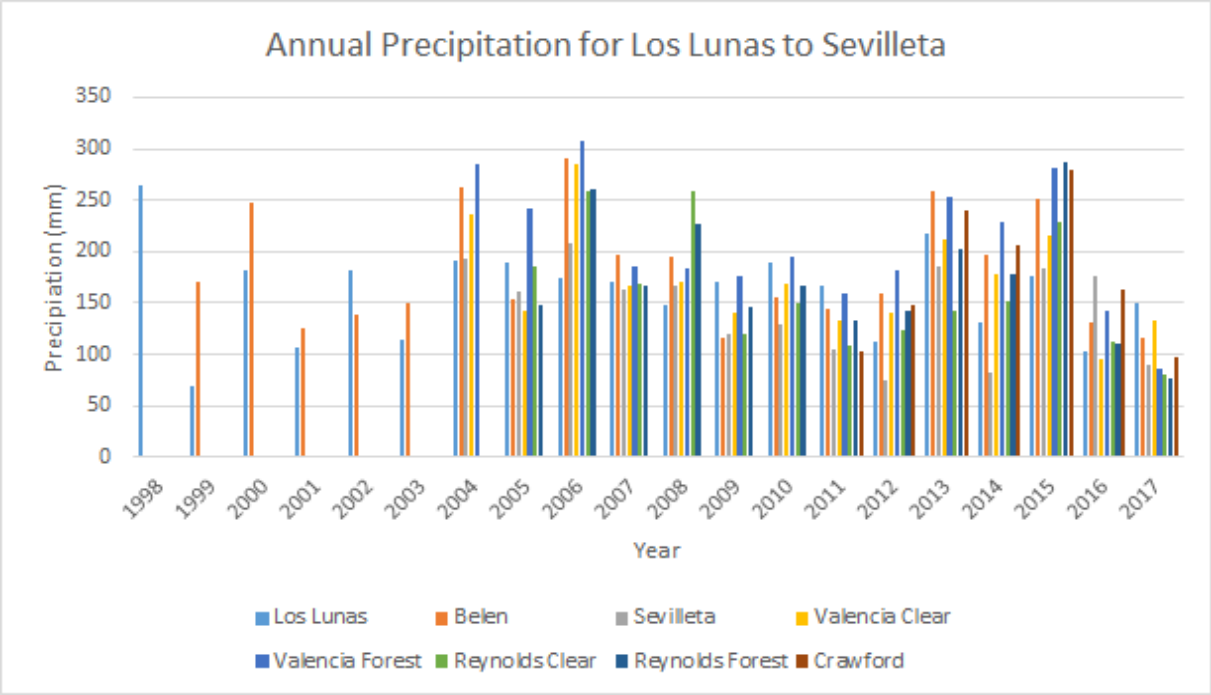

Figure 4: Average annual precipitation graph from 1998-2017

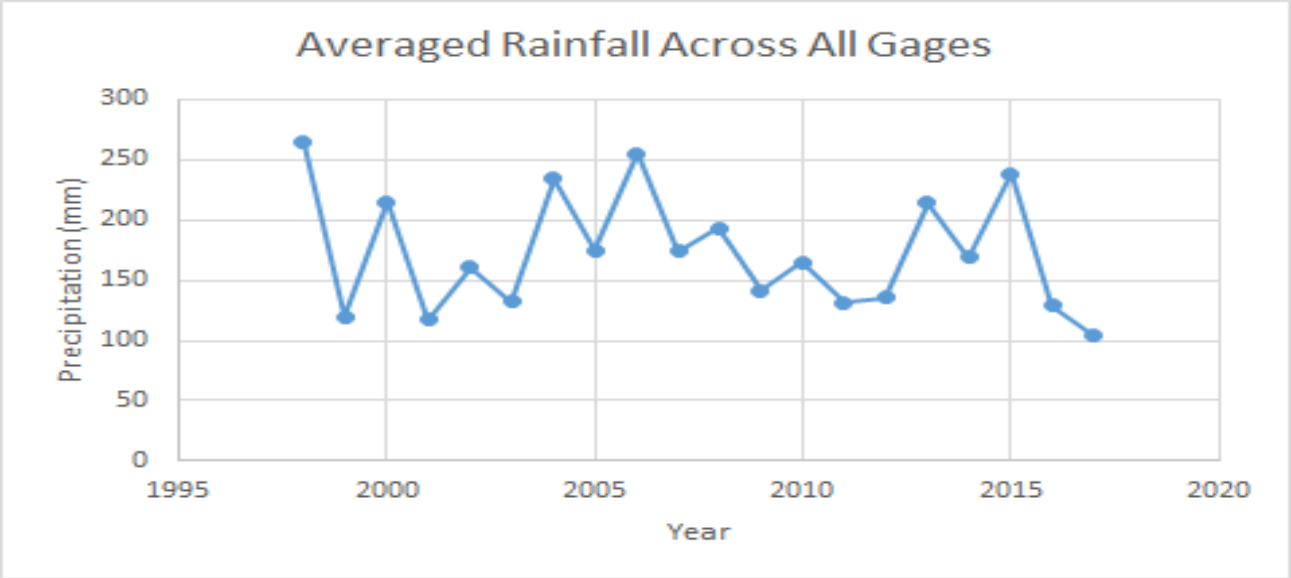

Figure 5: Averaged precipitation graph between Los Lunas to Sevilleta

Years 1998, 2006 and 2015 have peaks in precipitation. The driest years are around 2001 and 2011. Figure 6 shows monthly trends for the Los Lunas gage (the longest record).

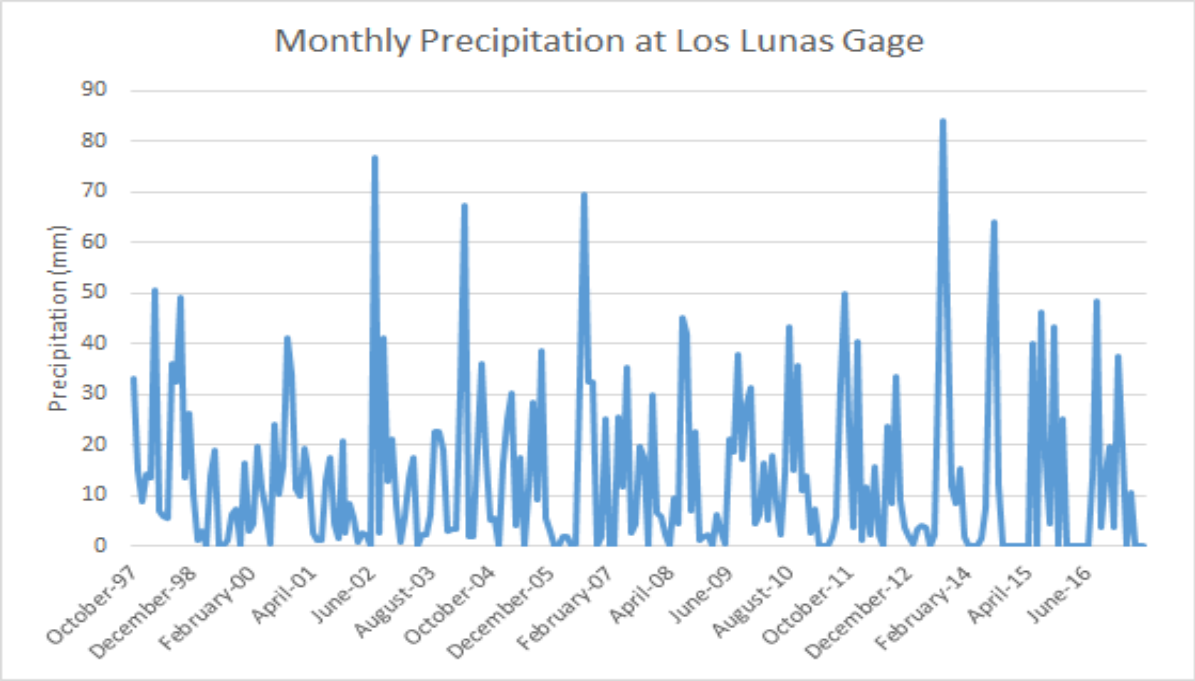

Figure 6: Monthly precipitation trends at the Los Lunas gage

The highest rainfall events tend to happen in late summer or early fall. Winter and early spring rain events still occur but are less common.

2.2. Flow Discharge

Available gages near the study reach are found in the USGS National Water Information System. Table 2 lists the gages that were analyzed in this report.

Table 2: List of USGS gages used in this study.

Station	Station #	Mean daily discharge	Suspended sediment
Rio Grande at Albuquerque	08330000	Oct 1989 - Current	Oct 1969 – Sep 2016
Rio Grande at Isleta Lakes Near Isleta	08330875	Oct 2002 - Current	
Rio Grande Near Bosque Farms	08331160	Oct 2007 - Current	
Rio Grande at State HWY 346 near Bosque	08331510	Oct 2006 - Current	
Rio Grande Floodway Near Bernardo	08332010	Oct 1990 - Current	Oct 1964 – Sep 2015
Rio Puerco near Bernardo	08353000	Sep 1939 - Current	Oct 1955 – Sep 2015
Rio Grande Floodway at San Acacia	08354900	Oct 1958 - Current	Oct 1959 – Sep 2016

The daily discharge of the Albuquerque (08330000), Bernardo (08332010) and San Acacia (08354900) are plotted in Figures 7-9. No data are available from July 2005 through September 2011 at the Bernardo gage. The plots show seasonal flow patterns: the high flow occurs in April through June, followed by low flow in July to October, and medium flow from November to March. The spring high flow is attributed to snow melt runoff. Spring flow has generally decreased since around 1980 through the Albuquerque gage (Figure 7). At the Bernardo gage, flows dramatically increased after 1985 and have declined since the mid-1990s (Figure 8). At the San Acacia gage, flows increased starting around 1980 and then also declined in the 1990s (Figure 9), following a similar pattern to that of the Bernardo gage. The Rio Puerco is unregulated and has large peak flows. Current peak flows are still lower than peak flows observed in the 1920s to the 1940s (MEI 2002 in Klein et al. 2018a). Similar trends can also be found in the 3D water magnitude plots of Rio Grande at Albuquerque, Bernardo, and San Acacia. At Albuquerque, Figure 8, the low flow periods after the 80's are not as severe as they were prior to Cochiti Dam.

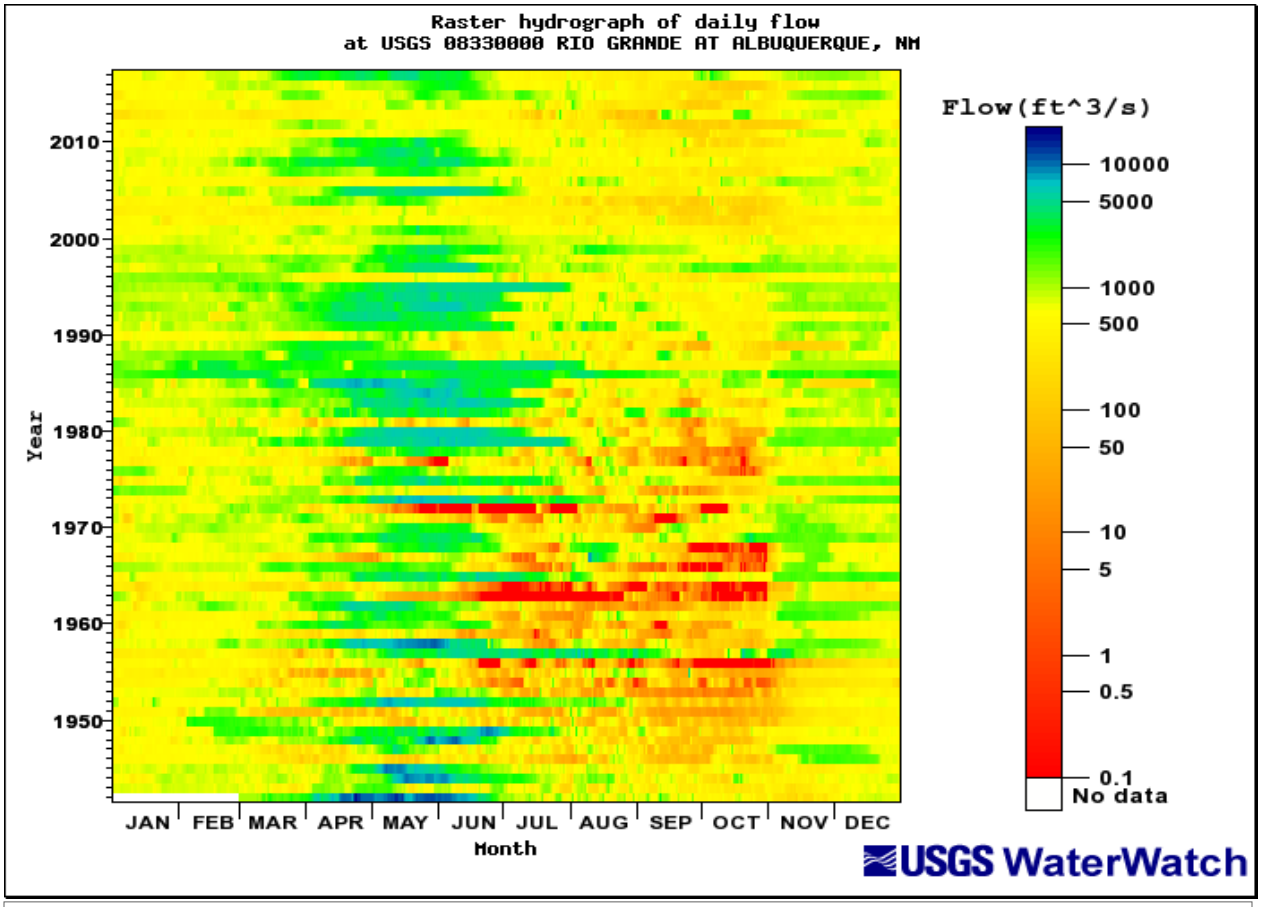

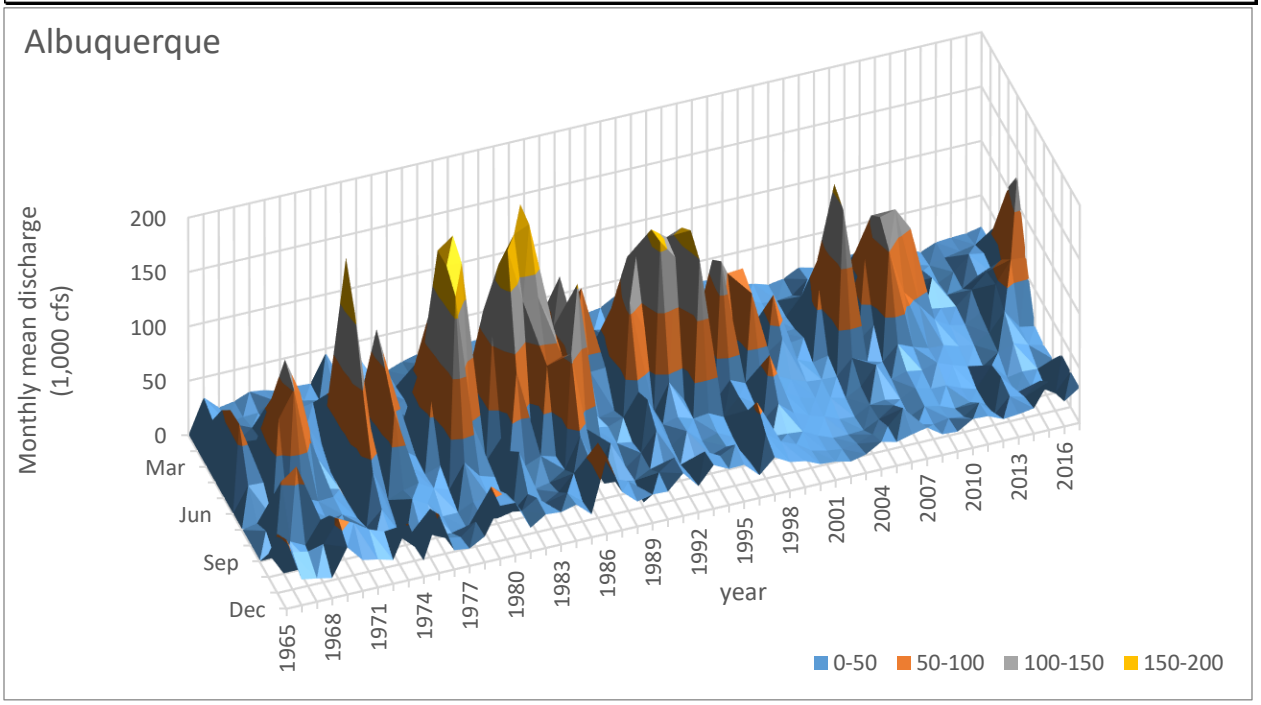

Figure 7: Raster hydrograph for the Rio Grande at Albuquerque (08330000): 1942 to 2017.

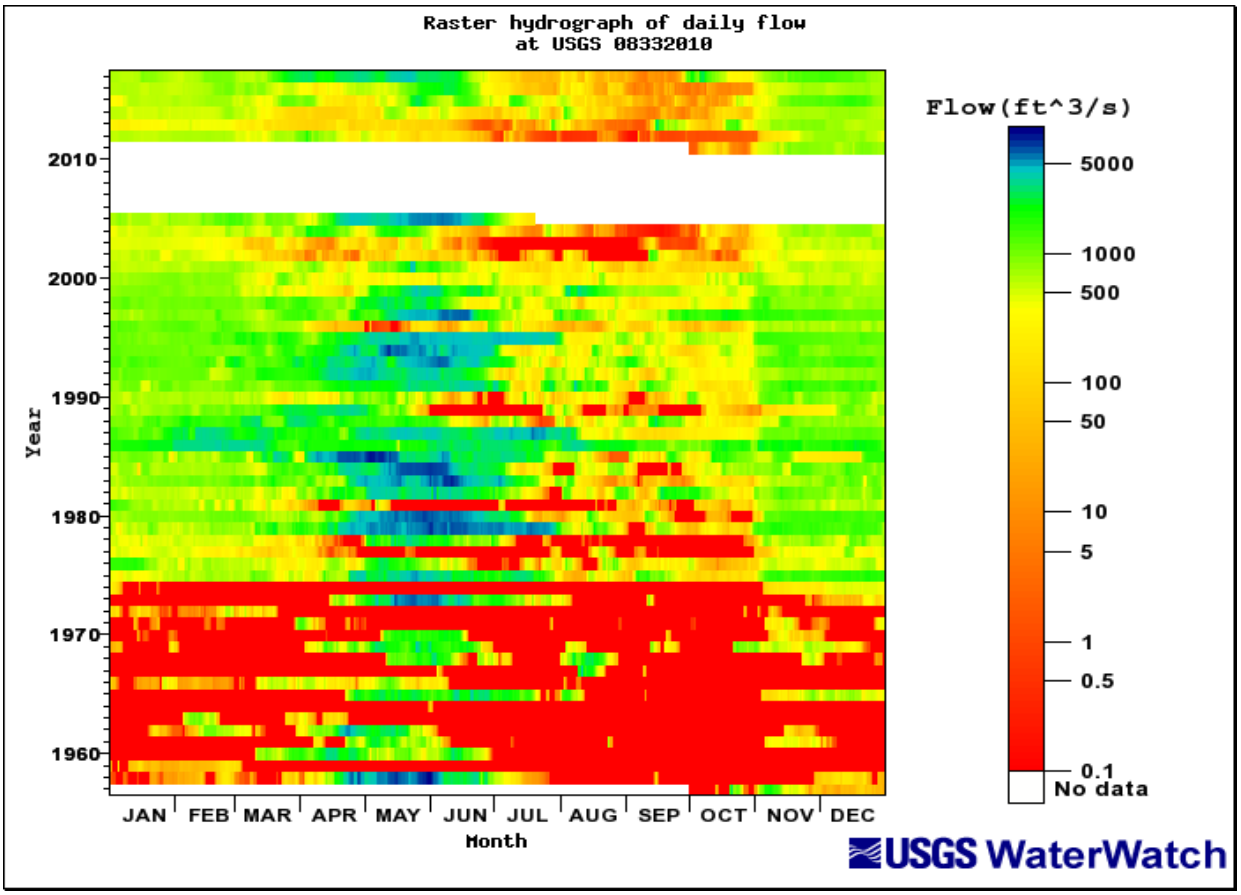

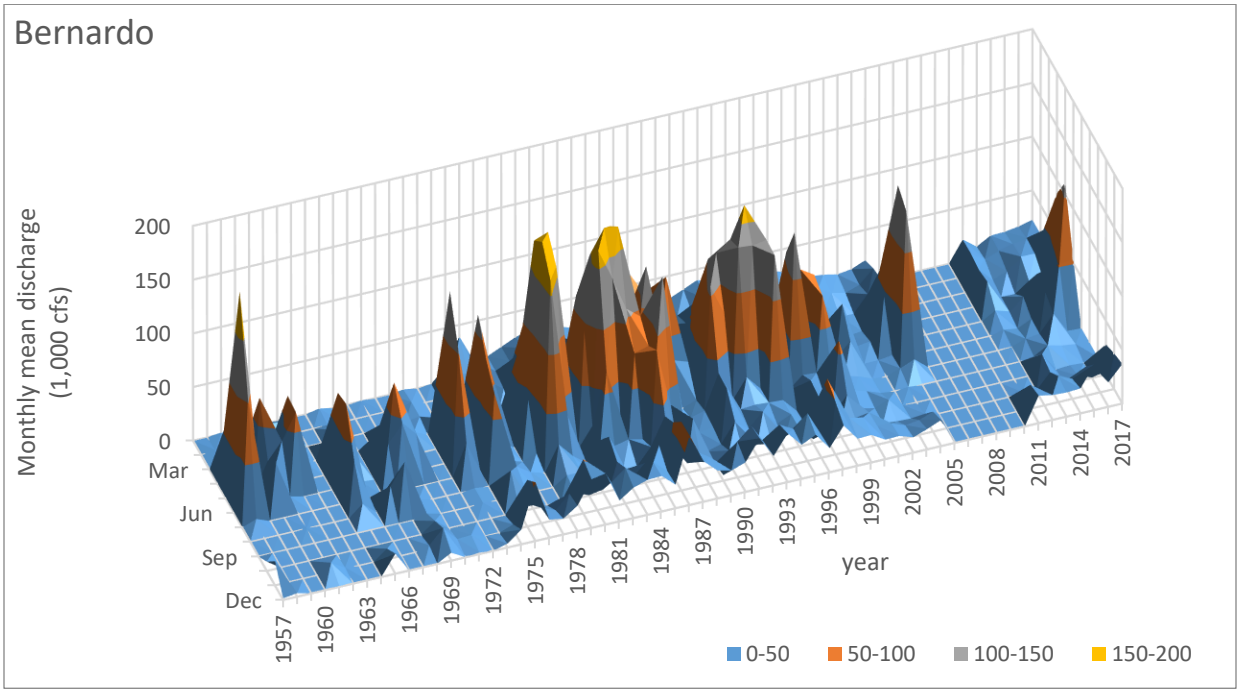

Figure 8: Raster hydrograph for the Rio Grande floodway near Bernardo (08332010): 1958 to 2017.

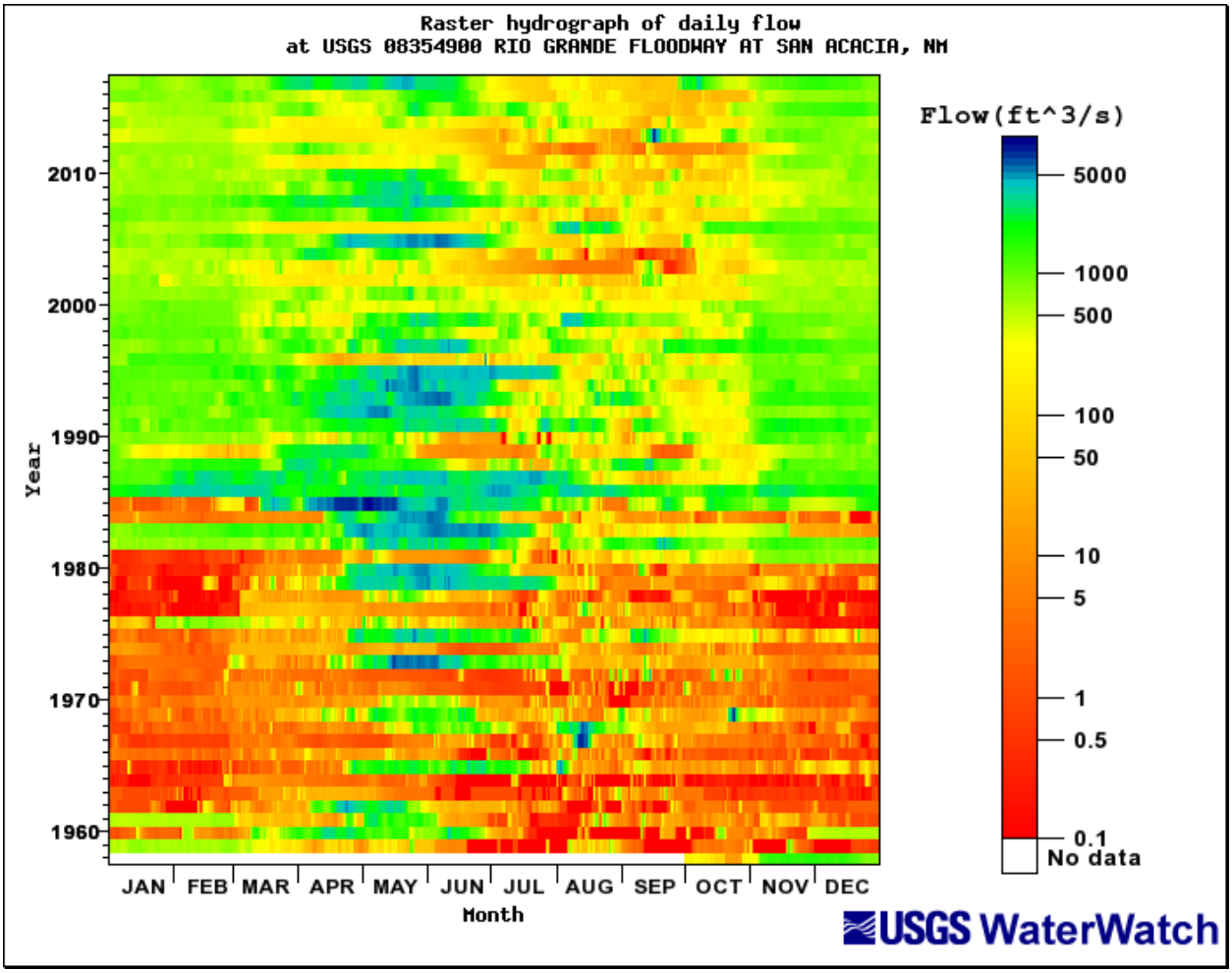

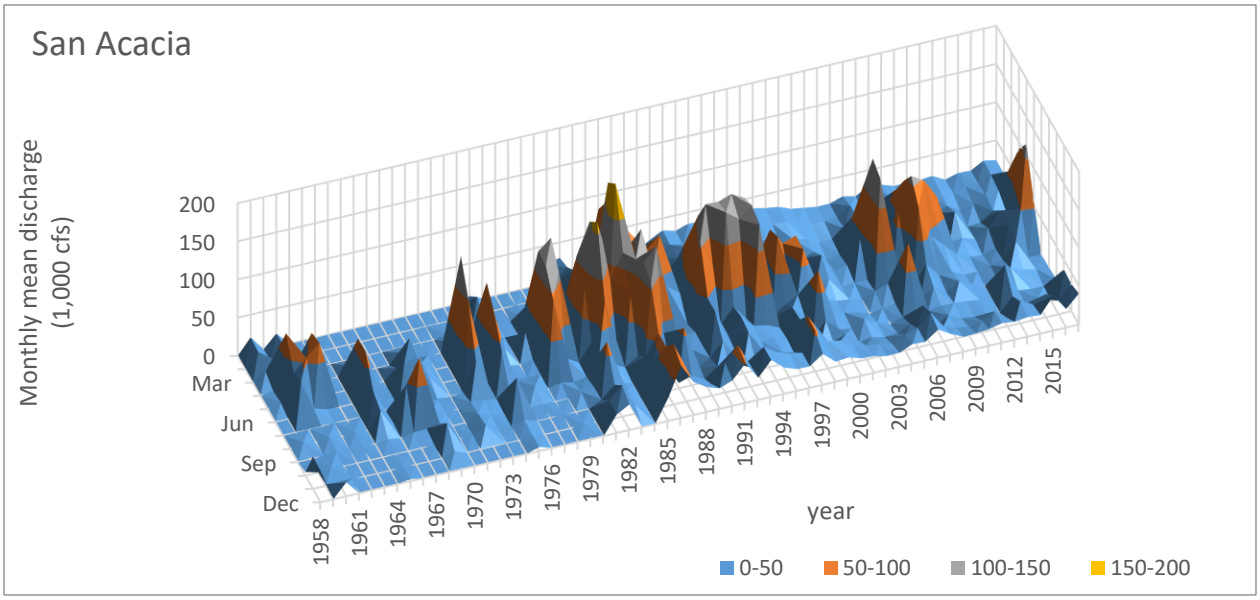

Figure 9: Raster hydrograph for the Rio Grande floodway at San Acacia (08354900): 1958 to 2017.

2.2.1. Cumulative Discharge Curves

Cumulative discharge curves are used to show changes in annual flow volume over time. The cumulative discharge is presented as a function of time in years. The slope of the line gives the mean annual discharge. Breaks in slope show changes in the flow volume. Figure 10 shows the flow mass curves of gages at Albuquerque, Isleta, Bosque Farms, Bosque, Bernardo, and San Acacia. The annual flow volume shows slight reduction in the downstream direction. The discharge mass curves are divided by the time periods 1942 to 1978, 1978 to 1980, 1980 to 1981, 1981 to 1987, 1987 to 1990, 1990 to 1995, 1995 to 2001, 2001 to 2004, 2004 to 2010, 2010 to 2014 and 2014 to 2017. The average discharge of each period is listed in Table 3. For the Albuquerque gage (08330000), the annual flow increases from 0.74 million acre-feet to 1.21 million acre-feet after 1978. A decrease in discharge between 1995 and 2010 and another decrease in discharge is found after 2010. Similar trends are found in the other stations as well.

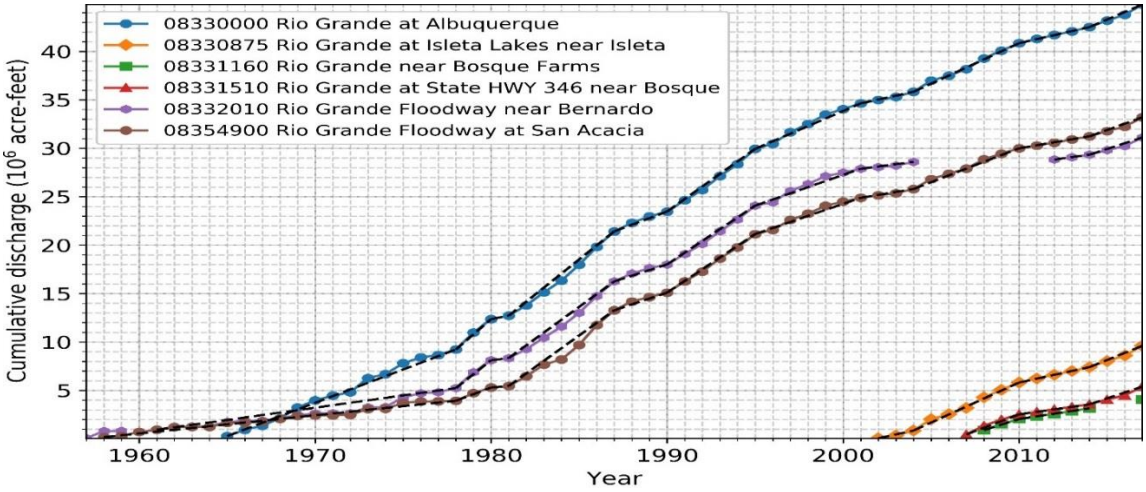

Figure 10: Cumulative discharge curves vs time.

Table 3: Average discharge at different time periods in million acre-feet.

Time	08330000	08330875	08331160	08331510	08332010	08354900
1958 - 1978	0.74				0.25	0.19
1978 - 1980	1.57				1.44	0.68
1980 - 1981	0.34				0.22	0.16
1981 - 1987	1.45				1.32	1.30
1987 - 1990	0.68				0.58	0.61
1990 - 1995	1.29				1.21	1.21
1995 - 2001	0.78				0.64	0.62
2001 - 2004	0.40	0.29			0.23	0.31
2004 - 2010	0.84	0.83	0.68	0.63		0.70
2010 - 2014	0.42	0.40	0.28	0.26	0.25	0.31
2014 - 2017	0.78	0.73	0.63	0.46	0.59	0.65

2.2.2. Recurrence Intervals

Using gages previously mentioned, recurrence intervals were calculated and presented in a report from the U.S. Bureau of Reclamation (USBR). The report from USBR, authored by Klein et al. (2018a) is closely related to this report, but the USBR geomorphic analysis is not broken up into subreaches, unlike this report. Therefore, the USBR report provides a great deal of background and summary of this reach, so is referenced frequently. Table 4 summarizes flood frequencies in the Klein et al. (2018a) report.

Table 4: Return periods (Klein et al. 2018a).

Discharge (cfs)	2 Year	5 Year	10 Year	25 Year	50 Year	100 Year
Albuquerque (MEI (2002))	5,410	7,600	8,940	10,100	11,600	12,600
Albuquerque (Wright (2010))	4,000	6,200	7,500	9,000	10,000	10,000
Albuquerque, 1993-2013	3,370	5,280	6,550	8,100	9,230	10,300
Bernardo (Wright (2010))	4,900	7,700	9,300	11,200	12,500	12,700
Bernardo, 1993-2013	3,290	5,610	7,090	8,820	10,000	11,100
San Acacia (Wright (2010))	7,800	12,000	14,500	17,400	19,300	20,100
San Acacia (Harris, 2016)	4,410	6,380	7,570	8,920	9,820	10,600

The number of days exceeding certain flow values was also examined. Flow is available at the Albuquerque, Bernardo and San Acacia gages. The data is analyzed in water years. Figure 11-13 show a reduction in peak flows, with flows above 6,000 cfs not seen after 2004 at any gages. Both the number of days where Q > 500 cfs and Q > 1,000 cfs show a general decrease at Albuquerque and San Acacia gages since 2000, perhaps with the exception of the Bernardo gage, because the missing data make it difficult to see the trend.

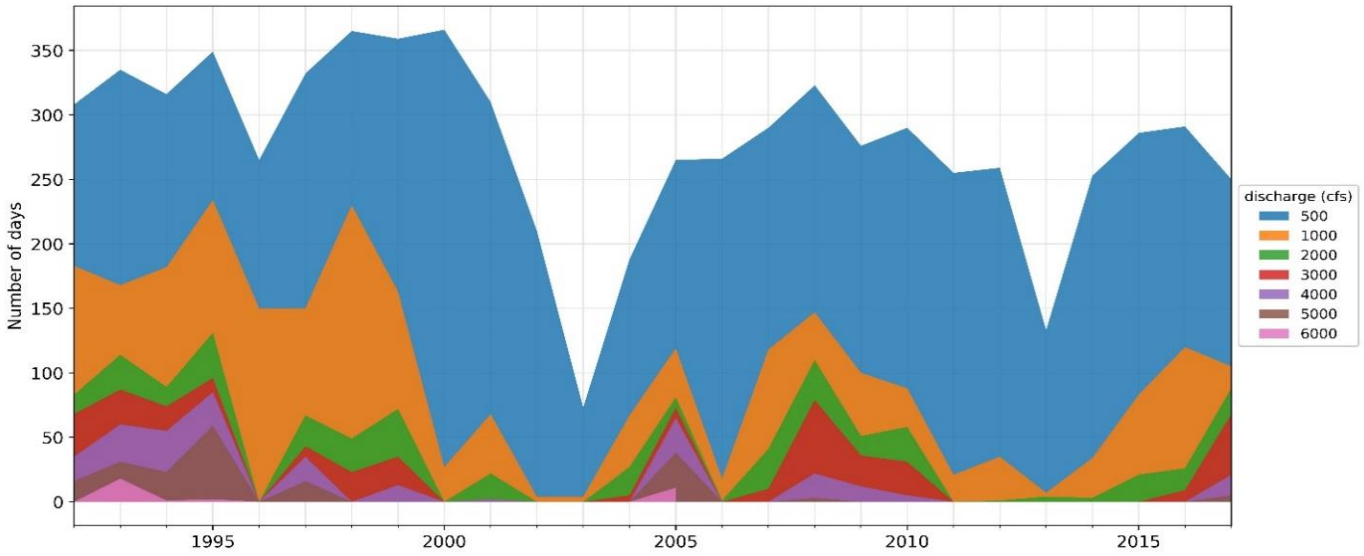

Figure 11: Graph of days exceeding flow values at Albuquerque (USGS Gage 08330000) (modified from Klein et al. 2018a).

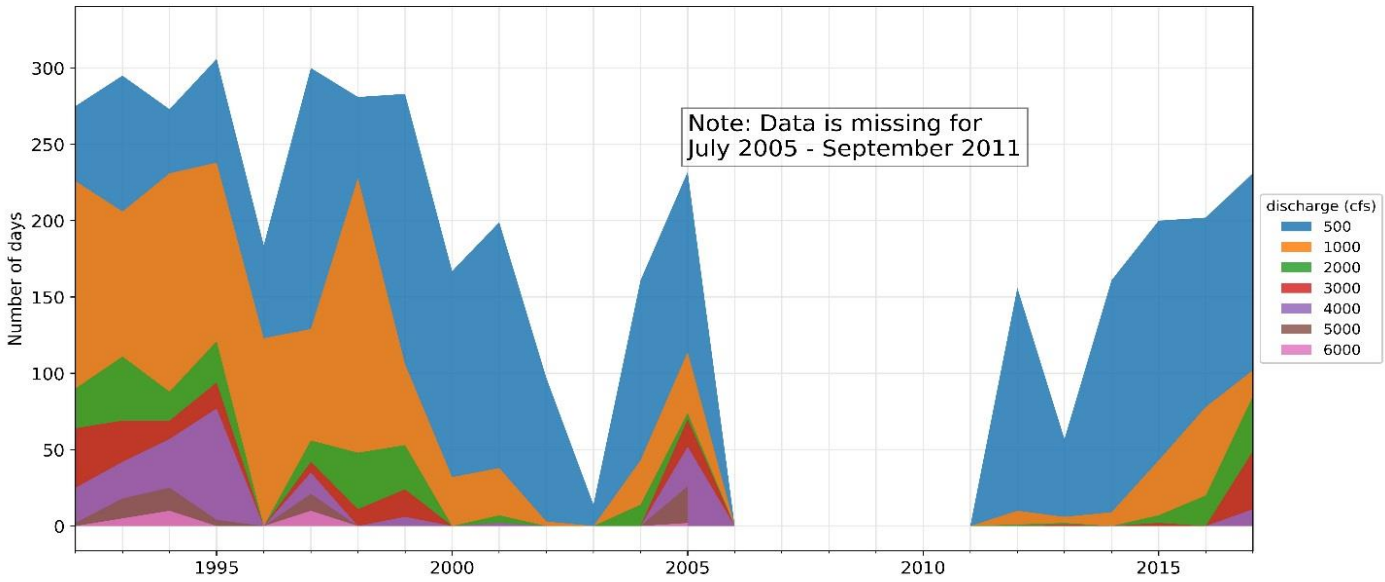

Figure 12: Graph of days exceeding flow values at Bernardo (USGS Gage 08332010) (modified from Klein et al. 2018a).

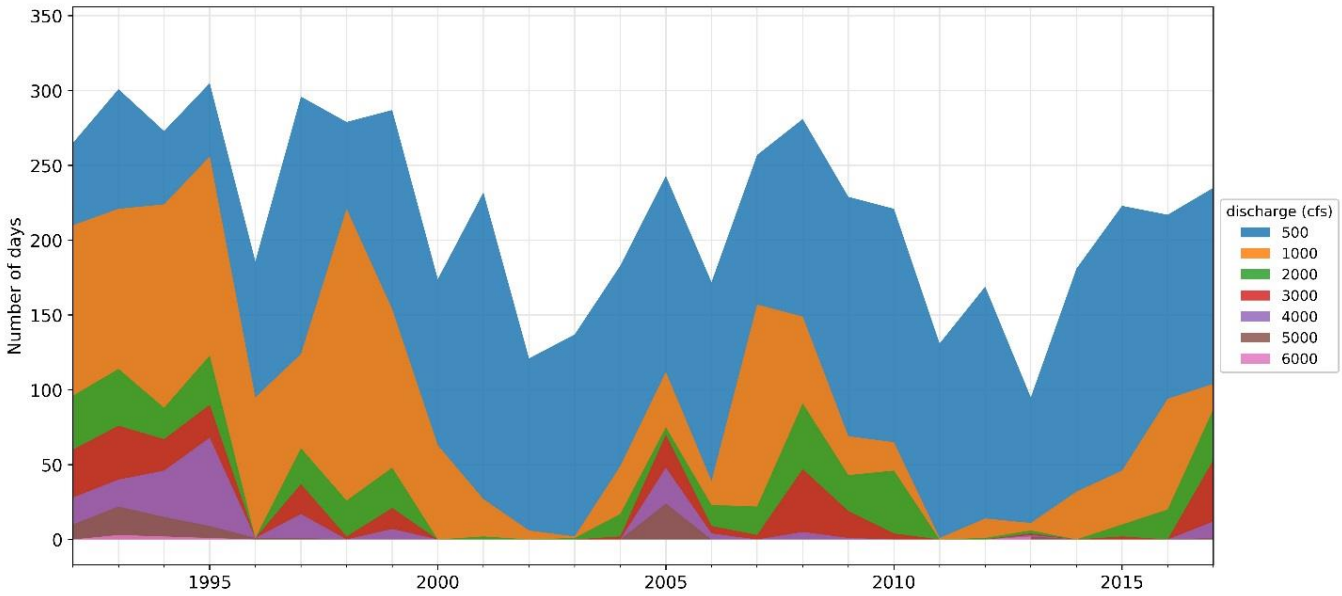

Figure 13: Graph of days exceeding flow values at San Acacia (USGS Gage 08354900) (modified from Klein et al. 2018a).

2.3. Suspended Sediment Load

2.3.1. Mass Curves

Single mass curves of cumulative suspended sediment flux (in millions of tons) are shown in Figures 14-16. Breaks in slope show the changes in flux. Data comes from the USGS gages at the Albuquerque (08330000) gage and Bernardo (08332010) gage upstream of the Rio Puerco confluence. The Rio Puerco gage (USGS 0853000) is used for the Rio Puerco single mass curve. The data on the graph is based on annual sediment amounts. show the suspended sediment curves.

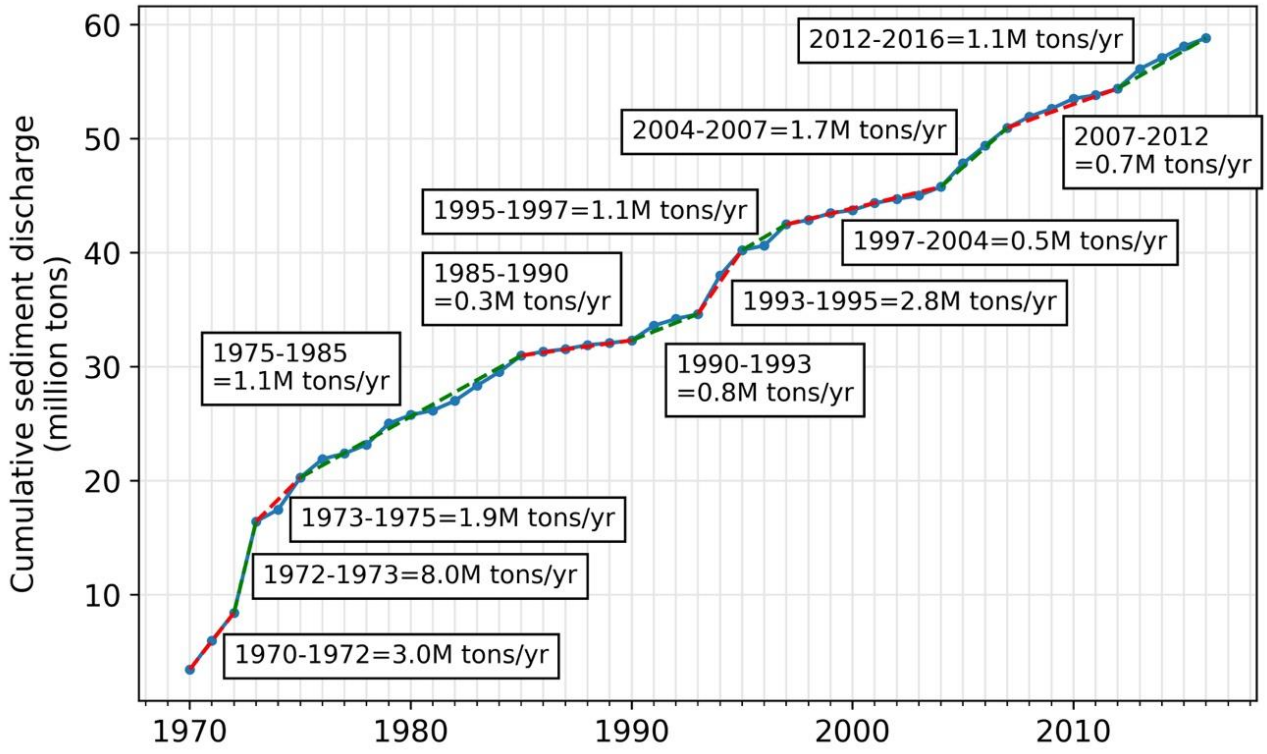

Figure 14: Single mass curve at Albuquerque (08330000) for suspended sediment (modified from Klein et al. 2018a).

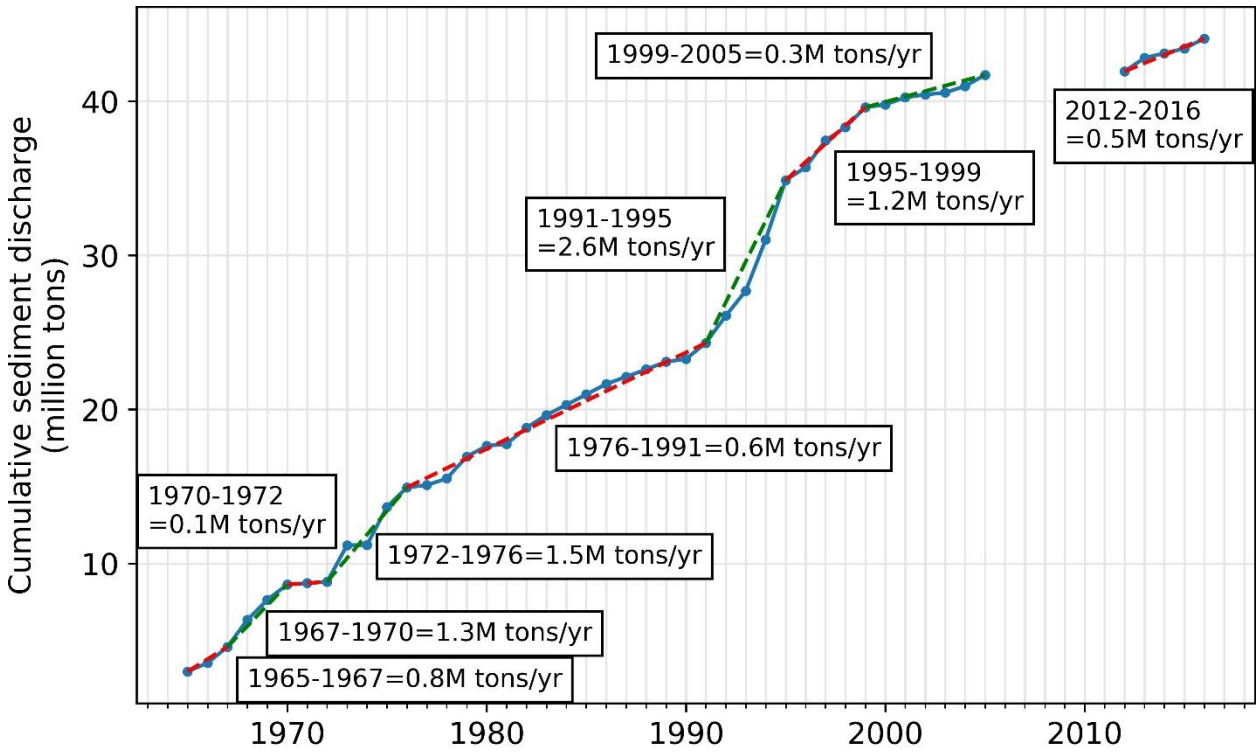

Figure 15: Single mass curve upstream at Bernardo (08332010) for suspended sediment (modified from Klein et al. 2018a).

Albuquerque experienced a larger decrease in sediment load after the mid -70's than the Bernardo gage, which can be attributed to the influence of Cochiti Dam. The sediment load at the Bernardo gage also was fairly high in the 90's, it also decreased to a fairly constant and sustained low suspended sediment load in the new millennium. The Bernardo and Albuquerque gage have alternated which transports more suspended sediment. For instance, the average suspended sediment load from 1991-93 was low at Albuquerque but high at Bernardo. Since 2000, the suspended sediment load at the Albuquerque gage appears to be larger than at Bernardo.

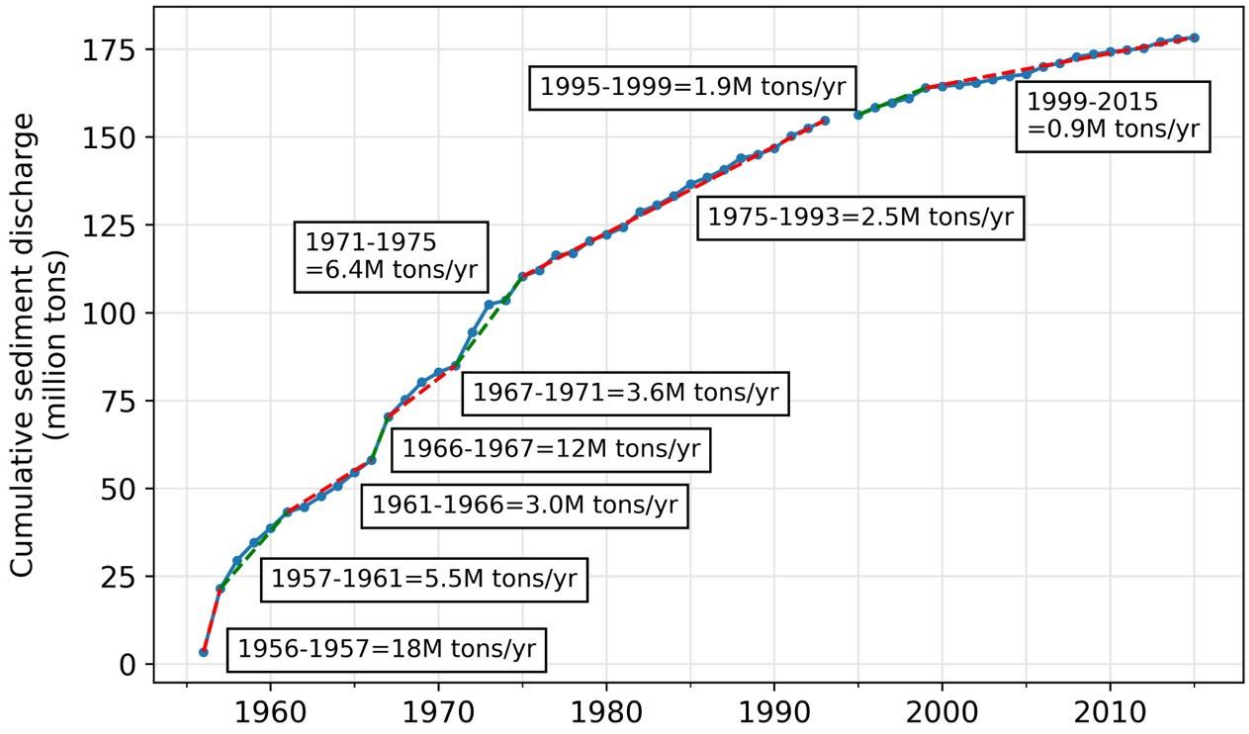

Figure 16: Single mass curve for suspended sediment on the Rio Puerco (08353000) (modified from Klein et al. 2018a).

The Rio Puerco's sediment discharge has gradually decreased since the 1970s. It contributed 70% of the annual suspended sediment volume recorded at the San Acacia gage from the late 1970s through the early 1980s. The contribution decreased to about 38% of the annual suspended sediment load (Klein et al. 2018a).

2.3.2. Double Mass Curves

Double mass curves are used to show how suspended sediment volumes pair with annual discharge volume. The slope of the double mass curves represents the mean sediment concentration. The double mass curves at Albuquerque and Bernardo are shown on Figures 17 and 18 respectively.

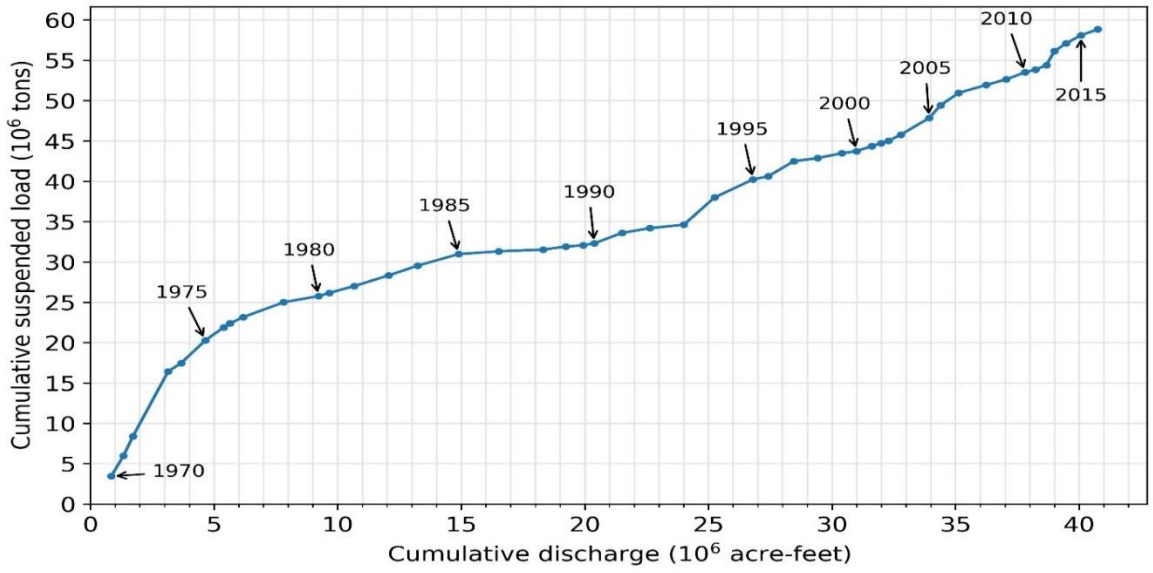

Figure 17: Double mass curve at Albuquerque gage (08330000) from 1970 to 2016.

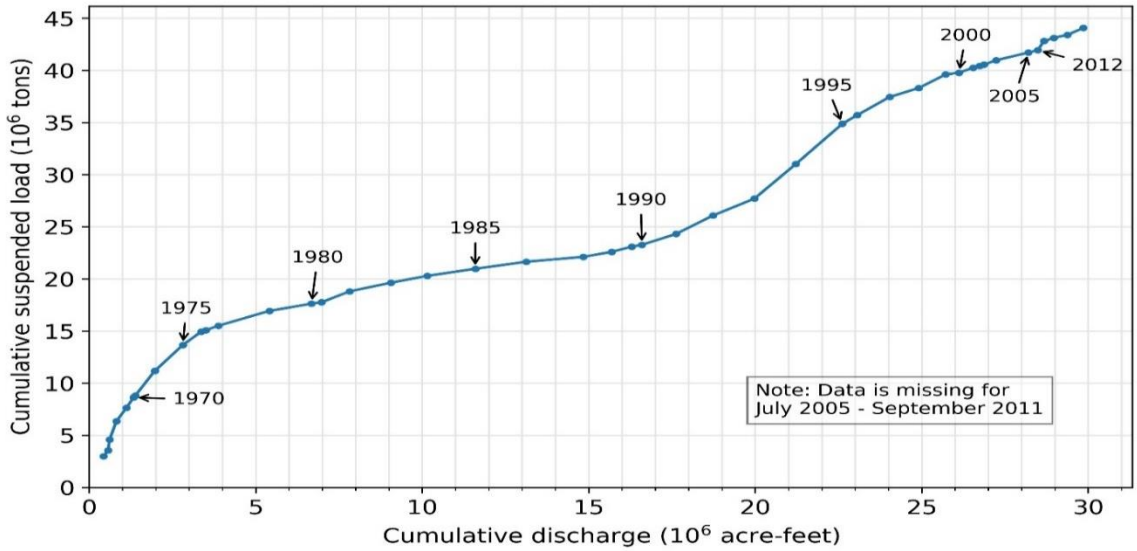

Figure 18: Double mass curve at Bernardo gage (08332010) from 1965 to 2016.

Overall, the mean annual suspended sediment concentration has decreased since the 1960s (Klein et al. 2018a). The highest concentration occurred prior to 1975 at Albuquerque gage (Figure 17). The Bernardo gage shows a similar trend to the Albuquerque gage, although the values are lower (Figure 18). Additionally, there is a more distinct increase in sediment concentration in the early 1990s at the Bernardo gage. From 1975 to 1993 the average sediment concentration was about 1,174 mg/l at Albuquerque and 1,270 mg/l at Bernardo. After 1993, the average suspended sediment concentration was 1,657 mg/l at Albuquerque and 1,864 mg/l at Bernardo.

2.4. Total Sediment Load

This section is divided into two parts: (1) BORAMEP analysis of the total sediment load from Klein et al. (2018a); and (2) Analysis of the total sediment load from SEMEP from Yang (2019).

2.4.1. BORAMEP

The total sediment load can be calculated from sediment concentration measurements and discharge using the Modified Einstein Procedure (MEP). The Bureau of Reclamation Automated Modified Einstein Procedure was developed by Holmquist-Johnson et al. (2009). The details of the calculations, methods and results on the Rio Grande were presented by Klein et al. (2018a). The total load was calculated using sediment data from the San Acacia gage downstream of the Diversion Dam (SADD). This is the only gage USBR used to calculate the total sediment load. The calculations using BORAMEP included the early 1990s through 2010. Figure 19 shows the total sediment discharge against the flow discharge. At a given discharge, silt or sand bed channel has a higher total sediment discharge (Figure 20). The San Acacia gage shows that the predominant material being transported is sand. Silts and clays are transported less than sand, and gravel is less than 1% of the total load. According to Klein et al. (2018a), sand loads are 5 times greater during summer or fall monsoon rain events compared to spring snow-melt runoff periods up to 2,000 cfs. Gravels move primarily during spring snow-melt periods, whereas sand and smaller particles move during both spring and summer peak flow periods. Figure 21 gives the total sediment rating curve at San Acacia.

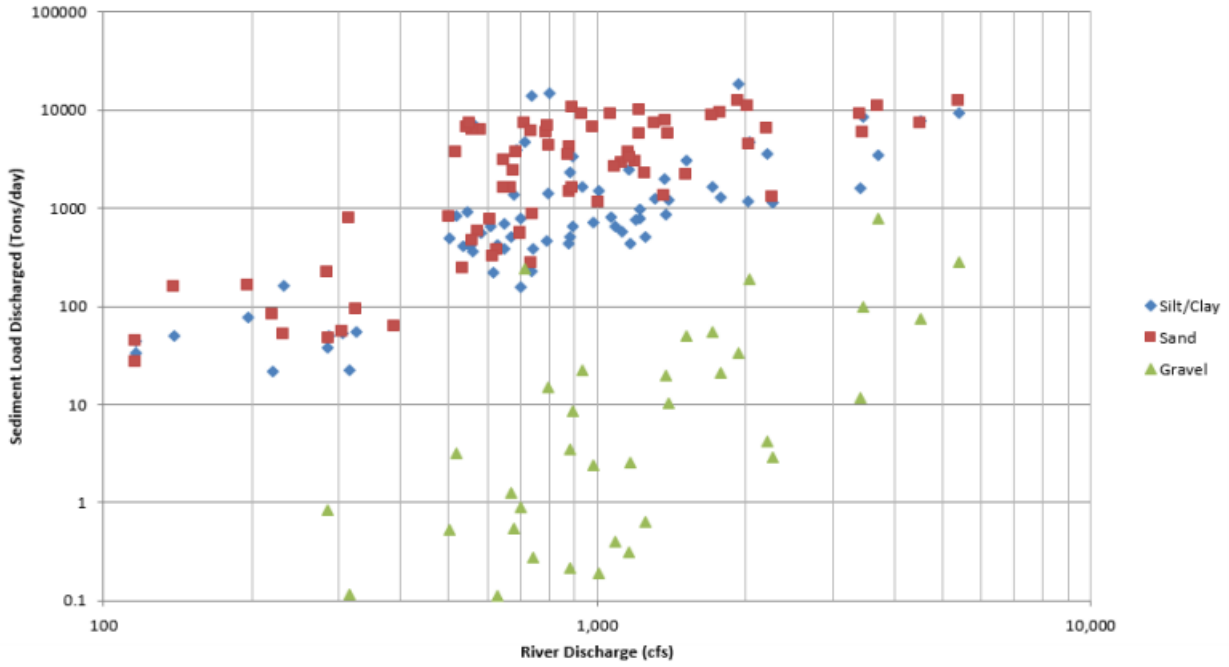

Figure 19: Graph of total load for gravels, sands and fines at the San Acacia gage from 1995-2010. Gravel data below 0.1 tons/day is omitted. (Klein et al. 2018a)

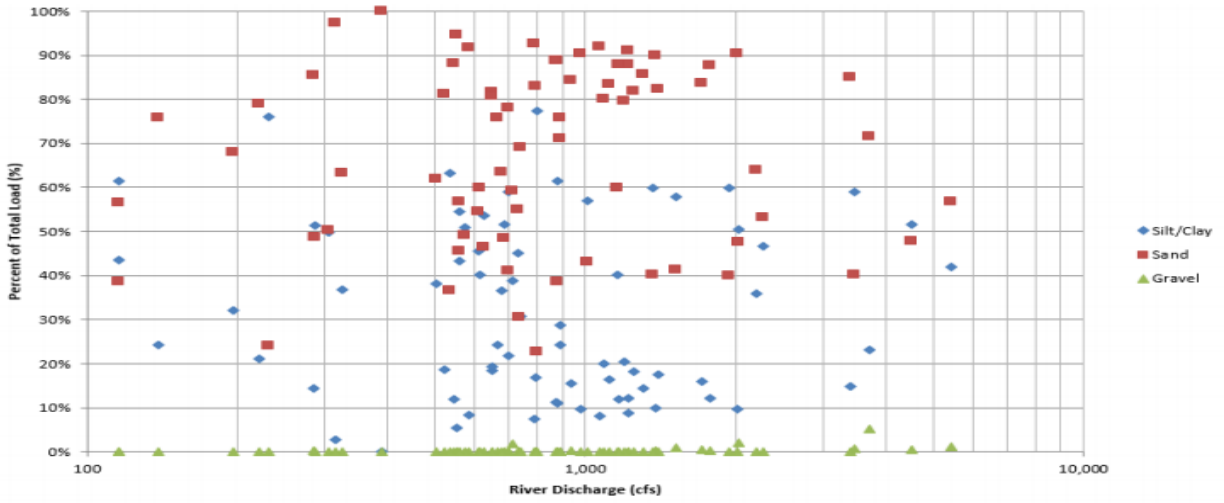

Figure 20: Percent of the total load in gravels, sands and fines as a function of discharge at San Acacia (Klein et al. 2018a)

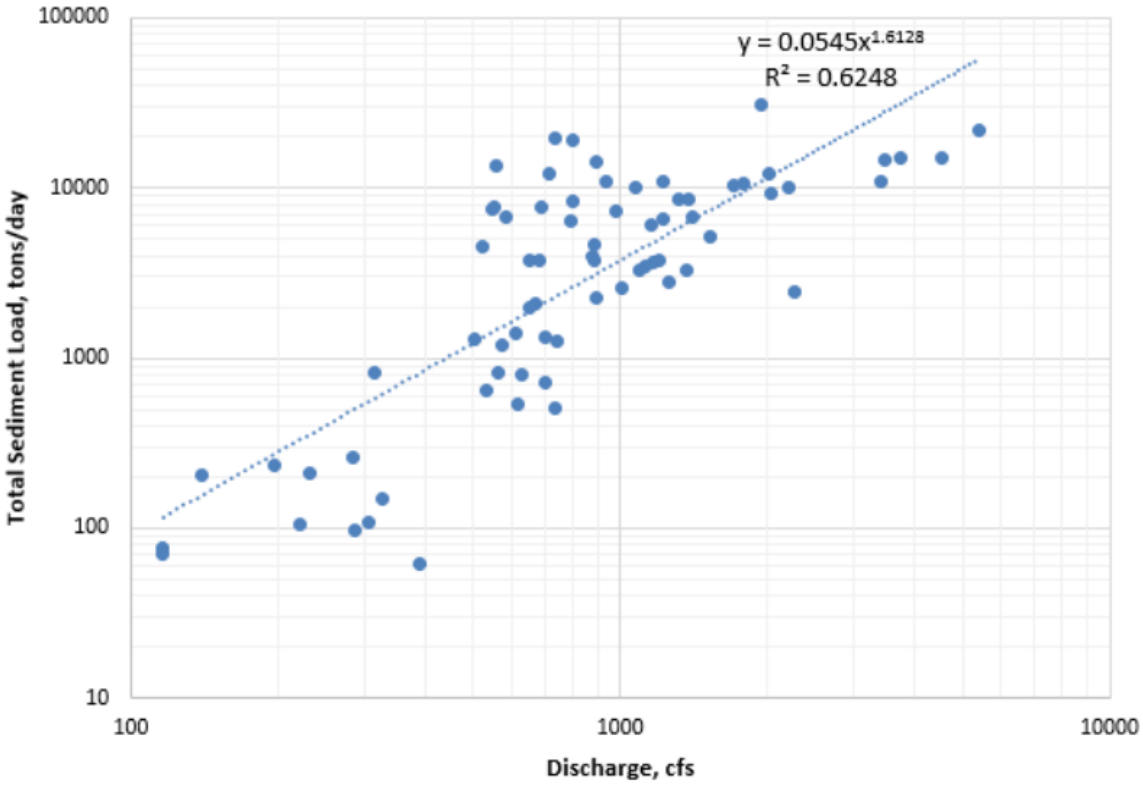

Figure 21: Total sediment load at San Acacia (Klein et al. 2018a)

2.4.2. SEMEP

The Series Expansion of Einstein Procedure (SEMEP) was also used in this study. The method was developed at CSU with the procedure detailed in Shah-Fairbank et al. (2011) as a function of shear velocity u_* and fall velocity ω. It was recently tested by Yang (2019) with applications on 35 rivers in South Korea. In this report, SEMEP is applied at three stations on the Rio Grande, at San Acacia gage 08354900, as well as Albuquerque and Bernardo at gages 08330000 and 08332010. The number of field samples calculated by the SEMEP are respectively 306, 211, and 173 samples at gages 08330000, 08332010, and 08354900. For these stations, the values of u_*/ω range from 1.5 to 37,600. According to Shah-Fairbank et al. (2011) and Julien (2010), SEMEP performs accurately when $u_*/\omega > 5$ so we expected good results from the applications on the Rio Grande.

It can be seen in Figure 22a that the SEMEP predictions and total sediment load measurements fall close to the 45 degree line of perfect agreement. Figure 23b also shows the prediction errors between SEMEP calculations and measurements as a function of u_*/ω. The mean absolute percentage error is 27% (Figure 23b). Figure 24-25 show the sediment rating curves for total sediment discharges at gages 08330000, 08332010, and 08354900.

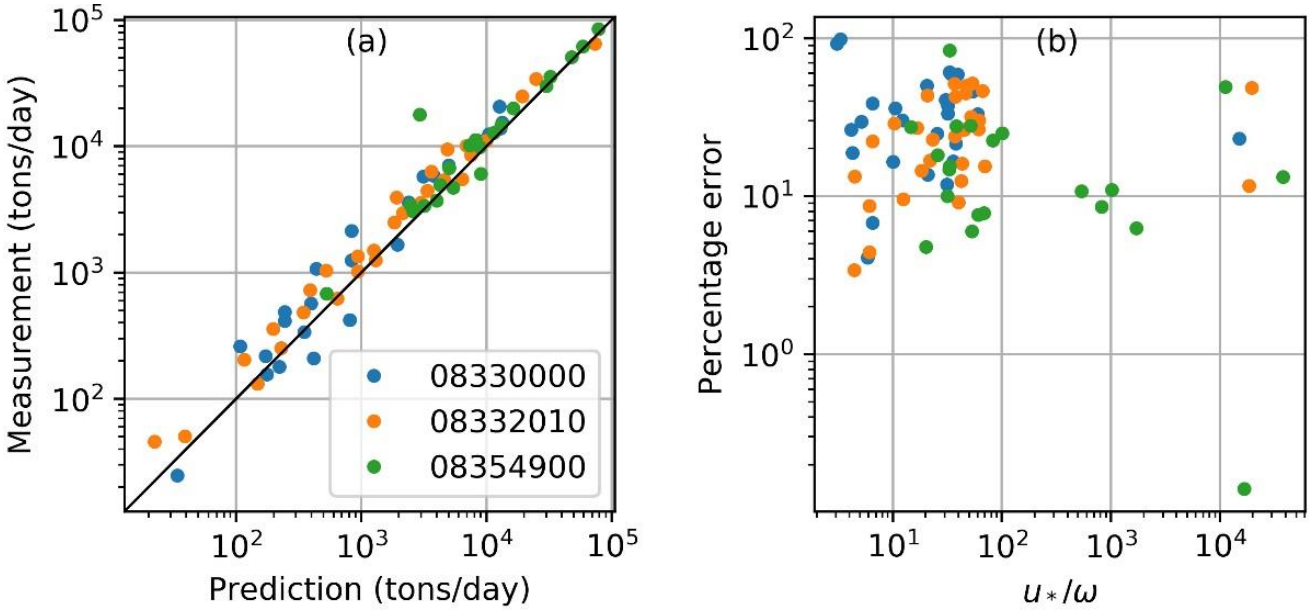

Figure 22: (a) Comparison between predicted and measured total sediment load, and (b) percentage error versus u_*/ω

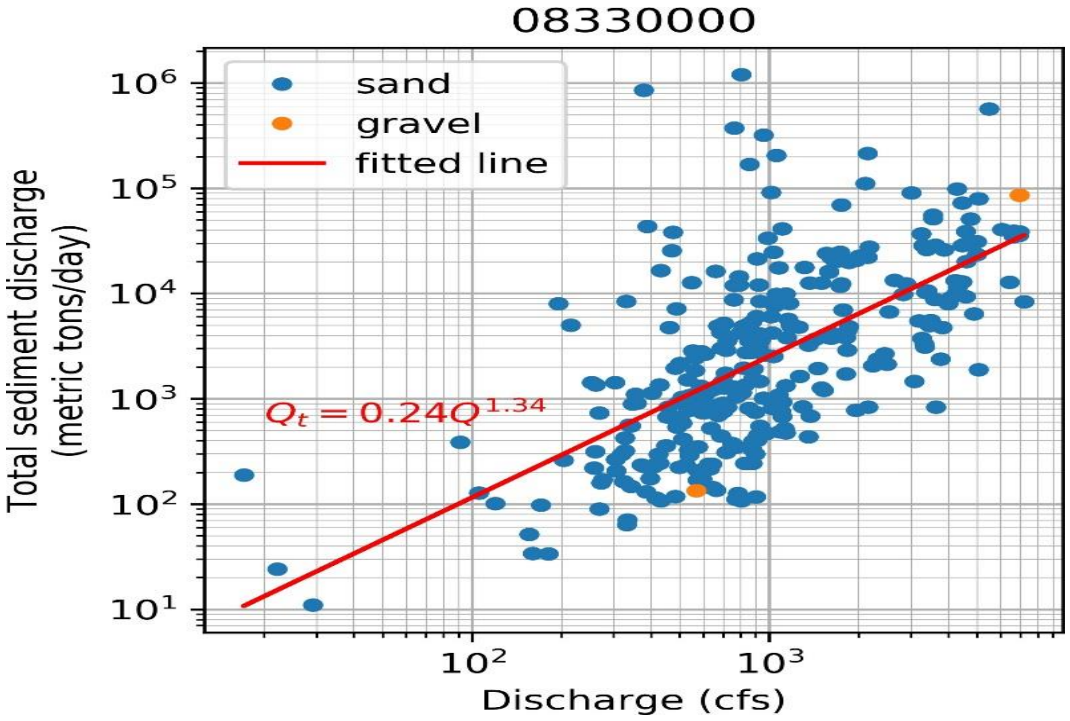

Figure 23: Total sediment rating curve at Rio Grande at Albuquerque (08330000)

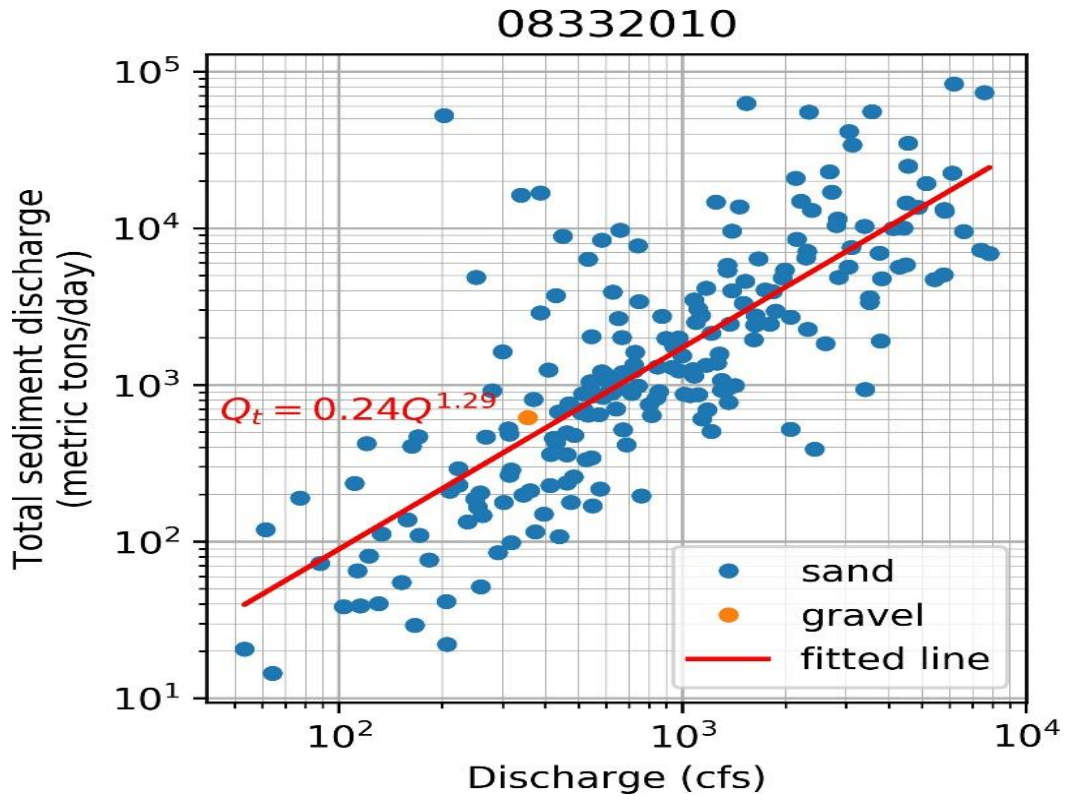

Figure 24: Total sediment rating curve at Rio Grande Floodway Near Bernardo (08332010)

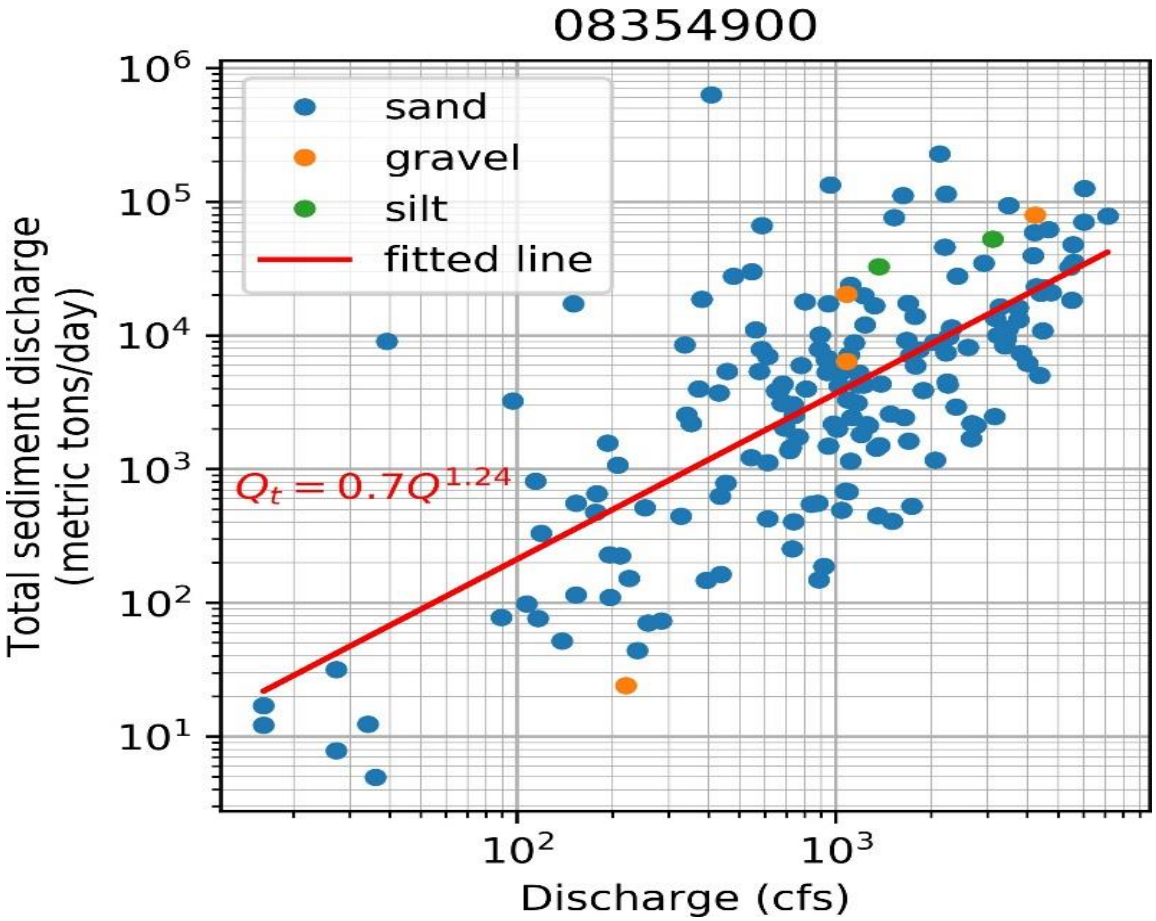

Figure 25: Total sediment rating curve at the Rio Grande Floodway at San Acacia (08354900)

The ratio of measured to total sediment discharge is a function of flow depth h, bed material d_s, and Rouse number Ro ($2.5/\text{Ro} = u_*/\omega$) according to SEMEP (Shah-Fairbank et al. 2011; Yang and Julien 2019). On the other hand, the ratio of suspended to total sediment discharge is a function of the ratio h/d_s of flow depth h to grain size d_s and Ro. The calculated ratio Q_m/Q_t of measured $Q_m$to total sediment discharge Q_t, and the ratio $Q_s/Q_t$of suspended Q_s to total sediment discharge Q_t are plotted with the analytical solutions in Figures 26 to 28 for the three different gaging stations. As expected, when the value of Ro is low (Ro < 0.3), the ratio Q_s/Q_t is close to 100% during floods when h/d_s > 100. These ratios are also in good agreement with the theory for both sands and gravels.

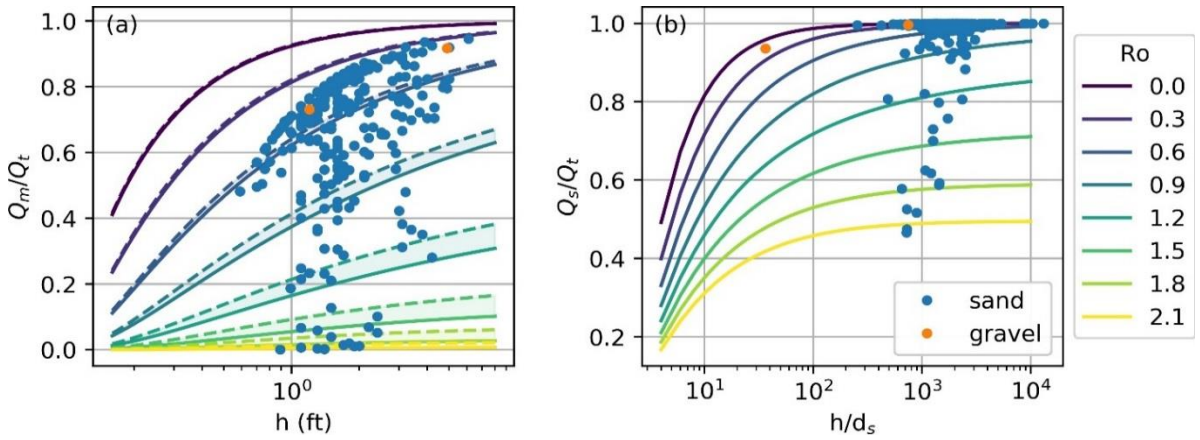

Figure 26: (a) the ratio of measured to total sediment discharge vs depth; and (b) the ratio of suspended to total sediment discharge vs h/ds at Albuquerque (08330000)

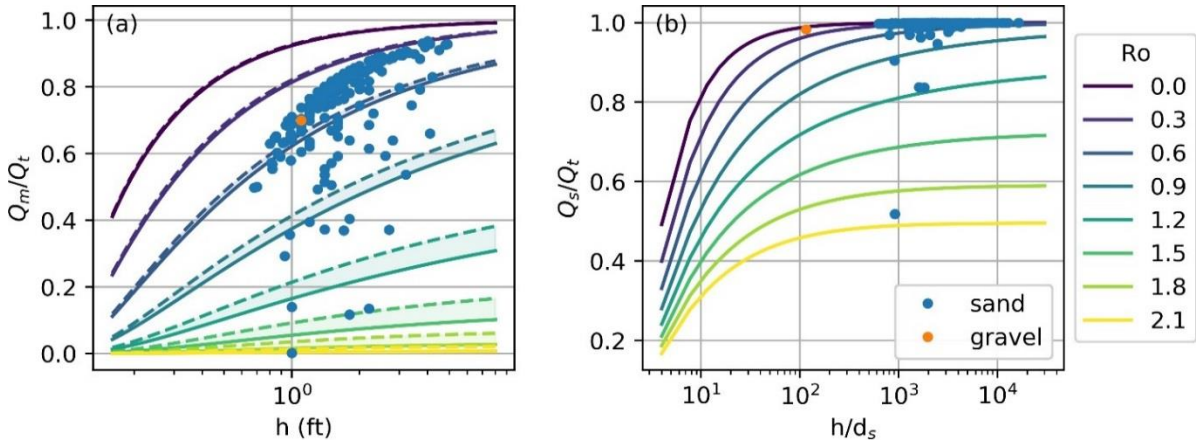

Figure 27: (a) the ratio of measured to total sediment discharge vs depth; and (b) the ratio of suspended to total sediment discharge vs h/ds at the Rio Grande Floodway Near Bernardo (08332010)

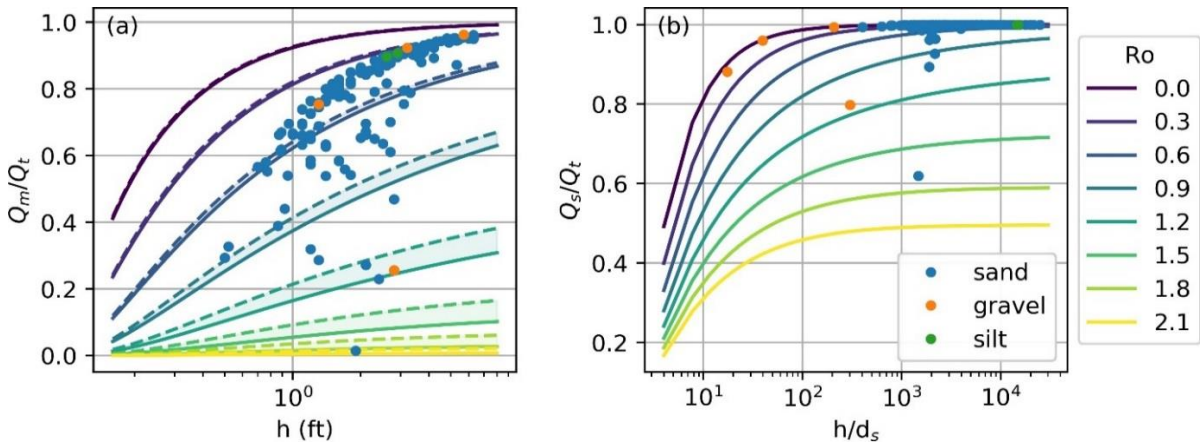

Figure 28: (a) the ratio of measured to total sediment discharge vs depth; and (b) the ratio of suspended to total sediment discharge vs h/ds at the Rio Grande Floodway at San Acacia (08354900)

3. Geomorphic River Characteristics

Geomorphic characteristics of the Middle Rio Grande have been changing due to the dynamic of flow and sediment regimes and the influence of human activities. In this section, the temporal change of the geomorphic attributes was analyzed. The analysis was conducted based on aerial photos, cross sectional surveys (agg/deg lines and range lines), and it also includes HEC-RAS simulations. The following parameters were tracked: sinuosity, active channel width, bed elevation, channel volume, and related hydraulic variables.

3.1. Sinuosity

As shown in Figure 29, sinuosity has been increasing slightly over time for the Isleta to Rio Puerco reach since the 1990s. Data on the entire reach was compiled from various sources. Years 1935 through 2006 came from Makar (2010), who calculated sinuosity as the active channel centerline divided by valley length using historic aerial photographs. The following years came from Klein et al. (2018a), who calculated sinuosity using active channel centerlines generated by various Reclamation contractors or Google Earth imagery.

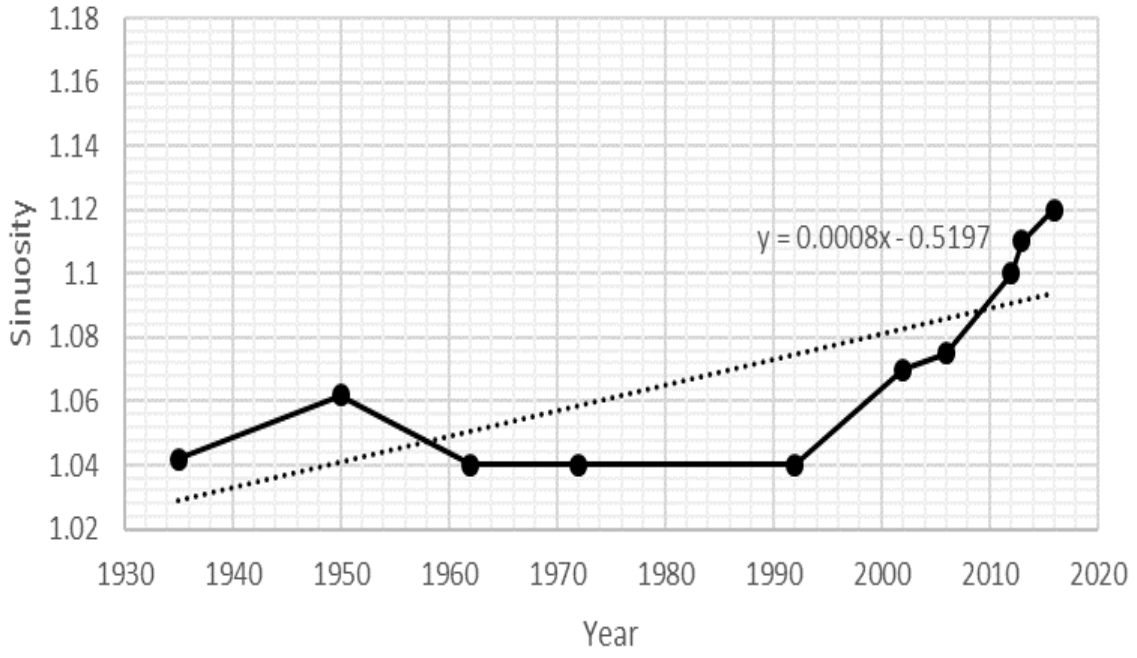

Figure 29: Trend of sinuosity from the Isleta diversion dam to Rio Puerco. A positive slope of 0.0008 is observed. The data for this graph was extracted from a graph provided by USBR (Klein et al. 2018a).

There is a small spike in 1950, which then decreases and stays constant until about 1990. This is likely due to channelization efforts from the USBR in the 1950s and 1960s and ongoing river maintenance through that period (Makar 2010). From 1990 onwards, sinuosity increases through 2016. This may be due to the reduction in sediment supply following the Cochiti Dam

construction and a change in management strategies by the USBR. Figure 30 shows the sinuosity for each subreach. Sinuosity was calculated for each individual subreach using digitized channel centerlines provided by the USBR's GIS and Remote Sensing Group. Aerial photographs and accompanying digital shapefiles were provided for years 1918, 1935, 1949, 1962, 1972, 1985, 1992, 2001, 2002, 2006, 2008, 2012 and 2016. The centerlines were then split up by subreach and divided by the length of the subreach as shown in Figure 30.

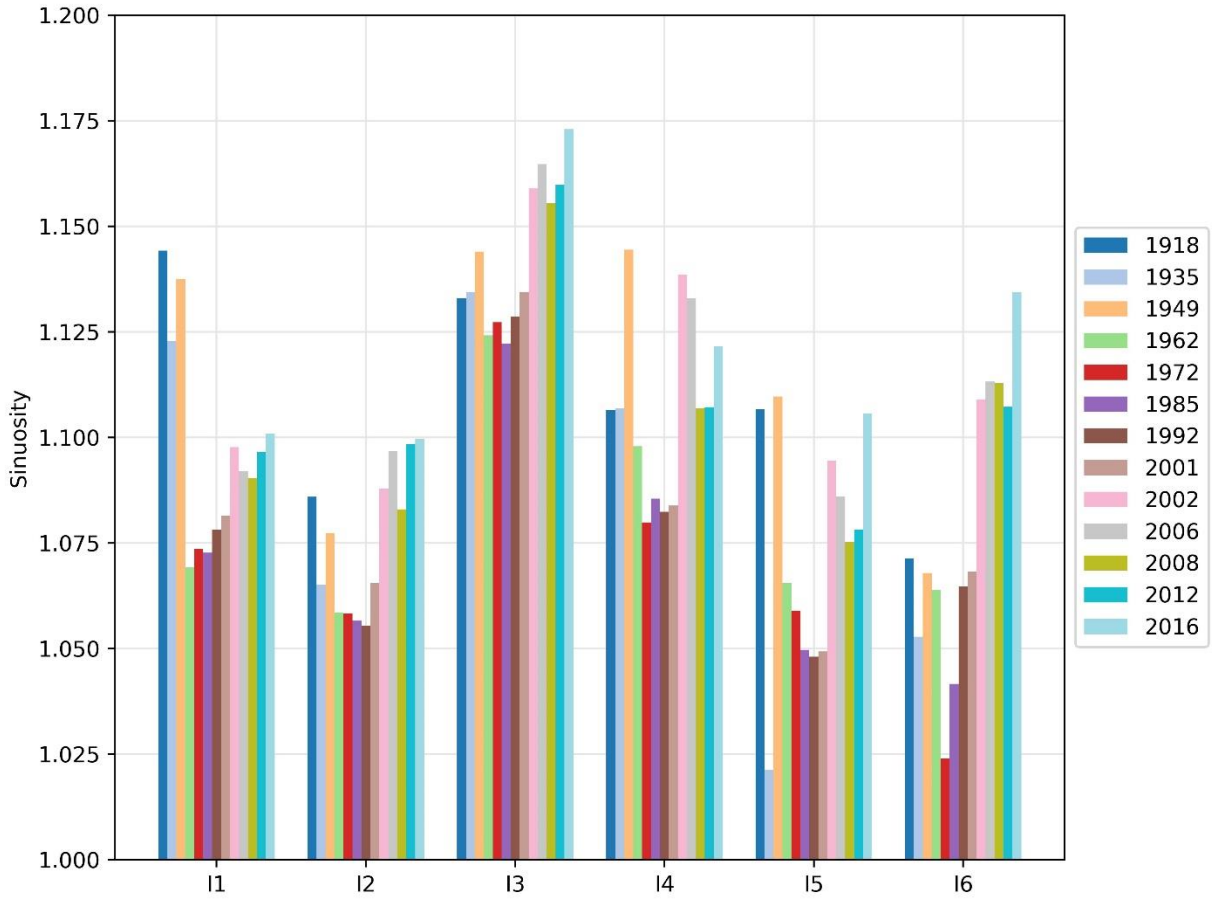

Figure 30: Sinuosity at subreach scale.

Subreach I3, Los Chaves to Abo Arroyo Confluence, is the most sinuous overall. The significant drop in sinuosity after 1949 in a few subreaches could be a result of channelization in the 1950s. For almost all subreaches, the years with the lowest sinuosity were 1962 through 1992. Overall, the sinuosity is near one which indicates a relatively straight channel.

3.2. Channel Width

The width has generally decreased over time since 1918 in this reach due to infrastructure construction, channelization, reduction in peak flows, upstream sediment reduction and vegetation encroachment (Culbertson and Dawdy 1964; Crawford et al. 1993; Berry and Lewis 1997; Bauer 2000; MEI 2002; Bauer and Hilldale 2006; Tashjian and Massong 2006; Parametrix 2008; Bauer 2009; Makar 2010; Makar and AuBuchon 2012; Baird 2014 in Klein et al. 2018a). This has made the widths more uniform as well (Crawford et al. 1993; Parametrix 2008; Makar and AuBuchon 2012 in Klein et al., 2018a).

Digitized data provided by the USBR's GIS and Remote Sensing Group from aerial photographs was used to analyze the active channel width at agg/deg cross-sectional lines. The active channel is defined as non-vegetated channel. Measurement of the active channel width was performed by clipping the agg/deg line coverage with the active channel polygon. Four lines (824, 873, 1061, and 1075) are deleted from the analysis because they are skewed with respect to the active channel for all years. The average width for each subreach is calculated by averaging the width of all agg/deg lines within the subreach (Figure 31).

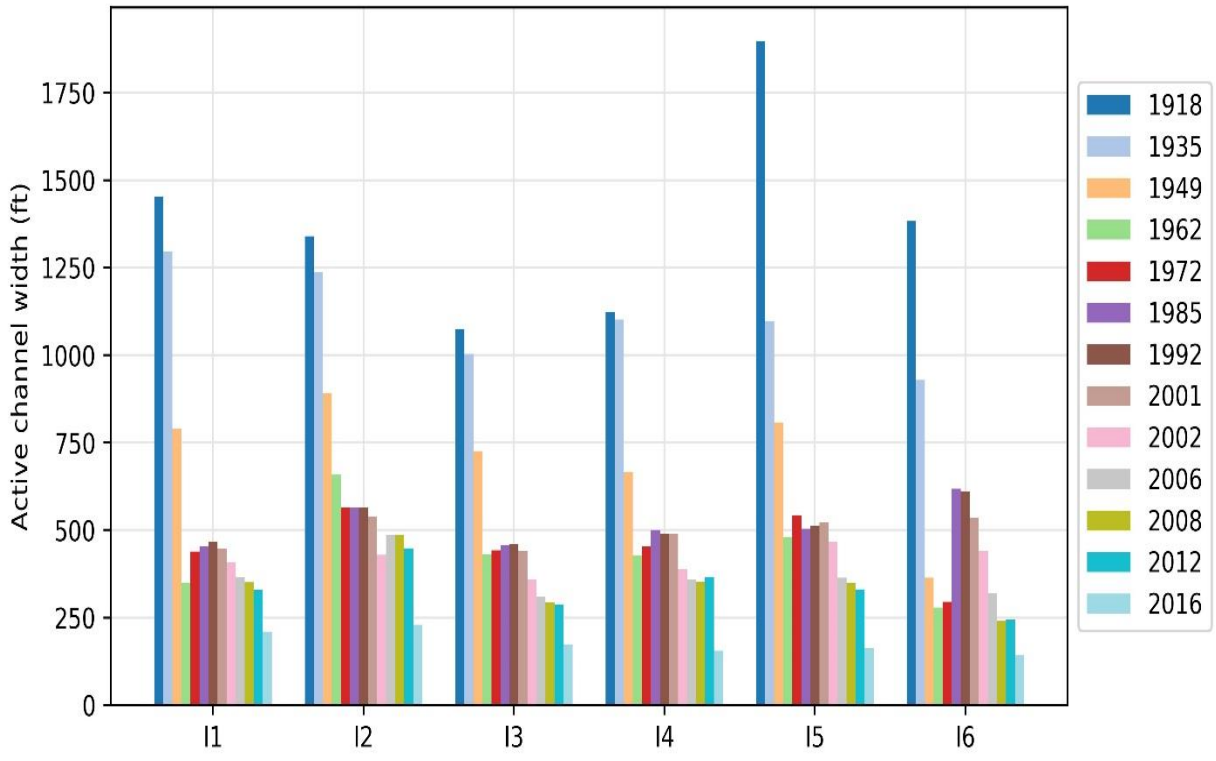

Figure 31: Reach averaged active channel width.

For each subreach, the width has decreased since 1918. At all subreaches, the most significant drop in channel width from occurs from 1918 to 1962. The biggest decrease is found at subreach I5: 1417 feet over 44 years. The widths across subreaches drop dramatically after 1949 because channelization with installation of jetty jack systems started around the 1950s (Easterling Consultants LLC 2015). There is an increase in channel width around the 1980s likely due to mechanical removal of vegetation (which stopped in the 1980s) and larger spring runoffs (Bauer and Hilldale 2006; Parametrix 2008 in Klein et al. 2018a). The average width began decreasing again starting in about 1992. The decreasing rate ranges from 5.9 ft/year (I2) to 18.3 ft/year (I6) between 1992 and 2012. This appears to be accelerating, with even steeper decreases starting in the 2010s, ranging from 25.2 ft/year (I6) to 54.5 ft/year (I2). The trend is similar to trend in the Cochiti Reach reported in Richard (2001).

3.3. Low Flow Channels

At low flows, the number of channels at each agg/deg line is measured from digitized planforms from the aerial photographs provided by the USBR. The average number of channels is calculated for each subreach and presented in Figure 32.

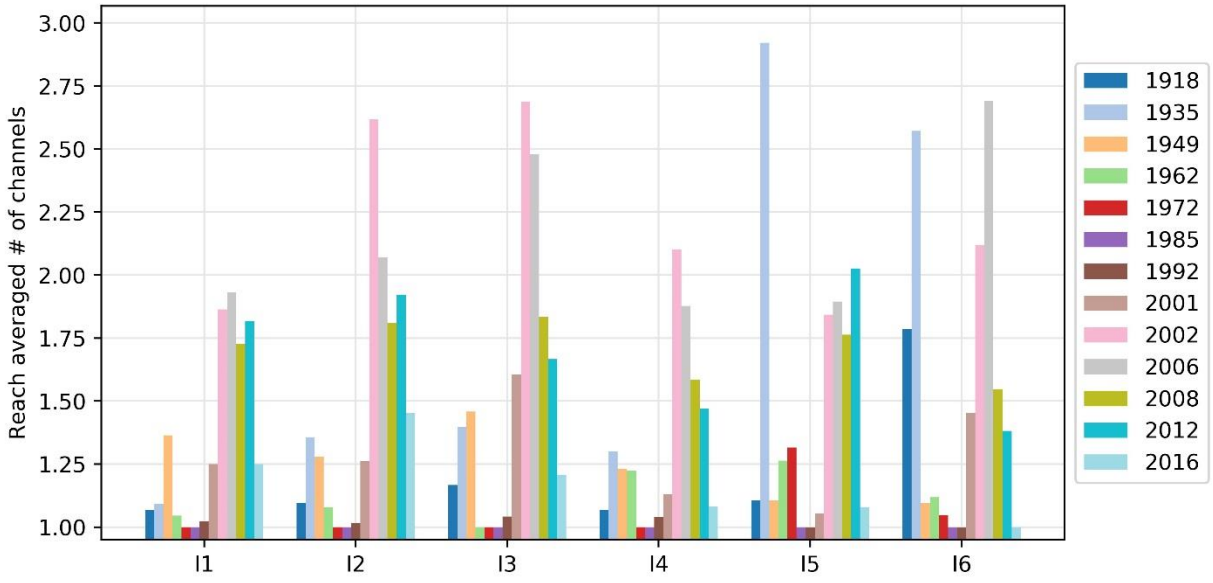

Figure 32: Average number of low flow channels at each subreach.

At high flows, the Isleta reach is a single threaded channel, but at low flows, it looks like a braided system. This explains how it is possible to see an increase in the number of channels coupled with a decrease in width. For instance, the number of channels is particularly low for 1962, 1972, and 1985, because the digitized planforms for these years did not capture the bars or islands in the channel due to either poor resolution or imagery quality, or high flows.

3.4. Bed Elevation

The mean bed elevation is used to compare the sketch the longitudinal profile in this report. Cross-section geometry models along agg/deg lines were developed by the Bureau of Reclamation Albuquerque Area Office. The geometry models are available for 1962, 1972, 1992, 2002 and 2012. For the models prior to 2012, the cross-section geometry is captured using photogrammetry techniques. The 2012 model is from LiDAR (Klein et al. 2018a). In addition, an underwater prism was developed (Varyu 2013). All the models were done using the NAV88 vertical datum. Figure 33 shows the long profiles of 1962, 1972, 1992, 2002, and 2012.

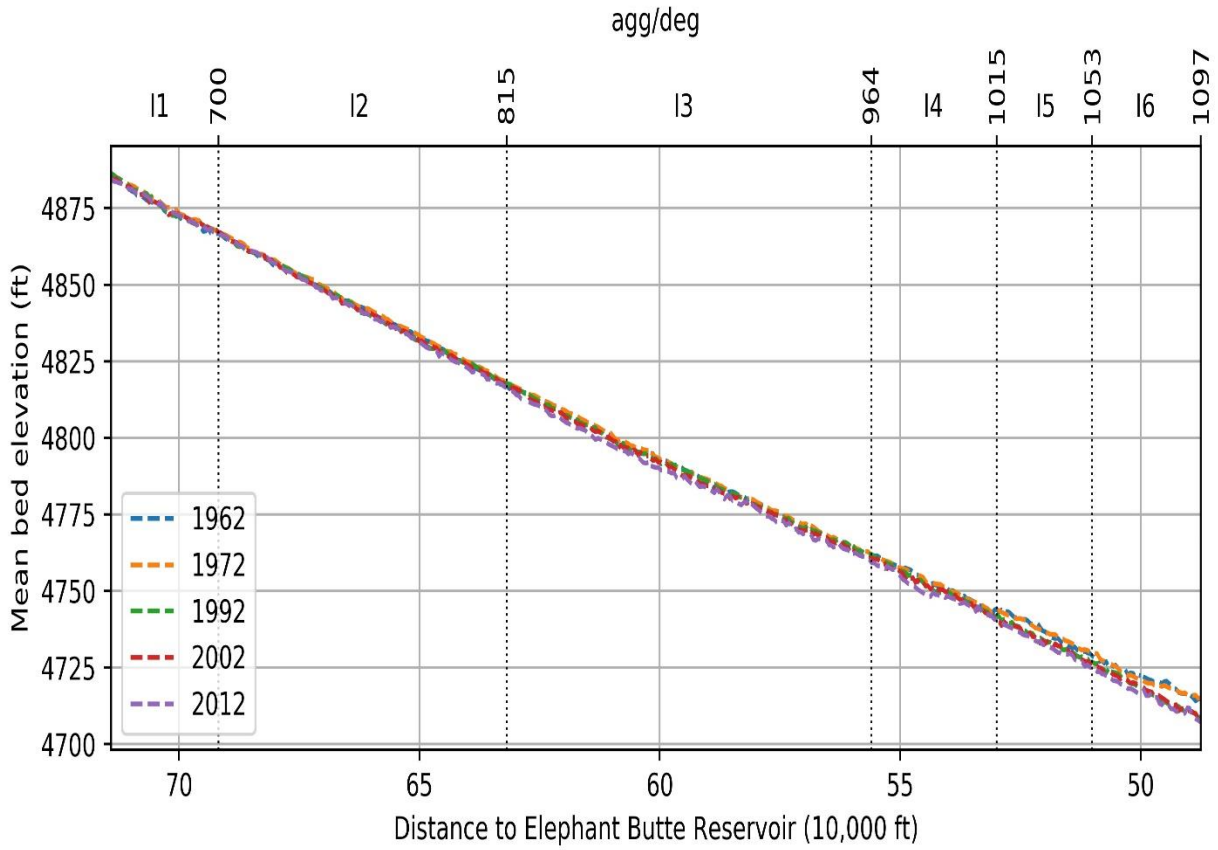

Figure 33: Longitudinal profiles for 1962, 1972, 1992, 2002, and 2012.

The longitudinal profiles of subreaches I1 and I2 are very similar between 1962 and 2012. Channel incision is found at subreaches I3, I4 and I5 after 1972. The average change in mean bed elevation for each subreach is listed in Table 5 and plotted in Figure 34.

Table 5: Change in mean bed elevation (ft).

Subreach	1962 - 1972	1972 - 1992	1992 - 2002	2002 - 2012
I1	1.32	-0.72	-0.06	-0.16
I2	0.68	-0.89	-0.13	-0.42
I3	0.55	-0.82	-0.74	-1.28
I4	0.09	-1.10	-0.43	-1.18
I5	0.22	-2.81	-0.52	-1.01
I6	-0.25	-3.70	-0.02	-1.29

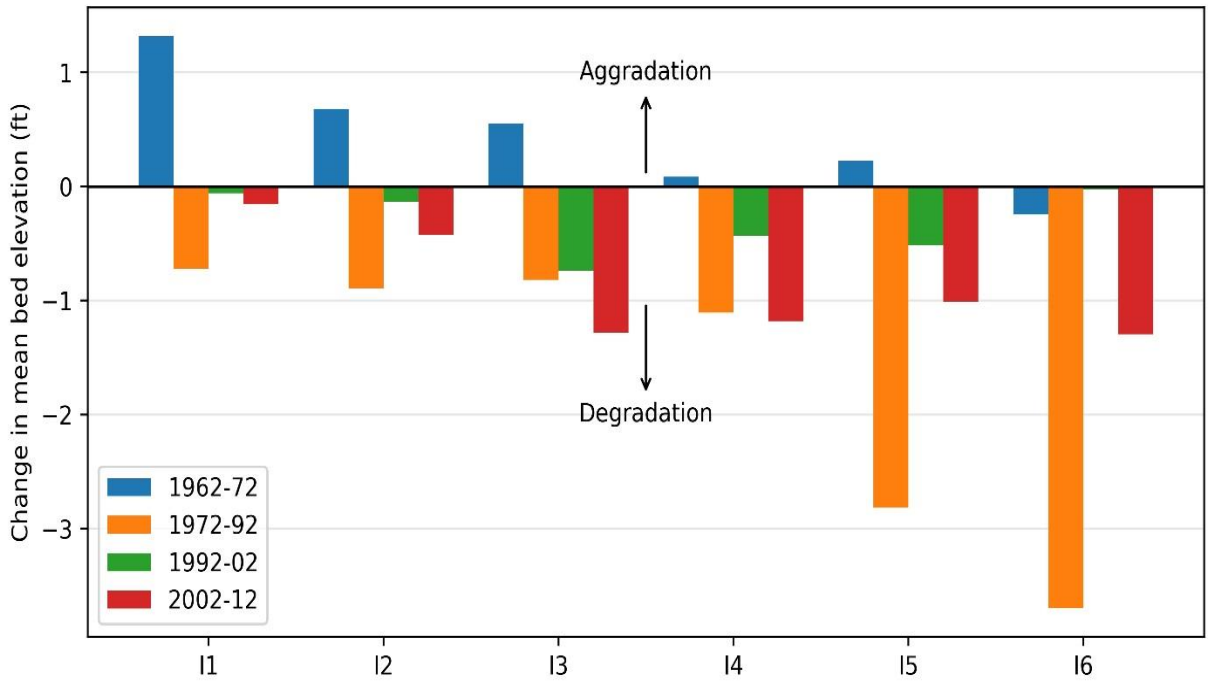

Figure 34: Change in bed elevation.

From 1962 to 1972, the channel aggraded in every subreach except in I5. I1 has the highest aggradation amount of 1.32 ft. The average aggradation varies from -0.25 ft to 1.32 ft. All of the reaches degraded following construction of Cochiti dam (November 1973). I6 has the highest degradation amount of 3.7 ft, during 1972 and 1992. Besides the influence of Cochiti dam, the degradation is likely associated to the decline in sediment load in Rio Puerco after 1975.

3.5. Volumetric Change

The change in main channel sediment volume for the time periods 1962 to 1972, 1972 to 1992, 1992 to 2002, and 2002 to 2012 is analyzed. This analysis follows a procedure by Varyu (2013) which provides an example of how to calculate the volume change. The extent of main channel is determined based on banklines. Banklines are given in the geometry models and are where the active channel intersects agg/deg lines. Due to the dynamic nature of the channel, banklines are likely to shift from year to year. The portion of the cross section within the outer-most right and outer-most left location of the banklines from two input datasets are defined as the main channel. The cross-section area between the banklines is then calculated for each of the two input datasets. Then the volume change is calculated as the difference in cross section area between two years multiplied by the length. The length is determined as half of distance of a cross section to its upstream cross section plus one-half the distance to the downstream cross section.

Figure 35 presents the main channel volume change of each subreach. A decrease in channel sediment volume shows degradation, while an increase shows aggradation. The change generally follows the trend in mean channel bed elevation.

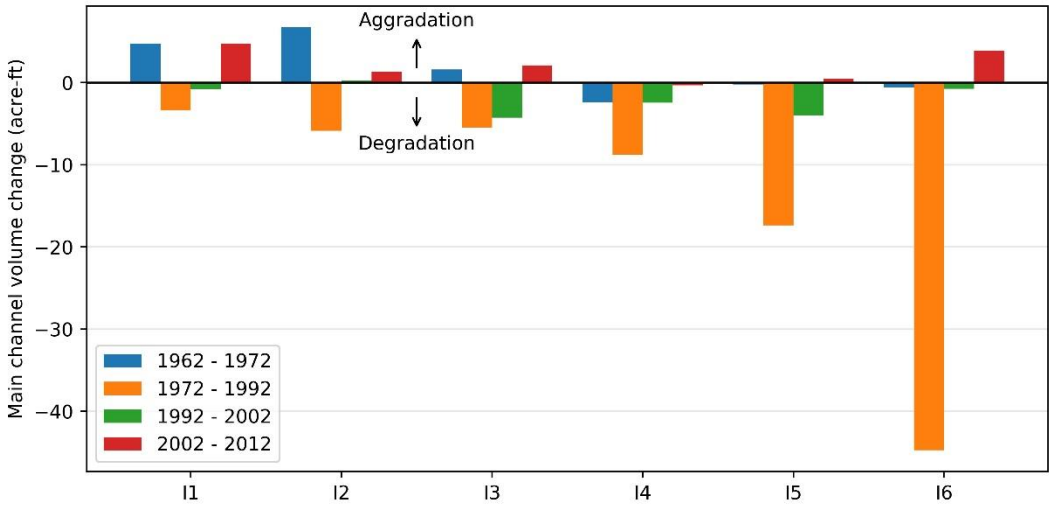

Figure 35: Main channel volume change.

Notice that from 2002 to 2012, most of the reaches show aggradation based on volume change but degradation based on the elevation change. It suggests that the channel is narrowing and incising.

3.6. Bed Material

Bed material samples were collected at rangelines that differ from the agg/deg lines. These rangelines do not date back as far as the agg/deg lines and are also spaced further apart. They are used in this analysis because bed material has been surveyed in these rangeline cross-sections. The sediment samples are grouped by decade and the statistical summary of the median grain size d_{50} is shown in Table 6. The typical d_{50} are medium sand (0.25 mm to 0.5 mm).

Table 6: d_{50} grain size statistics from the bed material samples in Isleta reach.

	Subreach	Min (mm)	Max (mm)	Mean (mm)	# of samples	# in sand only	# in gravel and sand
1990s	I1	0.19	0.48	0.41	20	20	0
	I2	0.13	0.51	0.39	38	38	0
	I3	0.03	0.96	0.36	366	366	0
	I4	0.19	0.46	0.32	13	13	0
	I5	0.36	0.18	0.24	8	8	0
	I6	0.16	0.41	0.30	12	12	0
2000s	I1	0.58	10.0	3.00	4	3	1
	I2	0.34	6.78	0.87	45	41	4
	I3	0.33	14.1	2.90	19	12	7
	I4	0.46	28.0	9.74	7	4	3
	I5						
	I6	0.24	45.3	5.52	11	9	2
2010s	I1	0.004	0.68	0.4	10	10	0
	I2	0.49	0.6	0.54	2	2	0
	I3	0.39	0.46	0.42	6	6	0
	I4	0.42	0.46	0.44	2	2	0
	I5	0.44	0.44	0.44	1	1	0
	I6	0.39	0.41	0.4	3	3	0

3.7. Flow depth, Velocity, Width, Wetted Perimeter and Slope

Flow depth, velocity, width, and wetted perimeter are obtained by using HEC-RAS 5.0.3 with a discharge of 3,000 cfs. A discharge of 3,000 cfs was selected because, anecdotally, it does not cause overbanking (Drew Baird, personal communication, June 19th, 2018). Available years of analysis with HEC-RAS include 1972, 1992, 2002, and 2012. The bed slope is calculated using both the cross-section from HEC-RAS and the channel length from the planform. The mean channel bed elevations at the beginning and the end of a subreach can be obtained from the HEC-RAS model. The difference of these two elevations divided the length of the subreach is the bed slope that is used here. The average value of each variable at subreach scale is plotted in Figure 37 and Figure 36. The change between ranges of years is summarized in Table 7.

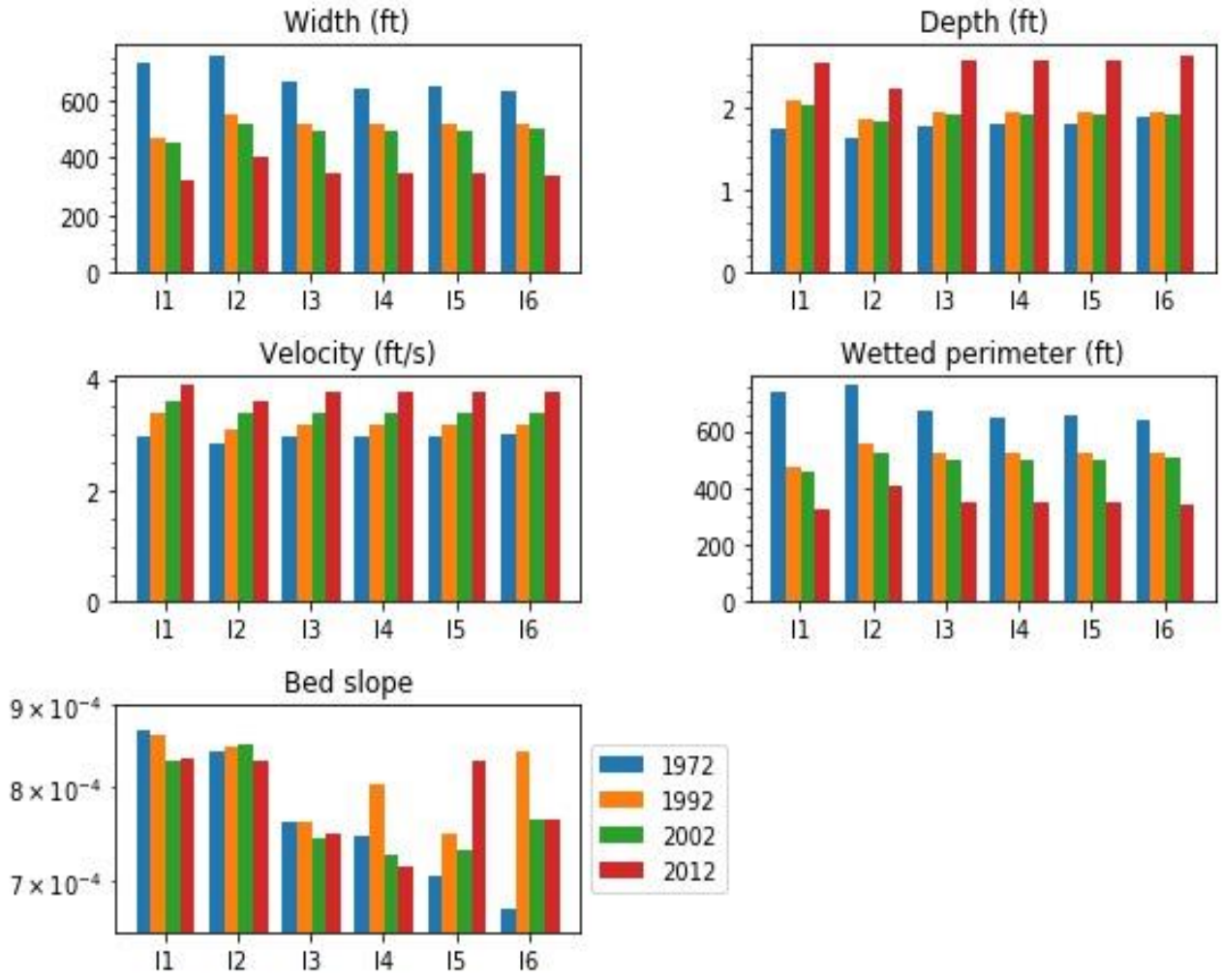

Figure 36: Width, depth, velocity, wetted perimeter, and bed slope at each subreach for 1972, 1992, 2002, and 2012 at 3,000 cfs

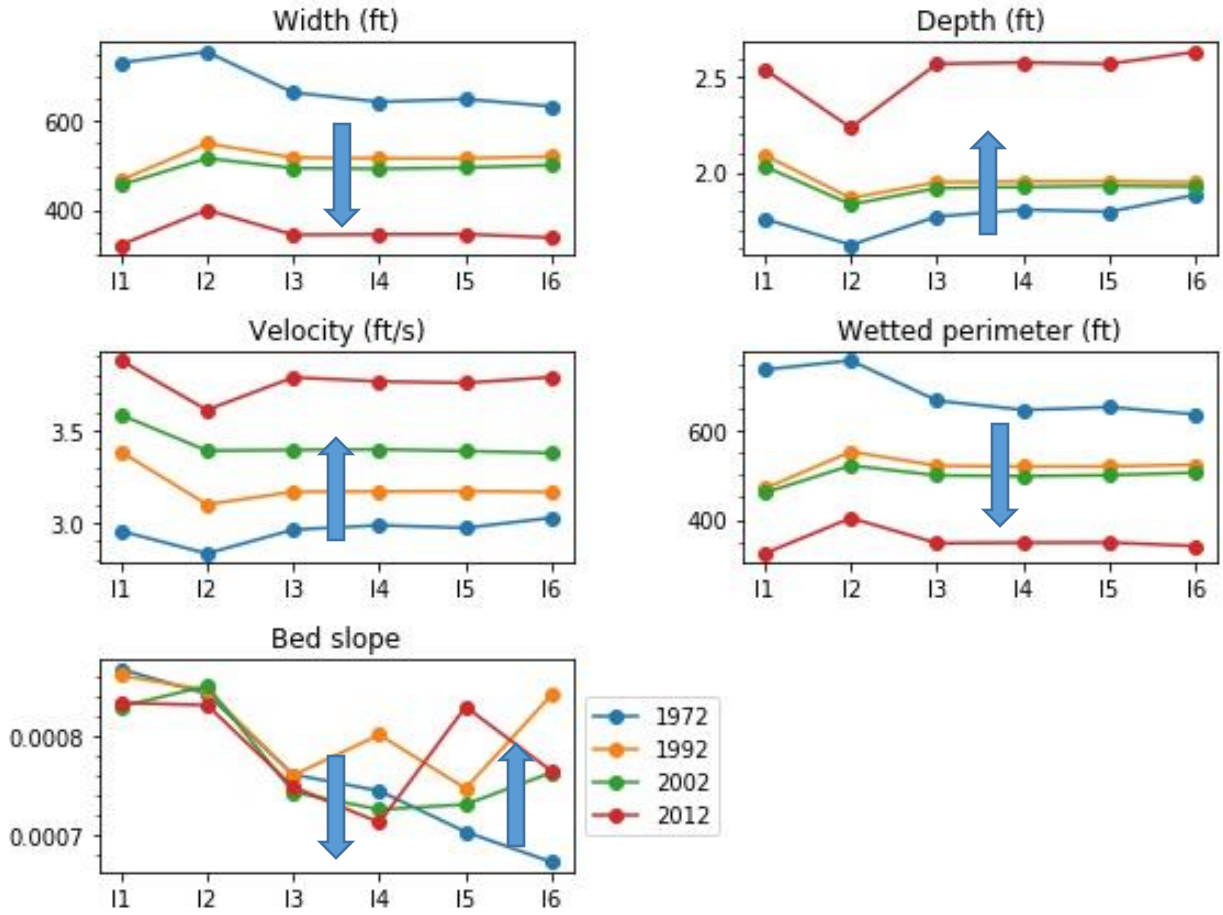

Figure 37: Width, depth, velocity, wetted perimeter, energy and bed slope at each subreach for 1972, 1992, 2002, and 2012 at 3,000 cfs.

Table 7: Isleta Reach channel geometry temporal change summary (+: increase in parameter value; -: decrease in parameter value).

Reach	Year	Width	Bed slope	Depth	Velocity	Volume	Bed elev.
I1	1972 - 92	-	-	+	+	+	-
	1992 - 02	-	-	-	+	+	-
	2002 - 12	-	+	+	+	-	-
I2	1972 - 92	-	+	+	+	+	-
	1992 - 02	-	+	-	+	-	-
	2002 - 12	-	-	+	+	-	-
I3	1972 - 92	-	-	+	+	+	-
	1992 - 02	-	-	-	+	+	-
	2002 - 12	-	+	+	+	-	-
I4	1972 - 92	-	+	+	+	+	-
	1992 - 02	-	-	-	+	+	-
	2002 - 12	-	-	+	+	+	-
I5	1972 - 92	-	+	+	+	+	-
	1992 - 02	-	-	-	+	+	-
	2002 - 12	-	+	+	+	-	-
I6	1972 - 92	-	+	+	+	+	-
	1992 - 02	-	-	-	+	+	-
	2002 - 12	-	+	+	+	-	-

The widths and wetted perimeter have decreased an average of about 420 ft across all subreaches since 1972. The decrease has been particularly prominent in subreach I1. Depth and velocity both are inversely proportional to width and wetted perimeter. The bed slope generally had the lowest values in 2012. The range of decrease is between 0.00003 and 0.00005. Subreach I2 exhibits a spike up or down for each of the parameters because it has a different geometry than the other subreaches.

3.8. Channel Response Models: Schumm's (1969) river metamorphosis

Schumm (1969) suggested the following dynamic responses of a channel to changes in water and sediment discharges.

$$Q_t^+ \sim W^+ h^- P^- L^+ S^+$$

$$Q^+ \sim W^+ h^+ L^+ S^-$$

$$Q^- Q_t^- \rightarrow W^- h^\pm F^- L^- S^\pm P^+$$

where Q is the flow discharge, Q_t is the percentage of the total sediment load transported as bedload, W is the channel top width, h is the flow depth, L is the meander wavelength, F is the width-depth ratio, S is the slope, and P is the sinuosity. The exponent, expressed as either a plus or minus, indicate whether the dimensions of the variables are increasing or decreasing.

Schumm's river metamorphosis model suggests qualitative changes in hydraulic geometry from a general decrease in water discharge and bed material load in Sections 2.2 and 2.3. Although some subreaches could not be evaluated by the model, overall the model suggests a response summarized in Table 8.

Table 8: Analysis of channel responses to water and sediment discharge based on the Schumm's model

Year	Subreach	W	h	S	F	P	Schumm's model
1972-1992	I1	-	+	-	-	+	$Q^- Q_t^-$
	I2	-	+	+	-	-	N/A
	I3	-	+	-	-	+	$Q^- Q_t^-$
	I4	-	+	+	-	+	$Q^- Q_t^-$
	I5	-	+	+	-	-	N/A
	I6	-	+	+	-	+	$Q^- Q_t^-$
1992-2002	I1	-	-	-	+	+	N/A
	I2	-	-	+	-	+	$Q^- Q_t^-$
	I3	-	-	-	-	+	$Q^- Q_t^-$
	I4	-	-	-	-	+	$Q^- Q_t^-$
	I5	-	-	-	-	+	$Q^- Q_t^-$
	I6	-	-	-	-	+	$Q^- Q_t^-$
2002-2012	I1	-	+	+	-	-	N/A
	I2	-	+	-	-	+	$Q^- Q_t^-$
	I3	-	+	+	-	+	$Q^- Q_t^-$
	I4	-	+	-	-	-	N/A
	I5	-	+	+	-	-	N/A
	I6	-	+	+	-	-	N/A

3.9. Equilibrium Width Predictors

The downstream hydraulic geometry of rivers was derived by Julien and Wargadalam (1995):

$$h = 0.2Q^{\frac{2}{6m+5}} d_s^{\frac{6m}{6m+5}} S^{\frac{-1}{6m+5}}$$

$$W = 1.33Q^{\frac{4m+2}{6m+5}} d_s^{\frac{-4m}{6m+5}} S^{\frac{-1-2m}{6m+5}}$$

$$V = 3.76Q^{\frac{2m+1}{6m+5}} d_s^{\frac{-2m}{6m+5}} S^{\frac{2m+2}{6m+5}}$$

where $m = 1/\ln(12.2\, h/d_s)$, h is the flow depth, W is the channel width, V is the velocity, Q is the flow discharge, d_s is the median grain size, and *S* is the slope. A discharge of 3,000 cfs, same as the HEC-RAS analysis, is used in order to compare the results to field observation. The values of grain size and slope are obtained from previous sections. The mean d_{50} of 1990s is used for 1992, 2000s for 2002, and so forth. The measured and predicted width can be found in Table 9. The method of Julien and Wargadalam predicts a channel equilibrium width between 216 to 225 feet, which is narrower than the observed channel widths for all subreaches and all years. This corroborates the observed channel width decrease noted in Section 3.2.

Table 9: Input and Output for Julien and Wargadalam's equations

Year	Subreach	Q (cms)	ds (mm)	Slope	Observed width (ft)	Predicted Width (ft)
1992	I1	85	0.41	0.000862	467	220
	I2	85	0.39	0.000847	550	221
	I3	85	0.36	0.000761	518	226
	I4	85	0.32	0.000802	517	224
	I5	85	0.24	0.000747	517	228
	I6	85	0.3	0.000843	520	222
2002	I1	85	3	0.000831	456	222
	I2	85	0.87	0.000851	517	220
	I3	85	2.9	0.000744	494	224
	I4	85	9.74	0.000726	493	222
	I5	85		0.000731	495	
	I6	85	5.52	0.000764	501	221
2012	I1	85	0.4	0.000834	320	222
	I2	85	0.54	0.000832	400	222
	I3	85	0.42	0.000749	343	227
	I4	85	0.44	0.000713	344	229
	I5	85	0.44	0.000830	345	222
	I6	85	0.4	0.000765	337	226

3.10. Geomorphic Conceptual Model

Massong et al. (2010) developed a channel planform evolution model for the Rio Grande based on historic observations. The sequence of the planform evolution is outlined in Figure 38. Stage 1 describes a large channel with a high sediment load and frequent floods such that a wide, clear channel is maintained. As water levels fall, Stage 2 occurs and dunes from Stage 1 begin to stabilize into bars. In Stage 3, this stabilization is maintained by encroaching vegetation, regardless of flow levels. Only after the third stage does sediment transport become important in determining future stages. A lack of transport capacity leads to avulsion, as the channel aggrades and eventually the main flow shifts on to the now lower floodplain, progressing to the A (aggrading) stages. Excessive transport capacity leads to the M (migrating) stages. Bends occur where bed and bank material erode both laterally and vertically. Transition between the M stages and the A stages can occur, however, a reset to Stage 1 requires a large, prolonged flood event (Massong et al., 2010). The gold color represents sand bars, while green represents vegetated bars.

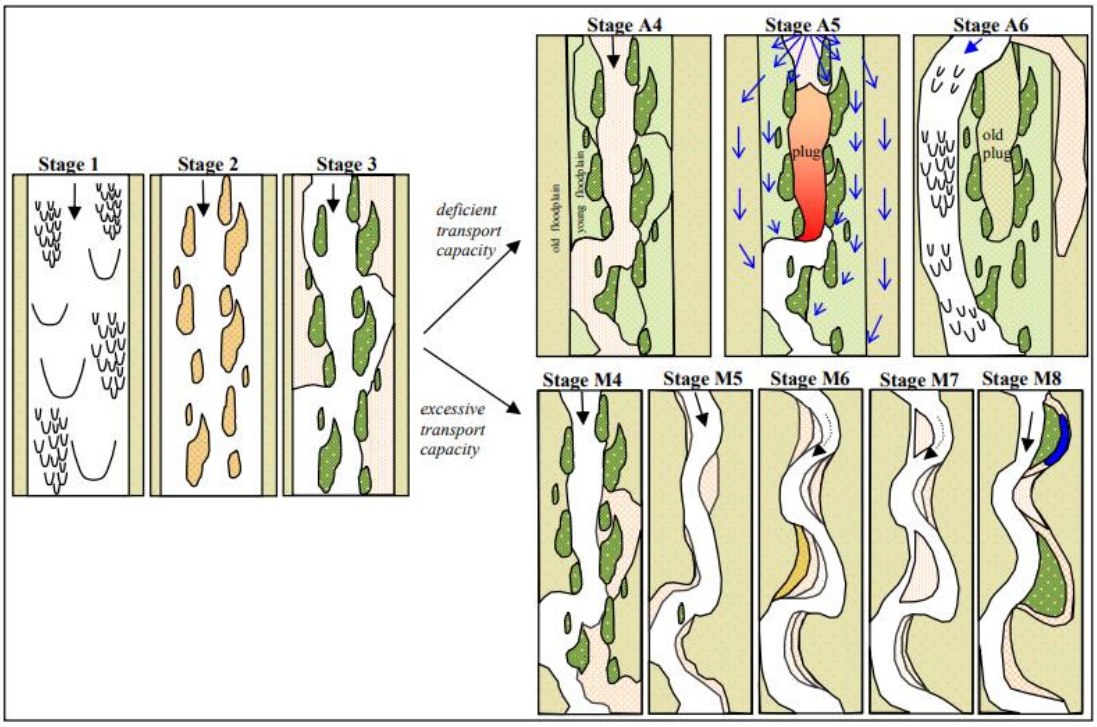

Figure 38: Planform evolution model from Massong et al. The river undergoes stages 1-3 first and then A4-A6 or M4-M8 depending on the transport capacity.

Stages M4-M8 are the most relevant to the Isleta Reach because it has an excessive transport capacity (Massong et al. 2010). The transition between Stage 1 and 2 occurred on much of the Middle Rio Grande from 1999-2004, during a long period of drought with minimal spring peak flows. During this time, considerable vegetation encroachment was also seen. In 2005, high

peak flows returned, but the bars were sufficiently stabilized to avoid a return to Stage 1. High water levels allowed vegetation to flourish, thus forming Stage 3 (Massong et al. 2010). The latest classification of the Isleta reach has been M5 and has undergone various stages since the early 1900s. USBR assigned planform stages to the Isleta reach over multiple years based on aerial photography in their report from 2018. Their results are shown in Table 10.

Table 10: Planform classification by stages (Klein et al., 2018a).

Years	Massong et al. (2010)	Schumm (1969)
1918	2	3
1935	1	3
1949	2	3
1962	3	2
1972	3	2
1985	3	8/9
1992	3	8
2002	3	9
2012	M4	8
2016	M5	7

Using these years of data and the classification from Massong et al. (2010), a conceptual model was considered. The intent is to understand how the river is changing and predict future planform of the river. The model is formed from a plan view and cross-sectional view of a typical cross-section and presented with the stages assigned by Klein et al. (2018a). The evolution of cross-section is evaluated by two randomly chosen agg/deg lines 658 and 939 (Figures 39 to 45). The planview was obtained using GIS, with HEC-RAS cross-section data.

The conceptual model only dates back to 1962 for the following reasons. Although cross section data and aerial photographs were available before 1962, agg/deg cross-sections can be difficult to identify before 1962 because the surveys were not consistent between the earlier years. This may be due to the agg/deg lines being established in 1962 (Posner 2017).

Comparisons of cross-sections from 1962 to 2016 can be found in Figures 39 and 40. The 2016 cross-section data were acquired from AutoCAD from rangeline IS-658 and CC-939, as shown in Figures 41-44. Over time the active channel has become narrower and more incised. This makes sense as the stages progress from Stage 3-M5 and become more of a narrow, single-threaded channel. The active channel width is based on planforms provided by USBR in GIS, and they may differ based on the flow when the photograph was taken. For instance, 1992, 2002, and 2012 are all around 650 cfs. 1972 is around 5 cfs and 2016 is at 40 cfs. The flow in 1962 is also about 650 cfs (Swanson et al. 2010). Based on observed trend, typical cross-sectional views with their corresponding stages are present in Figure 45.

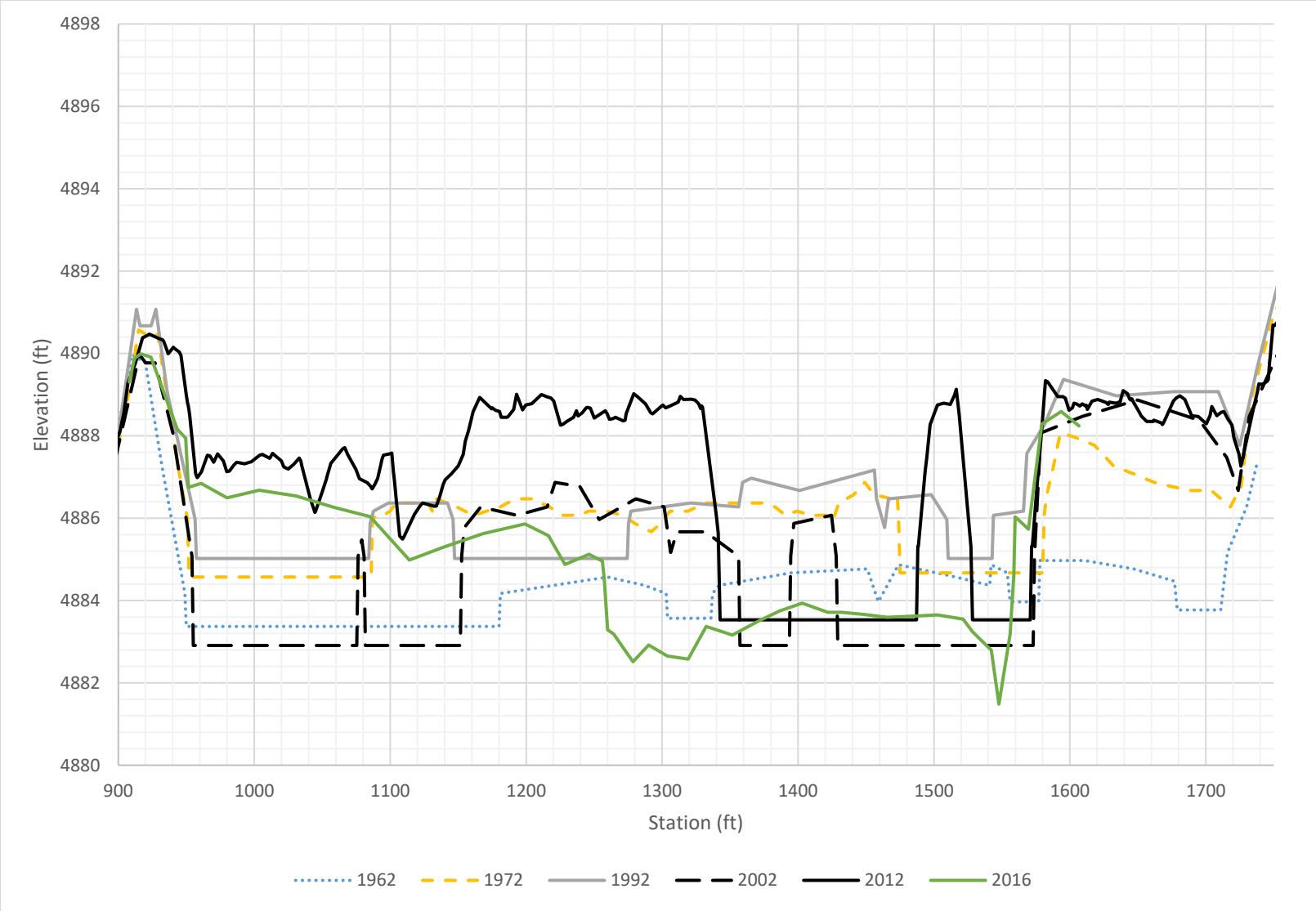

Figure 39: Comparison of cross-section 658 from 1962-2016. The corresponding stage can be found in Table 10.

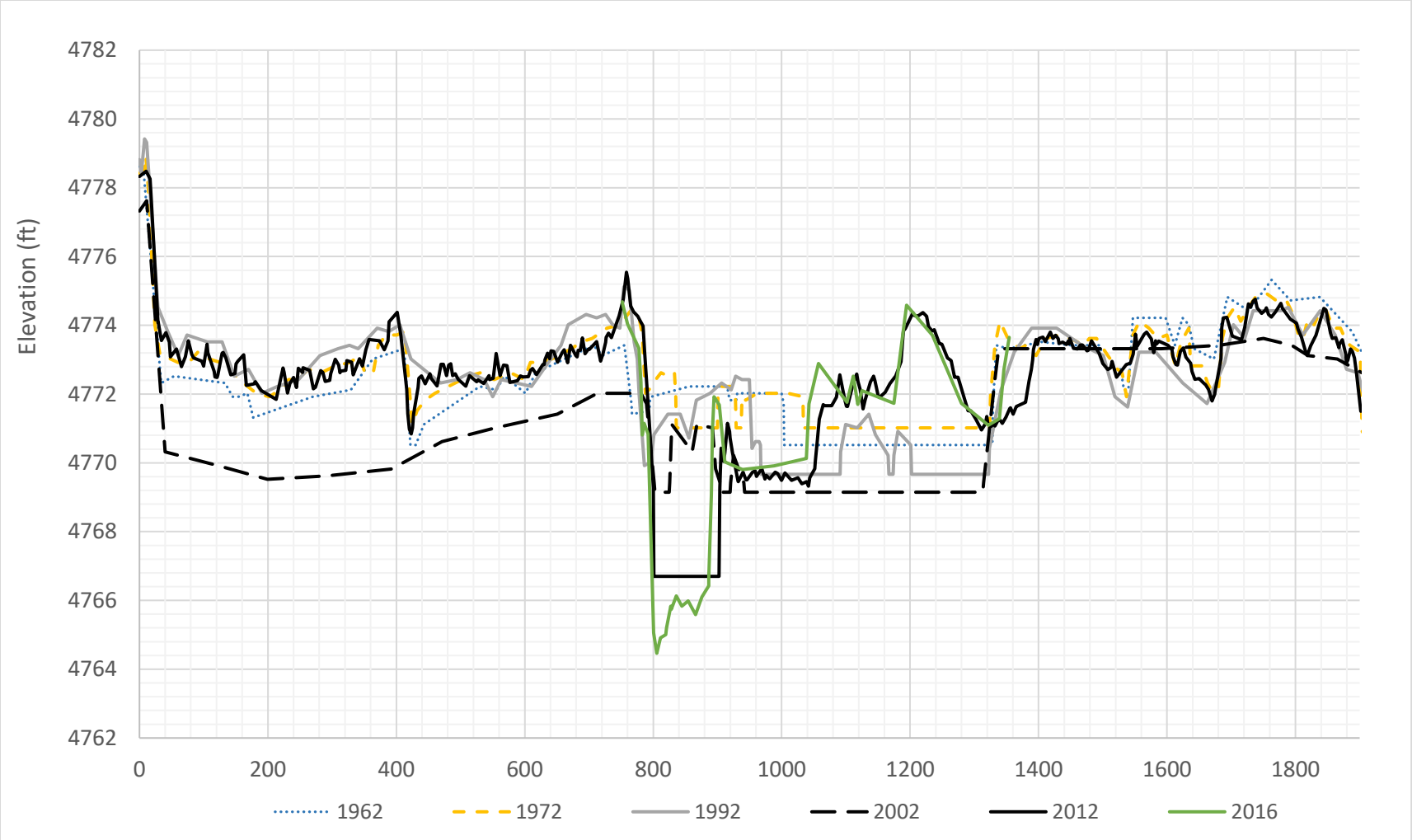

Figure 40: Comparison of cross-section 939 from 1962-2016.

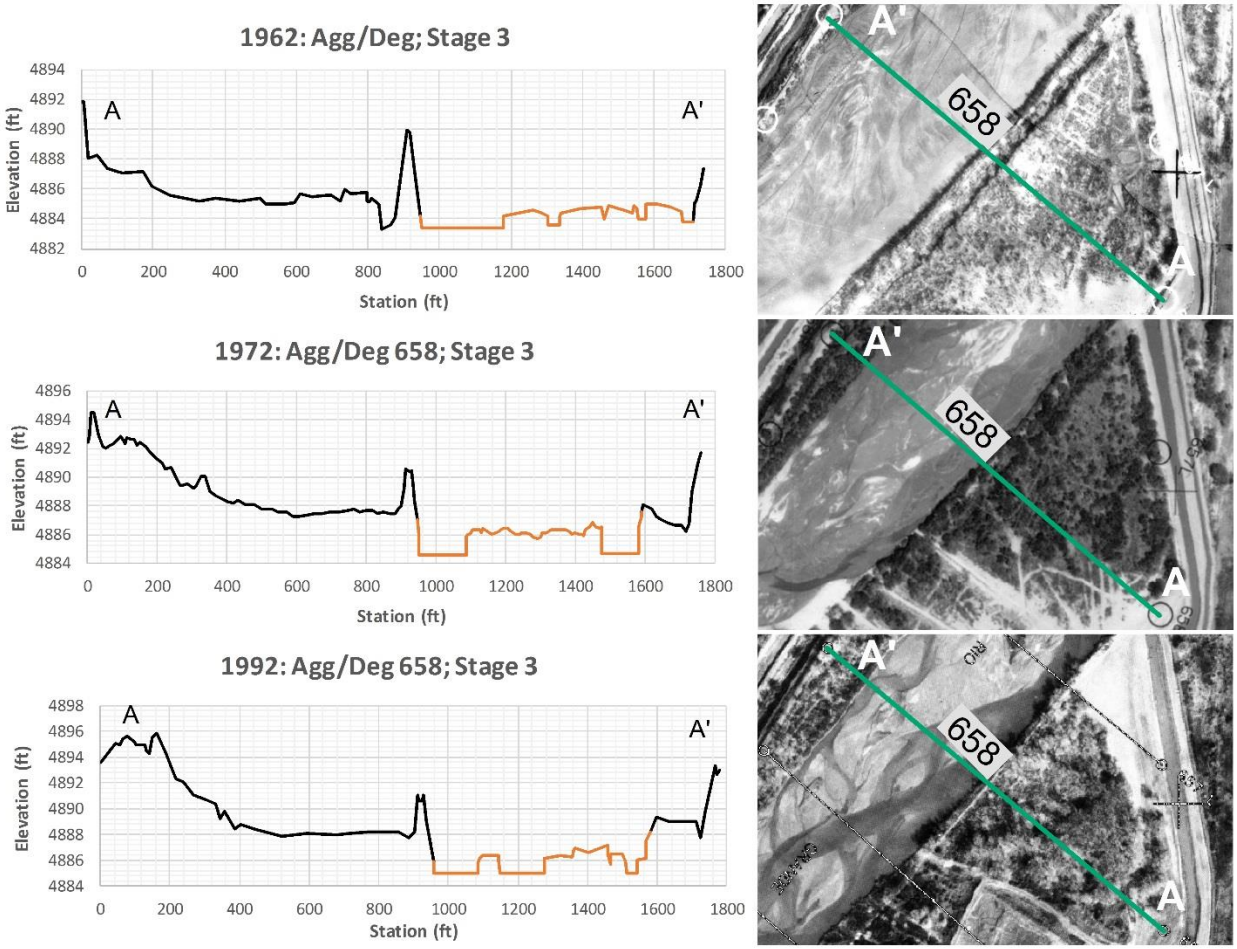

Figure 41: 1962, 1972, and 1992 cross-section 658 and planform views (planform to the right of each corresponding year). A denotes the left bank and A' denotes the right bank. The active channel is in orange the stage is denoted at the top of the graph.

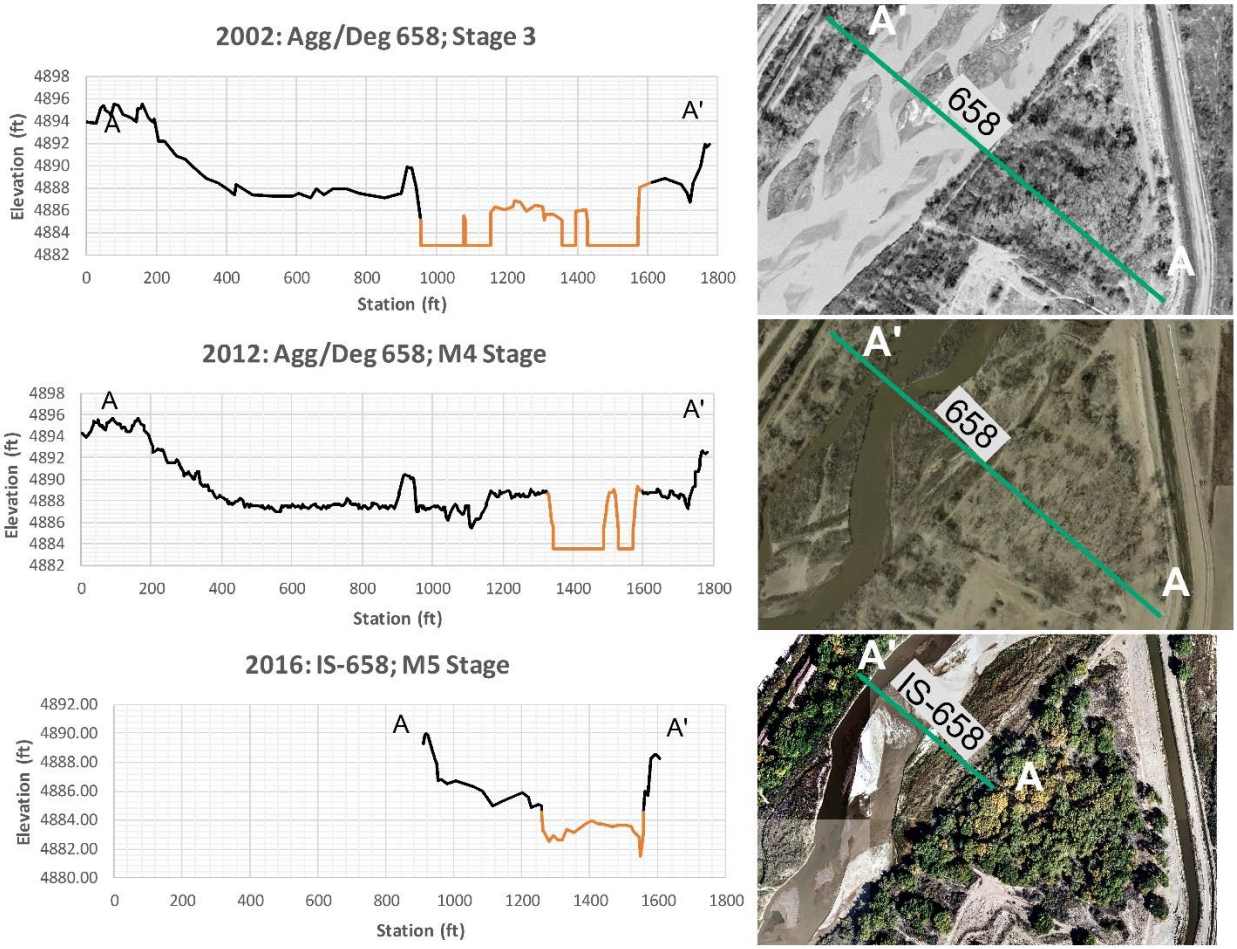

Figure 42: 2002, 2012, and 2016 cross-section 658 and planform views (planform to the right of each corresponding year). A denotes the left bank and A' denotes the right bank. The active channel is in orange the stage is denoted at the top of the graph.

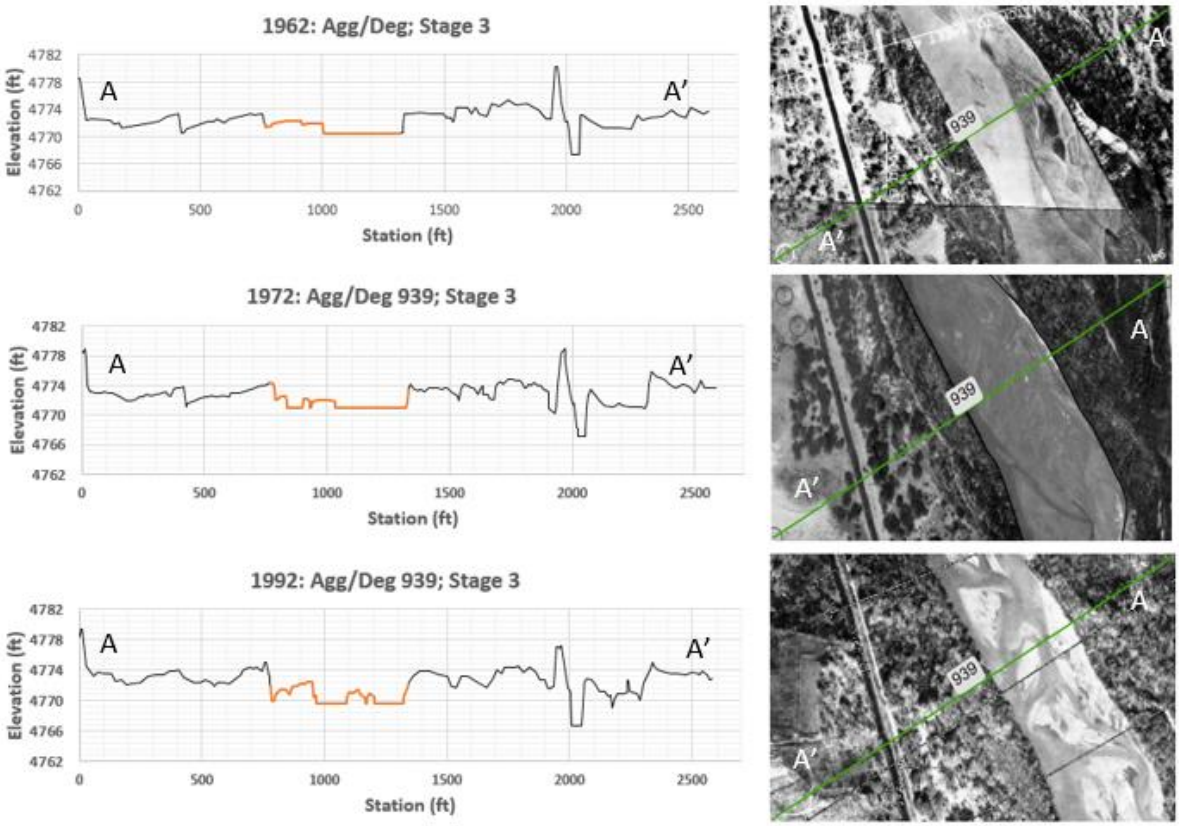

Figure 43: 1962, 1972, and 1992 cross-section 939 and planform views (planform to the right of each corresponding year). A denotes the left bank and A' denotes the right bank. The active channel is in orange the stage is denoted at the top of the graph.

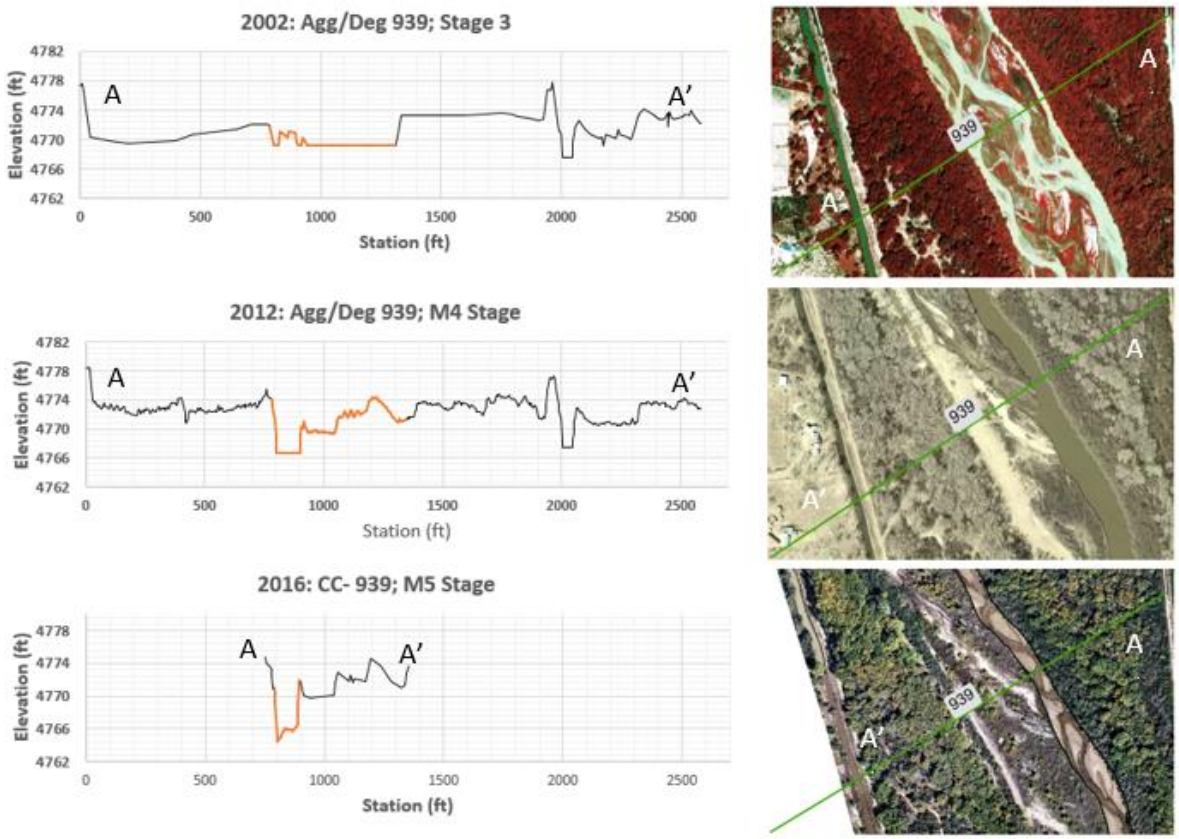

Figure 44: 2002, 2012 and 2016 cross-section 939 and planform views (planform to the right of each corresponding year). A denotes the left bank and A' denotes the right bank. The active channel is in orange and the stage is denoted at the top of the graph.

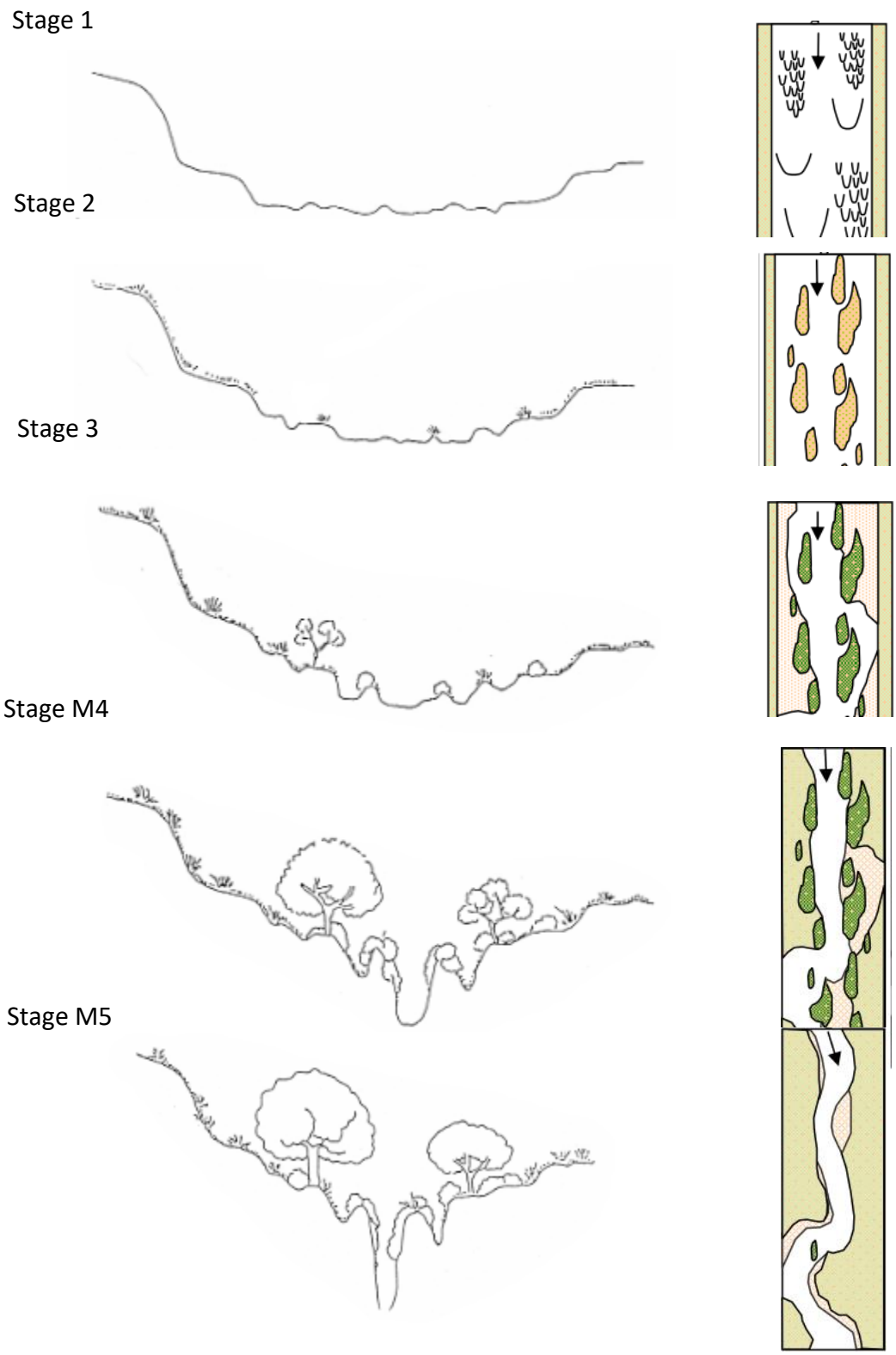

Figure 45: Cross-section view of the channel evolution model for stage 1, 2, 3, M4, and M5. (From Rozin and Schick, 1996)

4. Using HEC-RAS and GIS Analysis for Silvery Minnow Habitat

The potential for using HEC-RAS in combination with aerial photography in GIS is explored for a quantitative determination of the RGSM habitat quality. The preliminary analysis includes a set of three different discharges representing low, medium and high flow conditions, as well as three different hydraulic geometries as described from HEC-RAS files at three different decades (1992, 2002 and 2012).

4.1. Importance of the Rio Grande Silvery Minnow

Dams, levees, and channelization of the river have created an unhealthy riparian system and have led to an overall decline in ecological health of the Middle Rio Grande (U.S. Fish and Wildlife Service 2007; Marshall 2015). The silvery minnow is an indicator of the decline (Russo 2018). Silvery minnows became an endangered species in 1994 and currently, the silvery minnow occupies about only seven percent of its historic range (U.S. Fish and Wildlife Service 2010). It is believed to only occur in the Middle Rio Grande from Cochiti Dam to Elephant Butte Reservoir (Bestgen and Platania 1991; Dudley et al. 2005). The Isleta Reach falls inside of this range. Because silvery minnows are an indicator of the health of the river, great efforts are deployed to protect them.

The most important aspect of silvery minnow habitat is the connection of the main channel to the floodplain (Scurlock 1998; Cowley 2002; U.S. Fish and Wildlife Service 2010; Medley and Shirley 2013; Tetra Tech 2014; Dudley et al. 2016). Silvery minnow spawning is stimulated by peak flows in late April to early May. Ideally, these create shallow water conditions on floodplains, which are ideal nursery habitat for the silvery minnow (Mortensen et al. 2019). Peak flows that can inundate large areas of floodplains are essential to the recovery of silvery minnow populations. In-stream characteristics are also important. Silvery minnows most commonly occupy habitats with debris piles, pools and backwater. They thrive in mostly silt substrate and require low velocities and moderate depths, with slightly different requirements for juveniles and adults (Dudley and Platania 1997).

Dams, levees and diversion structures have heavily impacted the hydraulics and fluvial processes of the river. Sediment size has gone up overall, the floodplain is less connected than it has been in the past, water quality has decreased, and the river has become fragmented by dams (Osborne et al. 2012; Larsen 2007). These factors all decrease the habitat quality of silvery minnows. This is evident when looking at the decline of silvery minnow genetic diversity, densities, catch rates, and habitat range (Horner 2016). To prevent the silvery minnow from going extinct, we must study the river processes, understand how this impacts the ecological health of the system, and how to improve it. Looking at smaller scales such as reaches and subreaches may offer insight into how the rivers and minnows interact.

4.2. Relation between Flow and Population of RGSM

According to Dudley et al. (2016), the population of RGSM is "closely related to the timing, magnitude, and duration of flows in spring and summer". Figure 46 shows the relation between the population density of RGSM, spring peak discharge, annual mean discharge, and occurrence of flow higher than 2000 cfs at Albuquerque. Fish populations are positively correlated with the magnitude of the spring peak flow and the number of days with a flow exceeding 2000 cfs.

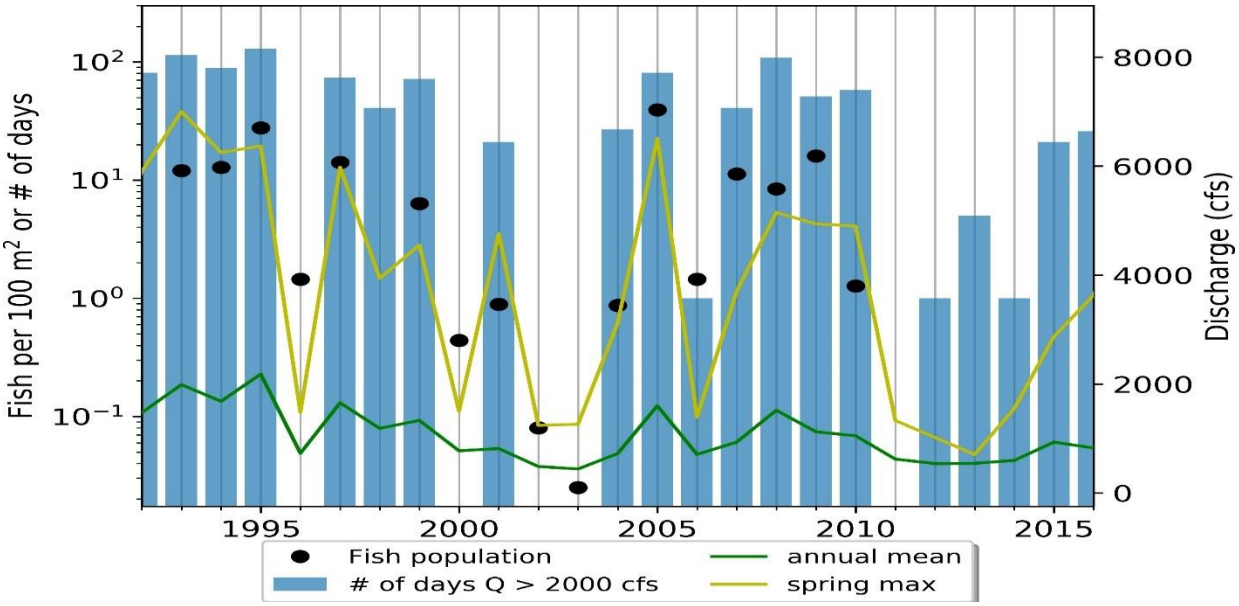

Figure 46: Population of silvery minnow vs annual mean discharge vs spring peak flow vs number of days that discharge is greater than 2000 cfs.

Figure 47 shows the scatter plots of fish population vs spring peak discharge and fish population vs number of days that discharge is higher than 2000 cfs.

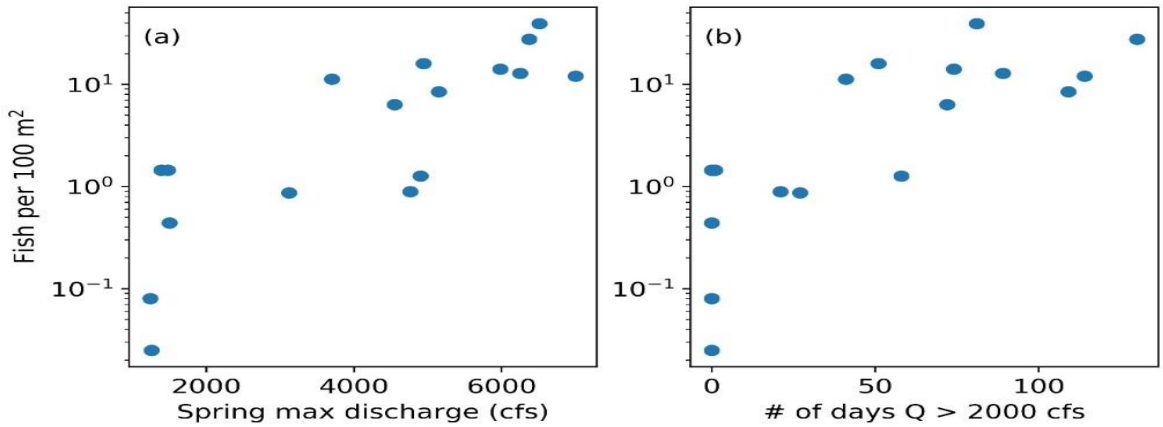

Figure 47: (a) Fish population density vs spring peak discharge, and (b) Fish population density vs number of days discharge is higher than 2000 cfs.

4.3. HEC-RAS

HEC-RAS models were set up for the Isleta reach at three different discharges (600 cfs, 1400 cfs and 3500 cfs). Certain depths and velocities are ideal for the minnows at various stages of their life cycle. A model allows one to find the percentage of area in a reach that matches these ideal flow characteristics. This can give a general estimate of the suitability of a reach for the RGSM. For more information on how this was performed, please see Appendix B and C – HEC-RAS Silvery Minnow Hydraulic Modeling.

Detailed HEC-RAS simulations are shown in Appendices B and C. For instance, Figure 48 shows that the best "spawning" and "feeding/rearing" habitats are at 3500 cfs (compared to 600 and 1400 cfs). These habitats tend to occur in subreaches I1, I2 and I3 due to better floodplain connectivity. The area of "good" habitat within the river is greatest at low flows of 600 cfs for subreaches I1-I4. The "good" habitat area also decreases from 1992 to 2012.

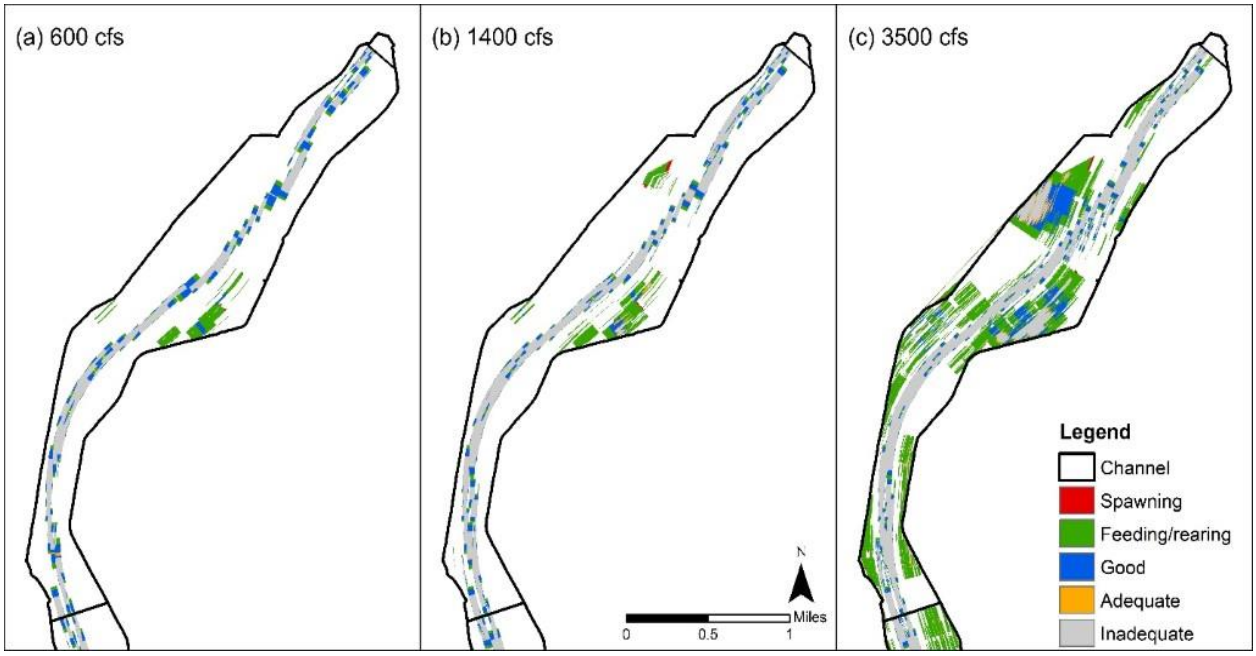

Figure 48: Hydraulic habitat at subreach I1 at flow rate 600, 1400, and 3500 in 2012

4.4. GIS (Aerial Photograph) Analysis

Aerial photographs provided by the USBR were analyzed for the RGSM habitat characteristics. Certain types of river features, such as shoreline complexity, bars, backwater, islands, and channels provide acceptable habitat for the RGSM. Each of these features can be assigned a numerical score, depending on complexity and type. By quantifying these points with in a reach and calculating their density between agg/deg lines, a measure of a reach's habitat suitability for the RGSM can be calculated. For more information on how this was performed, please see Appendix D and E – Silvery Minnow Habitat Scoring System.

For the GIS analysis in Appendices F-J, the best scores are found in earlier years or when the flow is high enough to inundate the floodplain (>3500 cfs). Subreaches I2 – I4 have the highest scores when comparing all years. By comparing the aerial photographs that were taken under similar flow conditions (~600 cfs), it shown in Figure 49 that subreaches I1 – I4 have the best habitat score. Similar results for all years are shown in Figure 50. The shoreline complexity was also analyzed with GIS. It does not have a consistent pattern over the years, but the highest score was found in 2005 with the flow just under 6000 cfs.

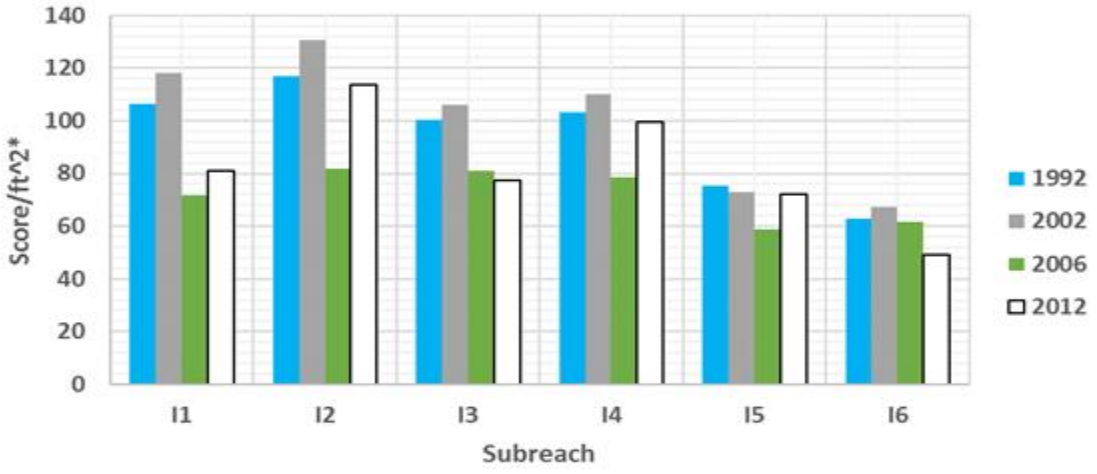

Figure 49: The column graph shows the overall habitat scores in each of the four comparable years in each subreach.

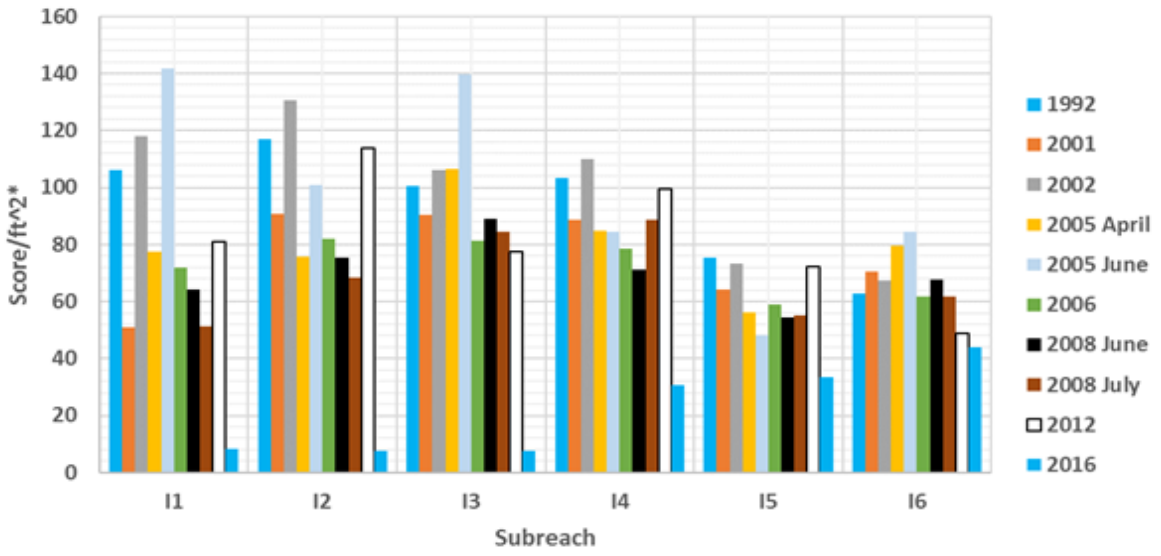

*Figure 50: The column graph shows the overall score in every year in each subreach. * Score/ft^2 is the score weighted for area of the subreach.*

A summary of all the habitat scores is presented in Table 11. It shows that the total habitat score is not always the highest at high flows, although the lowest score is at the lowest discharge. Also, under similar discharge, the score between different categories can change significantly.

Table 11: Summary of total habitat score, flows, and number of habitat types for each year. The comparable years are highlighted in blue.

				Shoreline Complexity			Main Channel Complexity		Side Channels					Backwater		Bars			Islands						Confluences	
Year	Month	Total Habitat Score	Flow (cfs)	1a	1b	1c	2a	2b	3a	3b	3c	3d	3f	4a	4b	5a	5b	5c	6a	6b	6c	6d	6e	6f	7a	7b
1992	February	4025	650[SA]	23	6	7	85	88	0	3	1	211	184	9	7	42	103	58	3	0	11	2	180	147	0	1
2001	February	3300	687[A]	26	6	0	125	103	0	0	3	111	111	1	1	45	26	8	5	6	26	8	216	83	1	1
2002	February	4335	600[SA]	17	10	0	153	45	0	10	4	181	142	3	12	73	158	28	19	7	16	16	293	45	0	0
2005	April	3447	4500[I]	138	16	5	168	59	8	2	4	84	84	2	0	101	8	0	0	1	0	10	118	81	3	0
2005	June	4395	5980[I]	340	8	1	55	50	8	16	7	64	128	16	2	140	23	0	0	9	5	24	147	79	1	1
2006	January	3081	580[SA]	45	33	2	42	76	8	75	3	124	65	21	14	24	140	33	6	2	16	7	156	56	2	1
2008	June	3050	4990[I]	81	9	0	30	22	0	0	1	193	39	8	1	143	16	1	0	33	0	33	148	82	2	0
2008	July	2905	1630[I]	38	35	11	7	35	7	31	24	165	123	12	8	17	40	13	3	109	9	54	128	45	1	1
2012	January	3501	740[SA]	65	35	5	68	57	23	146	11	82	89	6	5	43	79	29	14	58	19	35	135	76	2	0
2016	October	719	40[SA]	16	9	9	11	25	0	7	0	33	10	4	4	7	32	41	5	12	36	3	10	3	0	6

Note: Flows at different gages are given the follow subscripts: [I] Isleta gage daily average discharge, [SA] San Acacia gage daily average discharge, [A] Albuquerque gage daily average discharge

4.5. Combined HEC-RAS and Aerial Photograph Analysis

Ultimately, HEC-RAS and visual observations of aerial photographs with GIS were used to assess the habitat conditions in 1992, 2002, and 2012. All the results are shown in Appendices K and L and are briefly summarized here. It is found that subreaches I1-I3 have the best habitat and the overall habitat quality declines from 1992 to 2012. The decrease in habitat quality is likely due to: (1) a reduction in the frequency and magnitude of peak discharges; and (2) the channel narrowing and incising causing a loss of connectivity to the floodplain. For example, the summary of the combined analysis for Subreach I-1 is shown in Figure 51.

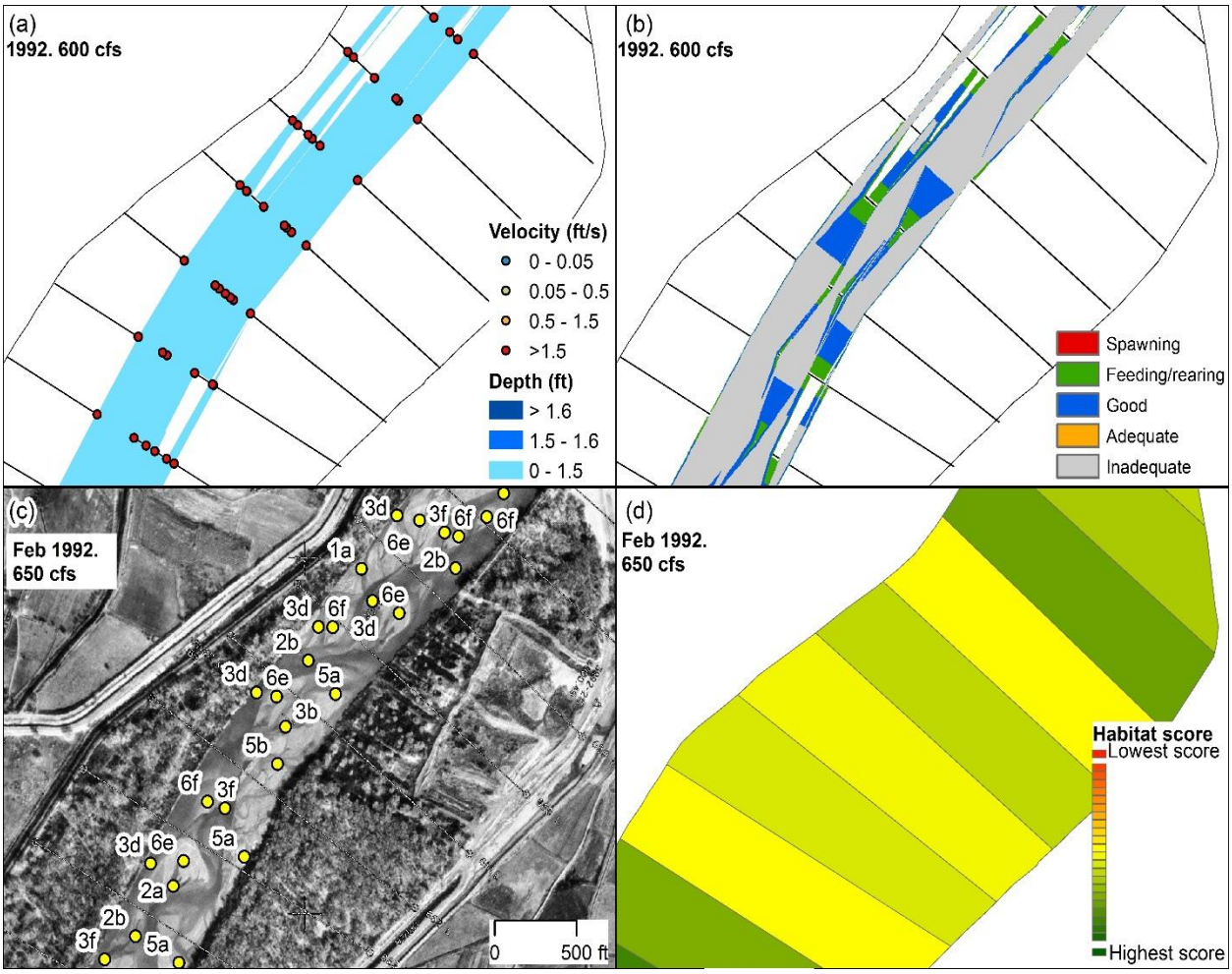

Figure 51: Summary of HEC-RAS and GIS habitat at subreach I1, agg-deg 657 to 665. (a) Velocity and depth of the simulation. (b) Habitat criteria mapped based on velocity and depth. (c) Habitat features mapped out by points and letters. (d) Habitat color scheme based on habitat features.

5. Conclusions

The Isleta reach was analyzed for hydrologic, hydraulic and geomorphic trends between 1918 and 2017. This reach covers about 42 miles from the Isleta Diversion Dam to the confluence with the Rio Puerco.

Hydrologic and hydraulic trends were based on past reports (recently compiled by Klein et al. 2018), but our analysis has been extended from 2014 until 2017 whenever data were available. HEC-RAS and GIS were used to find the geomorphic and river characteristics such as sinuosity, width, multiple channels, bed elevation, volume change, and other hydraulic parameters. These analyses were broken into six subreaches which enabled detailed results on a smaller scale. A conceptual geomorphic analysis also provides a schematic of prospective river changes.

The major findings include the following:

- The annual water volume has been reduced recently (since the 2000s). Peak discharges have become less frequent, shorter and have decreased in the past few decades.
- The annual suspended sediment discharge in the Rio Grande and Rio Puerco have decreased since the 1970s, although the average suspended sediment concentration increased after 1993.
- The predominant sediment size moving through the reach is sand, and finer material such silts and clay make up less of the total sediment load.
- The measured sediment load exceeds 80% of the total sediment load when the flow depth is larger than 5 ft.
- In most subreaches the flow depth, velocity, grain size and sinuosity increased. The wetted perimeter, energy slope and bed slope decreased.
- A conceptual geomorphic model shows the channel is becoming more incised and less connected to its floodplain.

A summary of a combined HEC-RAS and aerial photography analysis is presented here with ample details in Appendices B to L. Preliminary results on a HEC-RAS simulation for three different geometries and three different discharges characterize the RGSM habitat. Conditions favorable to “spawning”, “feeding/rearing”, or “good” habitat were identified. A GIS analysis of aerial photography was used to map habitat types and quality over different decades and over a range of discharges from 40 to 5980 cfs. This work deserves further consideration as it shows considerable potential for use in a later process linkage report.

References

Baird, D. (2014). *Historical Rio Grande Channel Width Design Literature Review Summary*, U.S. Department of the Interior, Bureau of Reclamation, Technical Services Center, Sedimentation and River Hydraulics Group. Denver, CO, 42 p.

Baird, D. C. (2016). *Rio Grande Silvery Minnow Habitat Restoration Design Review*, Department of the Interior, Bureau of Reclamation, Technical Services Center, Sedimentation and River Hydraulics Group. Denver, CO.

Bauer, T.R. (2000). *Morphology of the Middle Rio Grande from Bernalillo Bridge to San Acacia Diversion Dam, New Mexico*, Colorado State University, Fort Collins, CO.

Bauer, T.R. (2009). *Sediment Evolution on the Middle Rio Grande, New Mexico*, U.S. Department of the Interior, Bureau of Reclamation, Technical Services Center, Sedimentation and River Hydraulics Group. Denver, CO. 36 p.

Bauer, T.R. and Hilldale, R. (2006). *Sediment Model for the Middle Rio Grande – Phase 2: Isleta Diversion Dam to San Acacia Diversion Dam*. U.S. Department of the Interior, Bureau of Reclamation, Technical Services Center, Sedimentation and River Hydraulics Group. Denver, CO, 295 p.

BEMP Data (2017). *BEMP Database: Precipitation 1997-2017*. From Bosque Ecosystem Monitoring Program, BEMP, University of New Mexico, Albuquerque, NM. Online: http://bemp.org/data-sets/ Accessed on March 19, 2019.

Berry, K. L. and Lewis, K. (1997). *Historical Documentation of Middle Rio Grande Flood Protection Projects, Corrales to San Marcial*. Office of Contract Archeology, University of New Mexico, Albuquerque, NM.

Bestgen, K. R., Mefford, B., Bundy, J., Walford, C., Compton B., Seal S., and Sorensen T. (2003). *Swimming Performance of Rio Grande Silvery Minnow,* Final Report to U.S. Bureau of Reclamation, Albuquerque Area Office, New Mexico. Colorado State University, Larval Fish Laboratory Contribution 132, 70 p.

Bestgen, K.R., and Platania S.P. (1991). *Status and Conservation of the Rio Grande Silvery Minnow, Hybognathus Amarus*, The Southwestern Naturalist, 36 (2), 225-232

Bovee, K.D., Waddle, T.J., and Spears, J.M. (2008). *Streamflow and Endangered Species Habitat in the Lower Isleta Reach of the Middle Rio Grande*, U.S. Geological Survey Open-File Report 2008-1323.

Cluer, B., and Thorne, C. (2014). *A Stream Evolution Model Integrating Habitat and Ecosystem Benefits*, River Research and Applications, 30(2), 135–154.

Cowley, D.E. (2002). *Water Requirements for Endangered Species- Rio Grande Silvery Minnow (Hybognathus Amarus),* New Mexico Water Resources Research Institute, 97-107

Crawford, C. S., Cully, A. C., Leutheuser, R., Sifuentes, M. S., White, L. H., and Wilber, J. P. (1993). *Middle Rio Grande Ecosystem: Bosque Biological Management Plan*, Middle Rio Grande Biological Interagency team, Albuquerque, NM, 320p.

Culbertson, J. K., and Dawdy, D. R. (1964). *A Study of Fluvial Characteristics and Hydraulic Variables, Middle Rio Grande, New Mexico,* U.S. Geological Survey, Professional Paper 1498-F, Washington, D.C., 82 p.

Dudley, R. K., and Platania, S. P. (1997). *Habitat Use of Rio Grande Silvery Minnow*. Division of Fishes, Museum of Southwestern Biology, Department of Biology, University of New Mexico.

Dudley, R.K., Platania, S.P., and Gottlieb, S.J. (2005). *Rio Grande Silvery Minnow Population Monitoring Program Results from 2004*. American Southwest Ichthyological Research Foundation, Albuquerque, NM, 184 p.

Dudley, R. K., Platania, S. P., and White, G. C. (2016). *Rio Grande Silvery Minnow Population Monitoring Results from February to December 2015*, American Southwest Ichthyological Researchers, LLC, Albuquerque, New Mexico.

Easterling Consultants LLC, and Tetra Tech Inc. (2015). *Geomorphic and Hydraulic Assessment of the Rio Grande from the Rio Puerco to San Acacia Diversion Dam 1998 to 2015*, Middle Rio Grande Project Hydrographic Data Collection, U.S. Bureau of Reclamation, Albuquerque, New Mexico.

Happ, S.C. (1948). *Sedimentation in the Middle Rio Grande Valley, New Mexico,* Bulletin of the Geological Society of America. 59, 1191 – 1216

Holmes, R. and Hayes, J., (2011). *Broad-scale Trout Habitat Mapping for Streams (Using Aerial Photography and GIS)*, Cwathron Report, No. 1979, Nelson, New Zealand, 40 p.

Holmquist-Johnson, C., Raff, D. A., and Russell, K. (2009). *Bureau of Reclamation Automated Modified Einstein Procedure (BORAMEP) Program for Computing Total Sediment Discharge*, User's Manual, Denver, CO

Horner, C. (2016). *Middle Rio Grande Habitat Suitability Criteria*, Colorado State University, Fort Collins, CO.

Klein, M., Herrington, C., AuBuchon, J., and Lampert, T. (2018a). *Isleta to San Acacia Geomorphic Analysis*, U.S. Bureau of Reclamation, Reclamation River Analysis Group, Albuquerque, New Mexico.

Klein, M., Herrington, C., AuBuchon, J., and Lampert, T. (2018b). *Isleta to San Acacia Hydraulic Modeling Report*, U.S. Bureau of Reclamation, Reclamation River Analysis Group, Albuquerque, New Mexico.

Julien, P.Y. (2010). *Erosion and Sedimentation,* 2nd Ed., Cambridge University Press, New York

Julien, P.Y. (2018). *River Mechanics,* 2nd Ed., Cambridge University Press, New York

Julien, P. Y., and Wargadalam, J. (1995). *Alluvial Channel Geometry: Theory and Applications*, Journal of Hydraulic Engineering*,* ASCE, 121(4), 312–325.

Larsen, A. (2007). *Hydraulic Modeling Analysis of the Middle Rio Grande – Escondida Reach, New Mexico*, Colorado State University, Fort Collins, CO.

Makar, P. (2010). *Channel Characteristics of the Middle Rio Grande, New Mexico*. U.S. Department of the Interior, Bureau of Reclamation, Technical Service Center, Denver, CO, 48 p.

Makar, P. and AuBuchon, J. (2012). *Channel Conditions and Dynamics of the Middle Rio Grande*, U.S. Department of the Interior, Bureau of Reclamation, Upper Colorado Region, Albuquerque, NM, 108p.

Marshall, M. (2015). *Earth - What is the Point of Saving Endangered Species?* BBC News, BBC, <http://www.bbc.com/earth/story/20150715-why-save-an-endangered-species> (Jul. 4, 2018).

Massong, T., Paula, M., and Bauer, T. (2010). *Planform Evolution Model for the Middle Rio Grande, NM*, 2nd Joint Federal Interagency Conference, Las Vegas, NV, June 27 - July 1, 2010.

Medley, C. N. and Shirey, P. D. (2013). *Review and Reinterpretation of Rio Grande Silvery Minnow Reproductive Ecology using Egg Biology, Life History, Hydrology, and Geomorphology Information*, U.S. National Park Service Publications and Papers*,* 133.

MEI. (2002). *Geomorphic and Sedimentologic Investigations of the Middle Rio Grande between Cochiti Dam and Elephant Butte Reservoir*, Mussetter Engineering, Inc., Fort Collins, CO, 220 p.

MEI. (2006). *Evaluation of Bar Morphology, Distribution and Dynamics as Indices of Fluvial Processes in the Middle Rio Grande, New Mexico*, Report prepared for the New Mexico Interstate Stream Commission and the Middle Rio Grande Endangered Species Act Collaborative Program.

Mortensen, J.G., Dudley, R.K., Platania, S.P., and Turner, T.F. (2019). *Rio Grande Silvery Minnow Habitat Synthesis,* Draft report, University of New Mexico with American Southwest Ichthyological Researchers, Albuquerque, NM.

Osborne, M. J., Carson, E. W., and Turner, T. F. (2012). *Genetic Monitoring and Complex Population Dynamics: Insights from a 12-year Study of the Rio Grande Silvery Minnow*, Evolutionary Applications, 5(6), 553–574.

Parametrix. (2008). *Restoration Analysis and Recommendations for the Isleta Reach of the Middle Rio Grande, NM*, Parametrix, Inc., Albuquerque, NM, 292 p.

Perschbacher, J. (2011). *The Use of Aerial Imagery to Map In-Stream Physical Habitat Related to Summer Distribution of Juvenile Salmonids in a Southcentral Alaskan Stream*, University of Alaska Fairbanks, Fairbanks, AK.

Posner, A. J. (2017). *Channel Conditions and Dynamics of the Middle Rio Grande River,* Draft Report, U.S. Bureau of Reclamation, Albuquerque, New Mexico.

Richard, G. A. (2001). *Quantification and Prediction of Lateral Channel Adjustments Downstream from Cochiti Dam, Rio Grande*, NM, Colorado State University, Fort Collins, CO.

Richard, G.A., Julien, P.Y. and Baird, D.C. (2005). *Case Study: Modeling the Lateral Mobility of the Rio Grande below Cochiti Dam, New Mexico*, Journal of Hydraulic Engineering, ASCE, 131 (11), 931-941.

Rozin, U. and Schick, A.P. (1996). *Land Use Change, Conservation Measures and Stream Channel Response in the Mediterranean/Semiarid Transition Zone: Nahal Hoga, Southern Coastal Plain, Israel,* Erosion and Sediment Yield: Global and Regional Perspectives, Proc. Exeter Symposium, IAHS Pub. # 236, 1996.

Russo, B. (2018). *An Endangered Fish Out of Water*, Earth Island Journal. News of the World Environment, < http://www.earthisland.org/journal/index.php/elist/eListRead/an_endangered_fish_out_of_water/> (July. 4, 2018)

Schumm, S.A. (1969). *River Metamorphosis*, J. Hydraulics Division, ASCE, 95(1), 255-273.

Scurlock, D. (1998). *From the Rio to the Sierra: an Environmental History of the Middle Rio Grande Basin*, General Technical Report RMRS-GTR-5. Fort Collins, CO: US Department of Agriculture, Forest Service, Rocky Mountain Research Station, 440 p.

Shah-Fairbank, S. C., Julien, P. Y., and Baird, D. C. (2011). *Total Sediment Load from SEMEP using Depth-integrated Concentration Measurements*, Journal of Hydraulic Engineering, ASCE, 137(12), 1606–1614.

Swanson, B., Meyer, G., and Coonrod, J. (2010). *Coupling of Hydrologic/Hydraulic Models and Aerial Photographs through Time, Rio Grande near Albuquerque, New Mexico: Report Documentary 2007 Work*. U.S. Army Engineer Research and Development Center, Vicksburg, MS.

Tashjian, P. and Massong, T. (2006). *The Implications of Recent Floodplain Evolution on Habitat within the Middle Rio Grande, NM*, 2006 Federal interagency Sedimentation Conference, 9 p.

Tetra Tech. (2002). *Development of the Middle Rio Grande FLO-2D Flood Routing Model Cochiti Dam to Elephant Butte Reservoir,* Tetra Tech, Inc. 48 p.

Tetra Tech. (2014). *Ecohydrological Relationships along the Middle Rio Grande of New Mexico for the Endangered Rio Grande Silvery Minnow*. US Army Corps of Engineers, Albuquerque district, Albuquerque, New Mexico, 109 p.

Torres, L.T. (2007). *Habitat Availability for Rio Grande Silvery Minnow (Hybognathus Amarus) Pena Blanca, Rio Grande, New Mexico*, University of New Mexico, Albuquerque, New Mexico.

U.S. Bureau of Reclamation. (n.d.). *Projects and Facilities*, Central Valley Project - Mid-Pacific Region, Bureau of Reclamation, <https://www.usbr.gov/projects/index.php?id=130> (accessed Feb 1, 2019).

U.S. Bureau of Reclamation. (2012). *Middle Rio Grande River Maintenance Program - Comprehensive Plan and Guide*, Albuquerque Area Office, Albuquerque, New Mexico, 202p.

U.S. Fish and Wildlife Service. (2007). *Rio Grande Silvery Minnow (Hybognathus Amarus*), Draft Revised Recovery Plan, Albuquerque, New Mexico, 174 p.

U.S. Fish and Wildlife Service. (2010). *Rio Grande Silvery Minnow Recovery Plan*, First Revision, Southwest Region U.S. Fish and Wildlife Service Albuquerque, New Mexico, 210 p.

Varyu, D. (2013). *Aggradation / Degradation Volume Calculations: 2002-2012*. U.S. Department of the Interior, Bureau of Reclamation, Technical Services Center, Sedimentation and River Hydraulics Group. Denver, CO.

Varyu, D. (2016). *SRH-1D Numerical Model for the Middle Rio Grande: Isleta Diversion Dam to San Acacia Diversion Dam,* U.S. Department of the Interior, Bureau of Reclamation, Technical Services Center, Sedimentation and River Hydraulics Group. Denver, CO.

Yang, C.Y. (2019). *The Sediment Yield of South Korean Rivers*, Ph.D. Dissertation, Colorado State University, Fort Collins, CO.

Yang, C.Y. and Julien, P.Y. (2019). *The Ratio of Measured to Total Sediment Discharge*, International Journal of Sediment Research, 34(3), 262-269.

APPENDIX A

Subreach Delineation

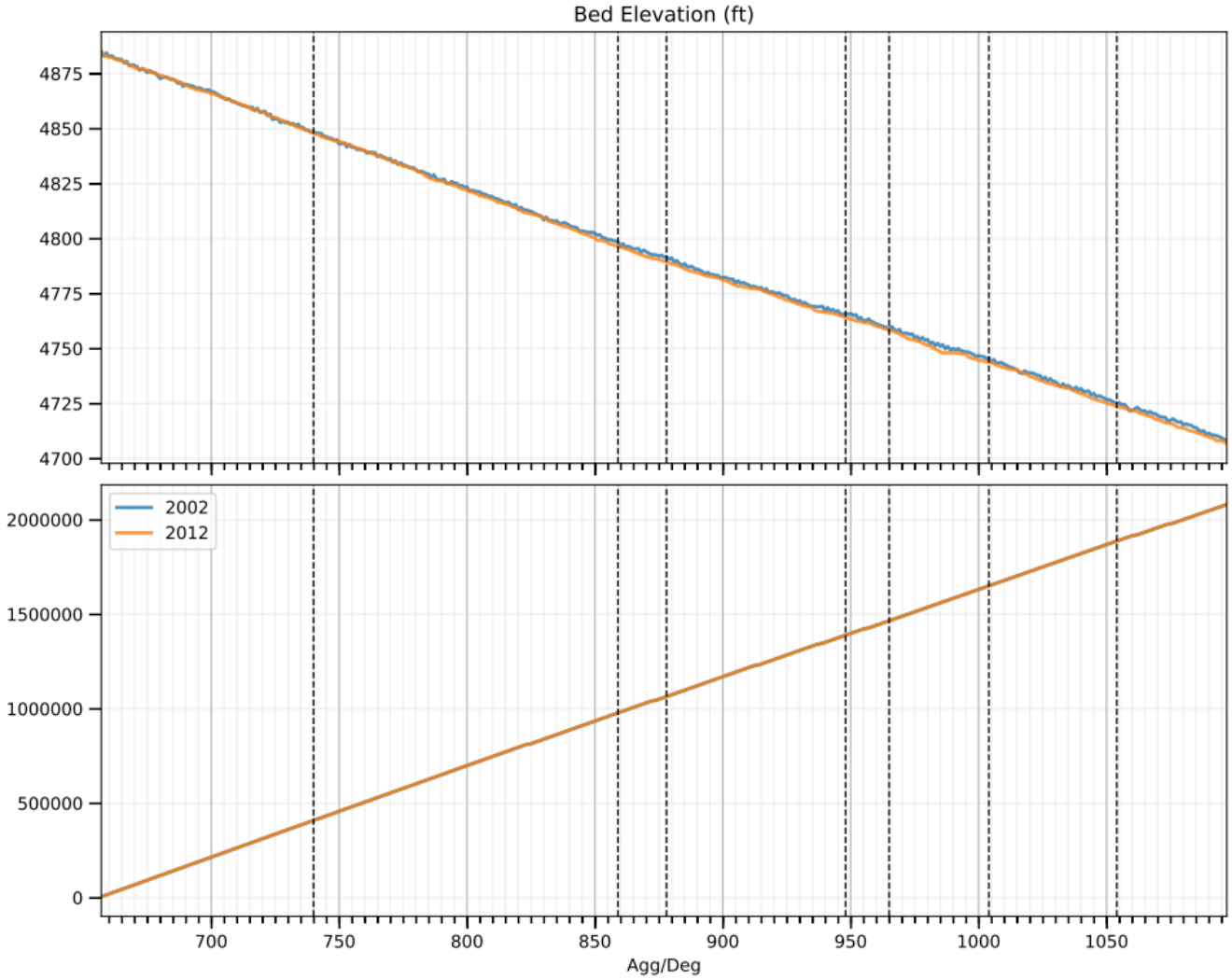
Bed Elevation (ft)
4875
4850
4825
4800
4775
4750
4725
4700
2002
2012
2000000
1500000
1000000
500000
0
700
750
800
850
900
950
1000
1050
Agg/Deg

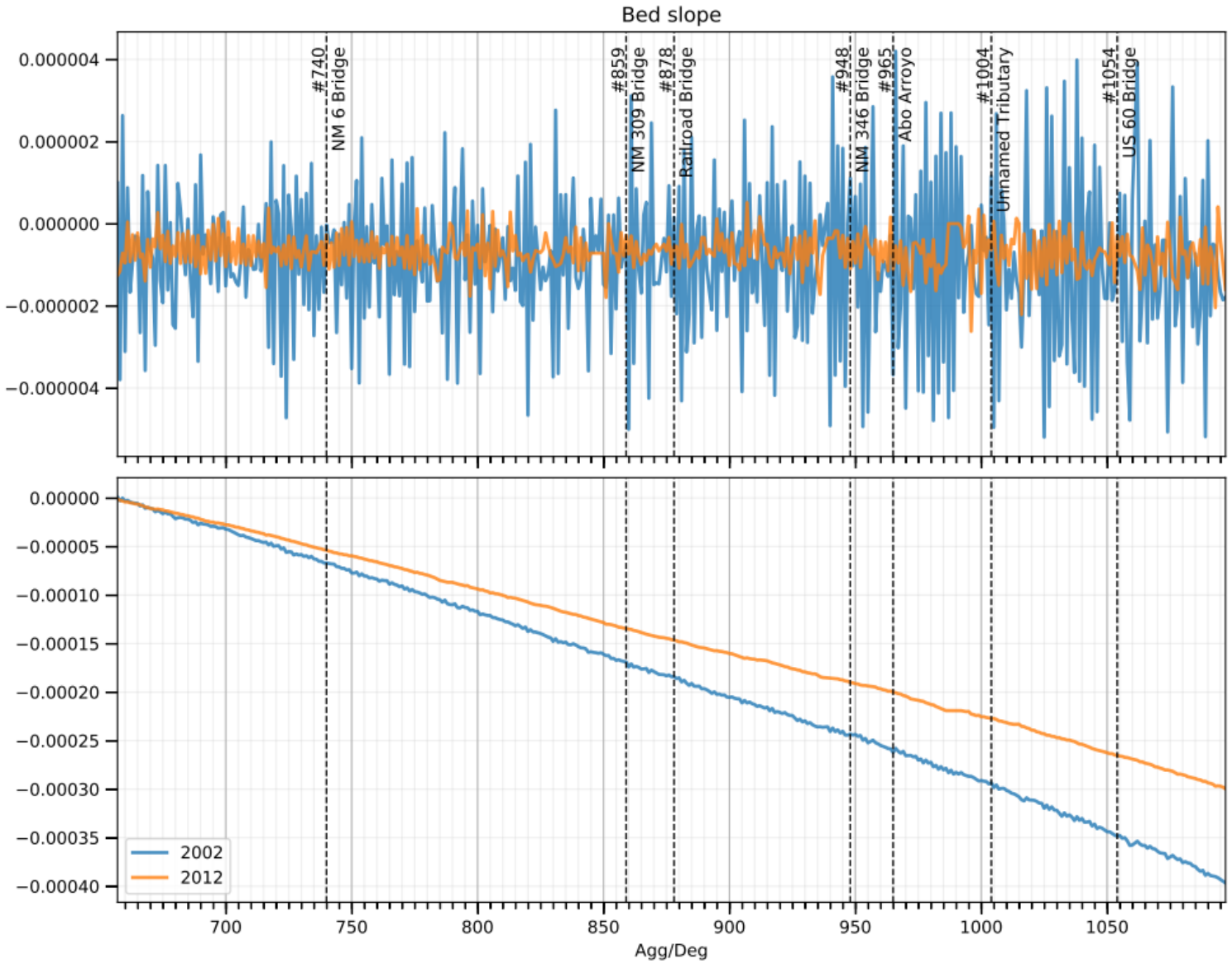
Bed slope
0.000004
0.000002
0.000000
−0.000002
−0.000004
#740
NM 6 Bridge
#859
NM 309 Bridge
#878
Railroad Bridge
#948
NM 346 Bridge
#965
Abo Arroyo
#1004
Unnamed Tributary
#1054
US 60 Bridge
0.00000
−0.00005
−0.00010
−0.00015
−0.00020
−0.00025
−0.00030
−0.00035
−0.00040
2002
2012
700
750
800
850
900
950
1000
1050
Agg/Deg

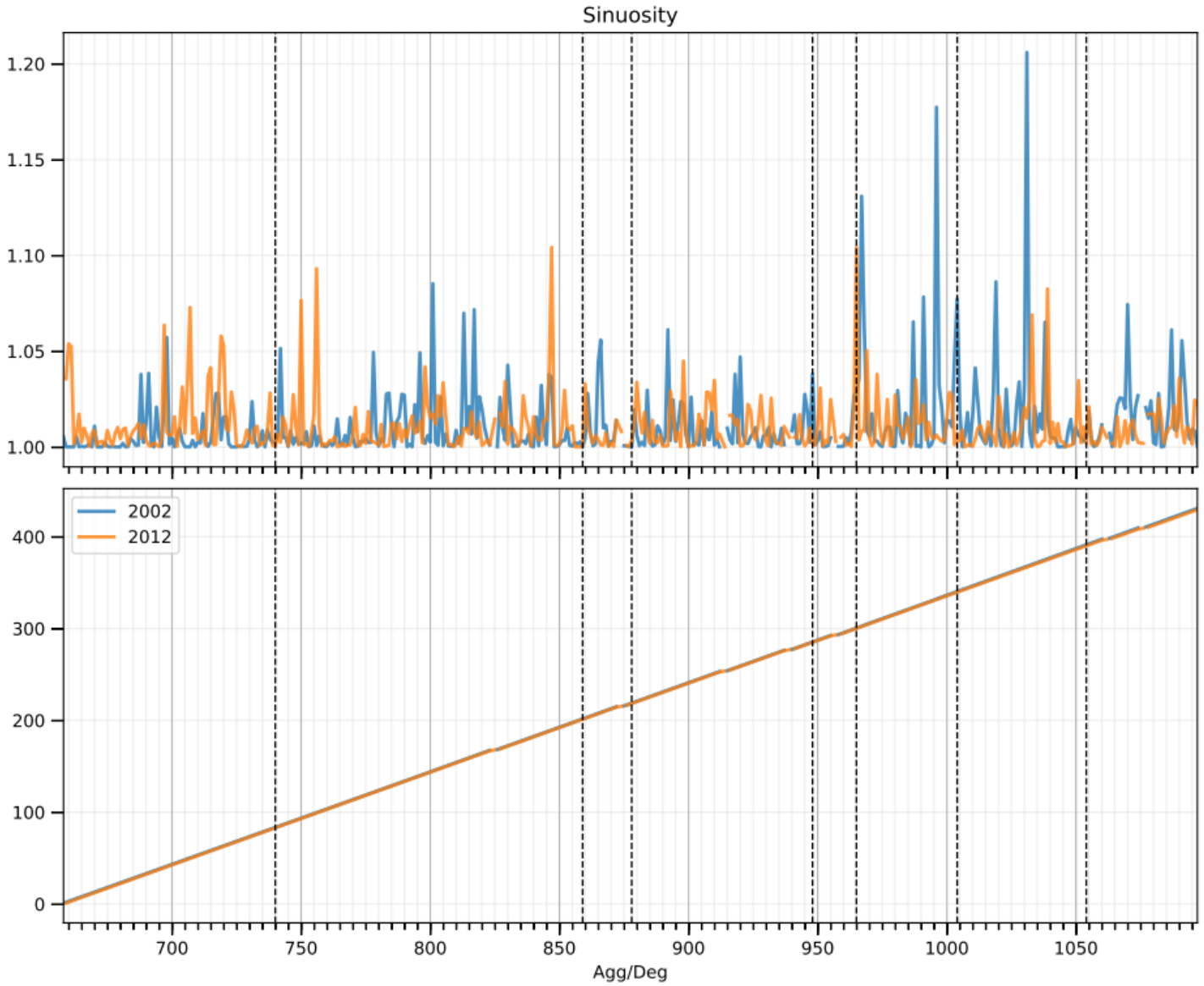
Sinuosity
1.20
1.15
1.10
1.05
1.00
2002
2012
400
300
200
100
0
700
750
800
850
900
950
1000
1050
Agg/Deg

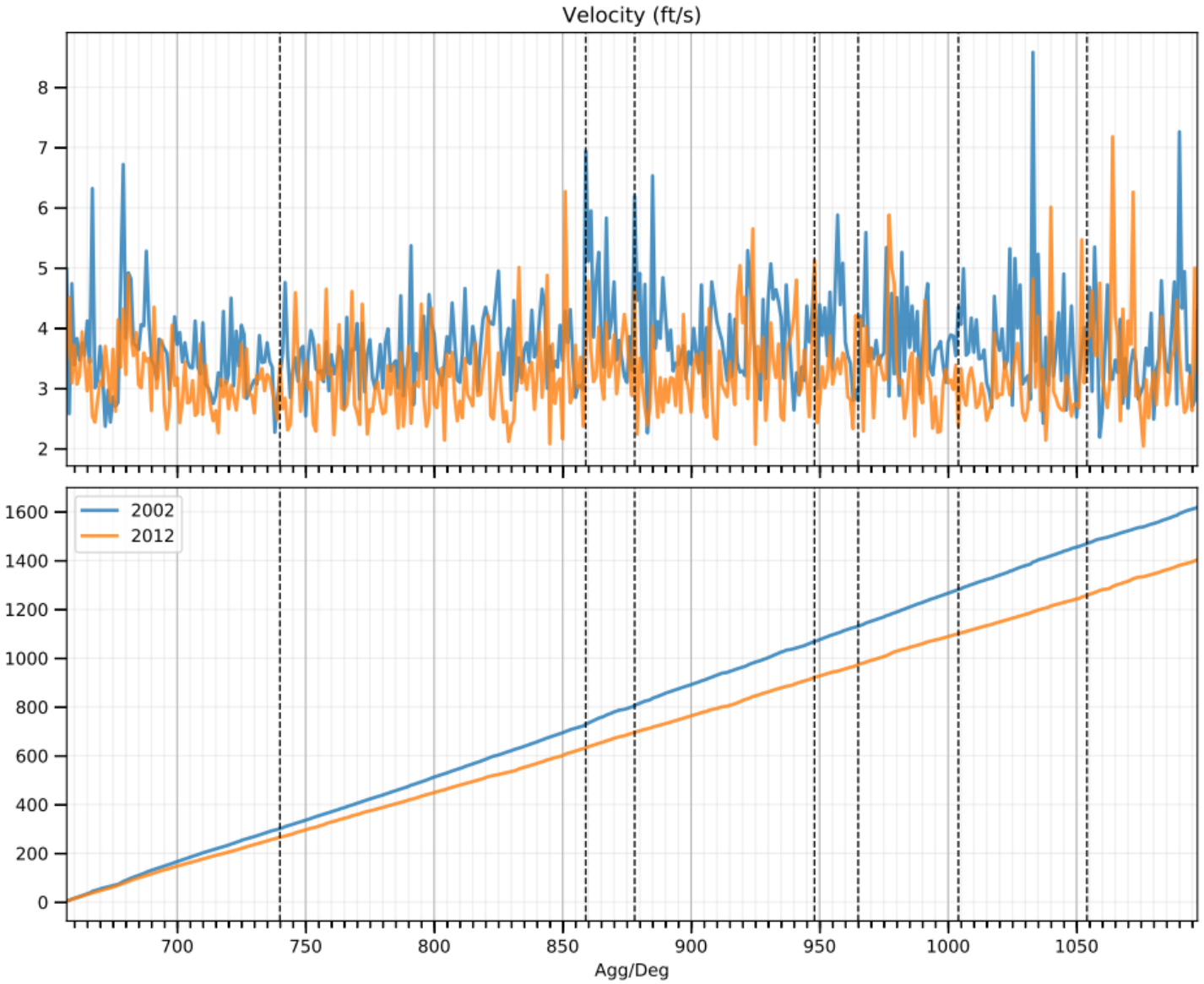
Velocity (ft/s)
8
7
6
5
4
3
2
1600
1400
1200
1000
800
600
400
200
0
2002
2012
700
750
800
850
900
950
1000
1050
Agg/Deg

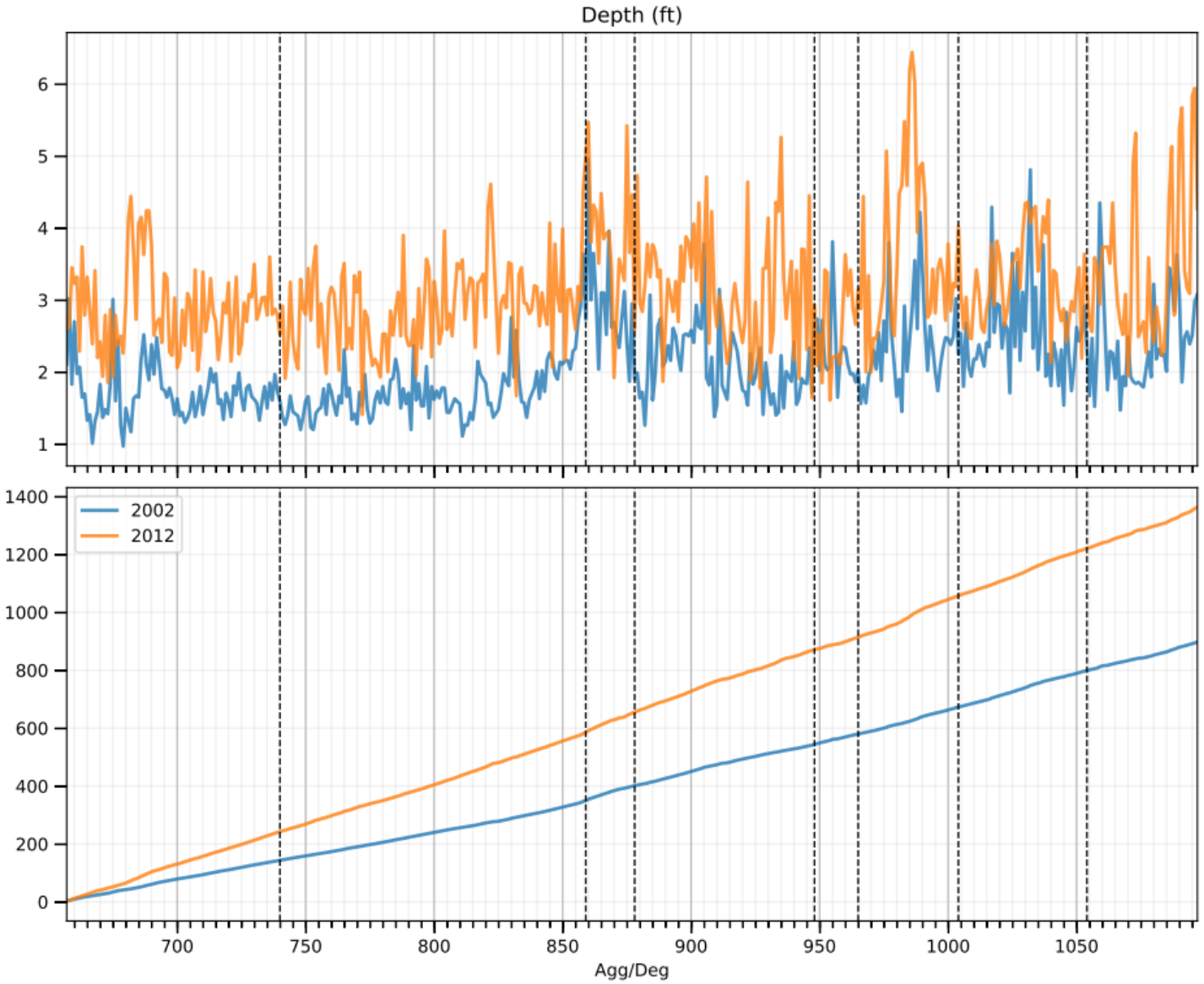
Depth (ft)
6
5
4
3
2
1
1400
1200
1000
800
600
400
200
0
2002
2012
700
750
800
850
900
950
1000
1050
Agg/Deg

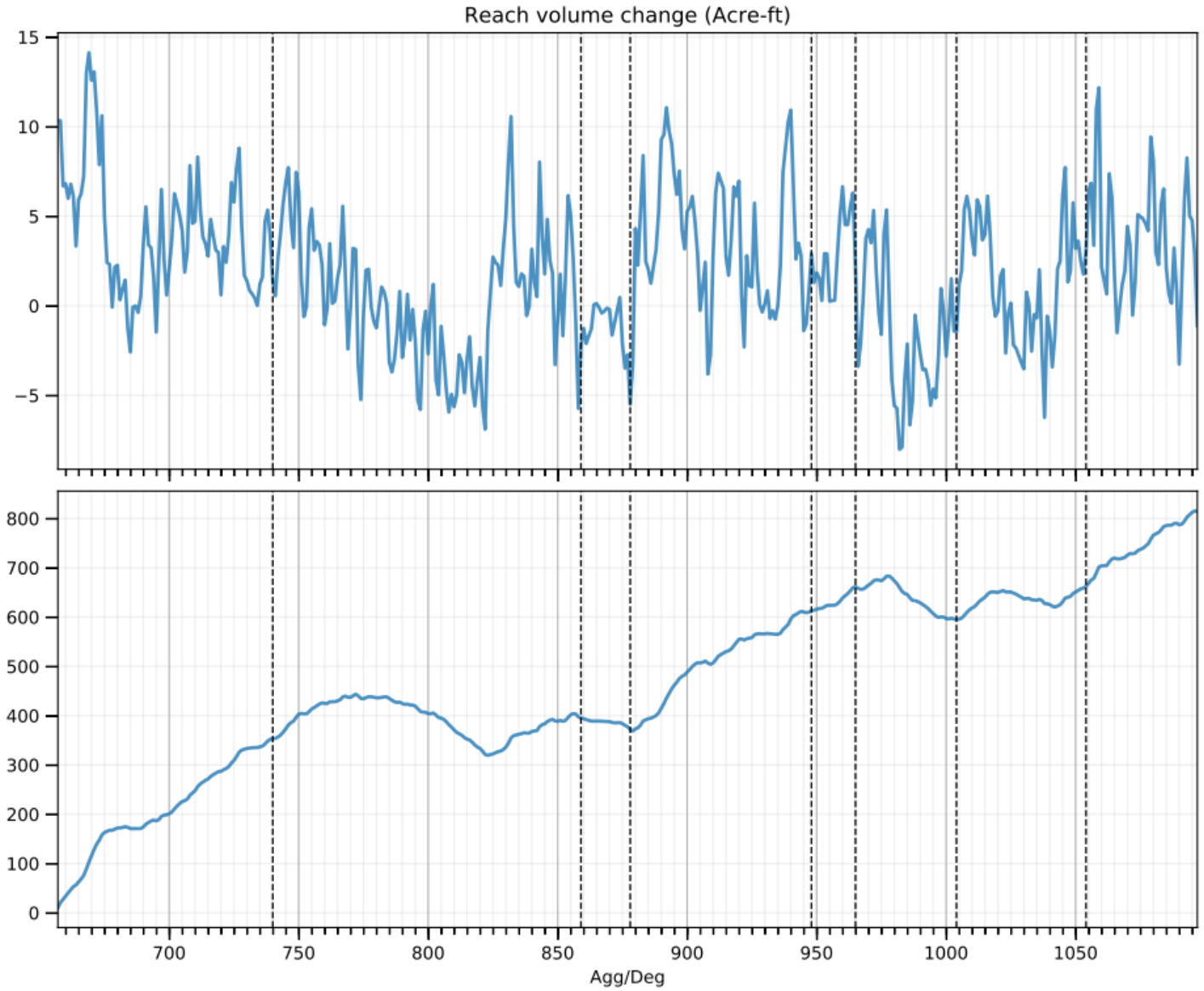
Reach volume change (Acre-ft)
15
10
5
0
−5
800
700
600
500
400
300
200
100
0
700
750
800
850
900
950
1000
1050
Agg/Deg

APPENDIX B

HEC-RAS Silvery Minnow Hydraulic Modeling

Flow depth and velocity determine the quality of habitat of RGSM. In this study, we use HEC-RAS 5.0.3 to analyze the flood extent and hydraulic condition at different discharges. The depth and velocity from HEC-RAS model are used to quantify the location and area of the habitat.

Habitat Criteria

The classification of habitat for silvery minnow used in this section is based on criteria and descriptions of habitat from Tetra Tech (2014). To understand the quality of silvery minnow habitat and how it is changing, it is useful to classify it into different types. These types of habitats indicate how good the habitat is and what it is used for. For instance, feeding, rearing and spawning habitats are necessary for silvery minnows to propagate. Feeding habitats for silvery minnows include benthic food sources, which includes organic detritus, algae, diatoms, and small invertebrates. For "feeding/rearing" habitat to form, it requires low velocity flow so that the river bed is stable (< 0.5 ft/s), and sufficient sunlight so the algae can grow. Also, spawning habitat is better if it is warm and has a low velocity so eggs do not drift downstream. The warm water triggers spawning, and algae begins to grow and therefore ensures food supply for larval development. "Spawning" is a rare habitat that has a velocity less than 0.05 ft/s and a depth less than 1.5 ft which ensures survival of eggs and larvae. Therefore, inundated floodplains are the perfect habitat for spawning. Other categories include "good", "adequate", and "inadequate". "Good" habitat describes the area where the silvery minnow is commonly found. Studies have shown that the silvery minnow is most commonly collected from water less than 1.6 ft (USFWS 2010 from Tetra Tech 2014). "Inadequate" meets none of the ideal habitat criteria and "adequate" meets some of the criteria.

These descriptions of habitats are translated into numerical ranges that fit certain depths and velocities. A summary of the depth and velocities and which habitats they represent is described in Table B-1.

Table B-1: Habitat Classification based on flow depth and velocity

Depth (ft)	Velocity (ft/s)			
	0 – 0.05	0.05 – 0.5	0.5 – 1.5	> 1.5
0 - 1.5	Spawning	Feeding/rearing	Good	Inadequate
1.5 – 1.6	Adequate	Adequate	Adequate	Inadequate
>1.6	Inadequate	Inadequate	Inadequate	Inadequate

Method

The amount of "inadequate", "adequate", "good", "feeding/rearing", and "spawning" habitat and where it is can be visualized and analyzed from the process outlined in this section. By looking at the simulated velocities and depths of the range of flows, we can have insight into silvery minnow habitat and how it changes with different flow regimes, spatially, and temporally.

HEC-RAS is employed to analyze the hydraulic condition at different flow conditions. Spring flow is targeted because the population of RGSM is highly correlated to the connectivity to floodplain in spring. The connectivity depends on the flow magnitude, flow duration and channel geometry. The flows used in HEC-RAS were based on past analyses and practicality. For instance, the 25-day exceedance spring runoff peak flow for dry, mean, and wet year are identified by MEI (2006) to be 1400, 3500, and 5600 cfs, respectively. Spring runoff for the last decade has been lower than the past runoffs, so we chose 600, 1400 and 3500 cfs for the fish habitat analysis. 600 cfs was chosen because several years with aerial photographs were taken with the flow discharge around this value (1992 at 650 cfs, 2002 at 600 cfs, 2006 at 580 cfs and 2012 at 740 cfs). This allows the comparison of HEC-RAS results with aerial photographs.

The available years of HEC-RAS geometries around when fish population started being collected include 1992, 2002, and 2012. The HEC-RAS geometry cross sections were developed by USBR. An example of a cross-section from 2002 is shown in Figure B-1. The 1992 and 2002 are derived by using photogrammetry and the 2012 geometry was derived from LiDAR. The reach from Isleta Diversion Dam to San Acacia was extracted from the entire Middle Rio Grande HEC-RAS file with additional 10 cross sections adjacent to upstream and downstream ends. Modifications were made to the main channel designation and levee stations to more accurately reflect the flood extent in the aerial photographs (Figure B-1). Aerial photographs from April of 2005 (4500 cfs), 2006 January (580 cfs), and 2008 July (1630 cfs), and a digitized flood map of 2005 June (5980 cfs) were used to identify the location of levees. Manning n was set as 0.019 for the main channel and 0.1 for the floodplain according to Klein et al. (2018b). The simulation was run under uniform steady condition.

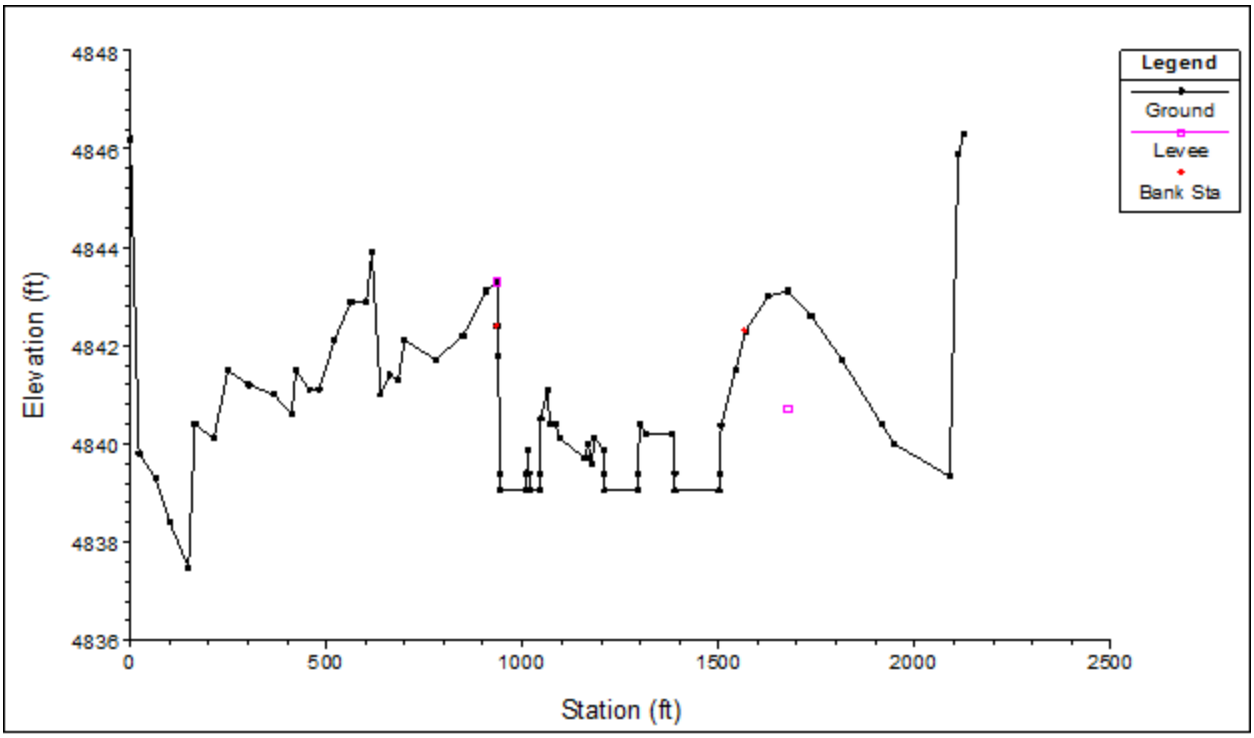

Figure B-1: Example of modified levee station: agg/deg 764 (river station 1177) in 2002. The 2005 flood map shows that the flow only overtopped at the right bank. Furthermore, the right bank side channel is found inundated in April of 2005 but not in the aerial photos in January of 2006, so the levee on the right bank is placed between side channel and main channel and at the elevation with flow between 1500 cfs and 3150 cfs. The levee on the left bank is placed at the top of the main channel banks.

Flow depth and velocity for each station are exported to ArcGIS to analyze the habitat spatially. The habitat quality is broken up into subreaches and compared. Because the HEC-RAS geometries are not geo-referenced, a program was developed to compute the coordinates at every station. A point polygon with flow depth, flow velocity, and xy-coordinate for a given flow condition can be generated. The point feature based on Table B-1 is used to create a TIN network with flow depth and velocity.

Results & Discussion

Figures B-2 and B-3 illustrate the simulation results of flow depth and velocity at subreach I1 with discharges at 600, 1400, and 3500 cfs in 2012. As shown in Figure B-2, we can identify the suitable habitat in terms of flow depth and velocity for the silvery minnows, based on Table B-1.

From the previous sections we learned that the Isleta reach transitioned from braided to single thread from 1992 to 2012. In addition, the channel width is decreasing. From the simulation, we saw that the main channel is narrower, and velocity and depth become greater over the years (Figures in Appendix C). There are areas with slow and shallow water around bars in 1992 and 2002. This feature is much less in 2012. As a result, we found loss of habitat over time, especially from 2002 to 2012.

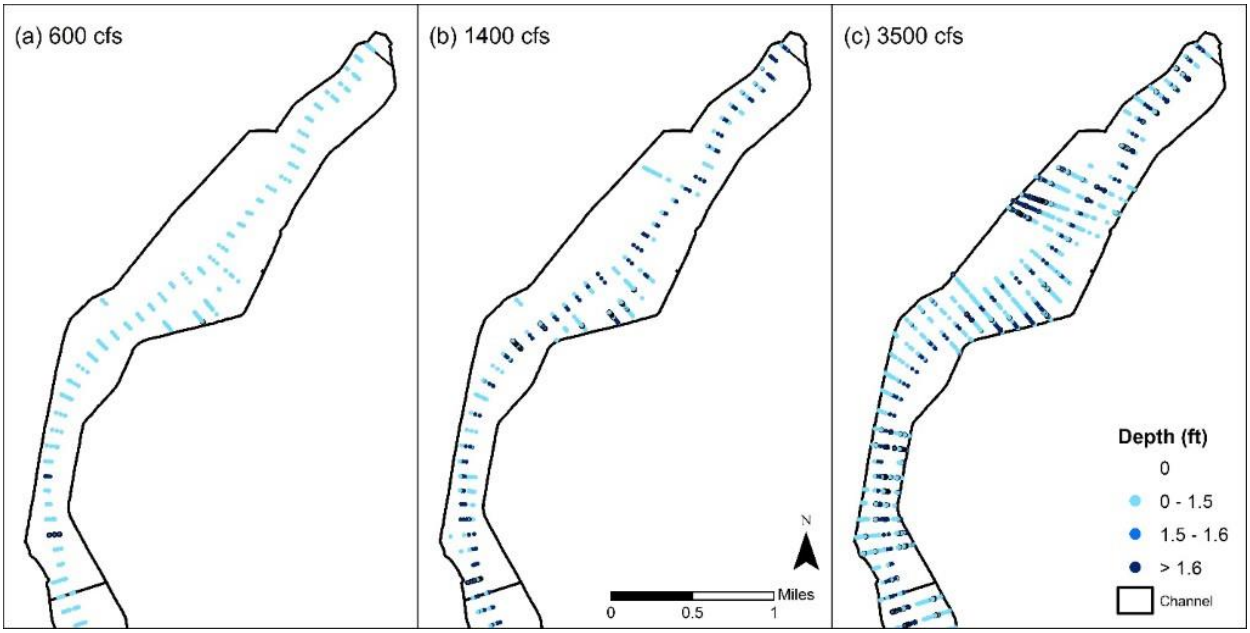

Figure B-2: Simulated depth at subreach I1 at flow rate 600, 1400, and 3500 cfs in 2012.

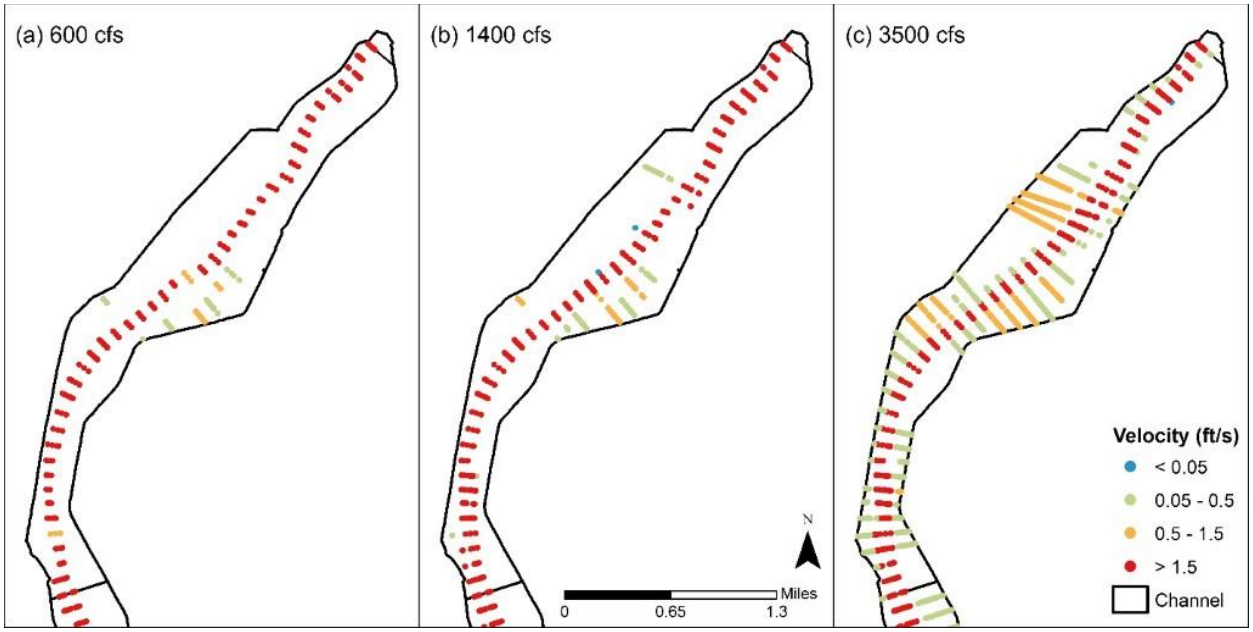

Figure B-3: Simulated velocity at subreach I1 at flow rate 600, 1400, and 3500 cfs in 2012.

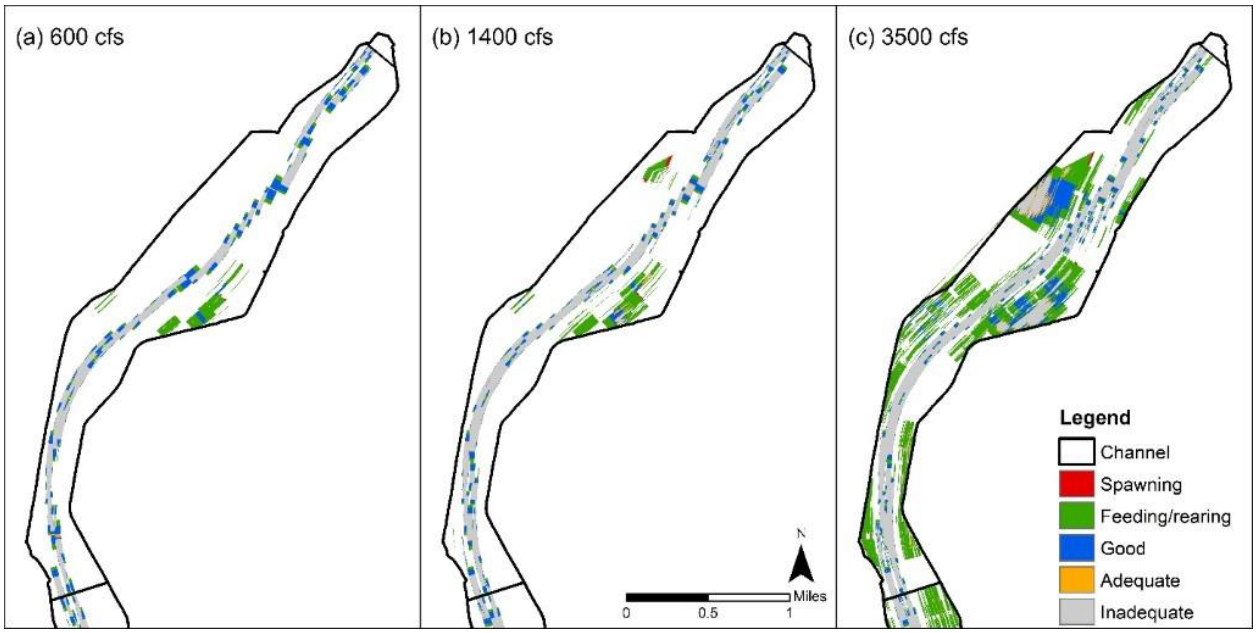

Figure B-4: Hydraulic habitat at subreach I1 at flow rate 600, 1400, and 3500 in 2012

Figures B-5, B-6, and B-7 show the areas and densities of "spawning", "feeding", and "good" habitat respectively of each subreach. The habitat density depicted in (b) in these figures gives a more meaningful representation of the habitat quality because it is weighted by subreach area.

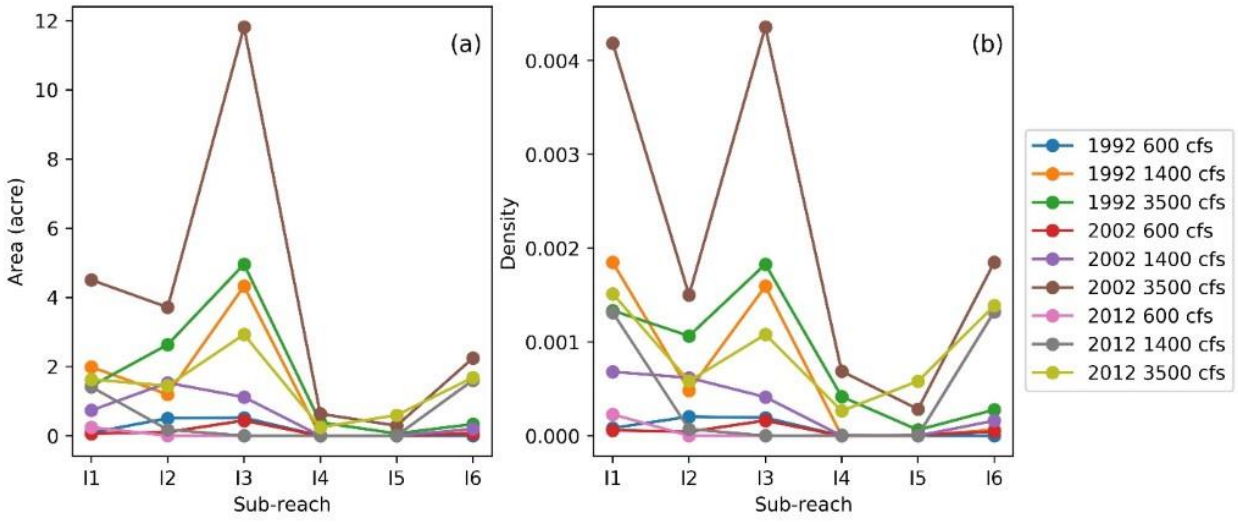

Figure B-5: "Spawning" habitat: (a) area, (b) density (area of habitat divided by area of subreach).

For all simulated years, the area of "spawning" habitat is largest when the flow is 3500 cfs (5.0 acre in 1992, 11.8 acre in 2002, and 2.92 acre in 2012 at I3). Figure B-5b shows that I1 and I3 have the highest weighted area by subreach of "spawning" habitat.

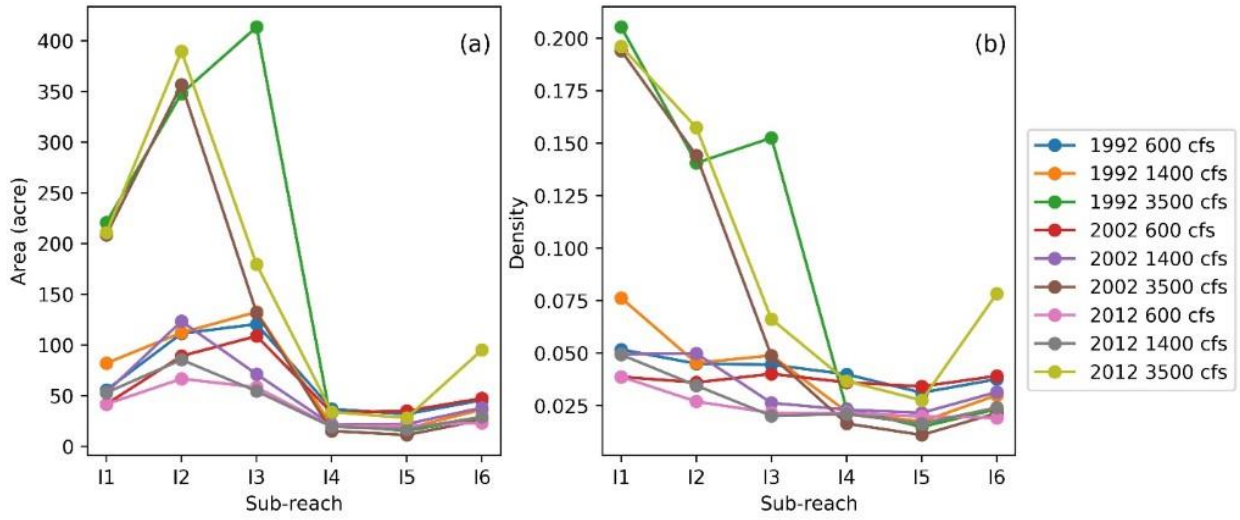

Figure B-6: "Feeding/rearing" habitat: (a) area, (b) density (area of habitat divided by area of subreach).

Area of "feeding/rearing" habitat shows a similar pattern to the spawning habitat. The best "feeding/rearing" habitat occurs in I1, I2 and I3 at 3500 cfs as shown in Figure B-6. The increase is attributed to floodplain inundation. Floodplain inundation begins at 3500 cfs for this reach, resulting in an increase in habitat quality (Tetra Tech 2014). This explains why there is more "feeding/rearing" and "spawning" habitat at 3500 cfs in this simulation. Also, while 2002 has the highest amount of "spawning" habitat at 3500 cfs, it has the least amount of "good" habitat at that flow compared to other years as shown in Figure B-7.

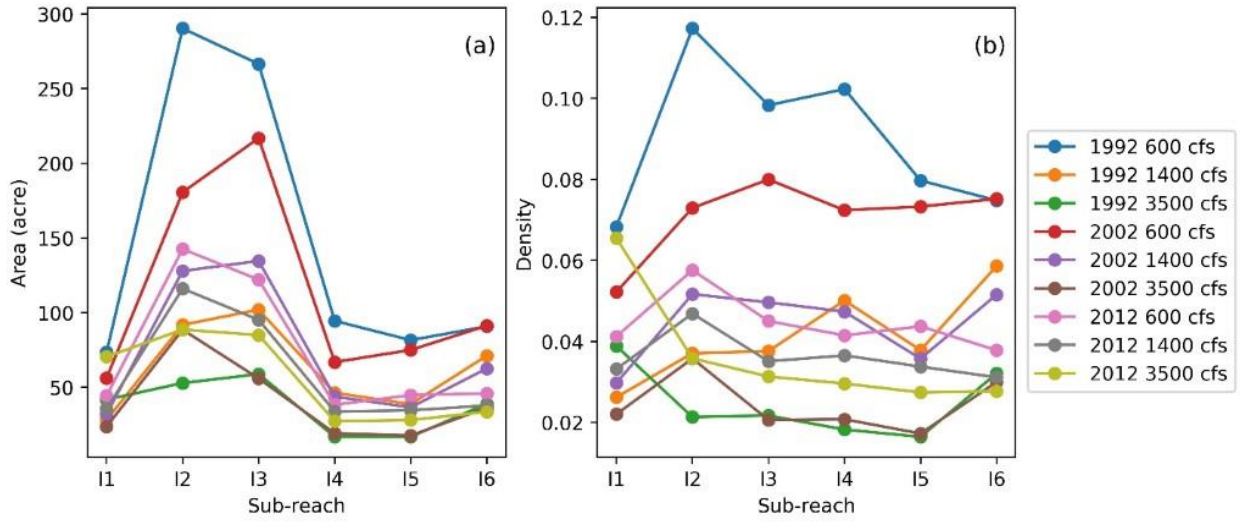

Figure B-7: "Good" habitat: (a) area, (b) density (area of habitat divided by area of subreach).

For the "good" habitat, the area is negatively related to discharge. Therefore, the highest density of "good" habitat is at the lowest flow of 600 cfs for all years. This could be due to more

accessible channels in the main channel, and shallower areas at low flow providing better habitat. Also, subreaches I2-I4 appear to have the majority of “good” habitat, but there is not an obvious trend when looking at the weighted area in Figure B-7b.

When the discharge increases, the area of low velocity in the channel decreases and therefore the area of “good” habitat decreases until floodplain inundation occurs. It would be expected that the “good” habitat would be lowest at 1400 cfs and higher at 3500 cfs when the floodplain becomes inundated (Bovee et al. 2008; Tetra Tech 2014), yet this does not occur. The “good” habitat is lowest at 3500 cfs. This is most likely because a very small amount of inundation occurs starting at 3500 cfs (Tetra Tech 2014), so that area become all “feeding/rearing” and “spawning” habitat. When significant inundation begins at flows such as at 5000 cfs, greater amounts of “good” habitat would be expected.

Overall, subreaches I1, I2, and I3 provide more in-channel and overbank habitat than I4, I5, and I6. The highest “spawning” and “feeding/rearing” habitat is at 3500 cfs. The majority of “good” habitat occurs at 600 cfs. As for the dry scenario (600 cfs), the greatest area for all habitats are found in 1992, followed by 2002, and the least in 2012 at all subreaches. The middle flow level of 1400 cfs never has the highest habitat area, and usually has the least amount of quality habitat.

APPENDIX C

Additional HEC-RAS RGSM Modeling Maps

A) 1992

I1

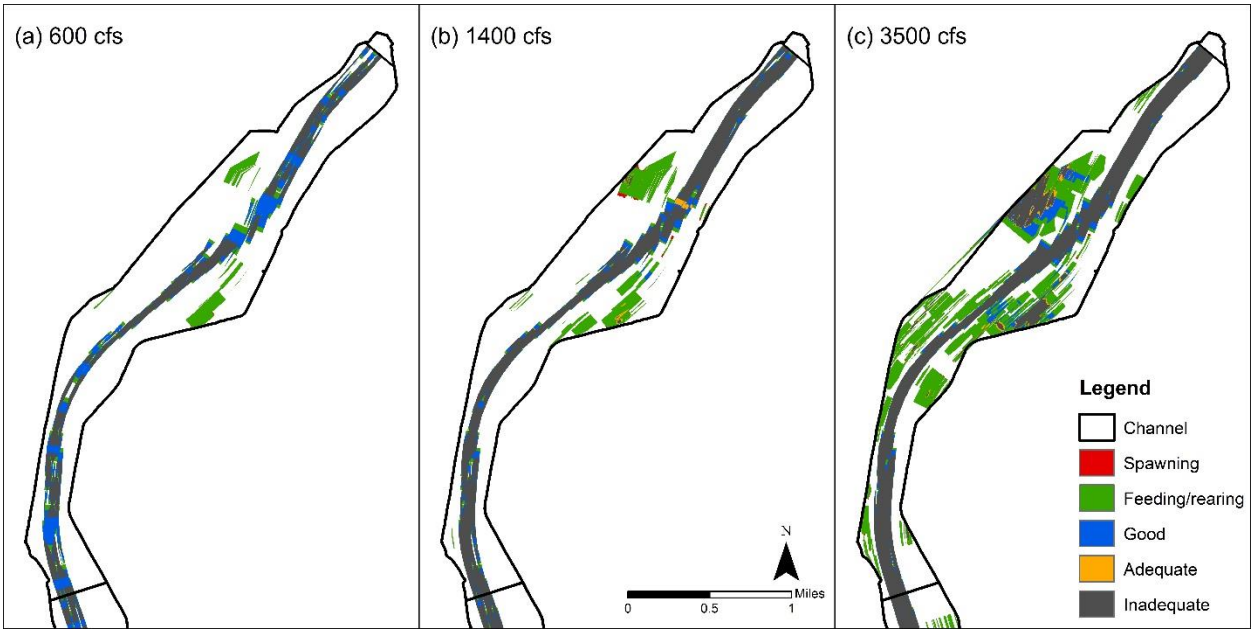
(a) 600 cfs
(b) 1400 cfs
(c) 3500 cfs
N
Miles
0
0.5
1
Legend
Channel
Spawning
Feeding/rearing
Good
Adequate
Inadequate

I2

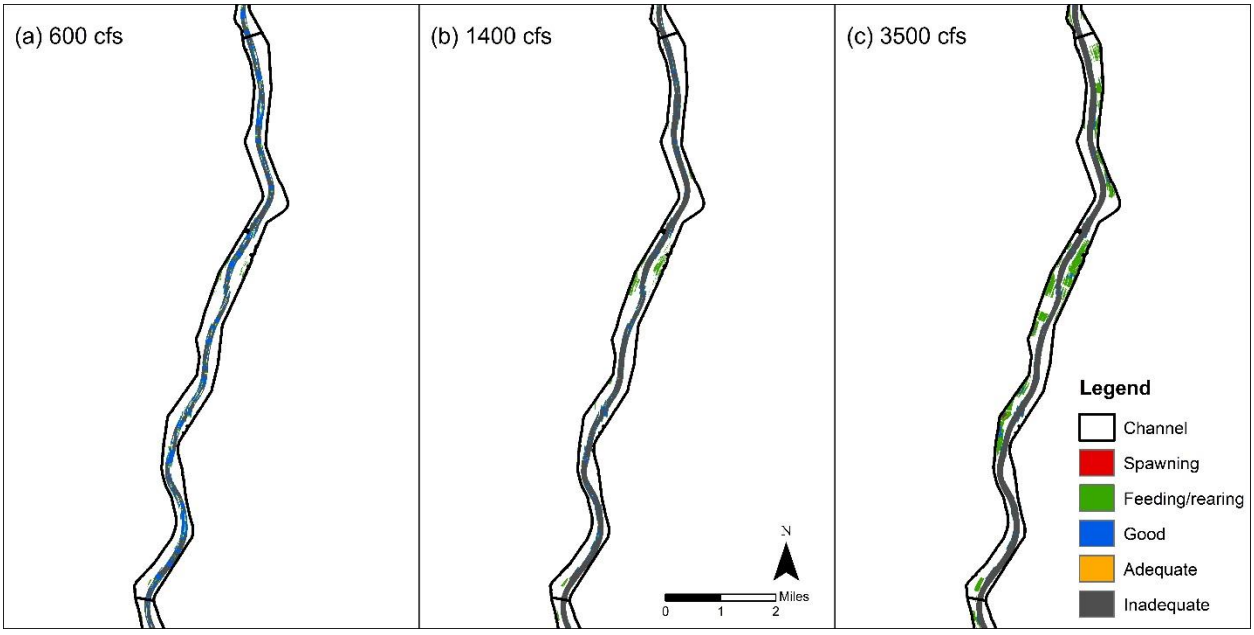
(a) 600 cfs
(b) 1400 cfs
(c) 3500 cfs
N
Miles
0
1
2
Legend
Channel
Spawning
Feeding/rearing
Good
Adequate
Inadequate

I3

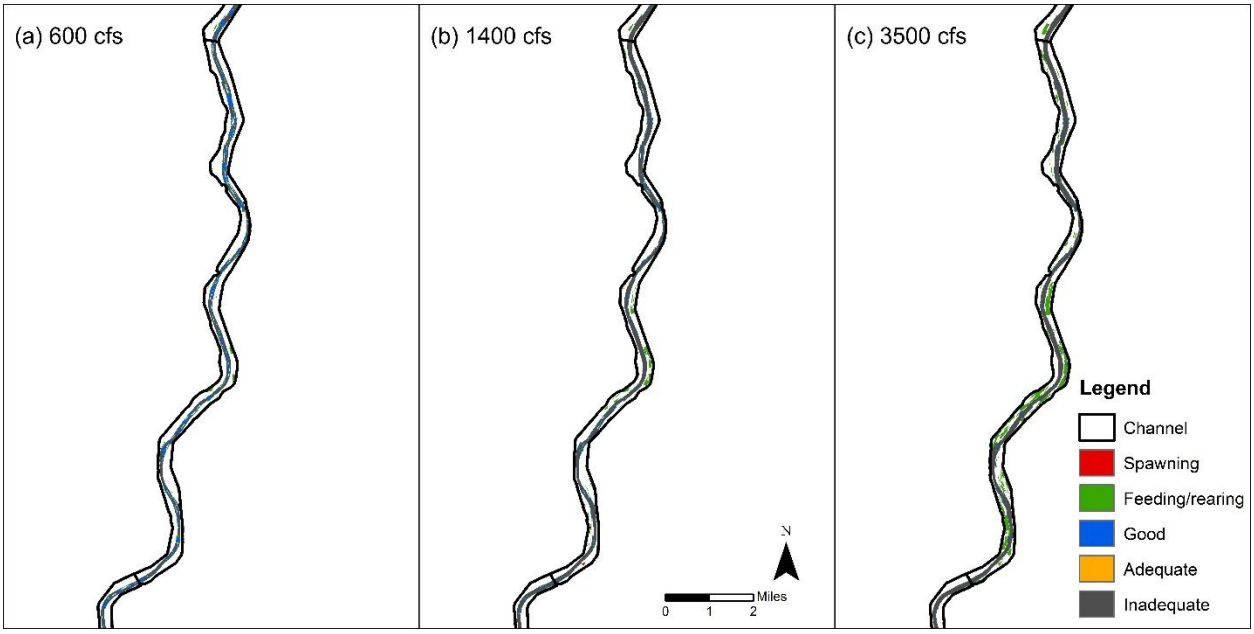
(a) 600 cfs
(b) 1400 cfs
(c) 3500 cfs
N
Miles
0 1 2
Legend
Channel
Spawning
Feeding/rearing
Good
Adequate
Inadequate

I4

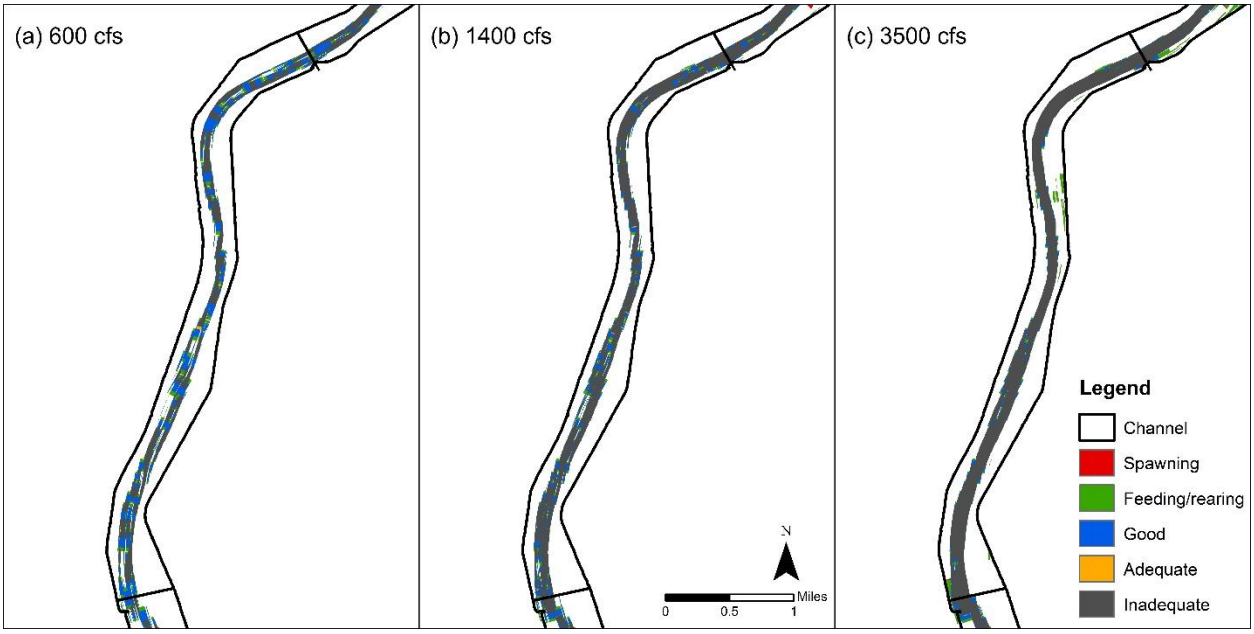
(a) 600 cfs
(b) 1400 cfs
(c) 3500 cfs
N
Miles
0 0.5 1
Legend
Channel
Spawning
Feeding/rearing
Good
Adequate
Inadequate

I5

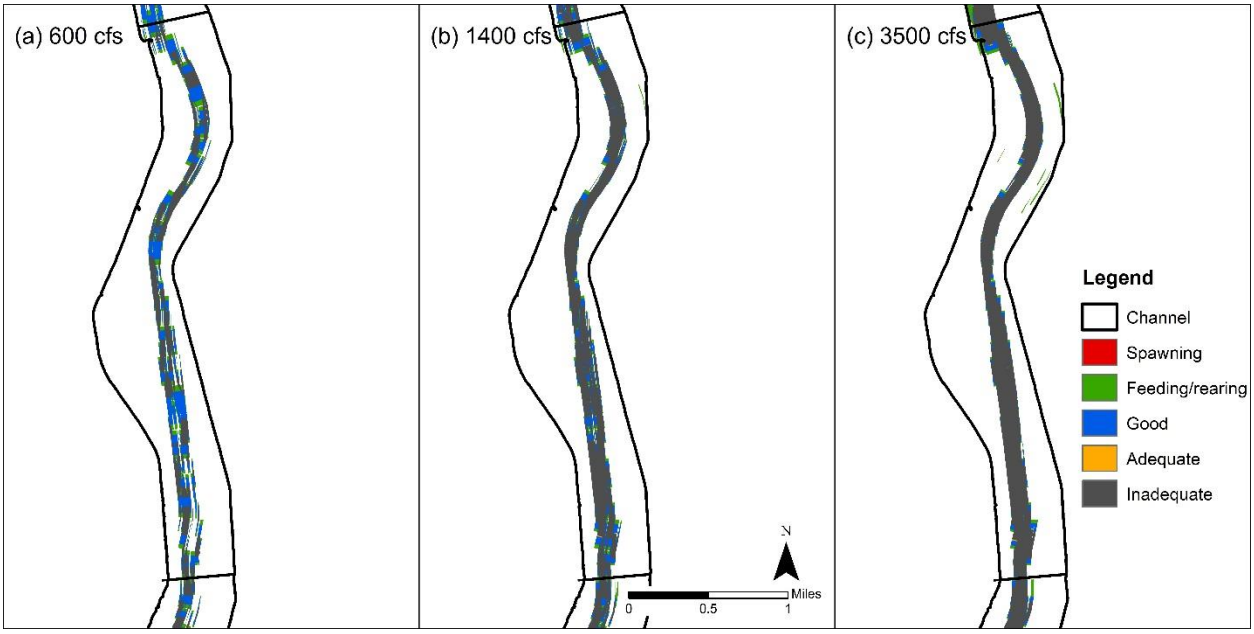
(a) 600 cfs
(b) 1400 cfs
(c) 3500 cfs
N
0
0.5
1
Miles
Legend
Channel
Spawning
Feeding/rearing
Good
Adequate
Inadequate

I6

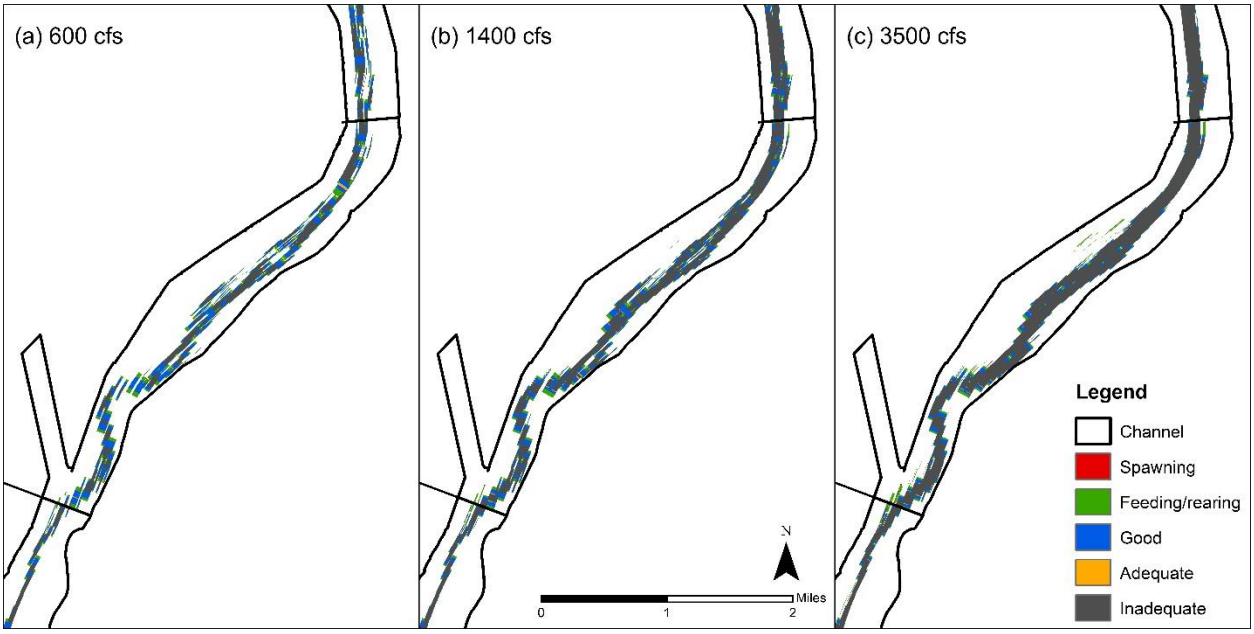
(a) 600 cfs
(b) 1400 cfs
(c) 3500 cfs
N
0
1
2
Miles
Legend
Channel
Spawning
Feeding/rearing
Good
Adequate
Inadequate

B) 2002

I1

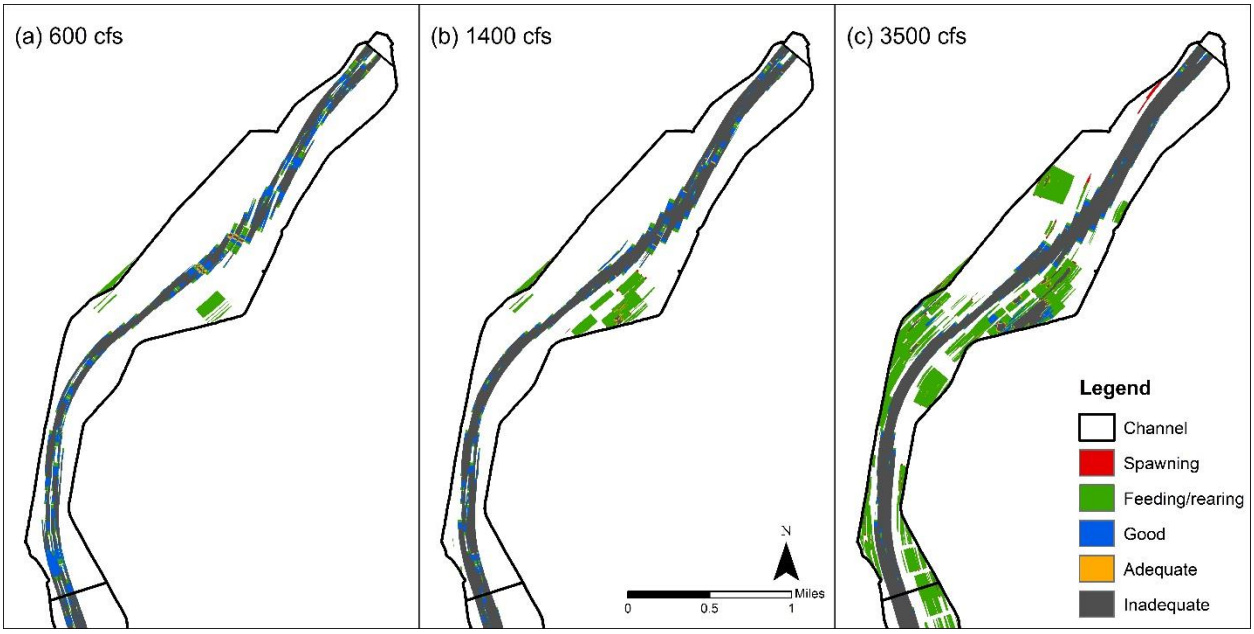
(a) 600 cfs
(b) 1400 cfs
(c) 3500 cfs
N
Miles
0
0.5
1
Legend
Channel
Spawning
Feeding/rearing
Good
Adequate
Inadequate

I2

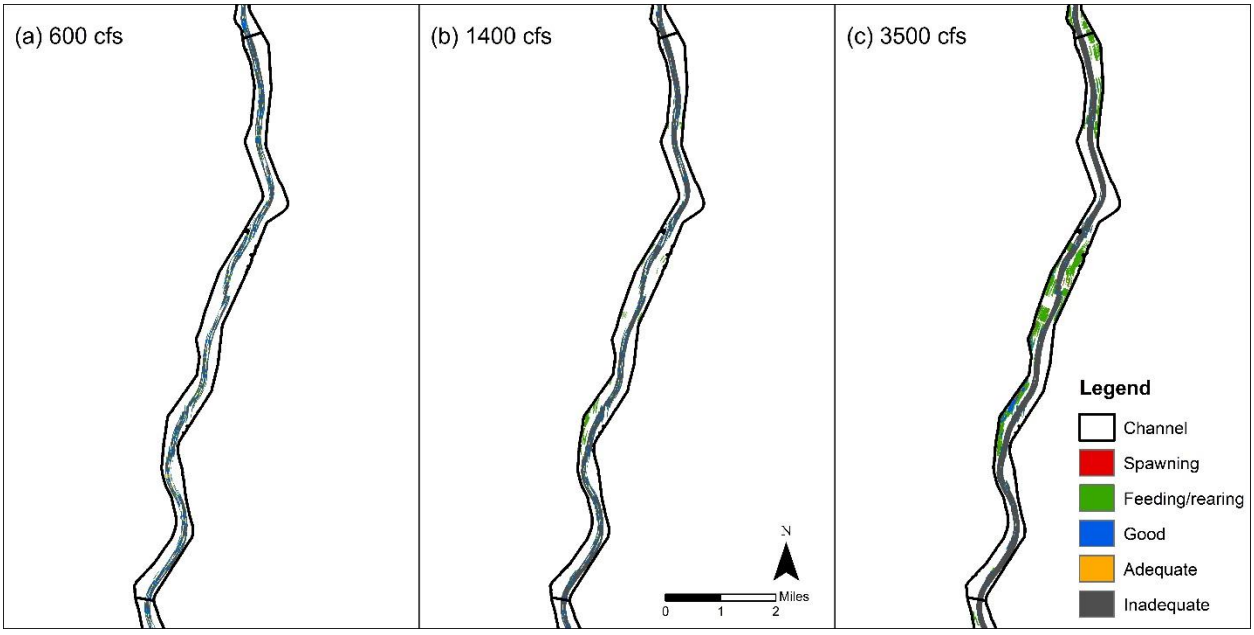
(a) 600 cfs
(b) 1400 cfs
(c) 3500 cfs
N
Miles
0
1
2
Legend
Channel
Spawning
Feeding/rearing
Good
Adequate
Inadequate

I3

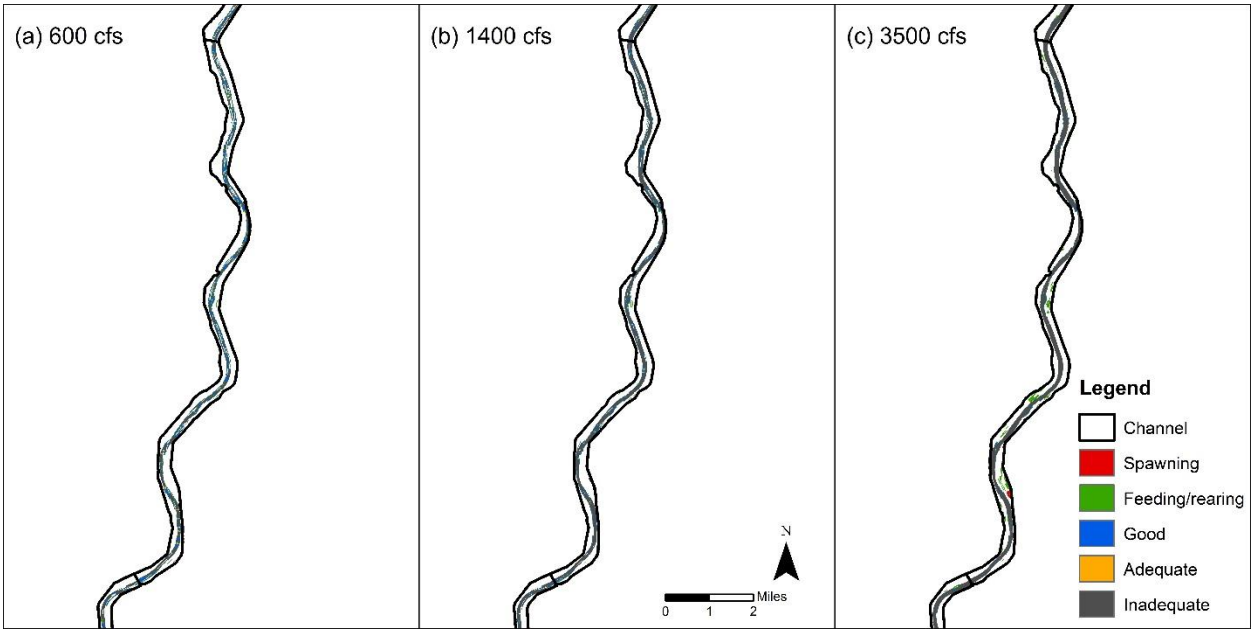
(a) 600 cfs
(b) 1400 cfs
(c) 3500 cfs
N
Miles
0 1 2
Legend
Channel
Spawning
Feeding/rearing
Good
Adequate
Inadequate

I4

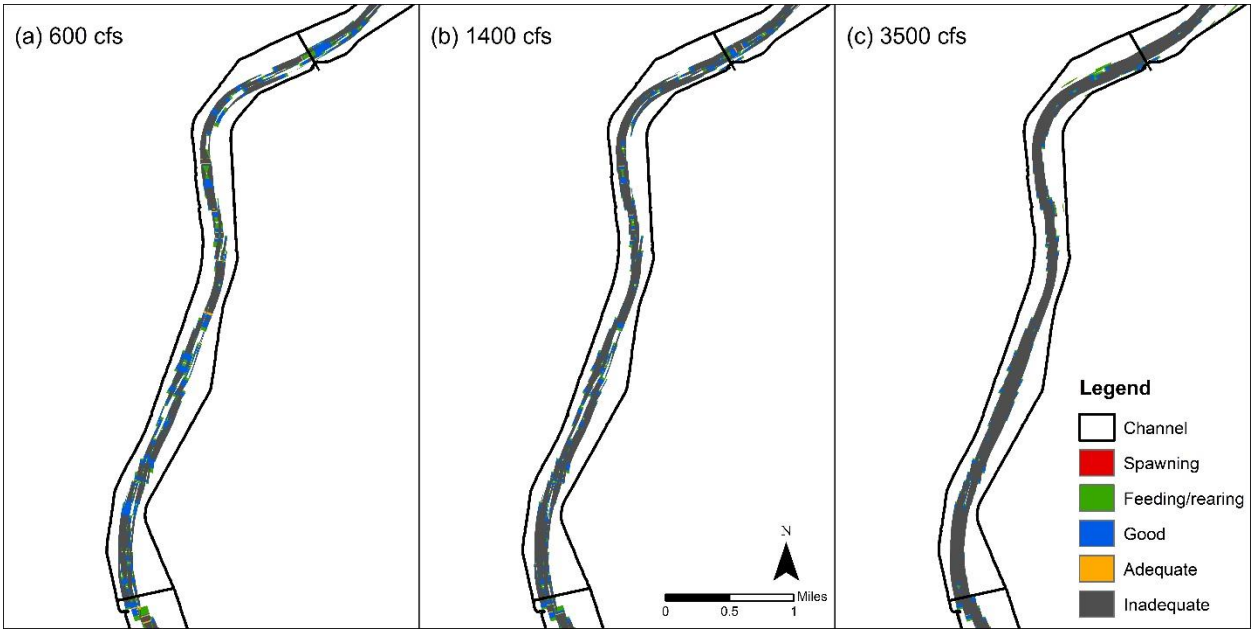
(a) 600 cfs
(b) 1400 cfs
(c) 3500 cfs
N
Miles
0 0.5 1
Legend
Channel
Spawning
Feeding/rearing
Good
Adequate
Inadequate

I5

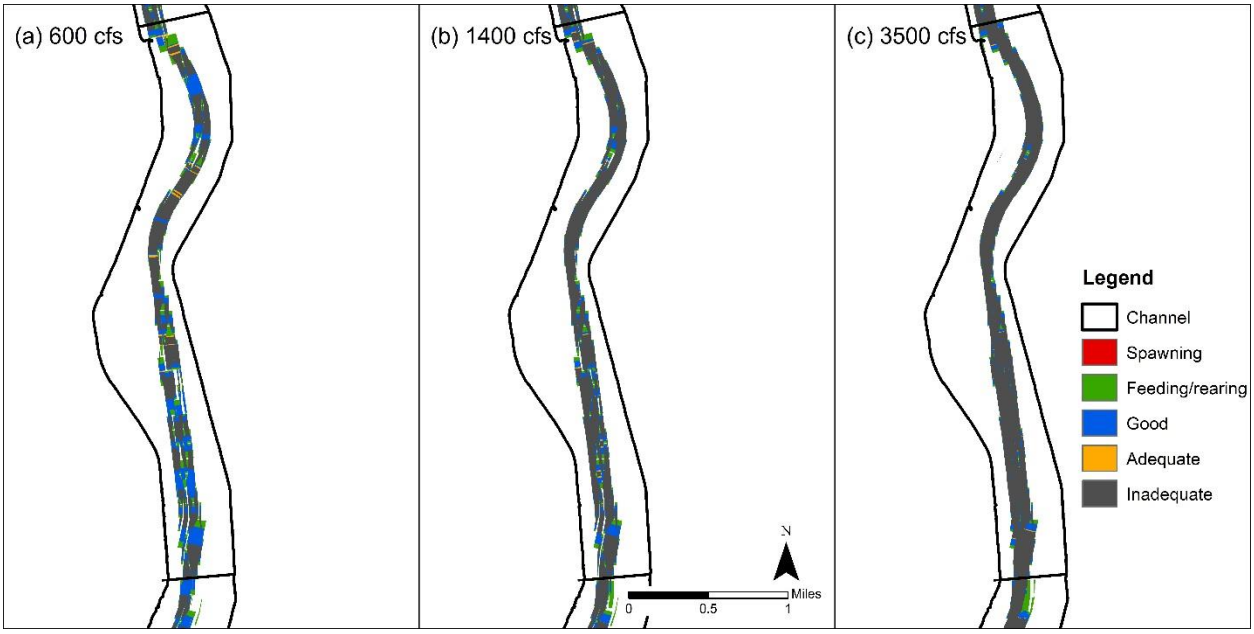
(a) 600 cfs
(b) 1400 cfs
(c) 3500 cfs
N
0
0.5
1
Miles
Legend
Channel
Spawning
Feeding/rearing
Good
Adequate
Inadequate

I6

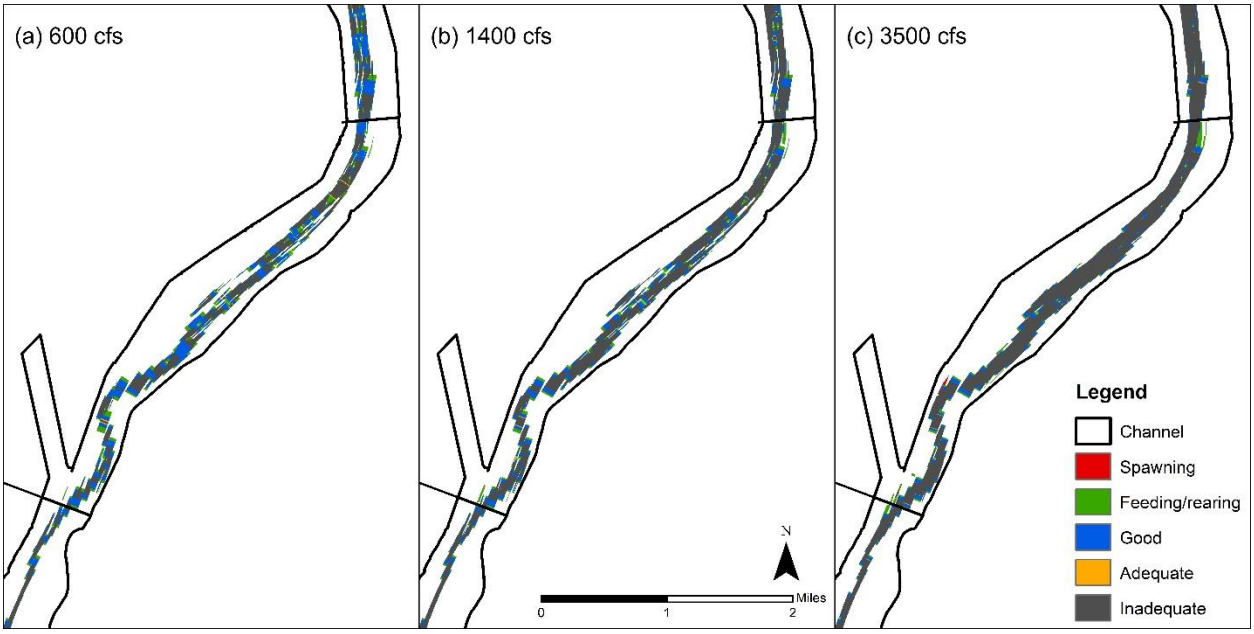
(a) 600 cfs
(b) 1400 cfs
(c) 3500 cfs
N
0
1
2
Miles
Legend
Channel
Spawning
Feeding/rearing
Good
Adequate
Inadequate

C) 2012

I1

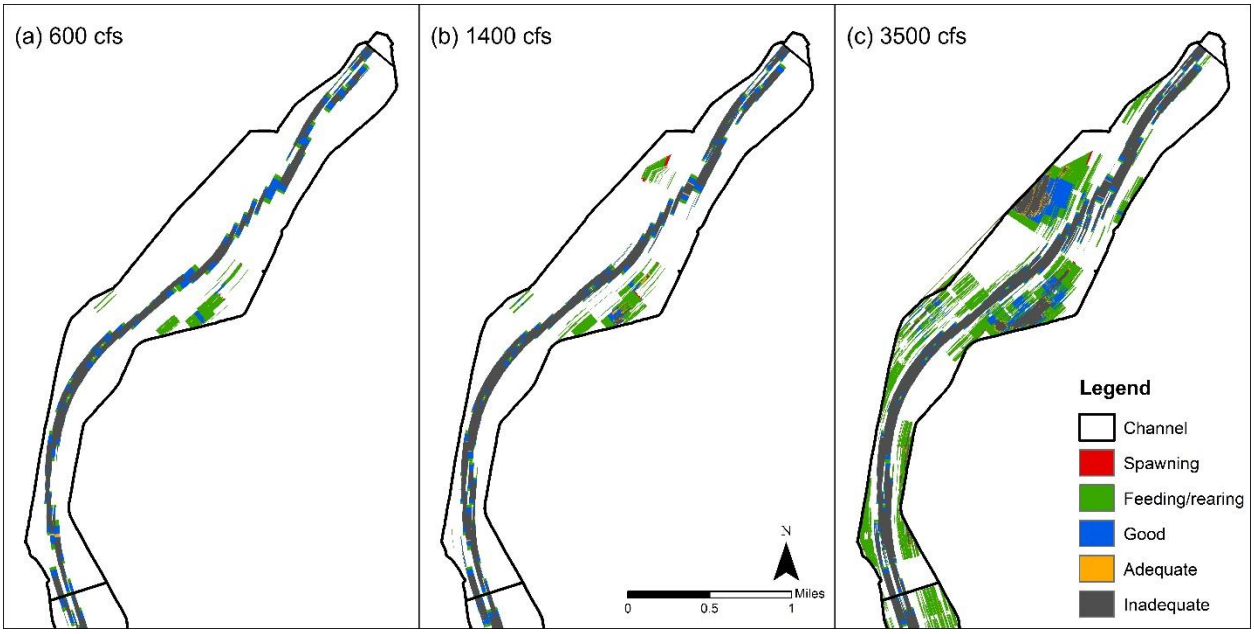
(a) 600 cfs
(b) 1400 cfs
(c) 3500 cfs
N
Miles
0
0.5
1
Legend
Channel
Spawning
Feeding/rearing
Good
Adequate
Inadequate

I2

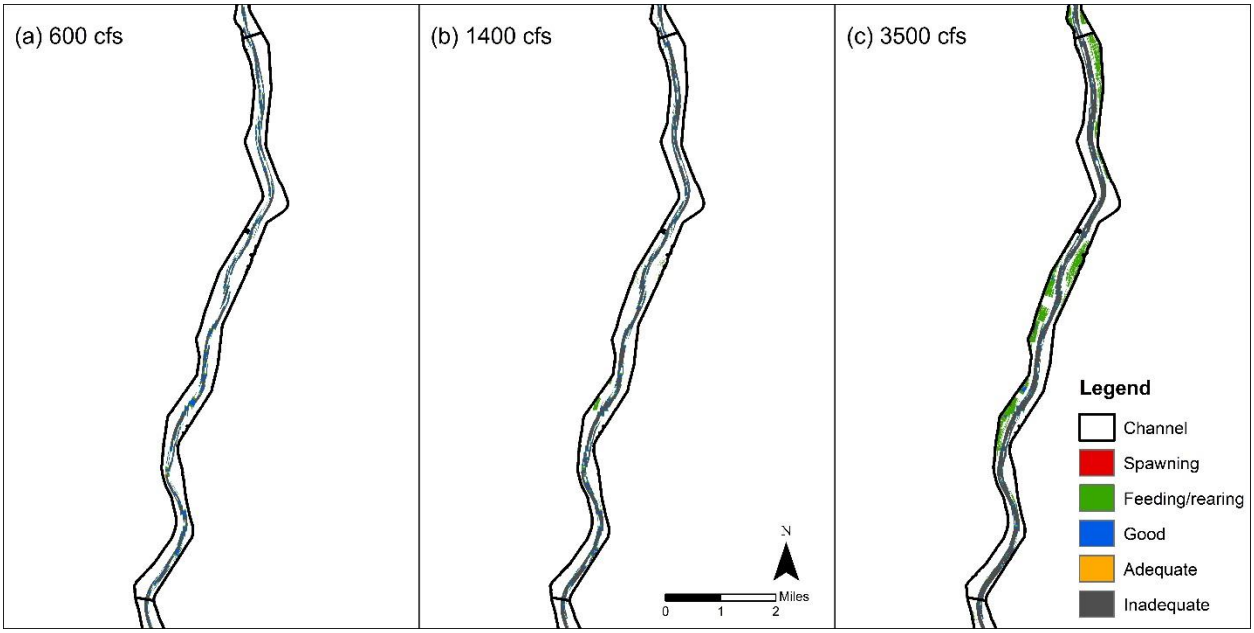
(a) 600 cfs
(b) 1400 cfs
(c) 3500 cfs
N
Miles
0
1
2
Legend
Channel
Spawning
Feeding/rearing
Good
Adequate
Inadequate

I3

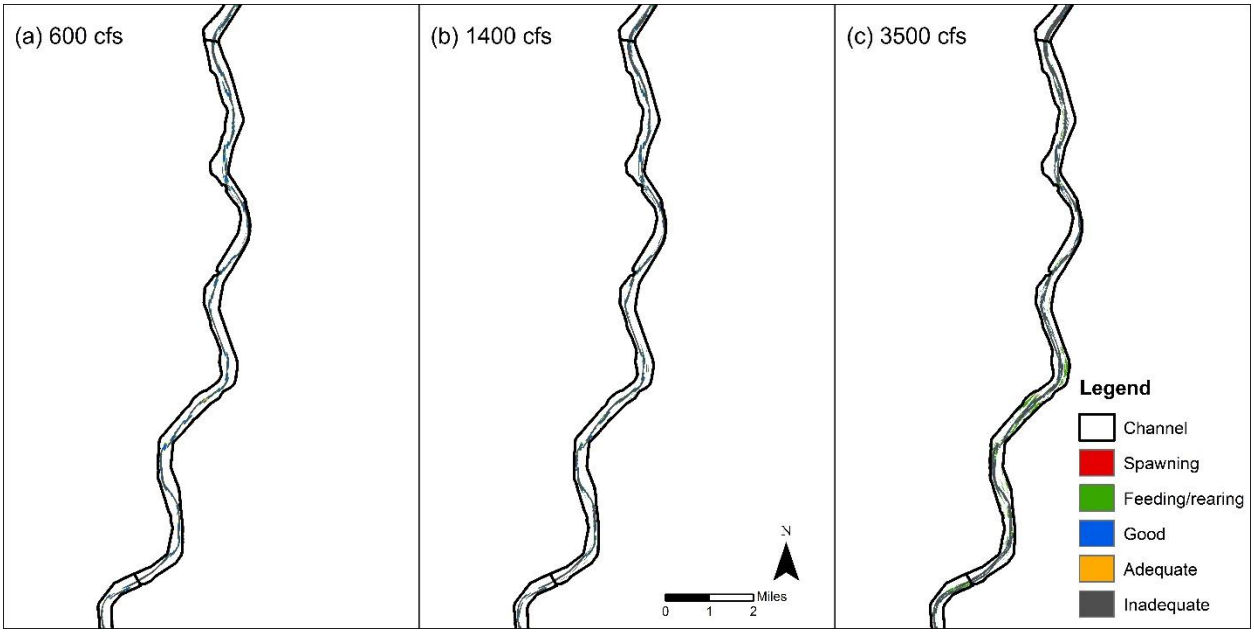
(a) 600 cfs
(b) 1400 cfs
(c) 3500 cfs
N
Miles
0 1 2
Legend
Channel
Spawning
Feeding/rearing
Good
Adequate
Inadequate

I4

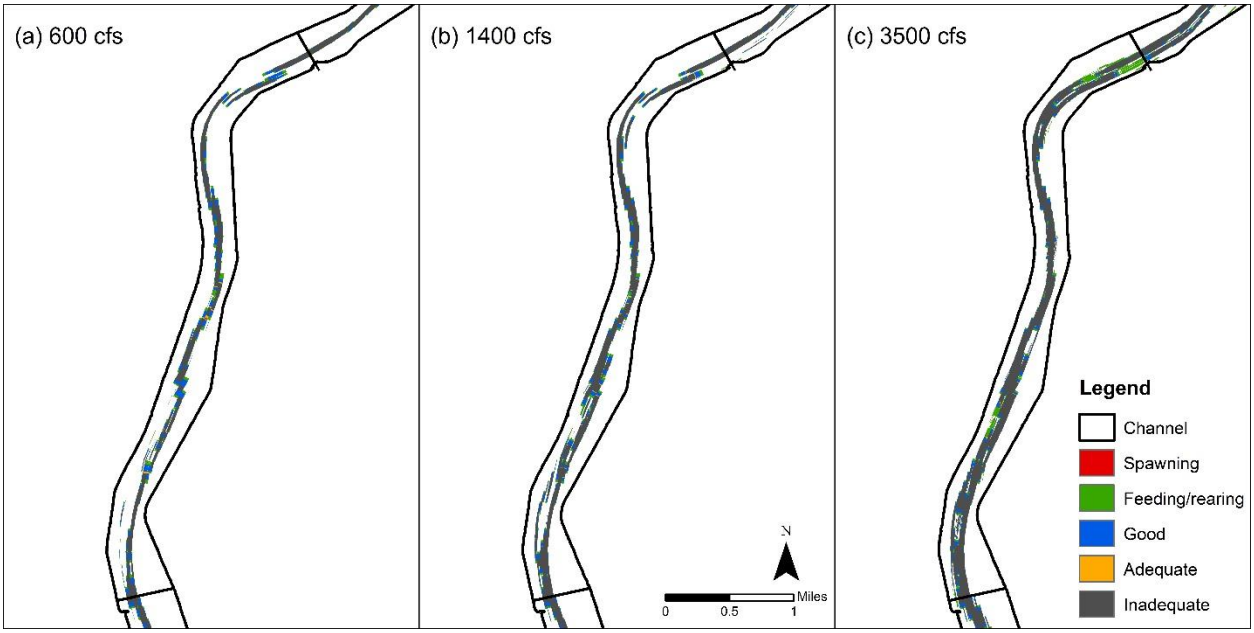
(a) 600 cfs
(b) 1400 cfs
(c) 3500 cfs
N
Miles
0 0.5 1
Legend
Channel
Spawning
Feeding/rearing
Good
Adequate
Inadequate

I5

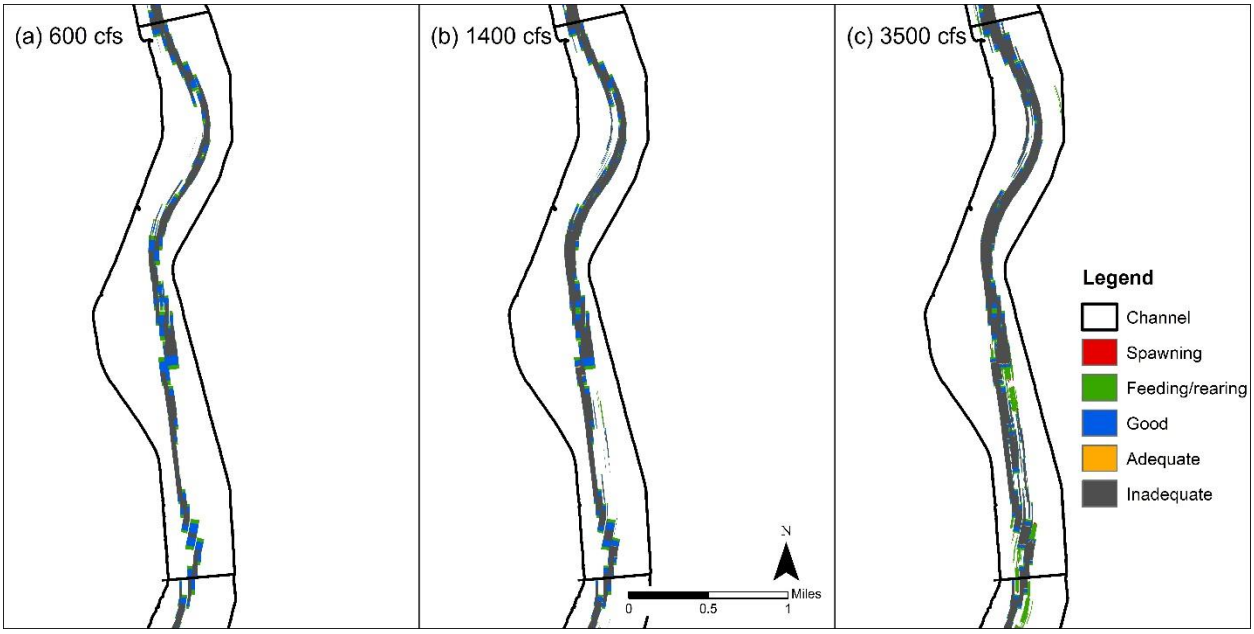
(a) 600 cfs
(b) 1400 cfs
(c) 3500 cfs
N
0
0.5
1
Miles
Legend
Channel
Spawning
Feeding/rearing
Good
Adequate
Inadequate

I6

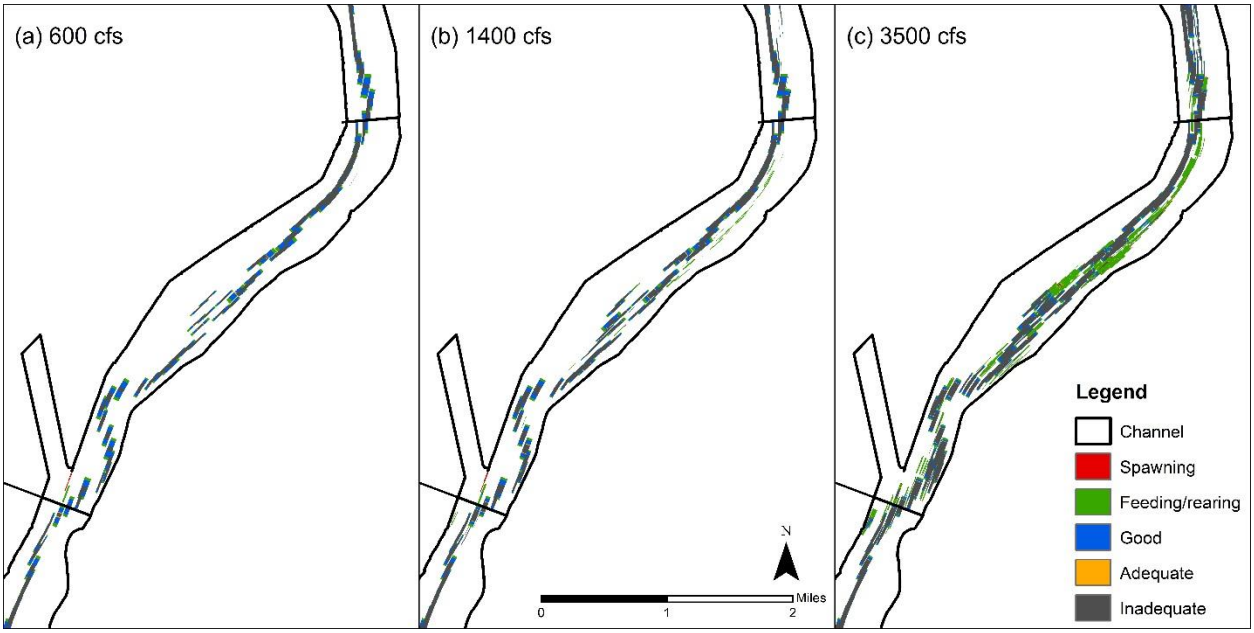
(a) 600 cfs
(b) 1400 cfs
(c) 3500 cfs
N
0
1
2
Miles
Legend
Channel
Spawning
Feeding/rearing
Good
Adequate
Inadequate

APPENDIX D

Silvery Minnow Habitat Scoring System

Introduction

This section outlines how silvery minnow habitat can be analyzed with GIS from aerial photography. It covers the methods, results and discussion of the findings. The analysis is based on finding what habitat features silvery minnows thrive in, identifying those features in the same reach over different years, and seeing how the habitat changes spatially and temporally. Our ultimate goal is to link this analysis to how fish population densities have changed with the habitat.

Methods

Data used/Aerial Photography

Analyzing orthographic aerial photography over many years can show how silvery minnow habitat has changed over time. Once we know how the habitat is changing and how this is related to fish population, habitat suitability can be improved. A link between habitat and population trends can be determined by looking at population data from population monitoring reports by Dudley and Platania (1997). They have been collecting data on the fish population throughout the Middle Rio Grande since 1993. The aerial photographs listed in Table D-1 were used to analyze habitat quality (1992 is also analyzed because it is the closest year to 1993 of aerial photography available):

Table D-1: The year, month and flow corresponding aerial photographs used for this study. Data from Klein et al. (2018a), Swanson et al. (2010) and GIS metadata provided by USBR.

Year	Month	Flow (cfs):
2016	October	40[SA]
2012	January	740[SA]
2008	July	1630[I]
2008	June	4990[I]
2006	January	580[SA]
2005	June	5980[I]
2005	April	4500[I]
2002	February	600[SA]
2001	February	687[A]
1992	February	650[SA]

[I] Isleta gage daily average discharge

[SA] San Acacia gage daily average discharge

[A] Albuquerque gage daily average discharge

The years analyzed are based on availability of data from USBR starting with 1992, so there is not a consistent spacing of years. The uncertainty created by varying image quality is also a limitation of analyzing the photographs. This is a known limitation based on many other studies using aerial photography to map fish habitat quality (Holmes and Hayes 2011; Perschbacher 2011). Other limitations include the flow being variable within the reach and between years, limited amounts of data, the analysis being subjective, limited data aids such as LiDAR and

thermal imagery, and ability to ground truth the data (Holmes and Hayes, 2011; Perschbacher 2011).

An effort can be made to address these limitations. For instance, picking only years that have the same flow can allow the habitat analysis to be compared. 1992, 2001, 2002, 2006, and 2012 all have flows around 650 cfs so these ones are chosen to compare to each other. To keep it as consistent as possible, 2001 is not used because the flow data is from a different gage than the others.

Though it would be useful to analyze habitat that meet the needs of different life history stages of silvery minnows, it is not plausible to do a thorough analysis of this with the given set of aerial photography. High flows around the same value across many years would be necessary to see how much the floodplain inundates and how the habitat quality changes over time. Aerial photography analyzed during low and peak flows can still be analyzed because this can give insight into habitat quality spatially and across different flow regimes. Still, the focus must be on analyzing adult silvery minnow habitat in the main channel because that is the available habitat for the comparable photographs at 650 cfs. Though there are a limited number of photographs to work with, analyzing this low flow of 650 cfs may be very useful because the Middle Rio Grande has experienced lower and less peak flows than it has in the past. This trend is expected to continue, so focusing on lower discharges that don't lead to floodplain inundation may be more a more realistic focus for improving silvery minnow habitat (Drew Baird, personal communication, June 19th, 2018).

To make the analysis as objective as possible, a detailed description of discernable habitat features will be given. This is still a challenge because distinctions between features such as islands, bars, bedforms and shoreline complexity are not always clear. Also, if more LiDAR or thermal imagery data were available that would help as well. Lastly, ground truthing to test the analysis with actual field surveys can be done in the future.

Even with limitations, there are advantages of using remote sensing for habitat analysis. The amount of habitat that can be mapped in a short amount of time can be very useful (Holmes and Hayes 2011; Perschbacher 2011). For this study, it took less than a day to map 50 miles of river habitat. This mapping technique allows a researcher to take a cursory look at a large area and find large-scale trends. Also, this exact type of habitat analysis for this exact reach has not been done before. Therefore, this analysis may yield interesting results (Torres 2007; Klein et al. 2018a).

Criteria Development

The criteria developed is based on literature that discusses physical features of silvery minnow habitat. That criteria from research is then simplified and shortened based on ability to analyze it based quality of aerial photography and practicality. Physical features determined to be

important based on literature include: bankline complexity, main channel complexity, side channels, backwater, bars, islands, confluences, pools, limited suspended sediment, suitable amounts of vegetation, and a correct range of temperatures. These features are important because they are representative of suitable silvery minnow habitat that requires low velocities, shallow depths, diverse habitat, silt and sand substrate, and good water quality (Tetra Tech 2014; Cluer and Thorne 2014; Bovee et al. 2008; Bestgen et al. 2003; Dudley and Platania 1997).

Even though all these features are important, only a handful of these can be accurately measured from aerial photography using GIS. The habitat requirements get narrowed down to low velocities, shallow depths, and habitat diversity (In this criteria diverse habitat is defined as anything that adds to complexity and diversity of the physical habitat topographically or with features such as debris piles). This creates of analyzable features that only include bankline complexity, main channel complexity, side channels, backwaters, bars, islands, and confluences.

There are a few reasons why certain features are not included. For instance, suspended sediment can sometimes be analyzed by looking at the color of the water, yet the aerial photographs vary so much spatially and temporally, it is impossible to analyze visually. Substrate is too hard to analyze because aerial photography from most years is not detailed enough. Also, temperature is something that cannot be seen on the imagery. Isolated pools can be seen from aerial imagery, but it is hard to determine how connected the pools are to the main channel, so they are removed as well.

Vegetation is not included in this list because vegetation is incorporated indirectly through certain habitat features. For instance, vegetation indicates complexity on bars, shorelines, or islands which affects habitat scores. It also affects how wide side channels are, which impacts the habitat area, and the likelihood that a channel would be inundated during high flows. It further adds complexity because vegetation provides shade to regulate temperatures and produces leaf litter. Leaf litter provides nutrients to feed algae and diatoms that in turn feed silvery minnows. Temperature regulation is also very important for the minnow (Tetra Tech 2014; Bovee et al. 2008; Bestgen et al. 2003; Dudley and Platania 1997). Therefore, vegetation density in the active channel is incorporated through other habitat features.

Also, though runs and pools would be useful to identify (Dudley et al. 2016), they are unable to be identified from the set of aerial photography given. Identifying runs and pools have been a focus of other studies identifying habitat features with remote sensing. They were able to do this by using ground truthing to identify where the pools and runs were and use that information to identify the features in aerial photography (Holmes and Hayes 2011; Perschbacher 2011). Ground truthing was not an option for this study. Using agg/deg cross-sectional data from HEC-RAS to identify pools and runs could be an option as well, but these lines are far apart so the data would not be as accurate.

The following schematic in Figure D-1 shows the main features that were considered for the criteria.

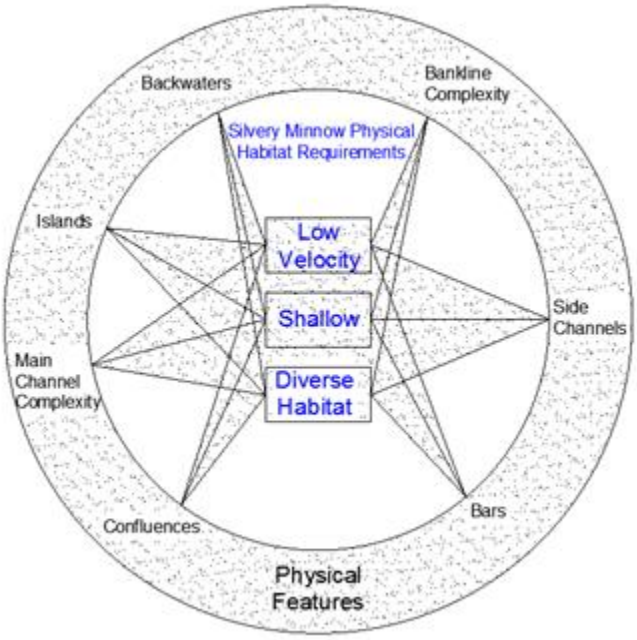

Figure D-1: Habitat requirements that can be seen from aerial photography. All of the physical features have three lines coming out of it and meeting the three requirements listed in the middle of the circle.

Overall, certain physical features that may indicate good quality silvery minnow habitat can be analyzed with GIS from aerial photography. These include features such as backwaters, secondary channels, and debris piles. These components of the river create low velocities, shallow depths and diverse habitats that are crucial for silvery minnow survival. By identifying features in the river, giving those features a score based on habitat suitability, and comparing the scores spatially and across time we can see how the physical habitat is changing.

General Guidelines for Scoring and Mapping

Each habitat feature is identified with a point using GIS and identified with a criterion comprised of a number and a letter. The criteria are correlated with a habitat feature (number), subdivided into the quality of that feature (letter), and given a score based on the quality of the habitat. The score is determined from literature review and is outlined in Appendix E. Tables D-2 to D-4 outline and briefly describe the criteria, what type of habitat it is and the score it receives. The entire outline of features which pictures and a description of what they are is given in Appendix E.

Table D-2: Habitat type, criteria and scores. Scores range from 1-5 and are further explained in Table D-4.

	Shoreline Complexity			Main Channel Complexity		Side Channels					Backwater		Bars			Islands						Confluences	
Criteria:	1a	1b	1c	2a	2b	3a	3b	3c	3d	3f	4a	4b	5a	5b	5c	6a	6b	6c	6d	6e	6f	7a	7b
Score:	4	3	2	4	3	4	3	2	3	5	5	4	5	2	1	3	2	1	1	4	3	4	3

Table D-3: Brief description of habitat types.

Complex Shoreline	1a
Less Complex Shoreline	1b
Less Complex, Less Accessible Shoreline	1c
Main Channel Complexity (Large)	2a
Main Channel Complexity (Small)	2b
Large, Easily Accessible Dry Side Channel	3a
Medium, Easily Accessible Dry Side Channel	3b
Small, Less Accessible Dry Side Channel	3c
Non-Complex Wetted Side Channel	3d
Complex Wetted Side Channel	3f
Large Backwater	4a
Small Backwater	4b
Complex Bar	5a
Simple Vegetated Bar	5b
Simple Unvegetated Bar	5c
Large Unvegetated Island	6a
Small Unvegetated Island	6c
Large Vegetated Island	6b
Small Vegetated Island	6d
Large Complex Island	6e
Small Complex Island	6f
Active Confluence	7a
Inactive Confluence	7b

Table D-4: Score Criteria. Each category depicts habitat that is beneficial to silvery minnows. Score 5 provides the most optimum habitat and score 1 provides the least amount of benefits.

Score	***Habitat Description***
1	Low chance of becoming inundated, in main channel, small features, and low complexity of topography.
2	Low chance of becoming inundated, in main channel or could be in margins, bigger features than 1 or smaller than 3, and low complexity of topography.
3	Medium chance of becoming inundated, in main channel or near shoreline, bigger features than 2 or smaller than 4, and medium complexity of topography.
4	High likelihood of becoming inundated on side channel, or inundated but not very complex in main channel. Bigger features than 3 or smaller than 5.
5	Areas that are currently inundated with water and form complex flow with shallow areas and low velocities. Tend to be isolated from the main channel. Large features with high topographic complexity.

The score given to various features is based on agg/deg polygons (area between each line). For instance, if an island spans over two agg/deg polygons it is given two points. The same is done for every feature including side channels. The longer the side channel, the more points it gets because it provides a larger silvery minnow habitat. Figure D-2a. depicts scoring with islands and channels across agg/deg lines.

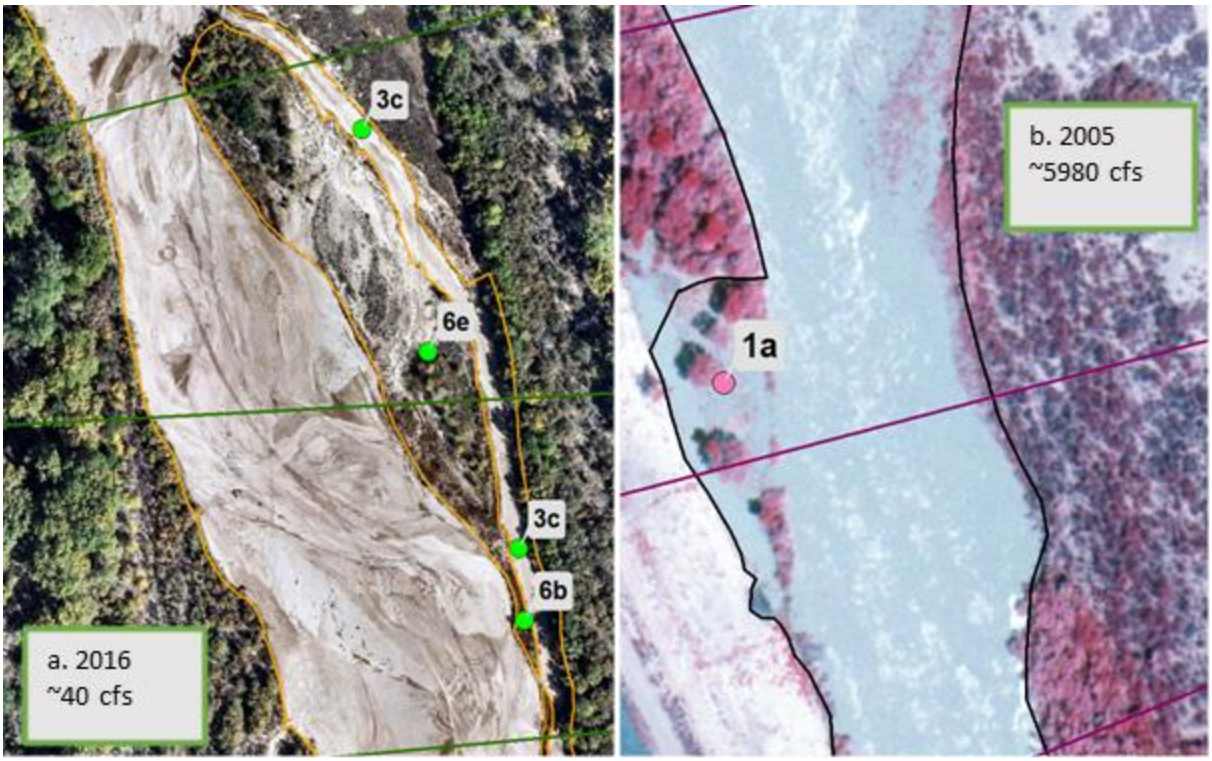

Figure D-2: a. A dry side channel (3c) and islands (6b and 6e) are depicted above in an aerial photograph from 2016. Agg/Deg lines are shown in green lines perpendicular to the main channel. The active channel is outlined in orange. b. 1a depicts shoreline complexity in an aerial photograph from June of 2005. Agg/Deg lines are shown in purple perpendicular to the main channel. The active channel is outlined in black. The flow is going to the bottom of the page for both images.

In Figure D-2a., the channel and the island span over two polygon lengths so they are each given a point in each polygon. This criterion is not exact, but instead an estimate of how many features there are. The criteria are not meant to be exact and map feature areas, but instead depict the number of features that offer suitable habitat to get a general idea of how change is occurring. In Figure D-2b. 1a is counted once instead of twice in this example. Even though the channel complexity spans over two agg/deg polygons, it only occupies the length of one agg/deg polygon, so it is counted once.

For each year, the points are located on a map and the scores are assigned and tabulated. The results are compiled and compared in a few different ways shown in the following sections.

Analysis

Overall Habitat Score

An overall score for each year was calculated as well as a count for how many of each habitat types there were in the Isleta reach.

Subreach Delineation

Each year with available photographs is analyzed. The points are broken up and grouped into subreaches using ArcGIS. Scores given to different habitat types are added up within each subreach and compared across years. Because the subreaches have different areas, the scores are weighted by area by computing the score per square ft. The score is divided by the area and multiplied by a multiple of 10 that makes the data easy to work with. Below is a sample calculation:

Raw score for I1 in 1992:493

Area for I1:46,386,142 ft^2

Multiple of 10: 10,000,000

Normalized score:49346,386,142$ft^2 * 10{,}000{,}000 = 106$

Also, the number of points in each subreach are counted and grouped into categories such as shoreline complexity, side channels, backwater etc. These scores are weighted as well. The following habitat features are grouped into the associated categories in Table D-5. This is done to reduce the number of graphs needed to compare how the habitat changes over time. When the habitat types are quite similar and mainly vary by size instead of quality they were grouped.

Table D-5: Habitat types grouped into broader categories.

Complex Shoreline	1a, 1b, 1c
Main Channel Complexity	2a, 2b
Easily Accessible Dry Side Channels	3a, 3b
Less Accessible Dry Side Channels	3c
Non-Complex Wetted Side Channel	3d
Complex Wetted Side Channel	3f
Backwater	4a, 4b
Complex Bars	5a
Simple Bars	5b, 5c
Unvegetated Islands	6a, 6c
Vegetated Islands	6b, 6d
Complex Islands	6f, 6e
Active Confluence	7a
Inactive Confluence	7b

Agg/Deg Line Delineation

Using ArcGIS, the points were broken up and grouped into agg/deg polygons divided by each agg/deg line. Each polygon was given one value. This value is the summation of the criteria score given to the points based on the type of habitat outlined in the precious section. The polygon was given a color based on its value. The colors in agg/deg polygons were visualized in the six subreaches using ArcGIS.

Results

Overall Habitat Score

Table D-6 summarizes the overall habitat score from 1992 to 2016. Overall, June of 2005 had the highest score and 2016 had the lowest score. The flows in the photographs in these years are also the highest and lowest respectively. The overall scores in between these two flows and those respective years vary and there is not a consistent trend. 1992 and 2002 also have high scores compared to the rest of the years.

Out of the comparable years, 1992 and 2002 are very similar and have higher scores than 2006 and 2012, which have close scores to each other as well.

June of 2005 has the highest score for "shoreline complexity" (1a) followed by April of 2005 because in both of those years the floodplain gets inundated, but less so in April. April of 2005 has the most "large main channel complexity features" (2a), and 2001 has the most "smaller main channel complexity features" (2b). In 1992, the channel has the greatest amount of "wetted side channels" (3d and 3f). The most "dry channels" occur in 2012. There are not any standout amounts of backwater or bars in any of the years. In July of 2008, the most "vegetated islands" occur (6b, 6d). There is not a trend for most "non-vegetated island". More "complex islands" occur earlier in time (6e,6f), and there is not a trend with "confluences".

Table D-6: Summary of total habitat score, flows, and number of habitat types for each year. The comparable years are highlighted in blue.

				Shoreline Complexity			Main Channel Complexity		Side Channels					Backwater		Bars			Islands						Confluences	
Year	Month	Total Habitat Score	Flow (cfs)	1a	1b	1c	2a	2b	3a	3b	3c	3d	3f	4a	4b	5a	5b	5c	6a	6b	6c	6d	6e	6f	7a	7b
1992	February	4025	650[SA]	23	6	7	85	88	0	3	1	211	184	9	7	42	103	58	3	0	11	2	180	147	0	1
2001	February	3300	687[A]	26	6	0	125	103	0	0	3	111	111	1	1	45	26	8	5	6	26	8	216	83	1	1
2002	February	4335	600[SA]	17	10	0	153	45	0	10	4	181	142	3	12	73	158	28	19	7	16	16	293	45	0	0
2005	April	3447	4500[I]	138	16	5	168	59	8	2	4	84	84	2	0	101	8	0	0	1	0	10	118	81	3	0
2005	June	4395	5980[I]	340	8	1	55	50	8	16	7	64	128	16	2	140	23	0	0	9	5	24	147	79	1	1
2006	January	3081	580[SA]	45	33	2	42	76	8	75	3	124	65	21	14	24	140	33	6	2	16	7	156	56	2	1
2008	June	3050	4990[I]	81	9	0	30	22	0	0	1	193	39	8	1	143	16	1	0	33	0	33	148	82	2	0
2008	July	2905	1630[I]	38	35	11	7	35	7	31	24	165	123	12	8	17	40	13	3	109	9	54	128	45	1	1
2012	January	3501	740[SA]	65	35	5	68	57	23	146	11	82	89	6	5	43	79	29	14	58	19	35	135	76	2	0
2016	October	719	40[SA]	16	9	9	11	25	0	7	0	33	10	4	4	7	32	41	5	12	36	3	10	3	0	6

Note: Flows at different gages are given the follow subscripts: [I] Isleta gage daily average discharge, [SA] San Acacia gage daily average discharge, [A] Albuquerque gage daily average discharge

Table D-7 shows that I3 and I2 have the highest scores followed by I4. Also, I5 and I6 score the lowest. The total scores for the four years with photographs taken around 650 cfs are compared in Figure D-3. Figure D-3 shows subreach I2 has overall highest scores for all years, whereas I5 and I6 contain the lowest scores of each of the years. For instance, in I6, the lowest scores occur for all years except for 2006 which occurs in I5. The scores in 2006 and 2012 generally tend to be slightly lower than those in 1992 and 2002.

Table D-7: Total weighted score by subreach. Summation of all years combined.

Subreach	Score
I1	771
I2	863
I3	884
I4	840
I5	591
I6	649

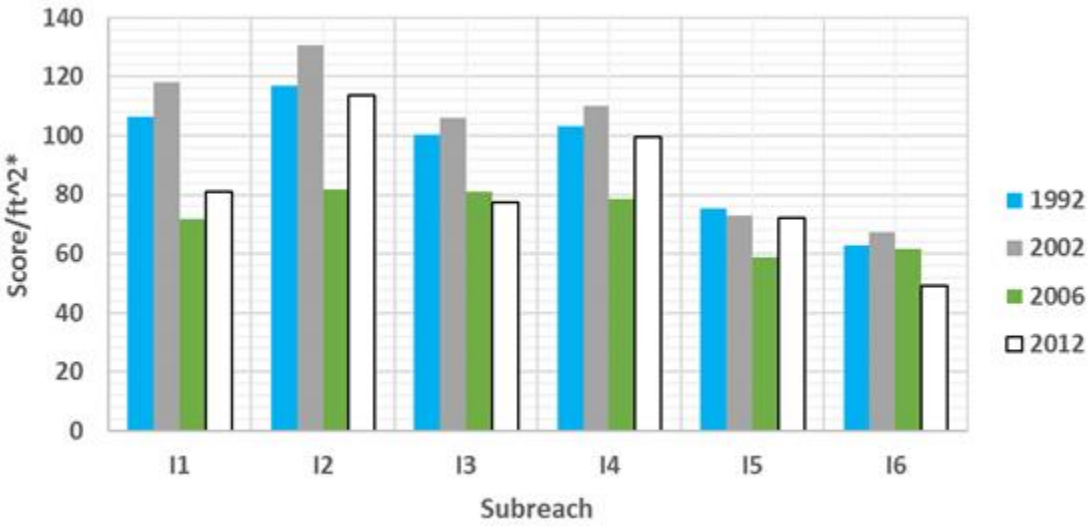

*Figure D-3: The column graph shows the overall habitat scores in each of the four comparable years in each subreach. *Score/ft^2 is the score weighted for area of the subreach as discussed in Appendix D.*

As seen in Figure D-4, the complex bars have shown to be decreasing over time. Complex bars seem to be more abundant in 1992 and 2002 compared to 2006 and 2012. Looking at similar graphs like this one that are listed in Appendix F, there are other trends that can be analyzed. For instance, complex islands, non-complex wetted side channels, and bedforms have generally decreased over time. Shoreline complexity, easily accessible dry side channels and vegetated

islands have increased over time. The rest of the parameters don't show consistent enough patterns to draw conclusions from.

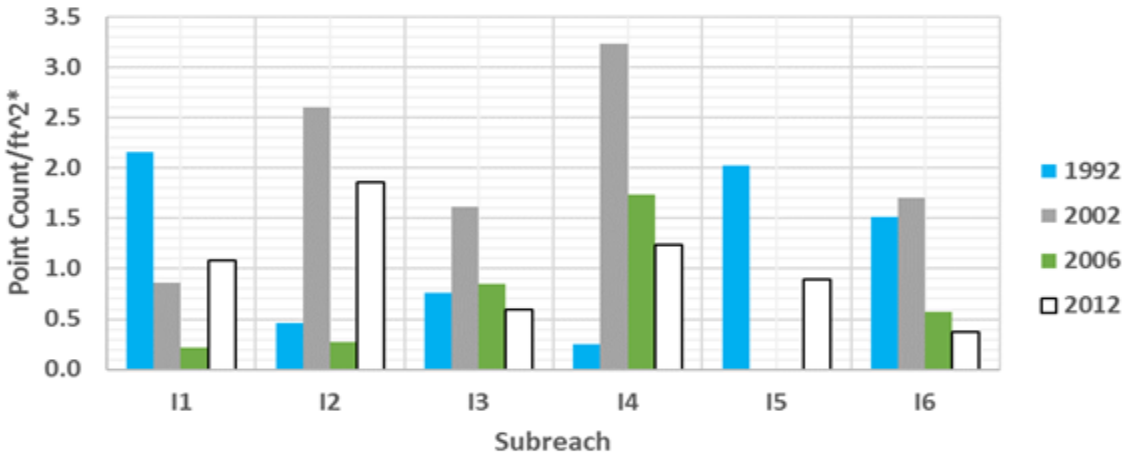

*Figure D-4: The column graph shows the amount of complex bars in each of the four comparable years in each subreach. *The point count/ft^2 is the number of points counted and weighted for area of the subreach as discussed in Appendix D.*

The overall scores comparing all years are shown in Figure D-5. The highest scores in the subreaches tend to occur in 1992, 2002, and June of 2005. The lowest scores occur in 2016 and July of 2008 somewhat consistently. All other years and flows vary and are middle of the range of high and low point counts/ft^2. Subreach I3 has the highest cumulative score when adding all years together. It is closely followed by I2. Subreaches I5 and I6 have the lowest scores.

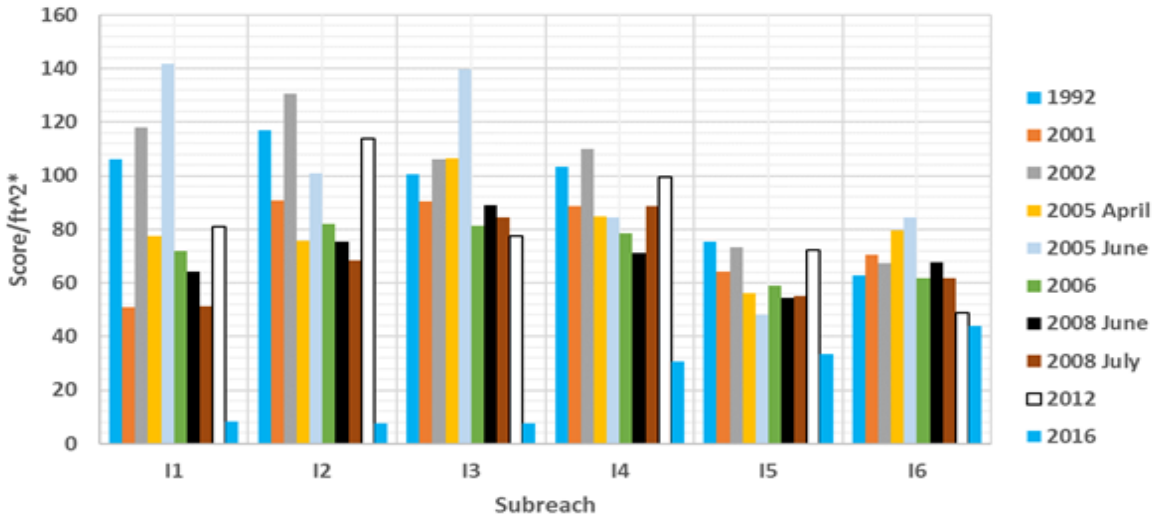

*Figure D-5: The column graph shows the overall score in every year in each subreach. * Score/ft^2 is the score weighted for area of the subreach as discussed in section 5.2.4.2.*

On Figure D-6, the green color illustrates the highest scores, red shows the lowest score, and yellow falls in the middle range of scores on the spectrum. In Figure D-6, the highest scores are shown in June of 2005 for subreach I1 because it appears to have the highest proportion of green polygons. 1992 and 2002 also have a high proportion of green and yellow polygons compared to other years, showing higher scores in more places. July of 2008 appears to have the lowest scores for the I1 subreach. The rest of the subreaches for the Isleta reach are in Appendix I.

Agg/Deg Line Delineation

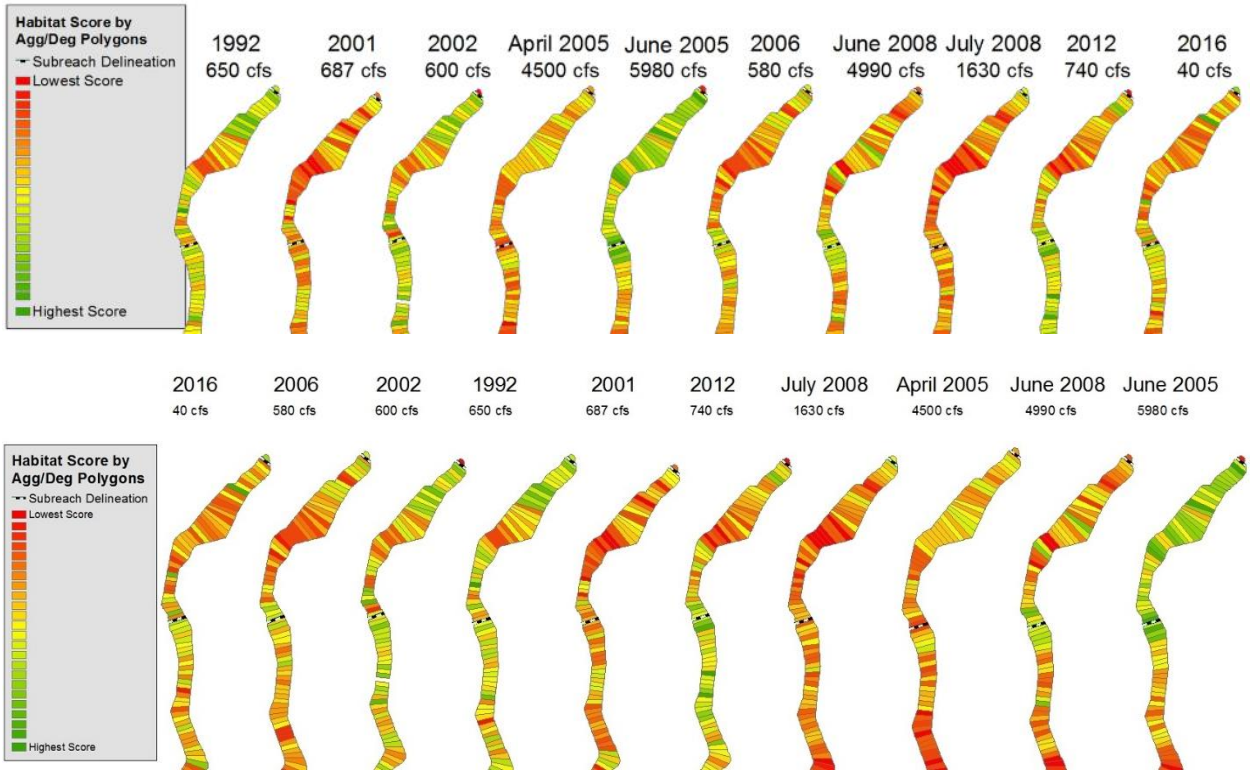

Figure D-6: Subreach I1 summation of habitat scores indicated by the color scheme in the legend and separated by agg/deg lines. All years are shown here with the discharge when the photographs used for this scoring scheme were taken. I1 is at the upper half of the images and the lower portions below the subreach delineation are part of the next subreach (I2). The upper figure shows the color-coded scores in chronological order. The lower figure shows the same results in order of increasing discharge.

All the subreaches vary in habitat quality over the years. There are not strong trends, but some years have more consistently higher or lower scores than the others. For instance, 2006, 2008 of July, and 2016 have higher proportions of red polygons. Also, 1992, 2001, 2002 June of 2005, and 2012 tend to have more green polygons in their subreaches.

Looking at four years with around the same flow, 1992 and 2002 appear to have higher scores in this subreach compared to later years (Figure D-7). Subreaches I2-I6 are in Appendix J. There is not a consistent trend when compared these four years over the whole reach. By taking a cursory look at how many green polygons appear in each subreach in each year, the order of higher to lower quality habitat can be estimated. Year 1992 has the highest number of green polygons, then 2012 and 2002 are very similar and 2006 has the lowest scores.

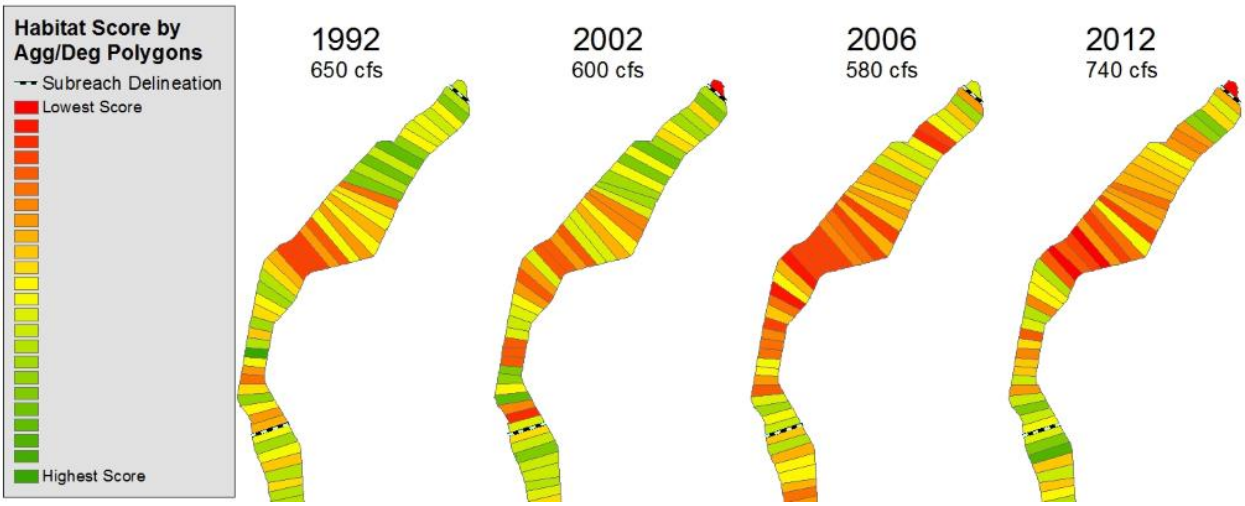

Figure D-7: Subreach I1 summation of habitat scores indicated by the color scheme in the legend and separated by agg/deg lines. Only years around 650 cfs are shown. 2001 is excluded because location of the gage is far away from this study site, so this information is not as accurate.

Discussion

The overall habitat score, subreach delineation scores, and agg/deg line delineation figures generally share the same results. Looking at the comparable discharges, 1992 and 2002 have better habitat than 2006 and 2012. This makes sense because habitat quality for silvery minnows in the Middle Rio Grande has been decreasing over time (Scurlock 1998; Bovee et al. 2008; Tetra Tech 2014).

When comparing all the years 2002, June and April of 2005, and 1992 consistently have the highest scores. Year 2006, July of 2008 and 2016 generally have the lowest scores. By subreach, I1-I3 have the highest scores for these years. Year 2016 has the lowest score by far because the river is dry for a lot of this reach, so it provides minimal habitat for silvery minnows. June of 2005 has the highest score mostly likely because of its high flow. By looking at the aerial photography, it is evident that the floodplain is inundated. This is further supported by the fact that there is significant overbank inundation at 5000 cfs in this reach (Tetra Tech 2014) and the aerial photographs in this year are taken when the flow was 5980 cfs. Habitat quality also increases with discharge from 3500 cfs-7000 cfs (Tetra Tech, 2014) as mentioned before. Floodplain inundation is extremely important for the survival of silvery minnows, especially during their spawning stages (Dudley and Platania 1997; Tetra Tech 2014; Bovee et al. 2008;

Klein et al. 2018a). Also, it has been shown that “prolonged high flows during spring were most predictive of increased density” (Dudley et al. 2016). It is also interesting to note that there are no other photographs that captured a flow above 5000 cfs which may be why the other sores are not as high as June in 2005. April of 2005 also has a flow that causes a small amount of inundation which would explain why it has higher habitat scores.

The scores may be low in July of 2008 due to the flow of 1630 cfs. This flow is sub-optimum for silvery minnow as suggested by a study done on silvery minnow by Bovee et al. (2008). The study was done in 2008 in a few small reaches (1-2 km each) downstream of the Rio Puerco and upstream of the San Acacia Diversion dam. They mapped out adult and juvenile hydraulic habitat in the study areas at flows up to 1000 cfs. Looking at connectivity, woody debris, depths and velocities, they found that habitat areas were reduced when flows exceeded 150 cfs mainly because of flow depth and velocity as shown in Figure D-8. In stream habitat such as connectivity and woody debris decreased over time as well for flows exceeding 150 cfs (Bovee et al. 2008).

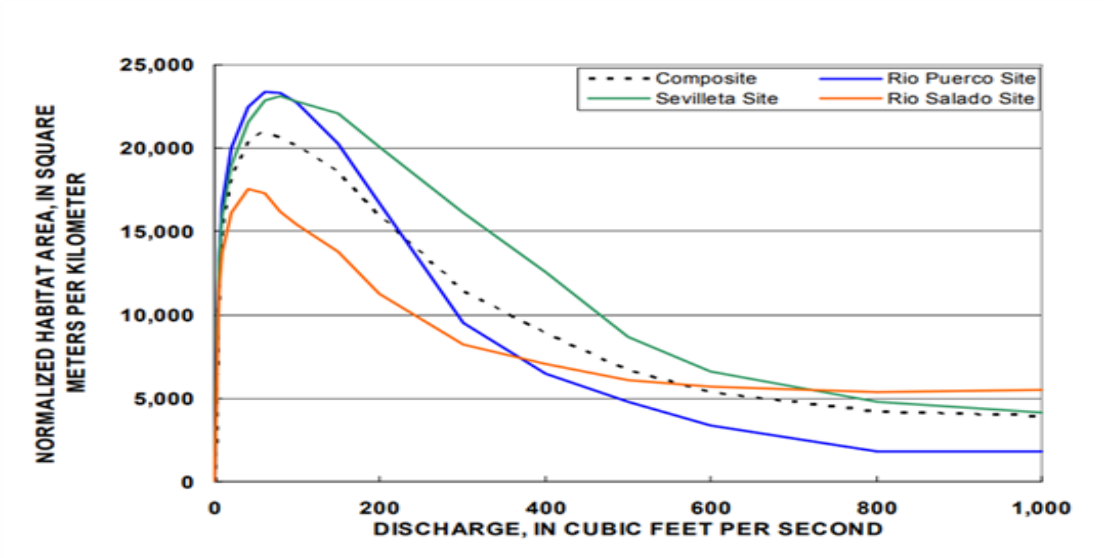

Figure D-8: Habitat area for silvery minnows (H. amarus) from Bovee et al (2008).

By subreach, I2 and I3 have the highest score and I5 has the lowest. This may be because subreach I3 is the most sinuous as shown in Figure 30. Subreach I2 has the highest width and wetted perimeter, as well as the lowest velocity and depth. These parameters are consistent with good habitat for silvery minnows. Subreach I5 has the least number of jetty jacks installed to channelize the river, so the opposite result would be expected. The density of the jetty jacks in other subreaches doesn’t vary greatly, so it does not help explain variations in those subreaches. There are not many obvious trends or geomorphic landmarks that would explain differences in the other subreaches either.

Complex islands, complex bars, wetted side channels, and bedforms decreasing could mean that overall, the channel is becoming less braided and complex. Dry side channels are also becoming more abundant as well as vegetated islands, meaning the main channel is becoming more incised and the side channels becoming abandoned. Vegetated islands also increase if higher flows are also less frequent. Vegetation has time to develop on islands and have strong roots before getting washed away if high flows don't occur often (MEI 2006).

APPENDIX E

Detailed Habitat Criteria

Bankline complexity:

Bankline complexity criteria

1a. Bankline juts out greatly, forms a small inlet, is rocky or has diverse substrate (vegetated islands, sandy banks and water inundating some parts of the bank). Provides a great amount of habitat, potentially causes eddies.	
1b. Bankline juts out or caves in slightly and is somewhat diverse. Provides some amount of habitat.	
1c. Possible access to more complex shoreline during higher flows (outside of active channel so it is less accessible)	

Bankline complexity scores

	Shoreline Complexity		
Criteria	1a	1b	1c
Score	4	3	2

Complex margins, or shorelines, are very important for silvery minnow habitat because they cause lower velocities, eddies, and shallower waters (Bovee et al. 2008). 1a has the most complex shoreline with inlets, channels that cause eddies, lower velocities, and diverse water

levels. This is not classified as backwater because backwater has a more definite channel away from the main flow. Backwater is also more isolated from the main channel, so it would have lower velocities and would score higher than 1a. Type 1b offers a refuge, yet it is a simple inlet and the area of complexity is not as large as 1a, so it counts for less habitat points than 1a. Type 1c is even less diverse and gets the lowest score for bankline complexity. It has the potential to become inundated and provide habitat, but it is less accessible than bankline in the active channel. Most banklines analyzed have an active channel outline (provided by USBR) that matches with the water surface. In 2016 though, the water surface is much lower than the active channel, so channel complexity is based on the active channel outline instead of the water surface.

Main Channel Complexity:

The clarity and quality of aerial photographs varies across years, within the reaches, and between different flow conditions. This makes it hard to analyze small features of the habitat criteria across the years of photographs provided. For instance, debris piles and bedforms can only be distinguished in highest quality photographs from 2016. Figure E-1 shows the difference in quality of the photographs.

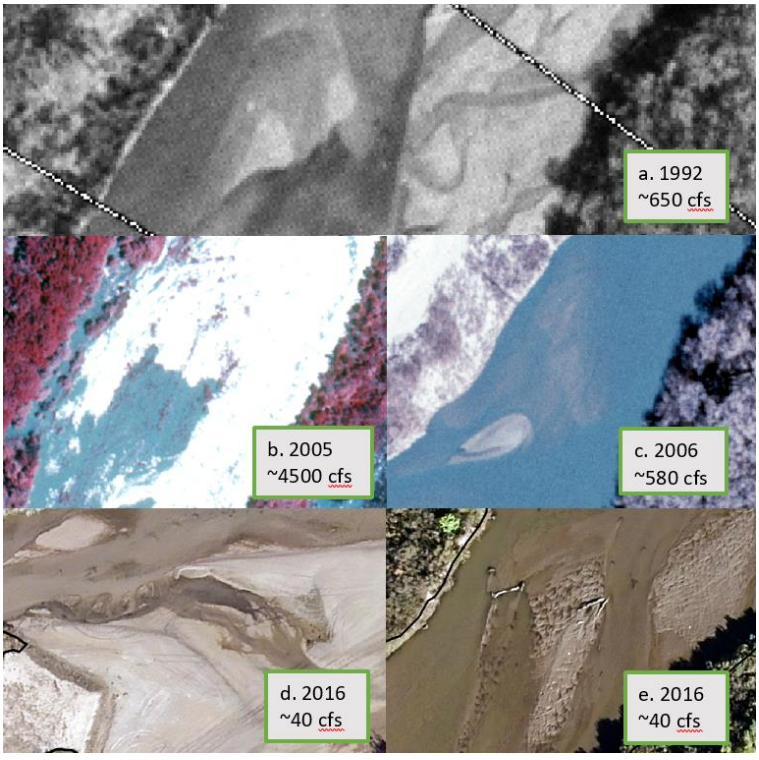

Figure E-1: A set of aerial photography that shows the differences in close-up quality. The zoom in each picture is as follows: a. 1:1000, b. 1:1500, c. 1:800, d. 1:600, e. 1:500). 1992 zoomed away by twice as much as 2016 gives a much more pixilated image than in 2016. 2016 has much better resolution even compared to 2006 (and 2008 which is not depicted here). 2005 has areas where light is reflecting off the water that makes it difficult to see what is happening in the channel. It also depicts the variability of flows and how that affects what is seen.

Therefore, lumping together features that require close-up analysis that create main channel complexity is necessary. These features include bedforms, low flow complexity, substrate or formations causing shallow waters, and debris piles.

All these images vary by a great amount, but they all depict low flow features that are diverse so they could all be identified as the same criteria (2a). Counting these smaller features together does not change the overall score very much because they all serve similar purposes of creating complex flow, eddies, and shallower waters. For example, in 2016 (2d.) more of the river is exposed, so it appears much more complex at a low flow. Type 2e. is in a higher flow area, yet it has debris piles and bedforms that cause ripples which could be suitable as well. In the bottom left corner of 2b. and center of 2c. images, bedforms or low geologic features could be the result of what is seen. These look like shallow and physically diverse areas, so they receive a high suitability score as well. In 1992, the complexity is hard to see at a small scale, but shallow areas with various geomorphic features can still be identified.

Main channel complexity criteria

2a. Large debris piles/low-flow complexity in the main channel (possibly braided). Large substrate/ formations create shallow depths	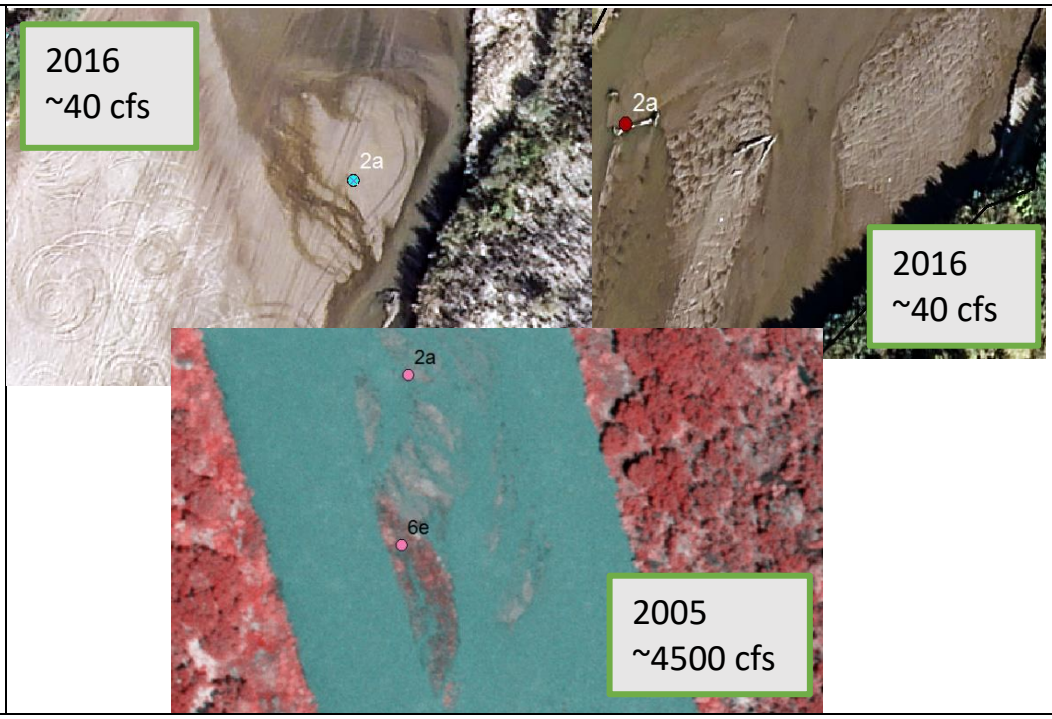

2b. Small to Medium sized debris piles/low-flow complexity in main channel. Medium substrate/ formations create shallow depths	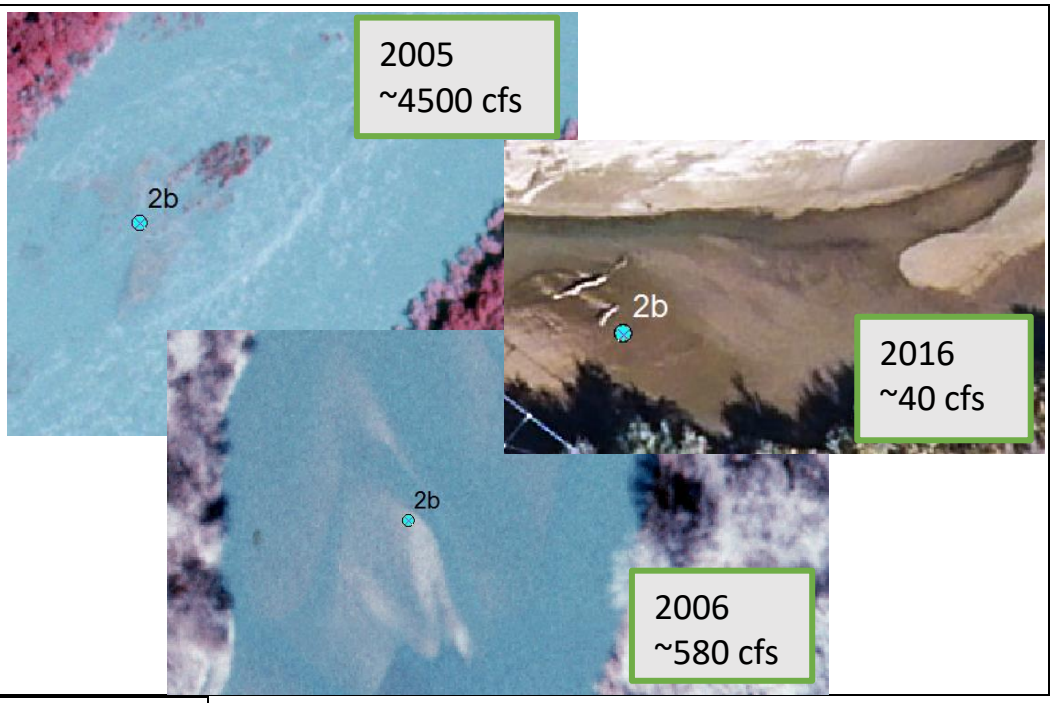

	Main Channel Complexity	
Criteria	2a	2b
Score	4	3

Main channel complexity scores

In-channel complexity, extensive debris piles, bedforms and formations are depicted in above. Bedforms, channel complexity and debris piles all offer suitable habitat for fish (Bovee et al., 2008, Cluer and Thorne 2013, Tetra Tech, 2014). Therefore, main-channel complexity scores are relatively height. In type 2b, there are images of debris piles and substrate formations that are less extensive as those depicted in 2a figures. Because both 2a and 2b are in the main channel that experiences higher velocities, the scores are not as high as backwater or complex side channels. They are still high because they offer refuge to silvery minnows when side channels or backwaters are not accessible at high flows. Type 2a is given one more point than 2b because it is bigger and generally more complex than 2b.

*Note: 2a is differentiated from an island or mid channel bar based on level of inundation. If the island is underwater so much that it is broken up into too many formations to count, or there is not an obvious continuous stretch of land, it is counted as substrate/formations.

Side channels:

Side channels criteria

3a. Dry bed- 3+ parallel side channels are in active channel. Channels appear accessible and wide	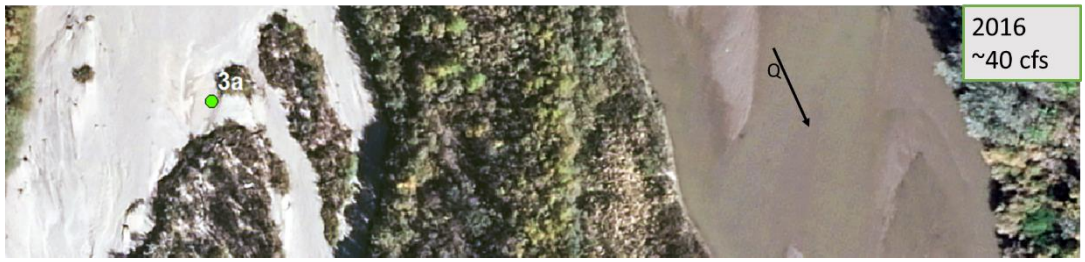
3b. Dry bed- 1-2 side channels are in active channel and appear accessible- wide (50 + feet)	
3c. Dry bed- 1-2 side channels are in active channel and appear accessible- narrow or not as accessible	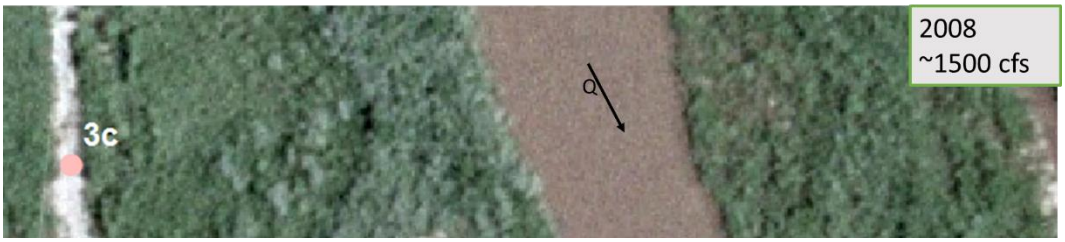

3d. Wet channel- simple and generally not braided- single threaded channel	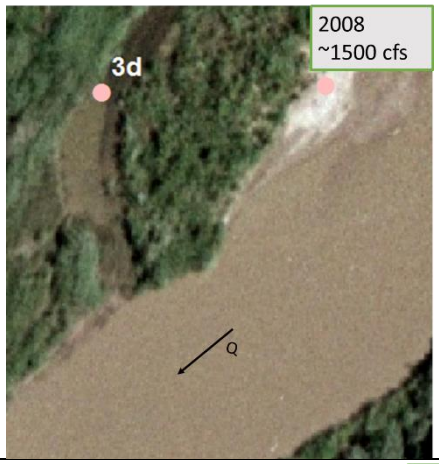
3f. Wet channel- Side channels are complex and winding (may cause eddies and slower flows). 2+ channels- braided	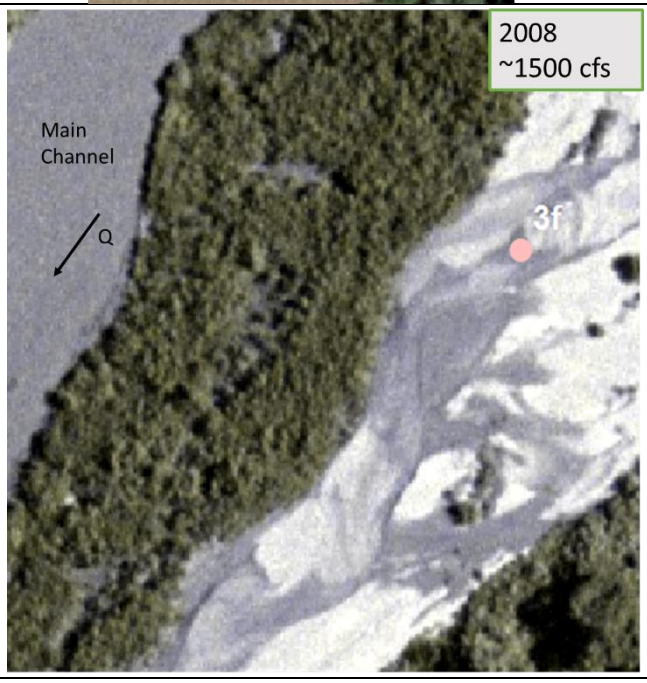

Side channels score

	Side Channels				
Criteria	3a	3b	3c	3d	3f
Score	4	3	2	3	5

A report by Tetra Tech found that complex, braided and anastomosing channels provide the best habitat suitability for silvery minnows (Tetra Tech 2014). Therefore, the more complex and accessible the side channel is, the greater the habitat score. For instance, type 3f has the highest score because it has braided features that create eddies and low velocity flows. Type 3f

is also underwater, so it is proven to be accessible. The next highest ranked is 3a because it is the most complex of the dry channels. If the river gets a large flow, this area could become inundated and create shallow, low velocity complex channels for silvery minnows to occupy (3a-3d and 3f are within the active channel delineated by USBR). Next, 3b and 3d are all ranked the same. Type 3b provides habitat during higher flows, but it is less complex and accessible than 3a channels. Type 3d is ranked similarly because while it is more accessible, there are higher velocities and deeper depths at higher flows. Finally, 3c offers the least suitable habitat because the channels are narrower than 3b channels. Narrow channels offer less habitat area. Also, 3c is narrower because there is a higher density of vegetation, which indicates that this area is less likely to become inundated and provide habitat. Overall, side channels are given relatively high scores because they are essential for high flow situations when the silvery minnow needs to be connected to more diverse areas with slower velocities.

Areas that can become inundated at very high flows are disregarded because they are too hard to analyze the areas beyond the active channel from year to year. The dry channels are identified by being within the active channel. Areas that could become inundated beyond the active channel are too subjective to analyze. For instance, the density of vegetation and previous years of flow areas give an idea of what channels could potentially become inundated. Using LiDAR data also helps with the analysis, but there is only LiDAR available for 2012. This makes analyzing areas that could be inundated in other years inconsistent. Even though potential channels for inundation are highly important for the life cycle of silvery minnows, there is not enough data to effectively analyze them. If there were aerial photographs compared across years that had the same high flow that inundate the floodplain, temporal trends in habitat could be analyzed.

As Middle Rio Grande has become more and more incised over time and peak flows are reducing, the availability of the floodplain habitat is greatly decreasing over the years (Tetra Tech 2014). Because the analysis is focused on the main channel for adult silvery minnows (all that can be analyzed across years at about 650 cfs), channels accessible during a large flood are not considered. This channel would be called 3e, but it was removed from the analysis.

*Note: Type 3f could be confused with 1a because it is near the shoreline. They are differentiated because 3f is generally a complete, yet braided, channel with many offshoots. Type 1a does not have continuous flow through that section and does not take the form of a channel. Type 3f is generally more extensive than 1a.

Hydraulic backwater:

Hydraulic backwater criteria

4a. Backwater extending back > 100 ft, wide and appear accessible	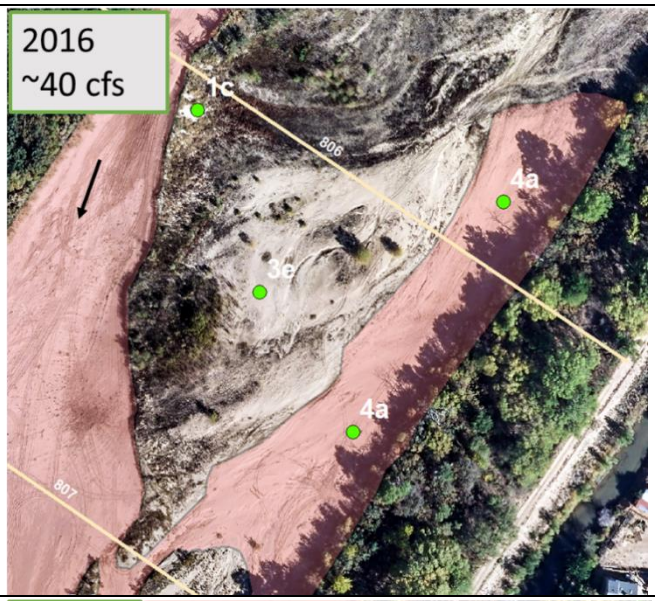
4b. Backwater extending back < 100 ft, not as accessible or wide	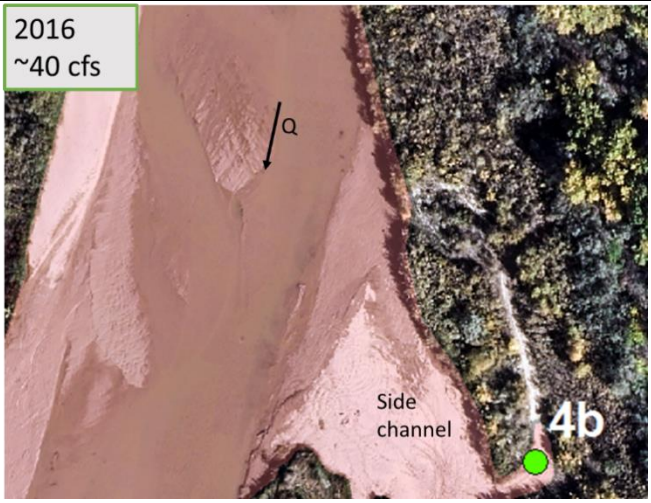

Hydraulic backwater scores

	Backwater	
Criteria	4a	4b
Score	5	4

The backwater is determined by the active channel outline provided by USBR. In the figures depicting 4a and 4b, the water does not actually flow in these channels, yet it has been delineated as a place where water would normally flow. Backwaters are an essential

component of silvery minnow habitat because they provide very low velocities that are near zero. The backwaters are especially important for larvae and juvenile silvery minnows when they first hatch and grow (Bovee et al. 2008). Type 4a is much larger than 4b so it provides more suitable habitat, and therefore receives a higher score.

Bank-attached bars:

Bank-attached bars criteria

5a. Bar is large and provides shallow channels and complex habitat	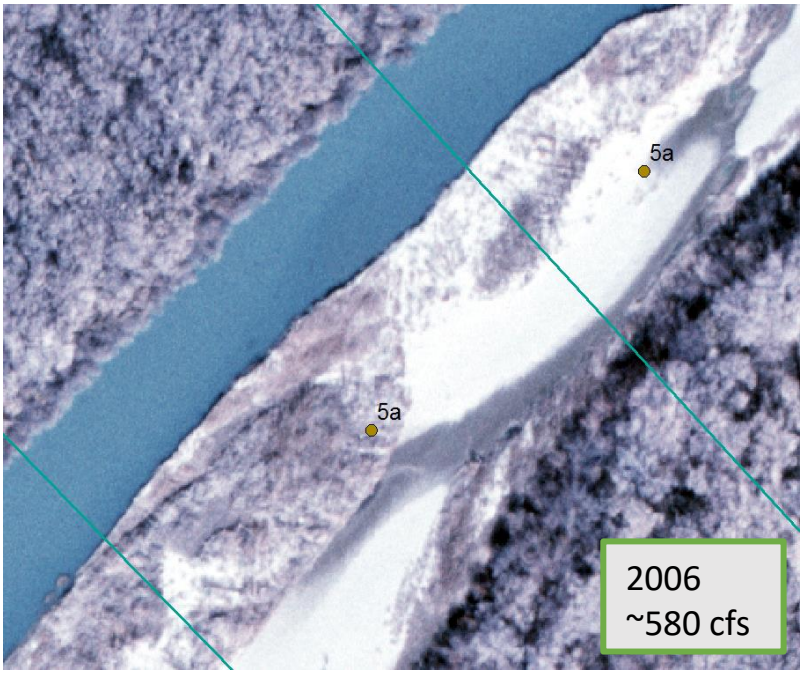
5b. Bar is small and provides some silvery minnow habitat (some vegetation)	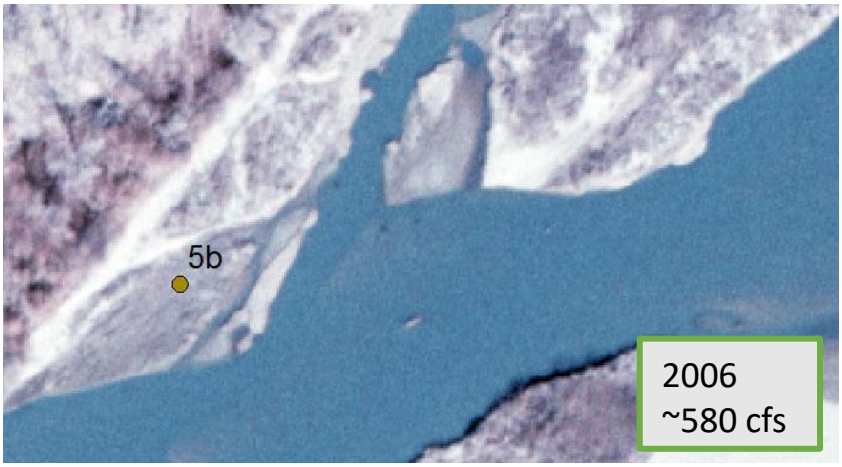

5c. Non-vegetated bar with little geomorphic variability	

Bank-attached bars scores

	Bars		
Criteria	5a	5b	5c
Score	4	2	1

Bars provide some habitat during high flows, yet they do not provide extensive spawning areas for silvery minnows. Because bank-attached bars are not very complex in their topography, only the most complex and extensive structural features provide in-channel habitat. Even when their complexity is evident and may provide some in channel habitat for adults, this does not always translate into optimum spawning habitat (Tetra Tech 2014). Bars still provide important habitat features during higher flows because they offer shallower habitat than the main channel if they become inundated, so they are given a relatively high score. The more complex the bar, the more suitable the habitat is for silvery minnows. For instance, 5a is generally characterized by having more complex geomorphic features, small side channels or vegetation that would provide lower velocity areas and shelter from predators (Cluer and Thorne 2014). Type 5a bears similarity with 1a (shoreline complexity), but they must be differentiated. Type 5a is identified as being much larger and wider than 1a. Type 5b has less of these features, and 5c does provide overall shallower habitat at higher flows, yet it adds little topographic complexity to the habitat.

Islands/Mid-channel Bars:

Islands/mid-channel bar criteria

6a. Large and non-vegetated 6c. Small and non-vegetated	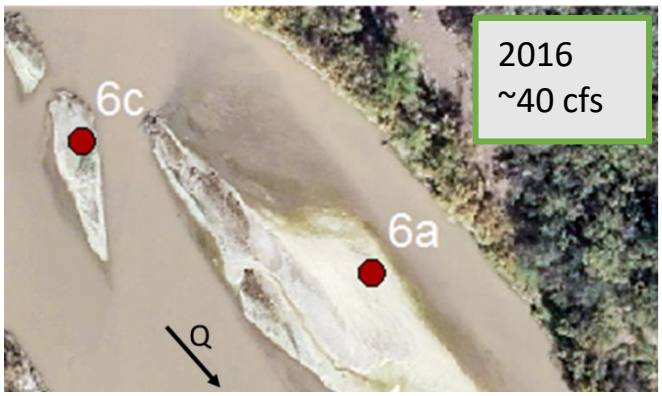
6b. Large and vegetated 6d. Small and vegetated	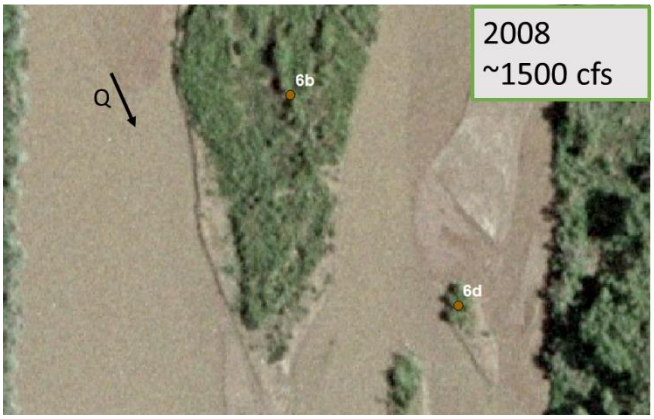
6e. Large- Some vegetation and some bare ground (Around 50% uniform veg cover over whole island). Could also have shoreline complexity or braided features within island. 6f. Small- Some vegetation and some bare ground (Around 50% uniform veg cover over whole island). Could also have shoreline complexity or braided features within island.	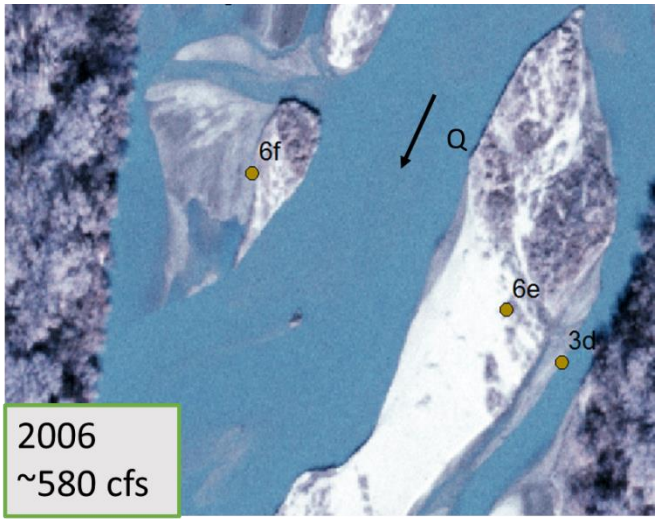

Islands/mid-channel bar scores

	Islands					
Criteria	6a	6b	6c	6d	6e	6f
Score	3	2	1	1	4	3

Islands in this section area defined as not being attached to the bank and are also referred to as mid-channel bars. An island or mid-channel bar is differentiated from a bank-attached bar based on what it is surrounded by. If there is an obvious, continuous separation from the bar and the shoreline, it is considered an island/mid-channel bar. It can be surrounded by water on both sides, a dry channel on both sides, or water on one side and dry channel on the other. A bank-attached bar has no major side-channels going through it that cause obvious and continuous separation from the bank.

Islands provide habitat to silvery minnows in a similar manner to bank-attached bars. During higher flows, the islands could become partially or fully inundated which helps in-channel habitat, yet it is not necessarily most suitable for spawning (Tetra Tech 2014). Type 6e gets the highest score because it generally has some vegetation, small channels or backwaters within the island providing complex topography and habitat. Type 6f is a smaller version of 6e so it gets a lower score by one. 6a has no vegetation which indicates it is more accessible at higher flows, and 6b is less accessible because it is densely vegetation. Therefore, 6a has a slightly higher score than 6b. Small islands that are not complex have little to no impact on habitat suitability (Tetra Tech 2014) so these are given the lowest score (6b and 6c). A large island (6a,6b,6e) is considered to reach across one agg/deg polygon, and a small island (6c,6d,6f) spans across half or less of the polygon. Exceptions to this rule may occur when an island is very skinny so it may be considered small instead of large even if it spans across the entire polygon.

Confluences:

Confluences criteria

7a. Active confluence- wet	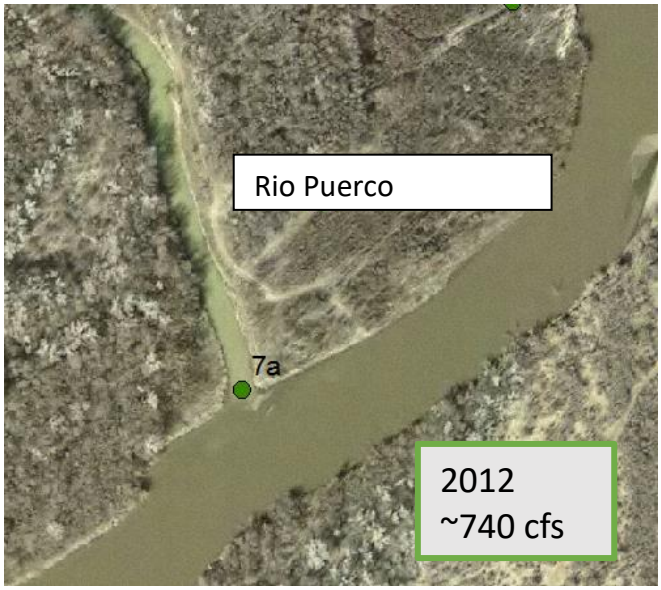
7b. Active confluence- dry	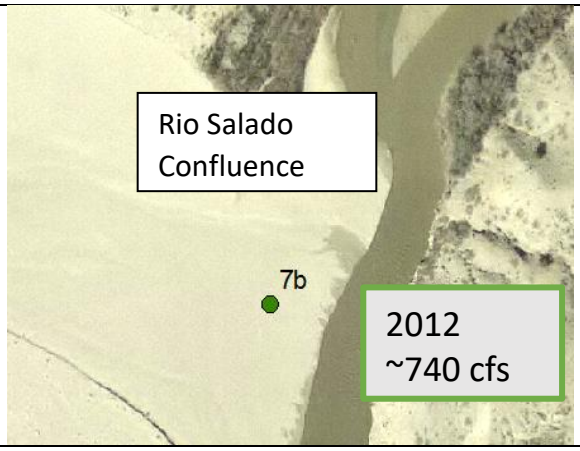

Confluence scores

	Wet Confluence	Dry Confluence
Criteria	7a	7b
Score	4	3

Confluences are spots where eddies, accelerating and decelerating velocities, sediment deposits, and large wood tend to accumulate. These factors create ecological hotspots (Cluer and Thorne 2014). Confluences are given a relatively high score because of this. If the confluence does not appear to be active or is disconnected from the Rio Grande, it is not

included in the analysis. Also, spots where irrigation canals are not counted as confluences because their flow is variable and cannot be compared across years. While these aren't counted as confluences, they are designated as shoreline complexity or backwater depending on how the "irrigation confluence" interacts with the main channel. Wet, active confluences are given a higher score than dry ones because they provide habitat instead of just channel margin complexity.

APPENDIX F

Habitat Counts (Years with flows around 650 cfs)

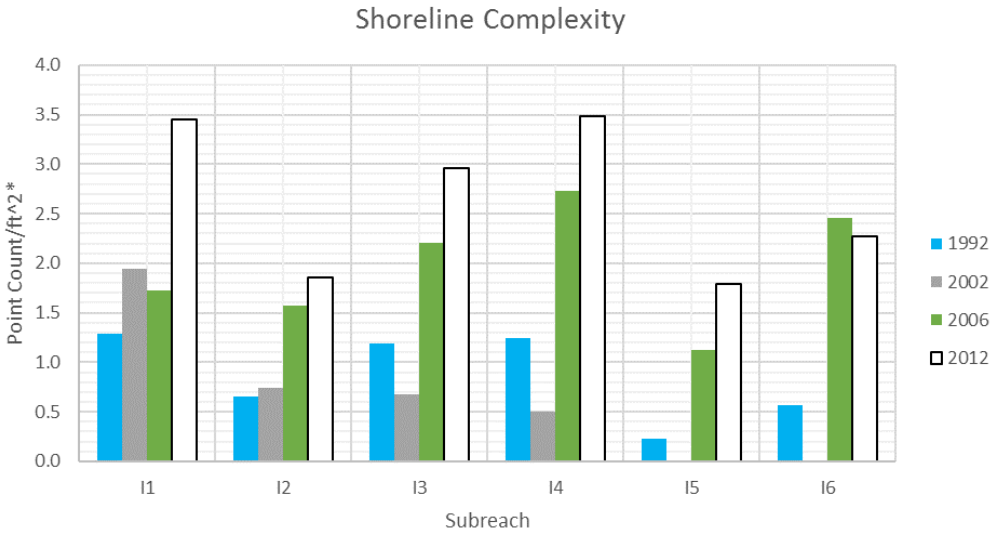
Shoreline Complexity
Point Count/ft^2*
4.0
3.5
3.0
2.5
2.0
1.5
1.0
0.5
0.0
I1
I2
I3
I4
I5
I6
Subreach
1992
2002
2006
2012

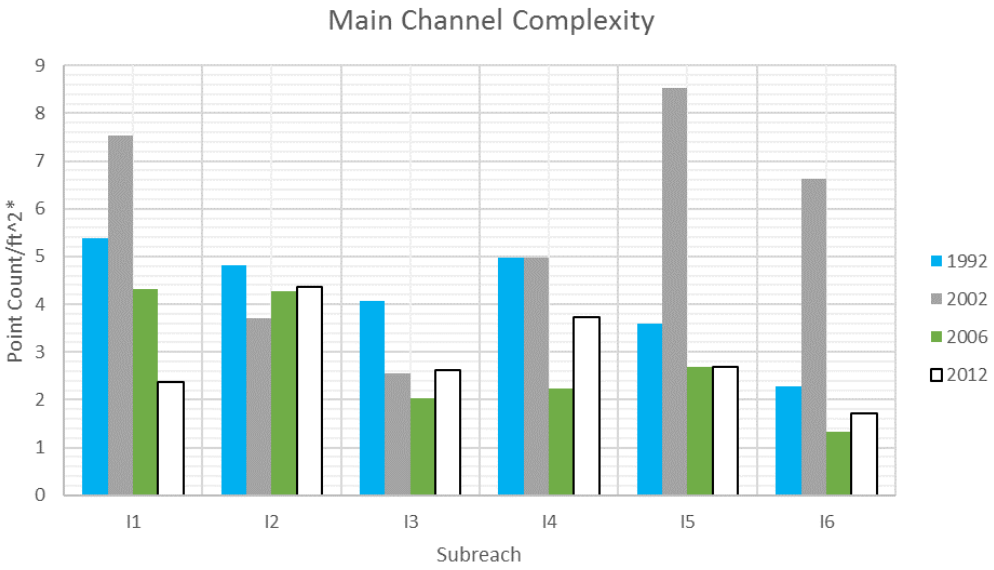
Main Channel Complexity
Point Count/ft^2*
9
8
7
6
5
4
3
2
1
0
I1
I2
I3
I4
I5
I6
Subreach
1992
2002
2006
2012

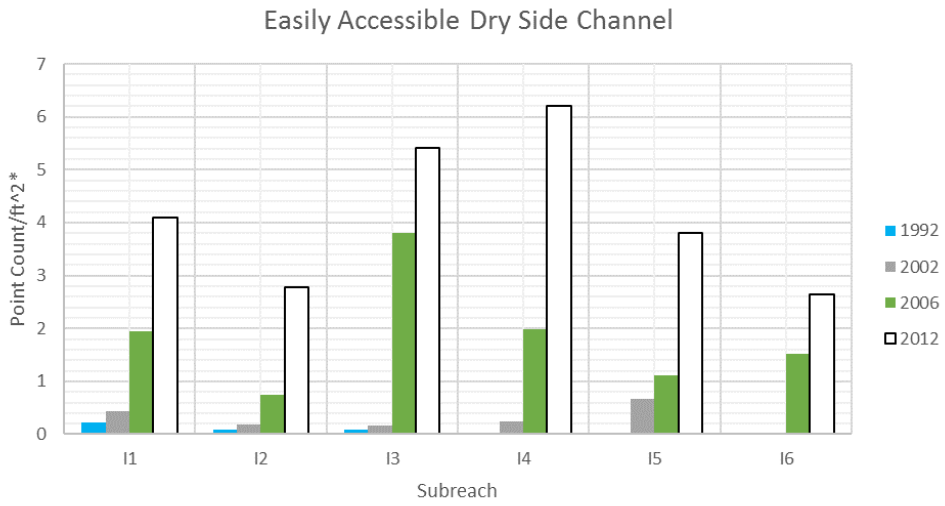
Easily Accessible Dry Side Channel
Point Count/ft^2*
0
1
2
3
4
5
6
7
I1
I2
I3
I4
I5
I6
Subreach
1992
2002
2006
2012

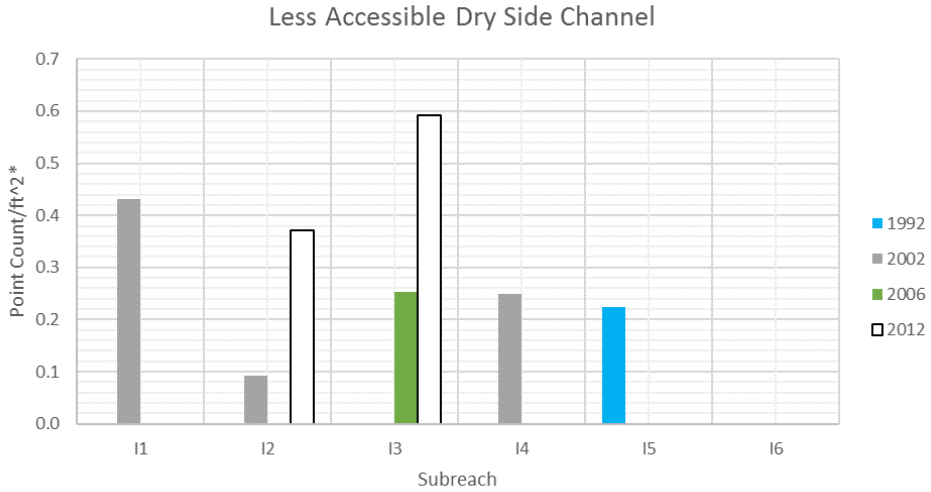
Less Accessible Dry Side Channel
Point Count/ft^2*
0.0
0.1
0.2
0.3
0.4
0.5
0.6
0.7
I1
I2
I3
I4
I5
I6
Subreach
1992
2002
2006
2012

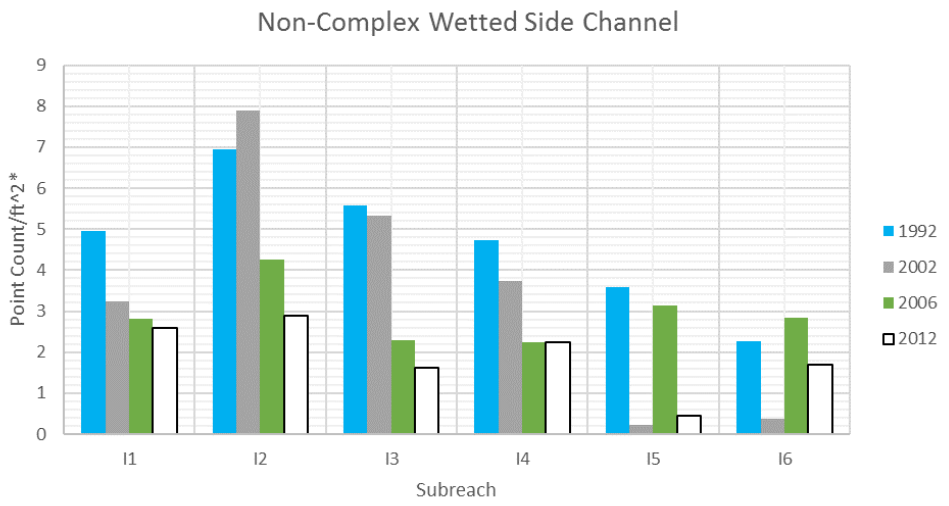
Non-Complex Wetted Side Channel
Point Count/ft^2*
0
1
2
3
4
5
6
7
8
9
I1
I2
I3
I4
I5
I6
Subreach
1992
2002
2006
2012

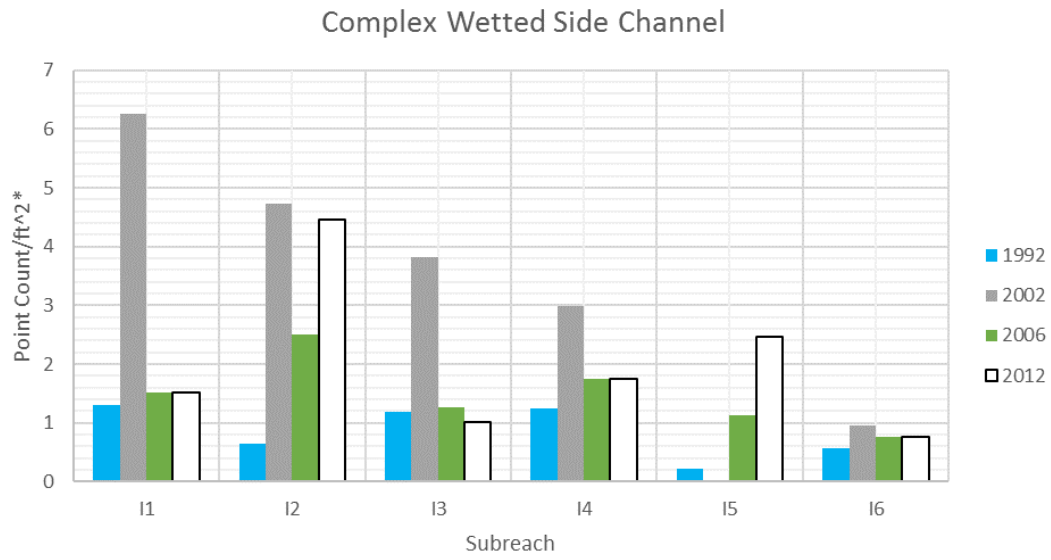
Complex Wetted Side Channel
Point Count/ft^2*
0
1
2
3
4
5
6
7
I1
I2
I3
I4
I5
I6
Subreach
1992
2002
2006
2012

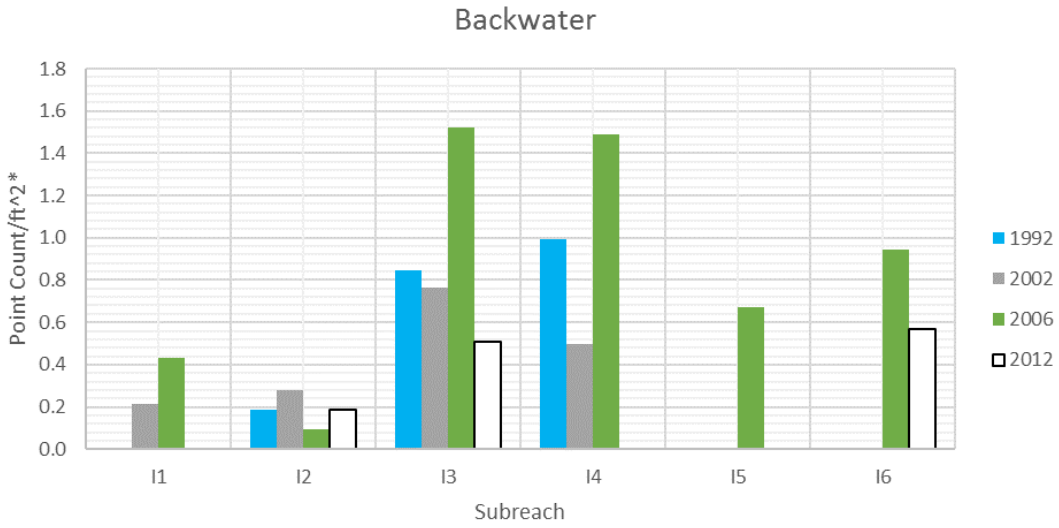
Backwater
Point Count/ft^2*
1.8
1.6
1.4
1.2
1.0
0.8
0.6
0.4
0.2
0.0
I1
I2
I3
I4
I5
I6
Subreach
1992
2002
2006
2012

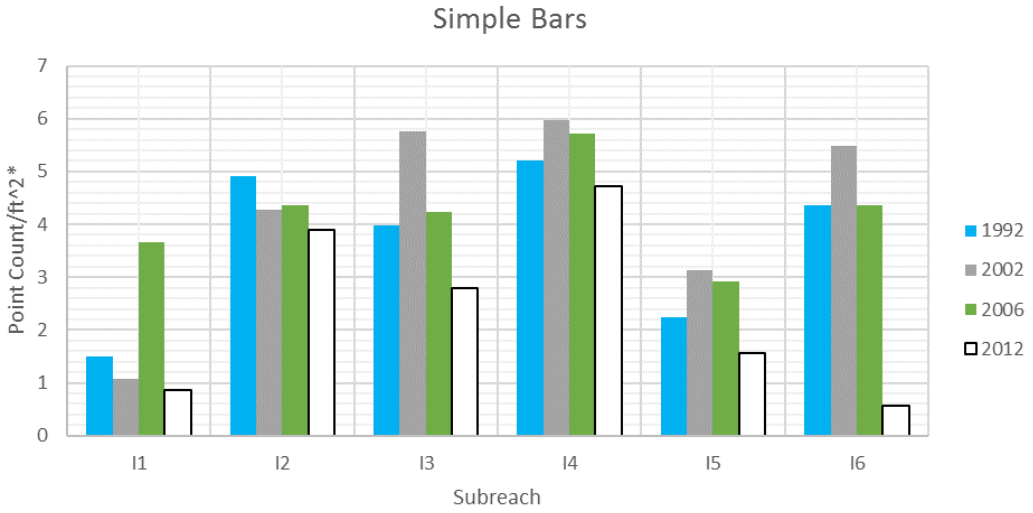
Simple Bars
Point Count/ft^2*
7
6
5
4
3
2
1
0
I1
I2
I3
I4
I5
I6
Subreach
1992
2002
2006
2012

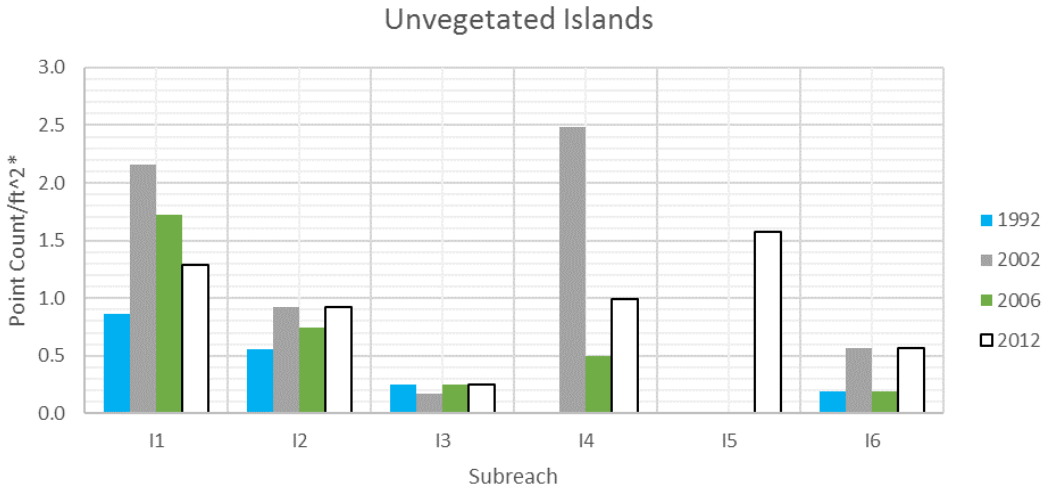
Unvegetated Islands
Point Count/ft^2*
3.0
2.5
2.0
1.5
1.0
0.5
0.0
I1
I2
I3
I4
I5
I6
Subreach
1992
2002
2006
2012

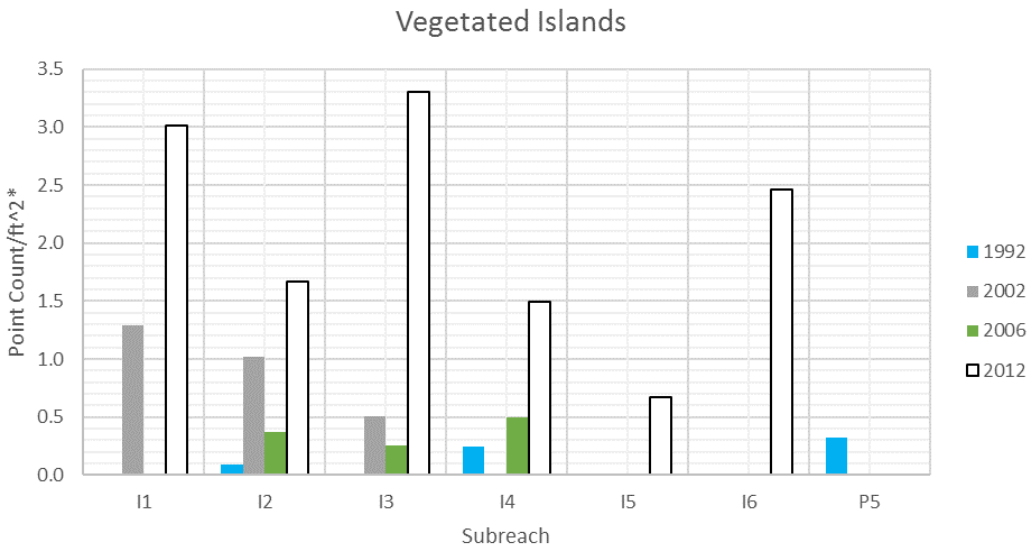
Vegetated Islands
Point Count/ft^2*
3.5
3.0
2.5
2.0
1.5
1.0
0.5
0.0
I1
I2
I3
I4
I5
I6
P5
Subreach
1992
2002
2006
2012

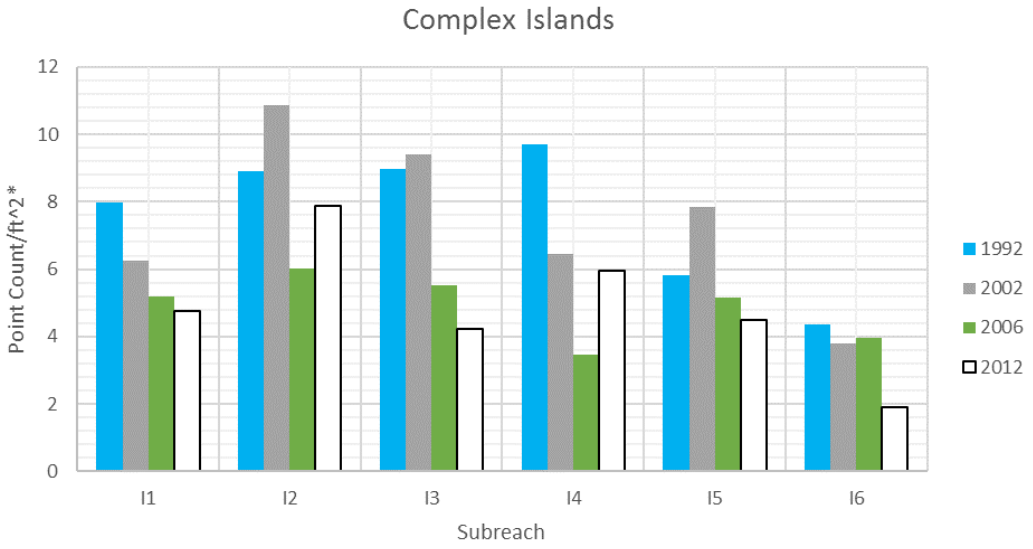
Complex Islands
Point Count/ft^2*
12
10
8
6
4
2
0
I1
I2
I3
I4
I5
I6
Subreach
1992
2002
2006
2012

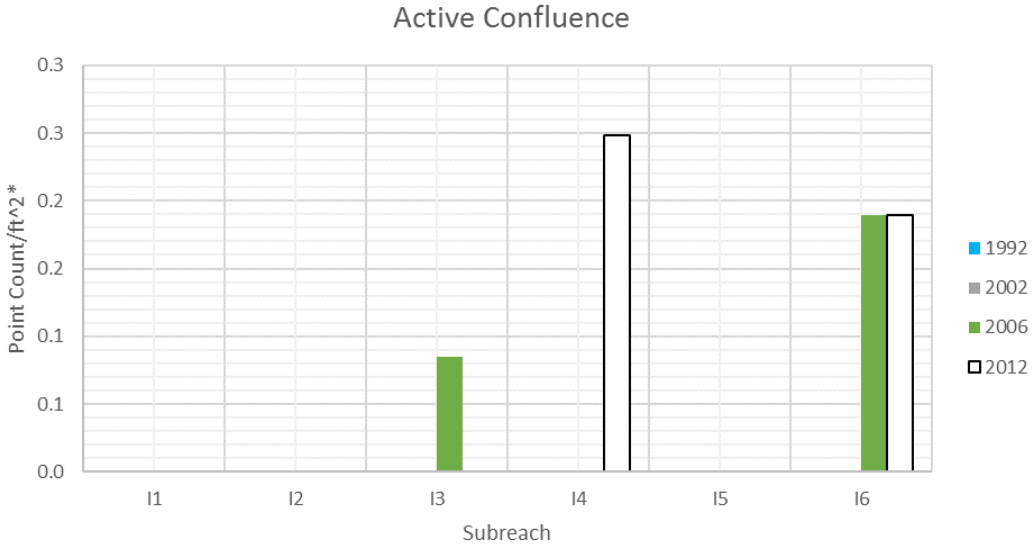
Active Confluence
Point Count/ft^2*
0.3
0.3
0.2
0.2
0.1
0.1
0.0
I1
I2
I3
I4
I5
I6
Subreach
1992
2002
2006
2012

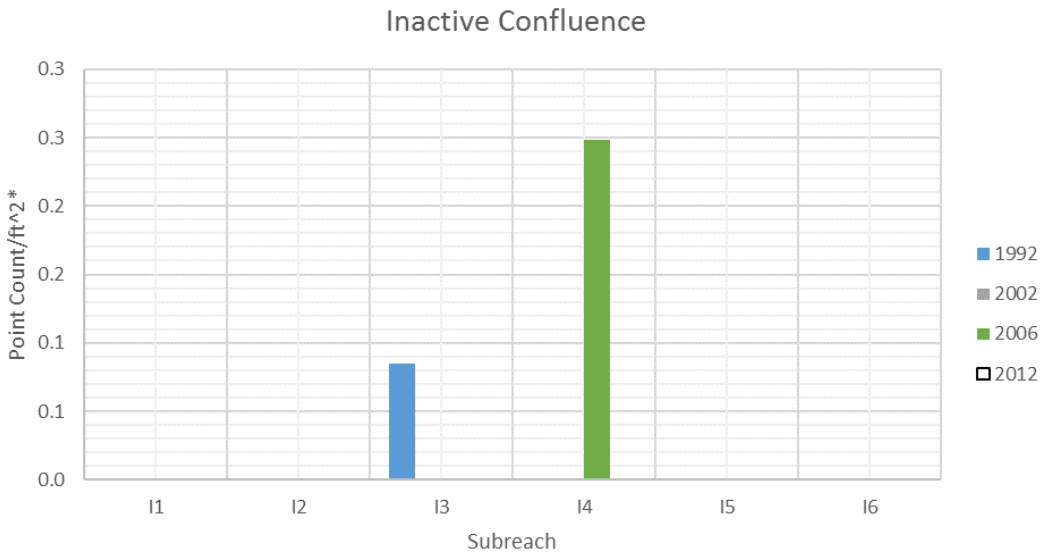
Inactive Confluence
0.3
0.3
0.2
0.2
0.1
0.1
0.0
Point Count/ft^2*
I1
I2
I3
I4
I5
I6
Subreach
1992
2002
2006
2012

APPENDIX G

Shoreline Complexity Analysis

Shoreline complexity incorporates some silvery minnow habitat criteria, yet also incorporates geomorphic parameters for its analysis. Because it combines aspects from various geomorphic characteristics, shoreline complexity stands alone as its own section.

Methods

Two aspects of the shoreline were analyzed: the length of the shoreline and habitat features that indicate complex shoreline. The set of data used to analyze these aspects is shown in Table G-1.

Table G-1: Years of the photographs used for analyzing the shoreline complexity.

1992	February
2001	February
2002	February
2005	June
2006	January
2008	July
2012	January
2016	October

These are the years with planforms supplied by the USBR available. Data before 1992 is not used for the same reason it is not used in the habitat criteria analysis. Records of fish population before 1993 is not available, so it would be impossible to relate fish population to geomorphic trends before the early 1990's. April of 2005 and June of 2008 are excluded because planforms were not drawn for these photographs. It is unknown how each year's planform was drawn and how they differed, so there may be inconsistencies that affect the lengths.

Features including complex shoreline (1a, 1b, and 1c), bank attached bars (5a, 5b, and 5c), backwater (4a, 4b), and confluences (7a,7b) were considered to impact shoreline complexity. These points and their scores were used to find a habitat shoreline complexity score. Whatever points fall into each subreach were multiplied by their corresponding score and added up to get an overall score for each subreach in each year. These scores were weighted by area by using the same method as outlined in Appendix D.

The length of the shoreline is also an indicator of complexity. It was measured using ArcGIS by breaking up the active channel outline provided by USBR into subreaches as shown in Figure G-1. The rest of the planform drawings are shown in Appendix H. The cumulative length of the right and left bank was used to compare each subreach in each year. To account for different sizes of the subreaches, the length was weighted. This was accomplished by drawing a straight line between each subsequent subreach delineation line perpendicular to the river. Then the

cumulative shoreline lengths were divided by the straight line and multiplied by 10 to get a weighted length index.

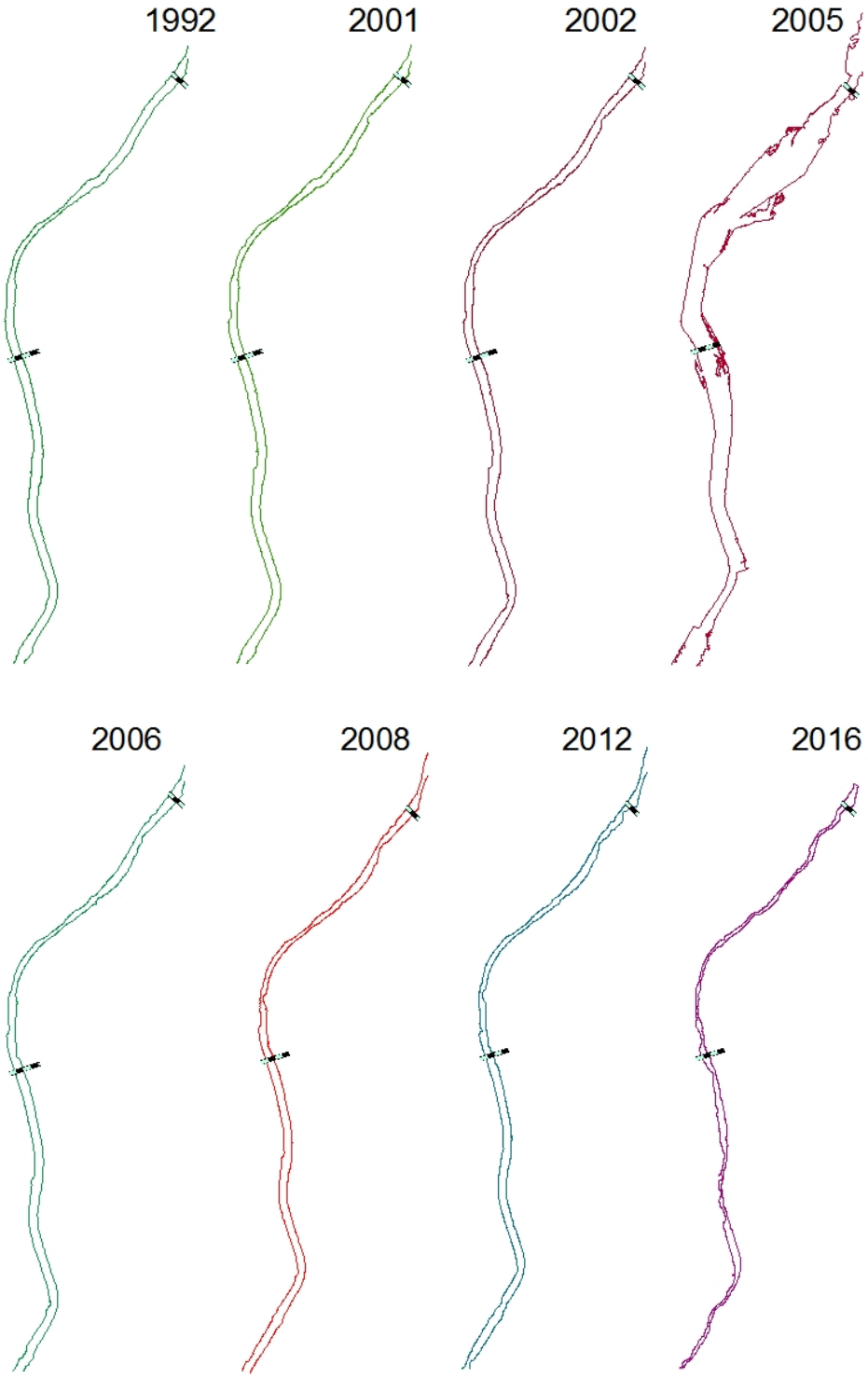

Figure G-1: Subreach I1 shoreline length shown with the planform drawing from USBR for each year.

The weight length index and the weighted habitat score were then added together to get an overall shoreline complexity score. They were weighted to be on the same order of magnitude so they when they were added up, each would equally impact the overall score. These overall scores were compared across all years and across the comparable years at 650 cfs. The length of each subreach was also compared across every year and in the comparable years with 650 cfs. The individual parameters were also compared to the overall scores for each year and subreach.

Results

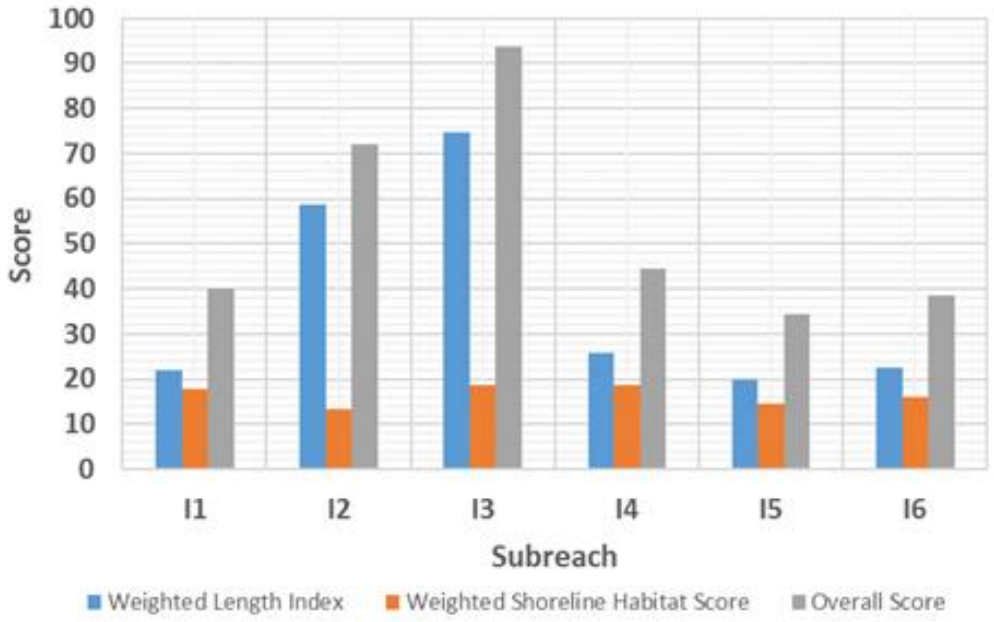

Figure G-2: Two parameters for analyzing shoreline complexity are compared and added up to show the overall score in 1992.

In Figure G-2, the overall complexity scores show that I3 is the most complex, followed by I2. The rest of the scores are very similar to each other. Every year in this subreach follows the same pattern, so the graphs for each year are essentially identical as shown in Appendix H. The score for the shoreline complexity and the length of the shoreline do not seem to be correlated.

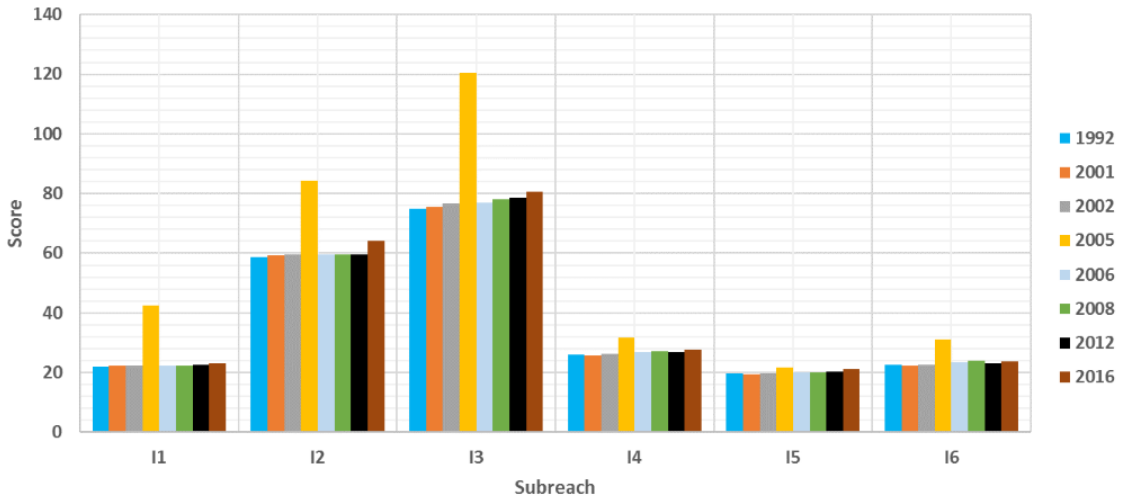

Figure G-3: The weighted length of the shoreline is compared over every subreach and every year.

As shown in Figure G-3, when comparing the lengths only across years, 2005 has the highest score and all the other scores are somewhat equal. In some subreaches, there is a slight increase in shoreline length over time.

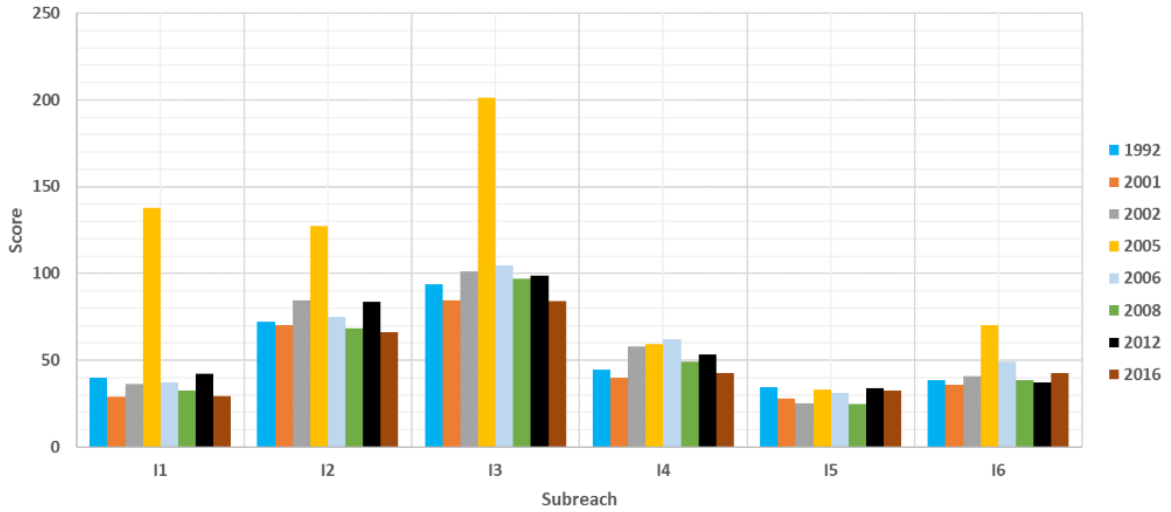

Figure G-4: The overall score for shoreline complexity is compared over every subreach and every year.

The overall score has more variation among the years, but 2005 still has the highest scores in each subreach (Figure G-4).

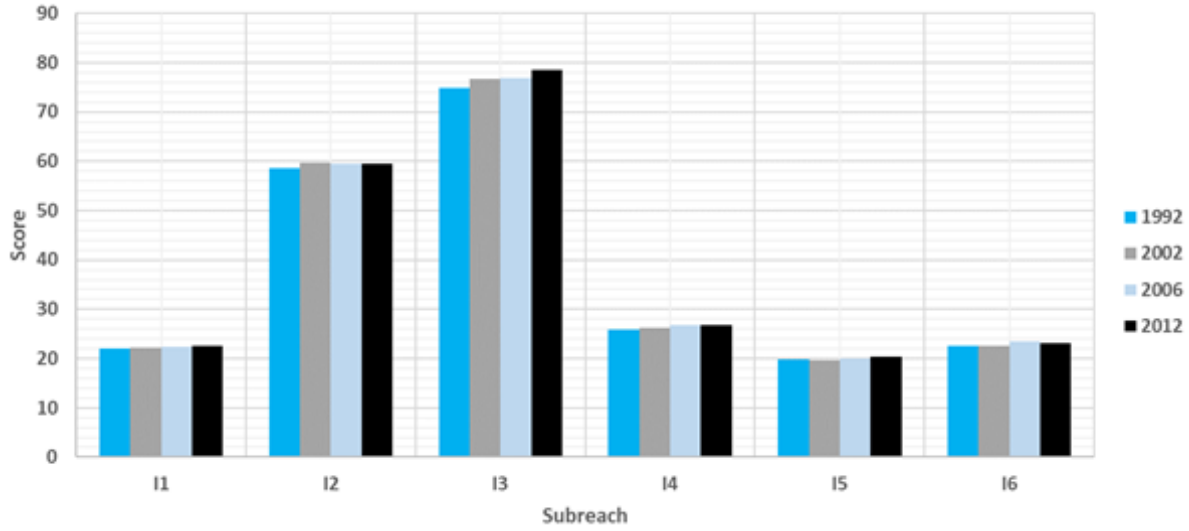

Figure G-5: The weighted length of the shoreline is compared over every subreach during years with a flow around 650 cfs when the aerial photograph was taken.

There is not much change in any of the subreaches over the years, but in some subreaches the complexity goes up slightly (Figure G-5).

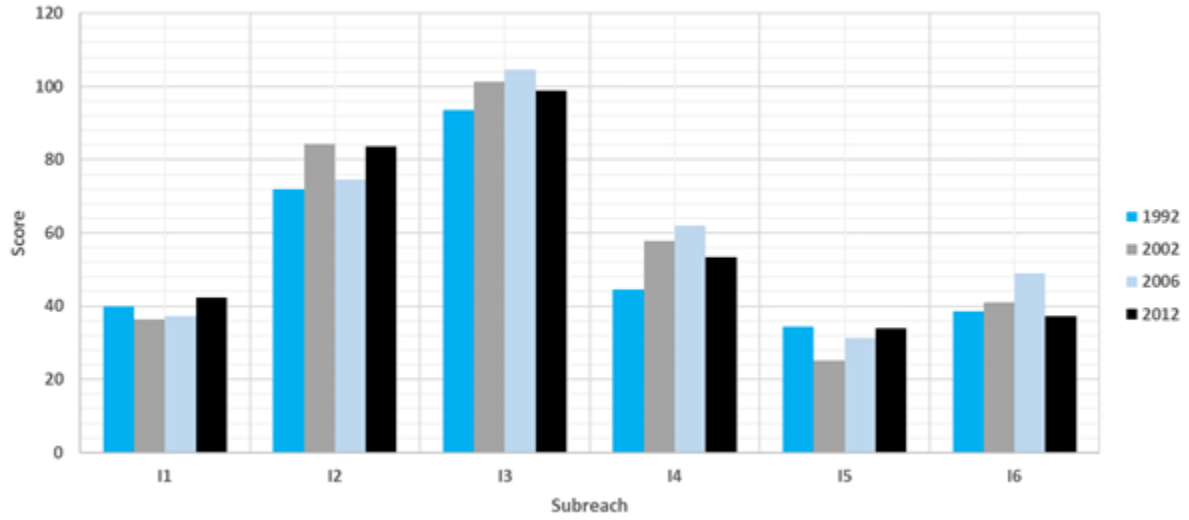

Figure G-6: The overall score for shoreline complexity is compared over every subreach during years with a flow around 650 cfs when the aerial photograph was taken.

Throughout these years, each subreach has a different trend. There is not much consistency for the overall score (Figure G-6).

In each of these figures where the years are compared, the overall trend is the same. I3 is the most complex, followed by I2. The rest of the subreaches have around the same scores and are consistently lower than I3 and I2.

Discussion

Subreach I3 has shown to be the most complex in the Isleta reach. This may be because I3 is the most sinuous reach as shown in Figure 30. I1 may have a lower score because it is just downstream of the Isleta Diversion Dam. The velocity and slope in I1 are higher than the other reaches, and the width is lower in I1 than the other reaches according to Figure 36: Width, depth, velocity, wetted perimeter, energy slope, and bed slope at each subreach for 1972, 1992, 2002, and 2012 at 3000 cfs. These parameters indicate a more incised channel, which would be consistent with the results of lower shoreline complexity. Subreach I2 is wider than I1 and has a lower velocity and energy slope than I2 as shown in Figure 36. This explains why the complexity jumps up at I2. The width, velocity, depth, wetted perimeter, bed slope and energy slope remain relatively constant from I3 through I6, so the variation in complexity may be due to other factors.

The complexity increasing over time since the 1990's may be due to sinuosity slightly increasing, and a decreased channel width and reduced tendency towards braiding. Because islands and side channels are not factored into the channel length and complexity, the results are not reflective of braiding decreasing, but instead just sinuosity increasing. This may be why it appears like the complexity is increasing over time.

APPENDIX H

Additional Shoreline Complexity Results

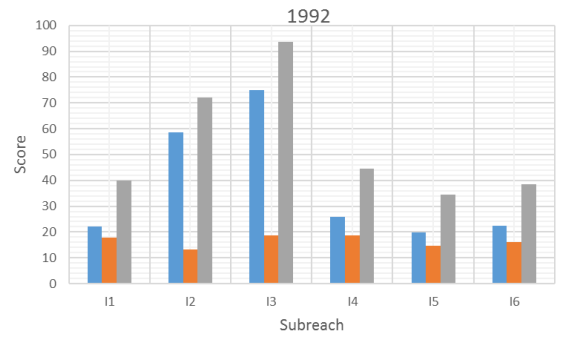
1992
Score
Subreach
I1
I2
I3
I4
I5
I6

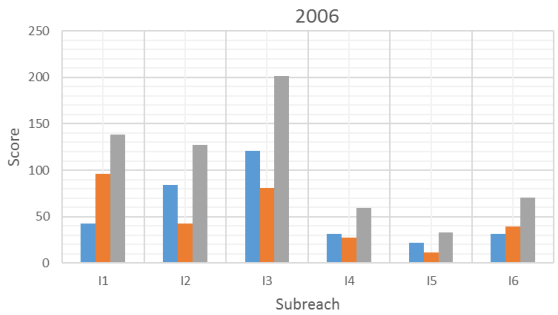
2006
Score
Subreach
I1
I2
I3
I4
I5
I6

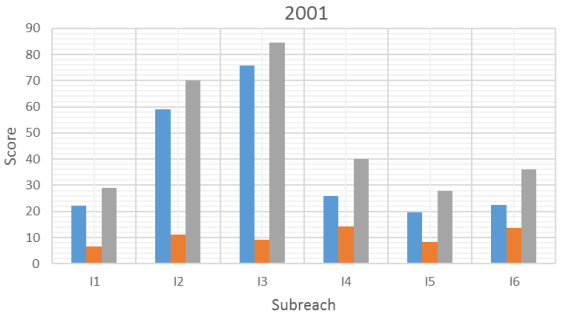
2001
Score
Subreach
I1
I2
I3
I4
I5
I6

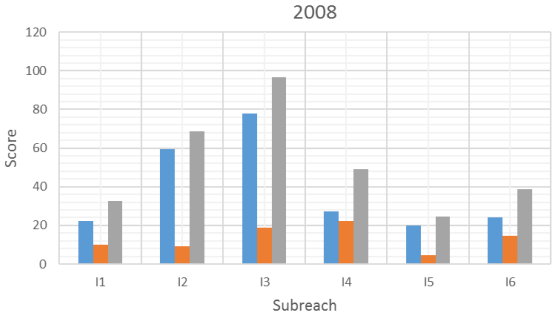
2008
Score
Subreach
I1
I2
I3
I4
I5
I6

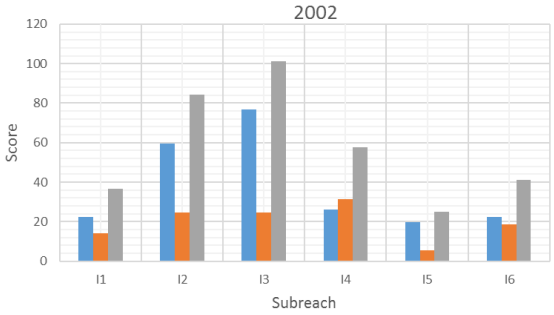
2002
Score
Subreach
I1
I2
I3
I4
I5
I6

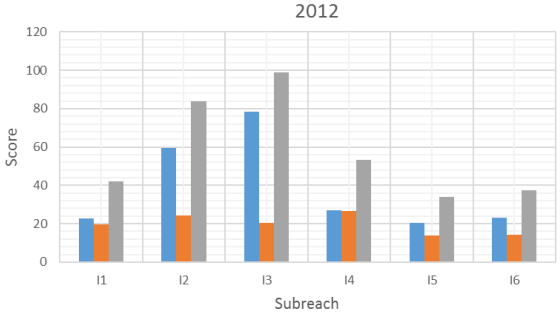
2012
Score
Subreach
I1
I2
I3
I4
I5
I6

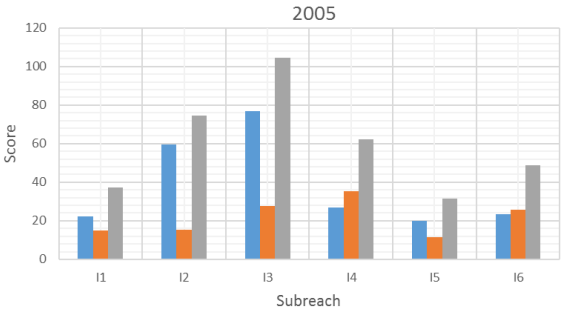
2005
Score
Subreach
I1
I2
I3
I4
I5
I6

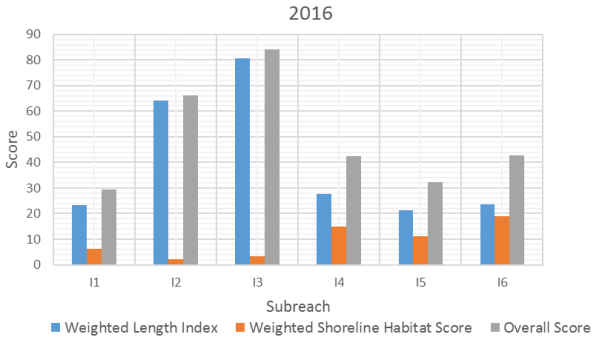
2016
Score
Subreach
I1
I2
I3
I4
I5
I6
Weighted Length Index
Weighted Shoreline Habitat Score
Overall Score

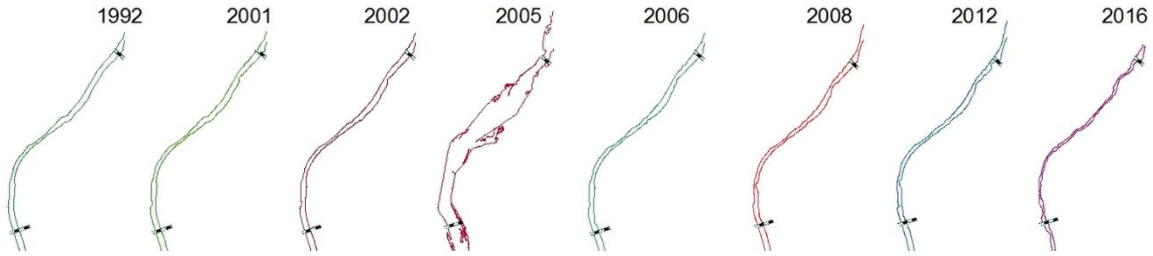
1992
2001
2002
2005
2006
2008
2012
2016

I1

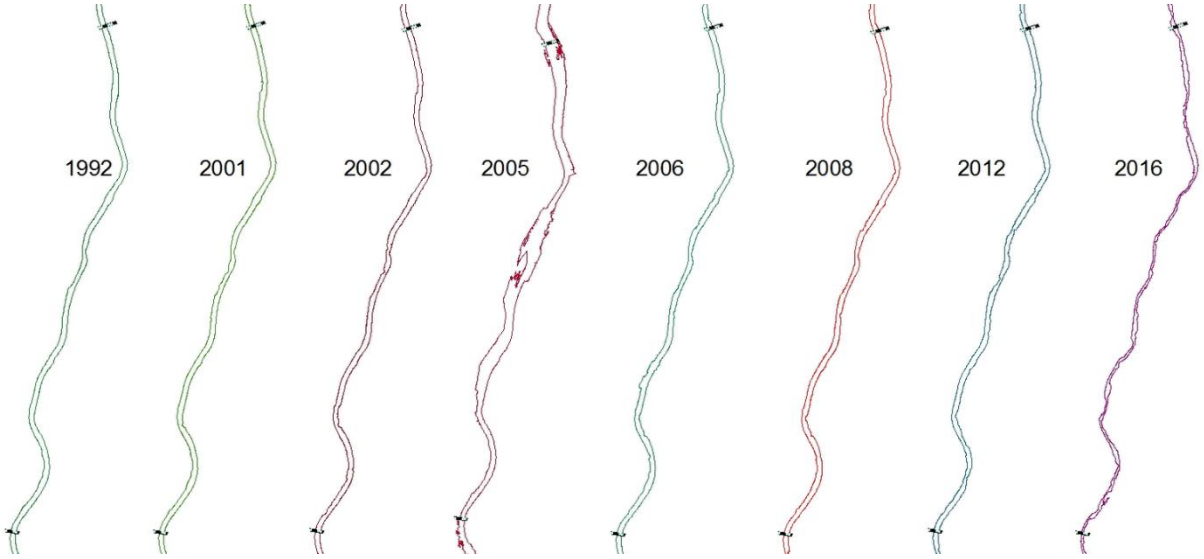
1992
2001
2002
2005
2006
2008
2012
2016

I2

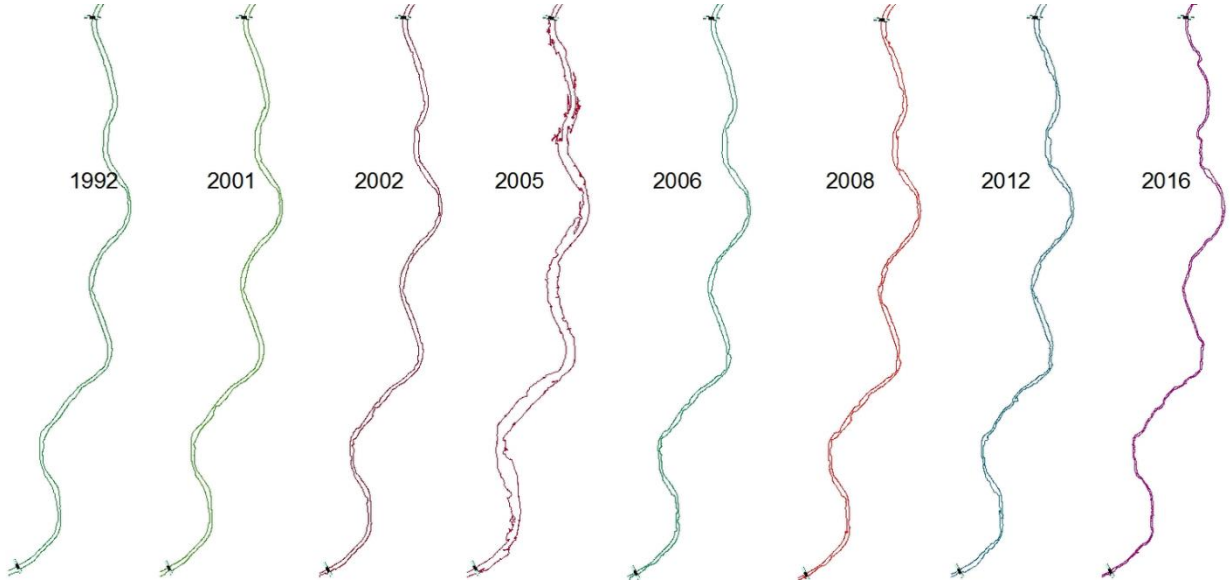
1992
2001
2002
2005
2006
2008
2012
2016

I3

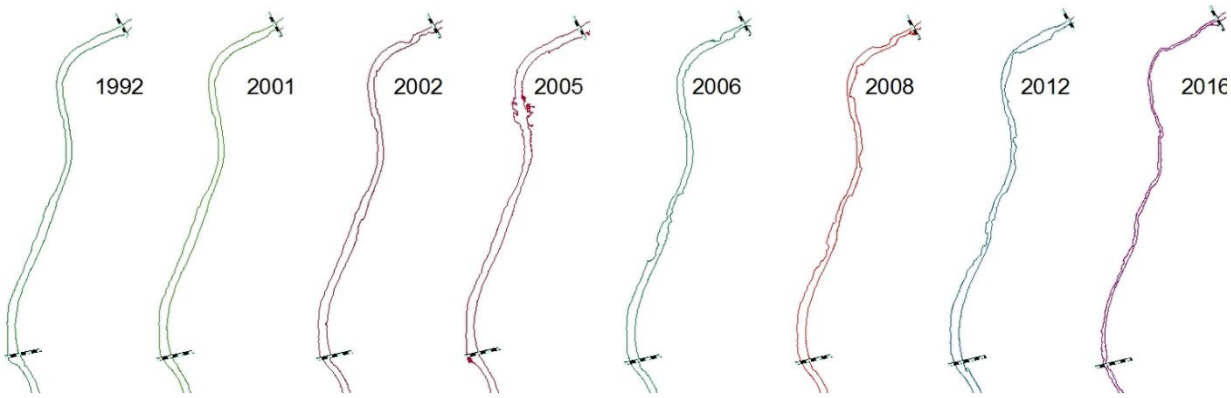
1992
2001
2002
2005
2006
2008
2012
2016

I4

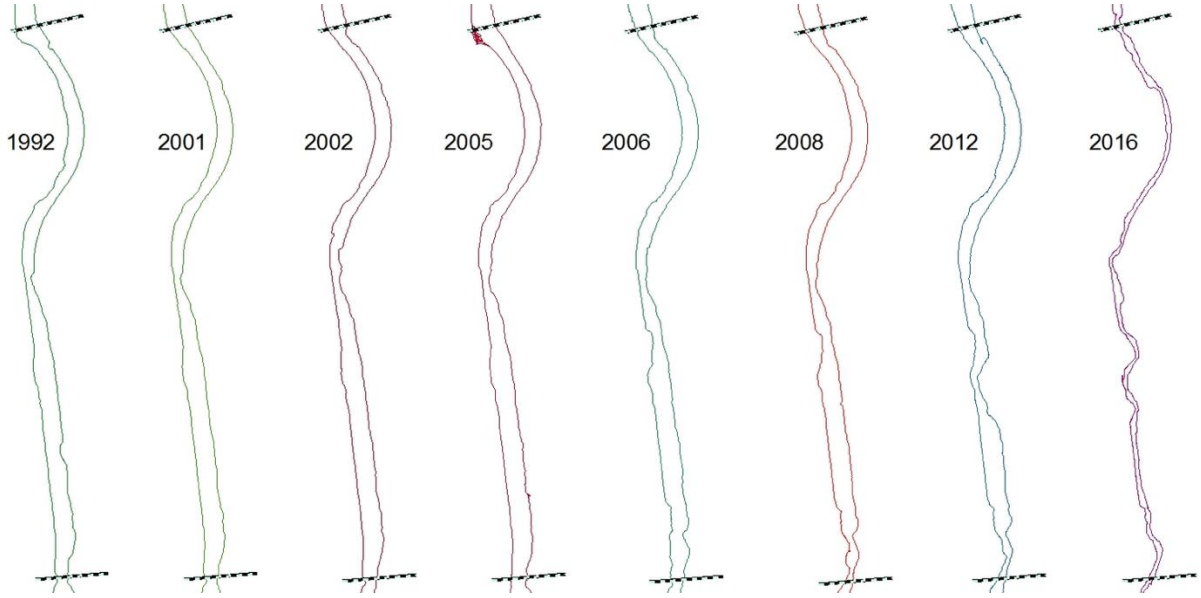
1992
2001
2002
2005
2006
2008
2012
2016

I5

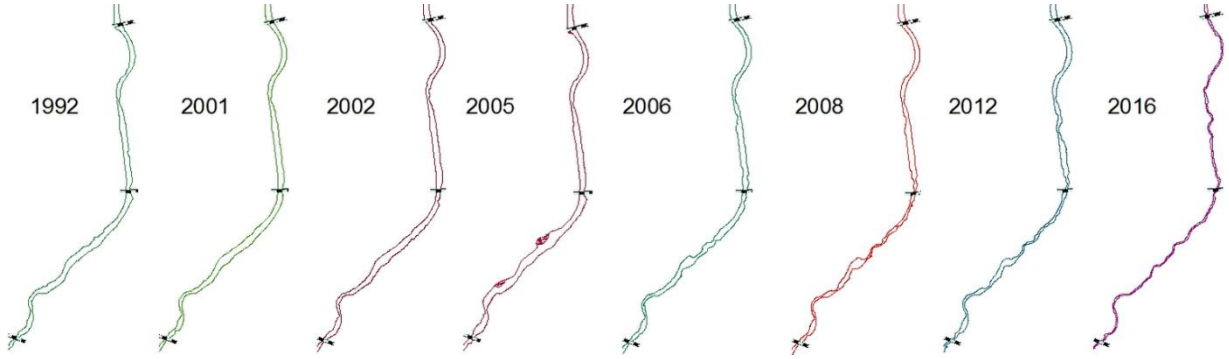
1992
2001
2002
2005
2006
2008
2012
2016

I6

APPENDIX I

Habitat Score by Subreach (All Years)

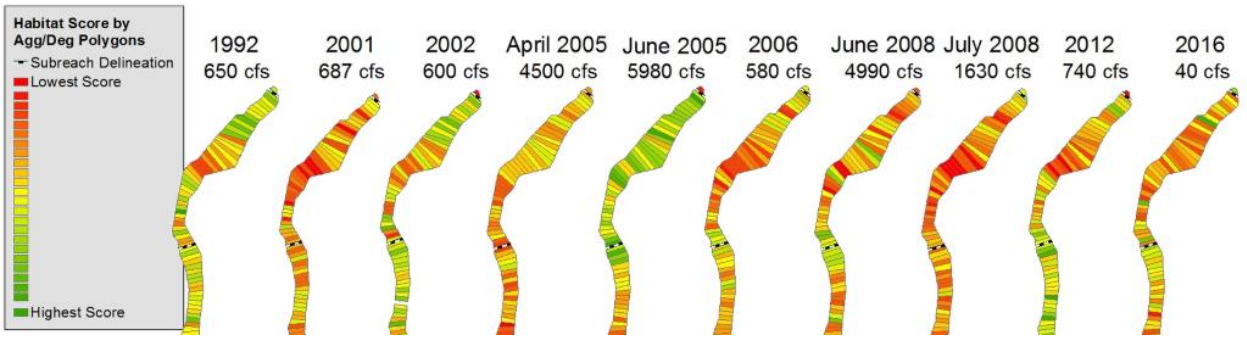

Subreach I1

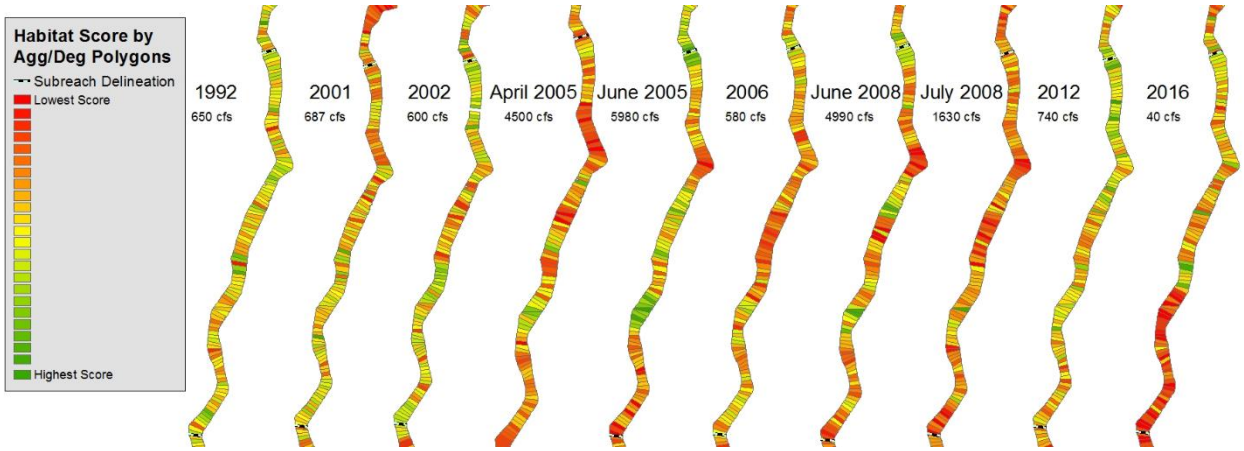

Subreach I2

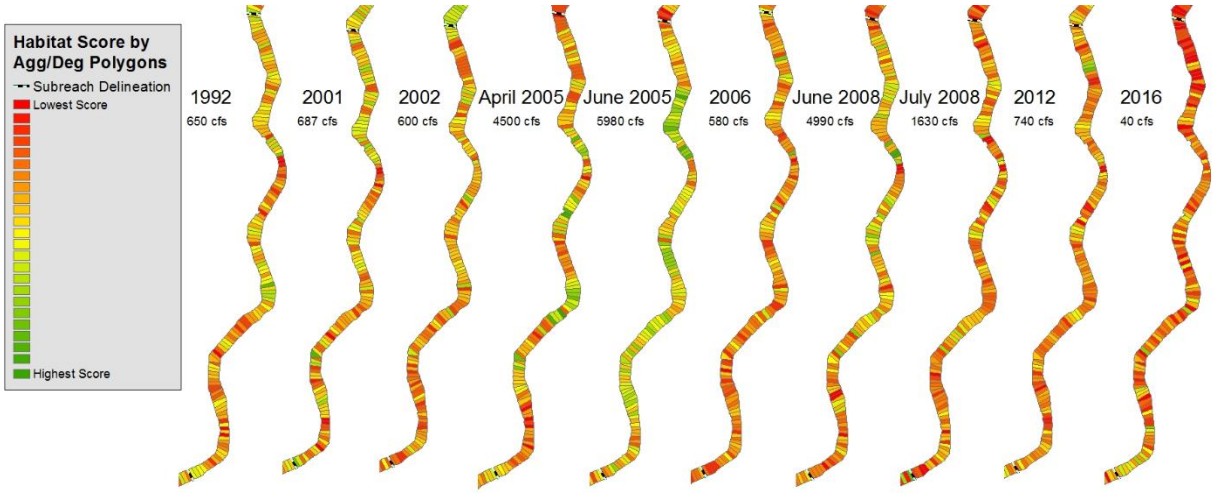

Subreach I3

Subreach I4

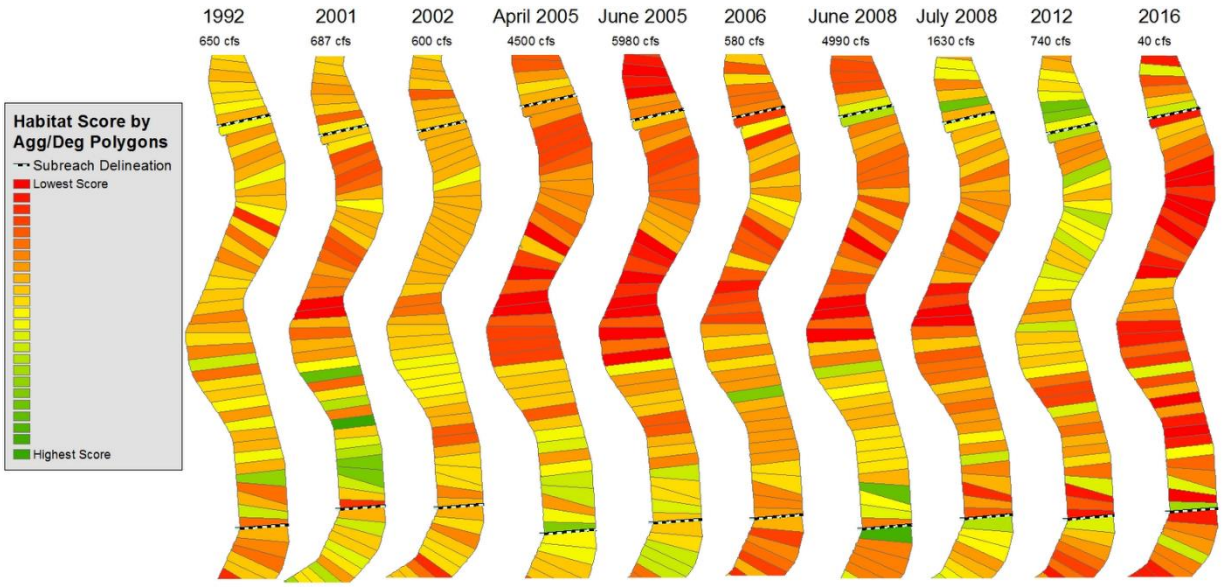

Subreach I5

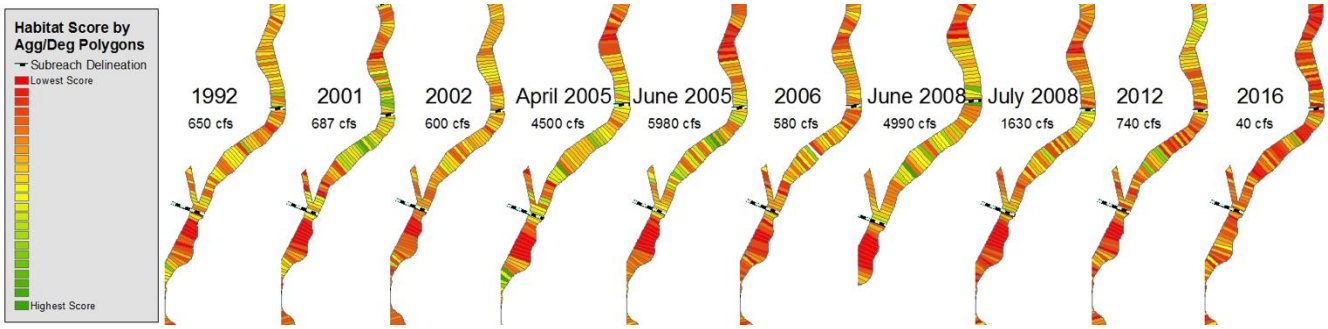

Subreach I6

APPENDIX J

Habitat Score by Subreach (Years with flows around 650 cfs)

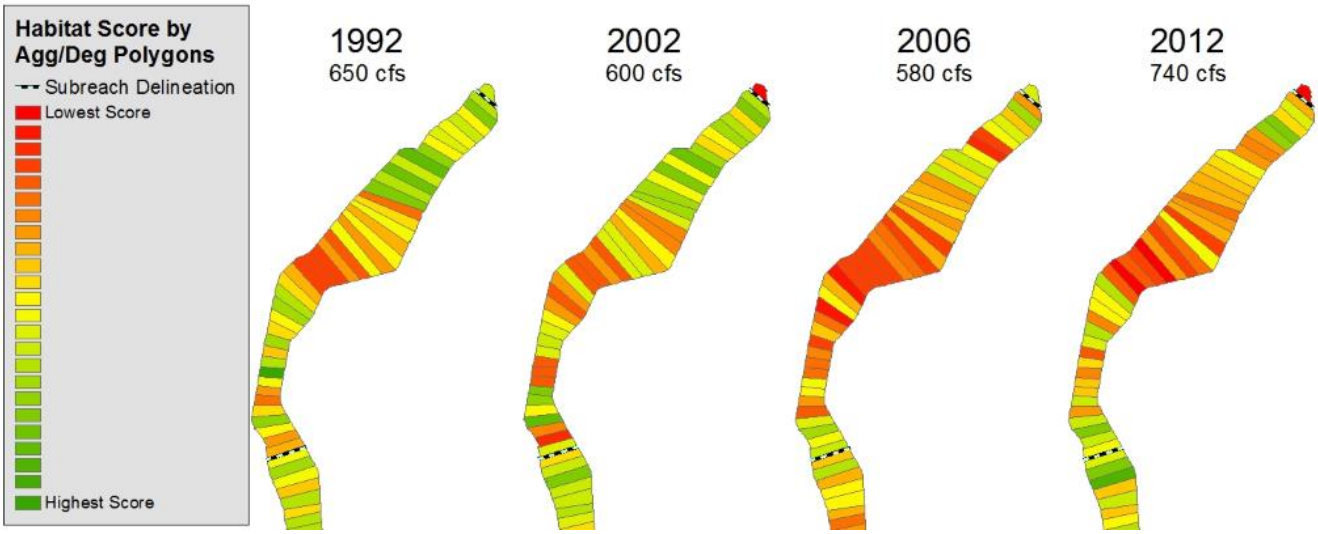

Subreach I1

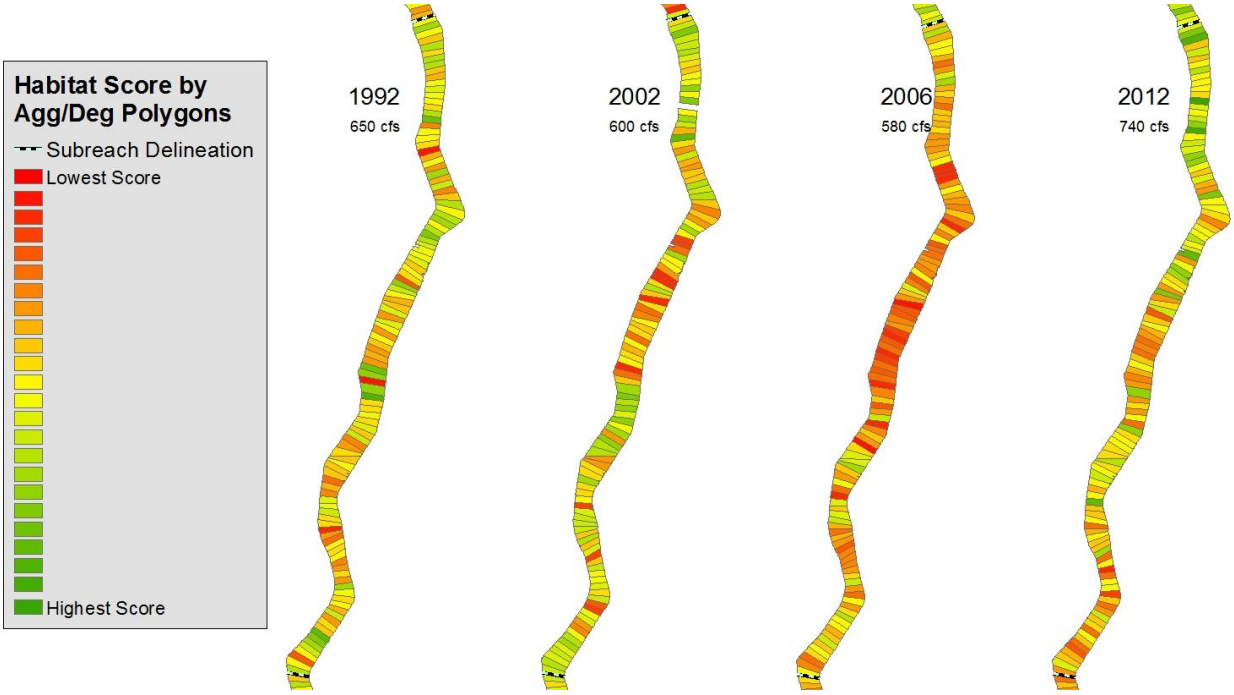

Subreach I2

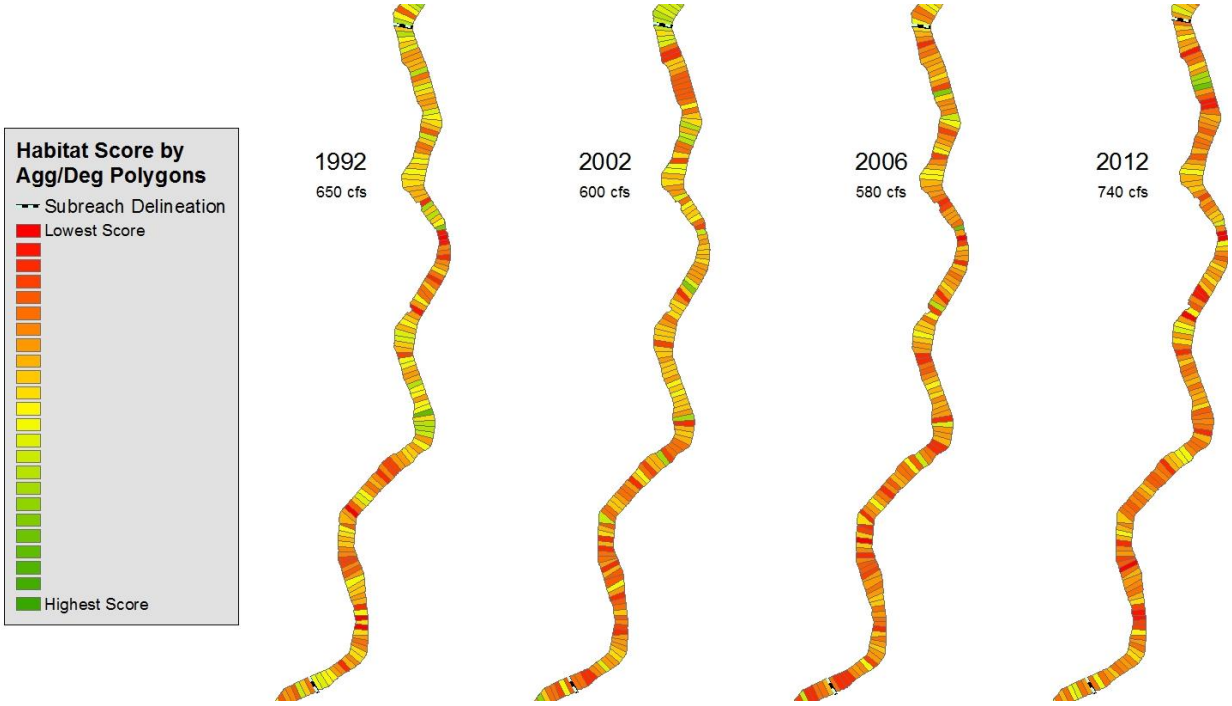

Subreach I3

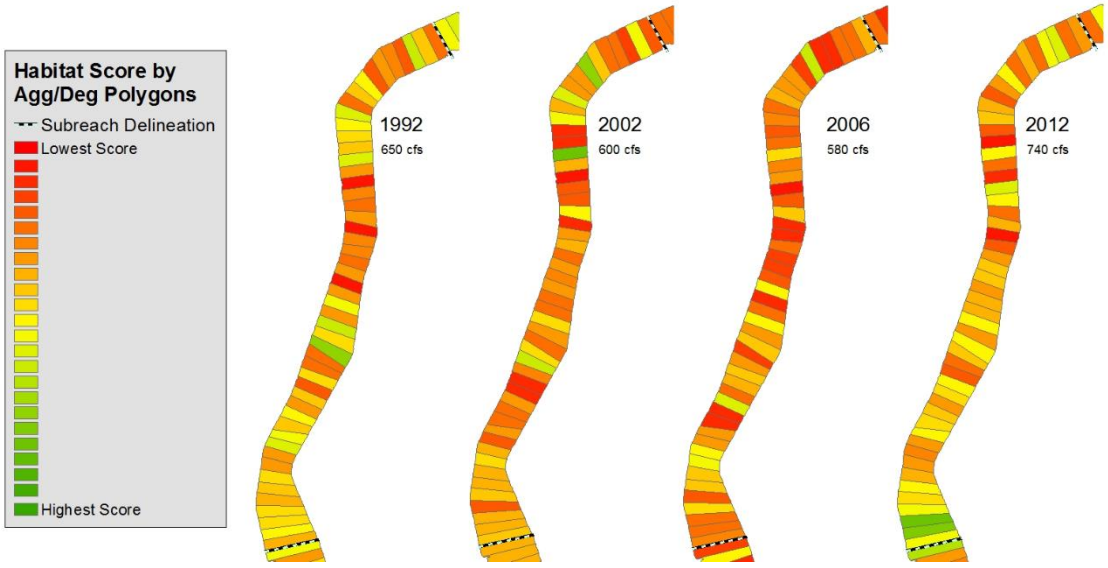

Subreach I4

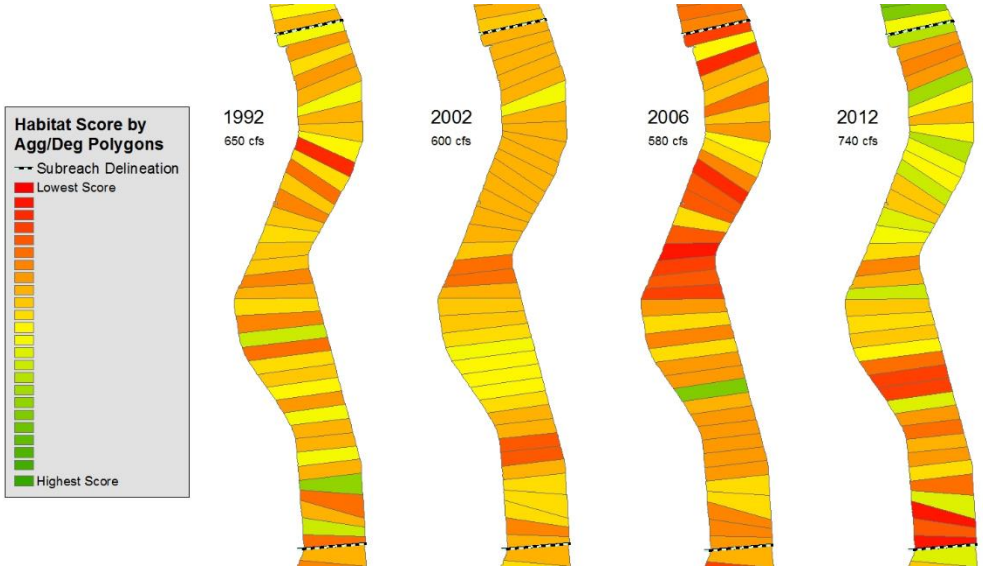

Subreach I5

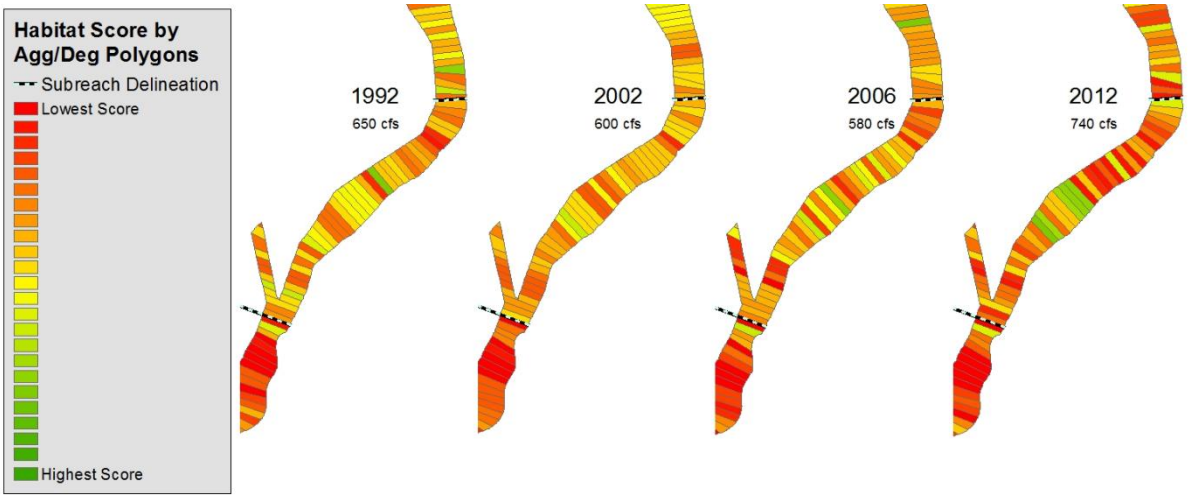

Subreach I6

APPENDIX K

Combined HEC-RAS and GIS Habitat Analysis for Subreach I1

To showcase the results for habitat analyses, figures representing one subreach at two flow conditions are presented. The rest of the subreaches at these flow conditions are in the appendix.

Subreach I1 is depicted in Figure K-1 and Figure K-2 because it is one of the subreaches that provides the best habitat. There is also a great amount of habitat variability in this subreach. This allows the analysis of how the habitats are different and what that difference looks like. Only a portion of the subreach is shown so the points and figures are decipherable.

The two different flow conditions are a low and high flow. The low flow analyzed is in 1992 at 650 cfs in GIS and 600 cfs in HEC-RAS shown in Figure K-1. The high flow is analyzed at 4500 cfs in 2005 in GIS and 3500 cfs in HEC-RAS in 2002 shown in Figure K-2. The difference in years and flows and the high flow analysis come from limitations in available data. The HEC-RAS simulation includes low, medium and high flows from 1992, 2002, and 2012. The only high flow data from aerial photographs analyzed is in 2005. The closest match for year and flow data to 3500 cfs from 2002 in HEC-RAS is aerial photography from April of 2005 at 4500 cfs. Therefore, the high flow results are not perfectly comparable because there is a difference in time and flow.

The top half of Figure K-1 and Figure K-2 (a) and (b) are from HEC-RAS and the bottom half (c and d) are from GIS. They both depict a portion of subreach I1. The results show that the HEC-RAS and GIS analyses are somewhat comparable. Where there is a large area of quality habitat from HEC-RAS there tends to be more habitat features mapped in GIS as seen in Figure K-1. The trend does not always occur such as in Figure K-2 which shows little correlation between the two analyses. This is mainly due to a limitation in seeing where the floodplain is inundated in the aerial photograph. The GIS mapping process is most accurate in the channel, yet HEC-RAS is more powerful at being able to map where the water inundates outside of the channel. These figures are mainly presented to get a visual idea of what the habitat and results look like.

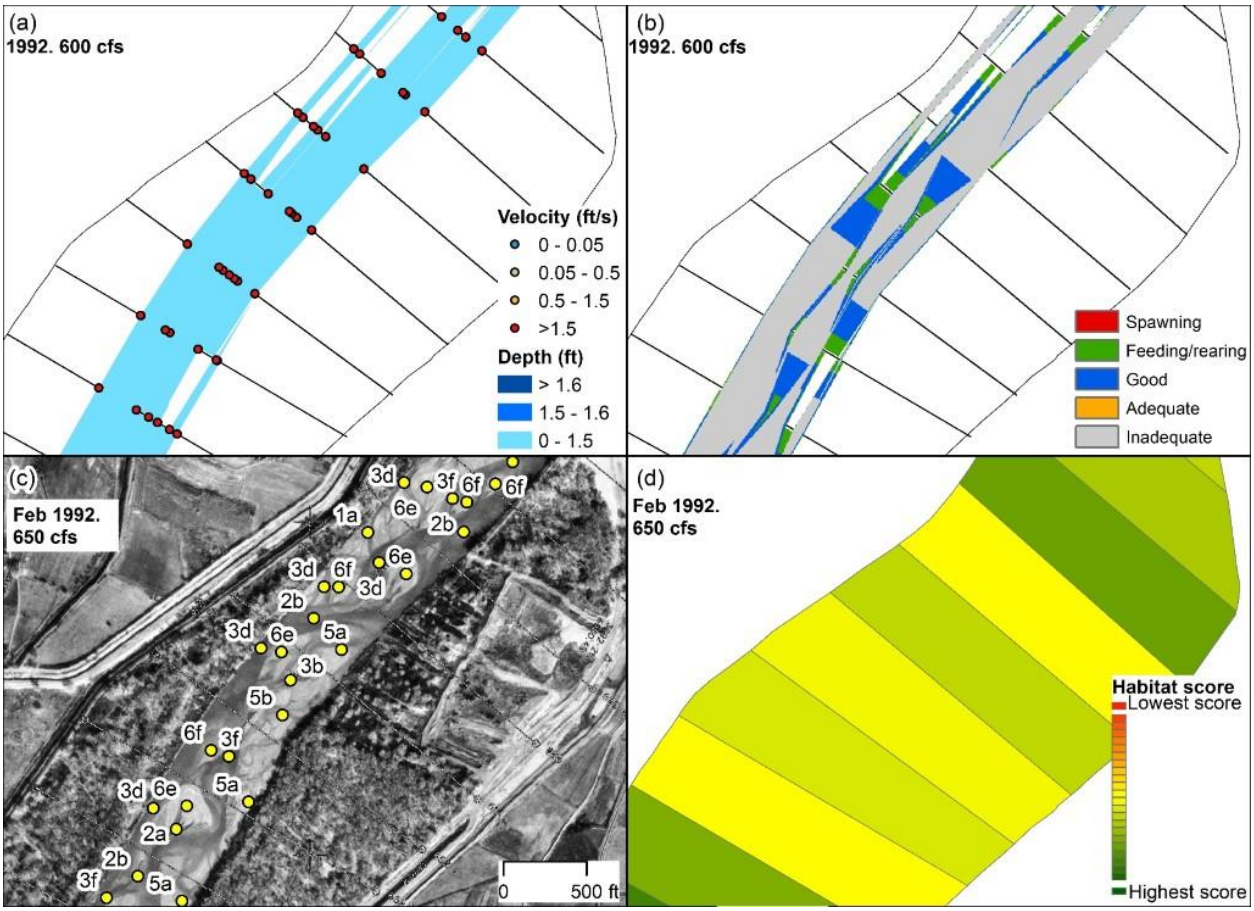

Figure K-1: Summary of HEC-RAS and GIS habitat at subreach I1, agg/deg 657 to 665. (a) Velocity and depth of the simulation. (b) Habitat criteria mapped based on velocity and depth. (c) Habitat features mapped out by points and letters. The description of these points is given in Appendix D (d) Habitat color scheme based on habitat features.

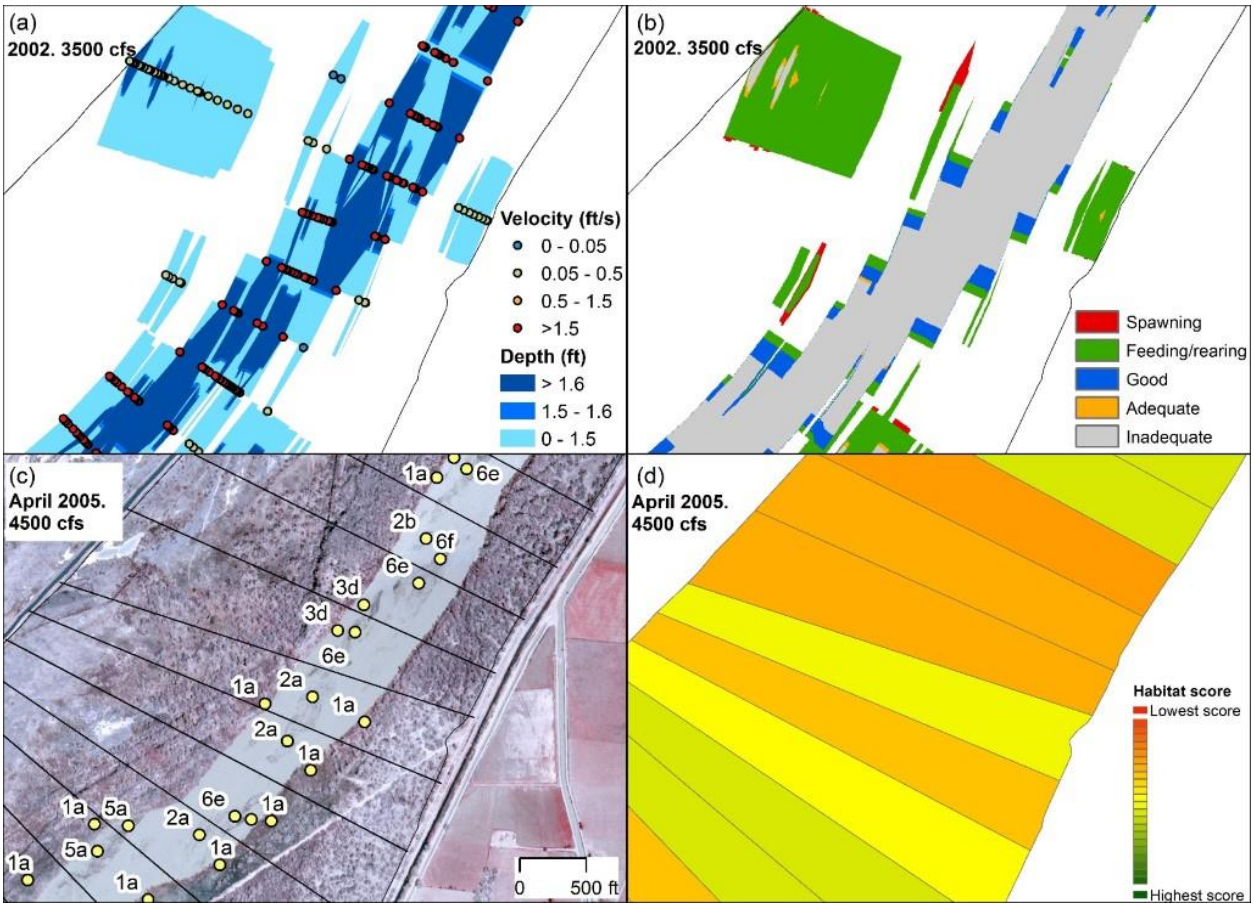

Figure K-2: Summary of HEC-RAS and GIS habitat at subreach I1, agg/deg 666 to 675. (a) Velocity and depth of the simulation at (b) Habitat criteria mapped based on velocity and depth. (c) Habitat features mapped out by points and letters. (d) Habitat color scheme based on habitat features.

APPENDIX L

Combined HEC-RAS and GIS Habitat Analysis for All Subreaches

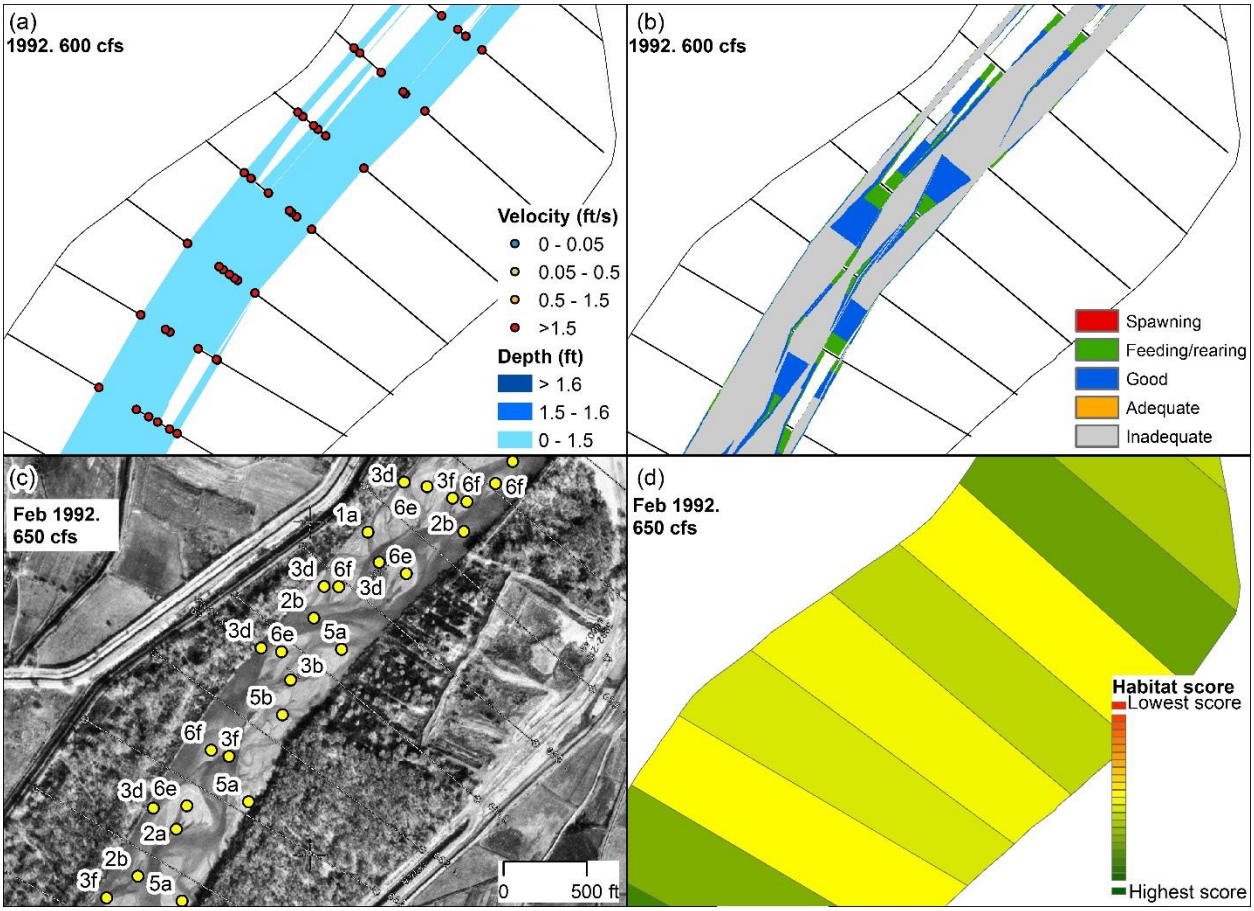

Summary of HEC-RAS and GIS habitat at subreach I1, agg/deg 657 to 665. (a) Velocity and depth of the simulation. (b) Habitat criteria mapped based on velocity and depth. (c) Habitat features mapped out by points and letters. (d) Habitat color scheme based on habitat features.

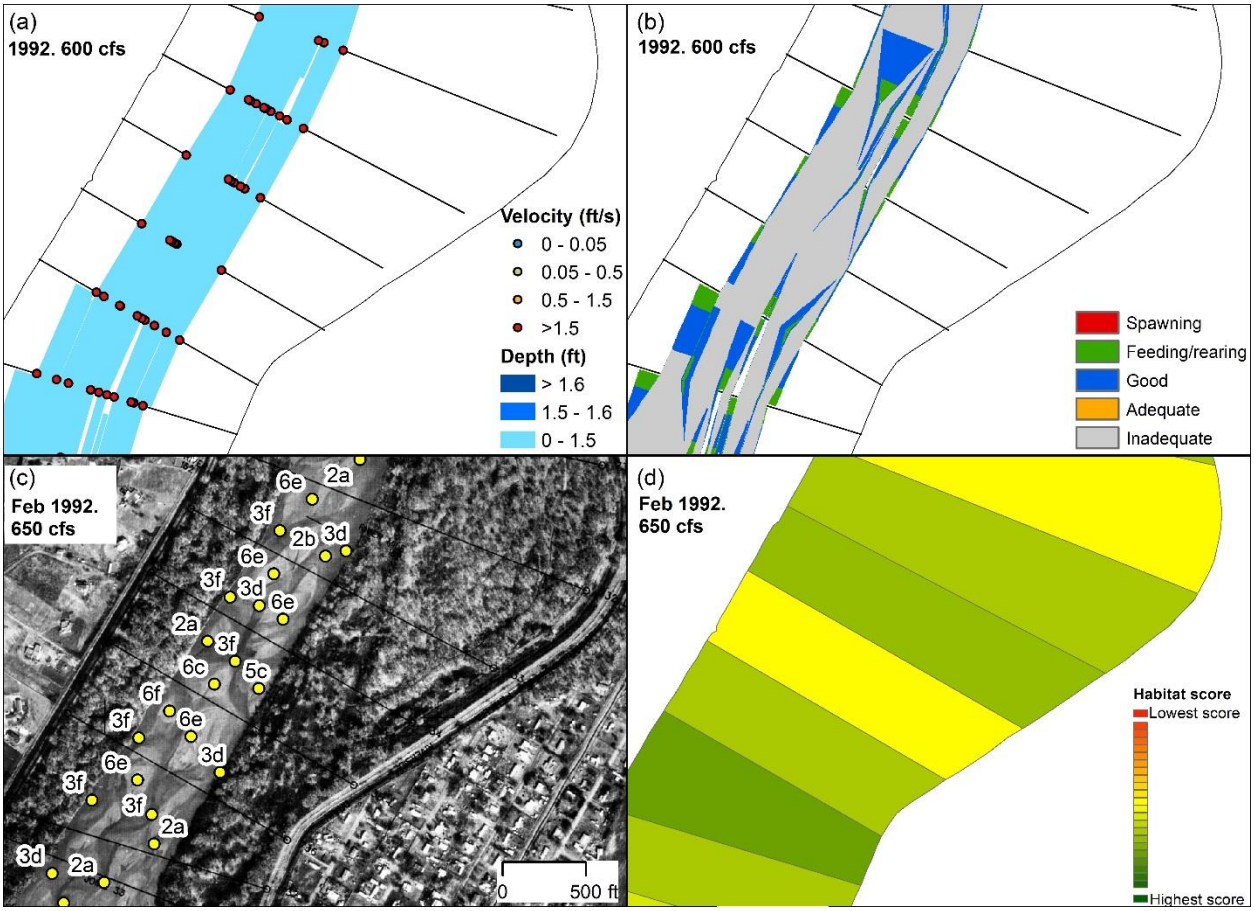

Summary of HEC-RAS and GIS habitat at subreach I2, agg/deg 732 to 737. (a) Velocity and depth of the simulation. (b) Habitat criteria mapped based on velocity and depth. (c) Habitat features mapped out by points and letters. (d) Habitat color scheme based on habitat features.

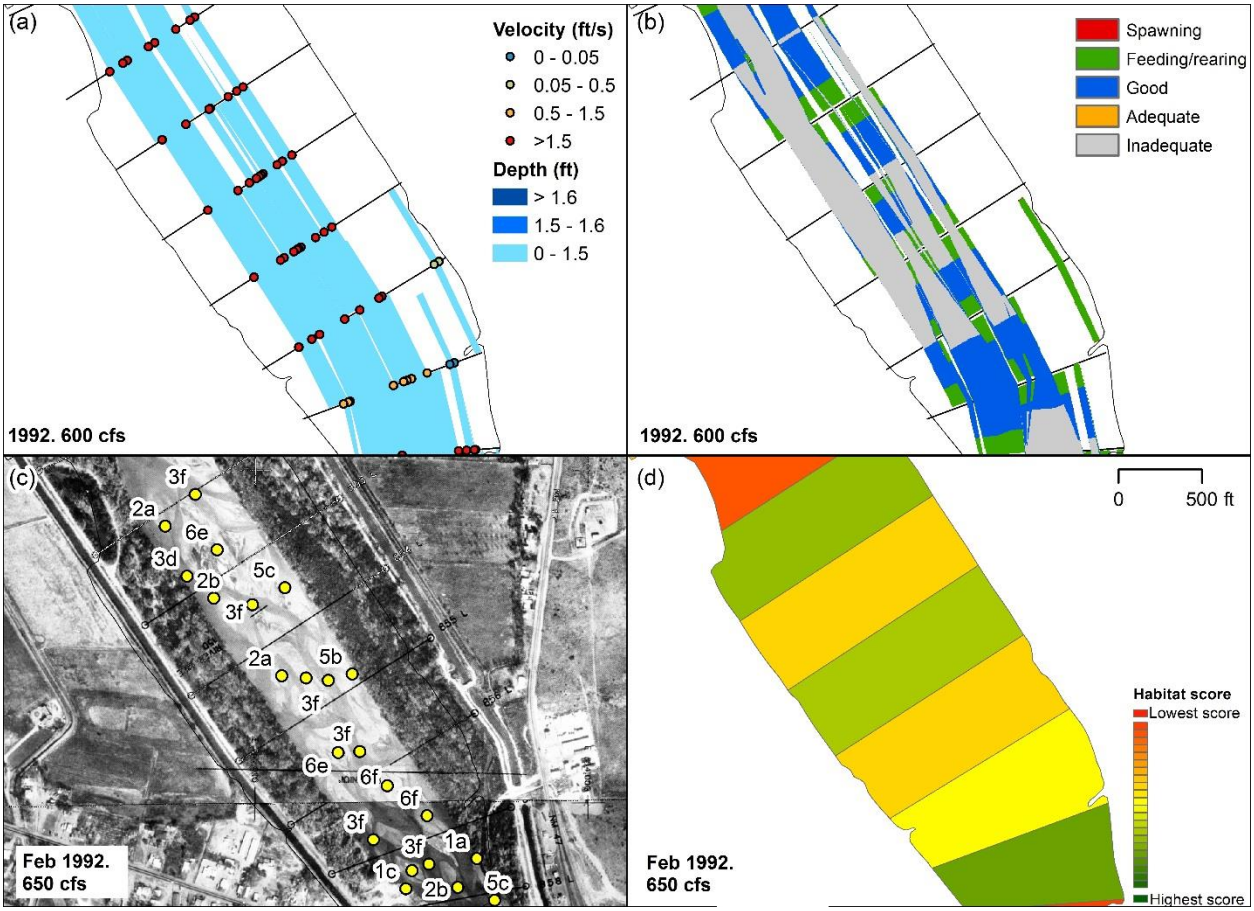

Summary of HEC-RAS and GIS habitat at subreach I3, agg/deg 852 to 858. (a) Velocity and depth of the simulation. (b) Habitat criteria mapped based on velocity and depth. (c) Habitat features mapped out by points and letters. (d) Habitat color scheme based on habitat features.

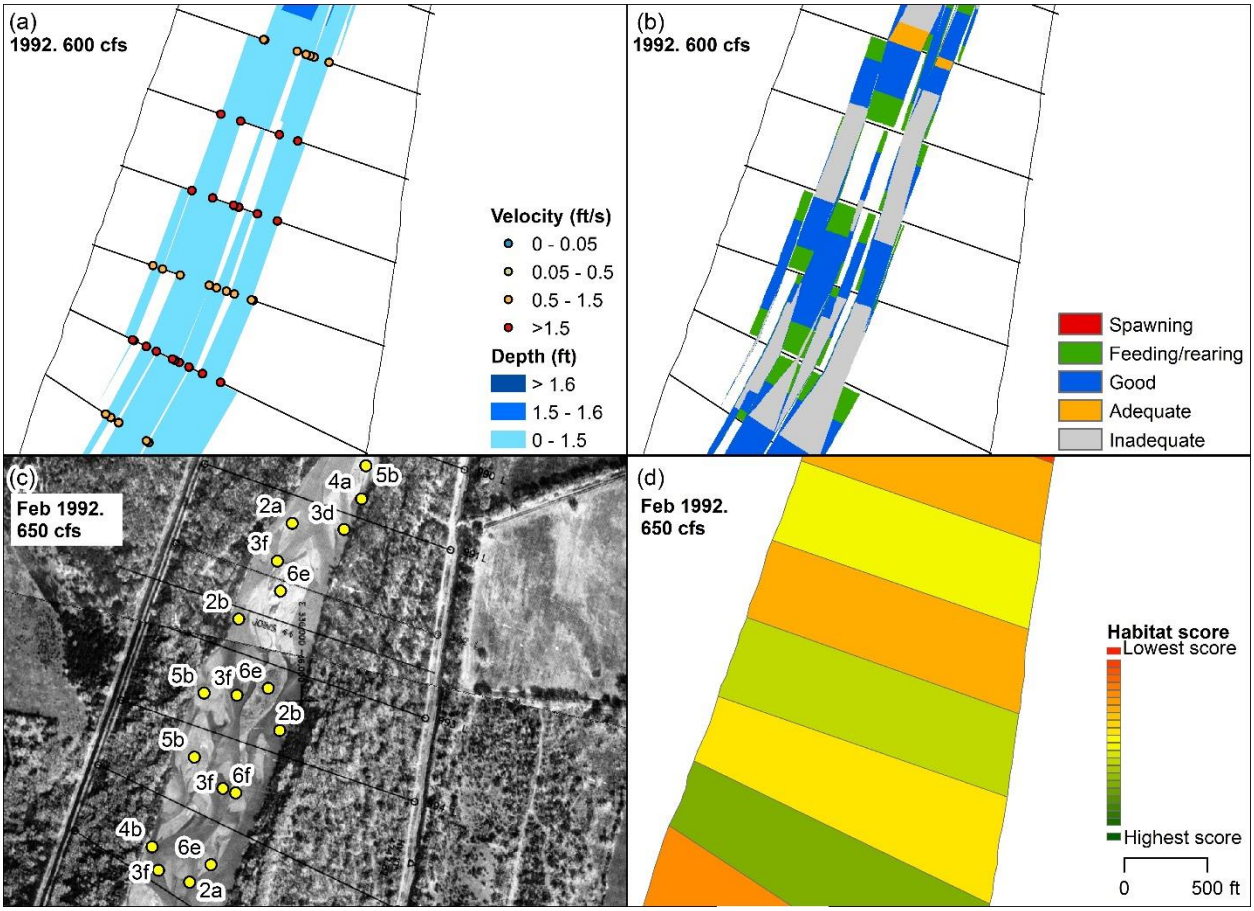

Summary of HEC-RAS and GIS habitat at subreach I4, agg/deg 991 to 996. (a) Velocity and depth of the simulation. (b) Habitat criteria mapped based on velocity and depth. (c) Habitat features mapped out by points and letters. (d) Habitat color scheme based on habitat features.

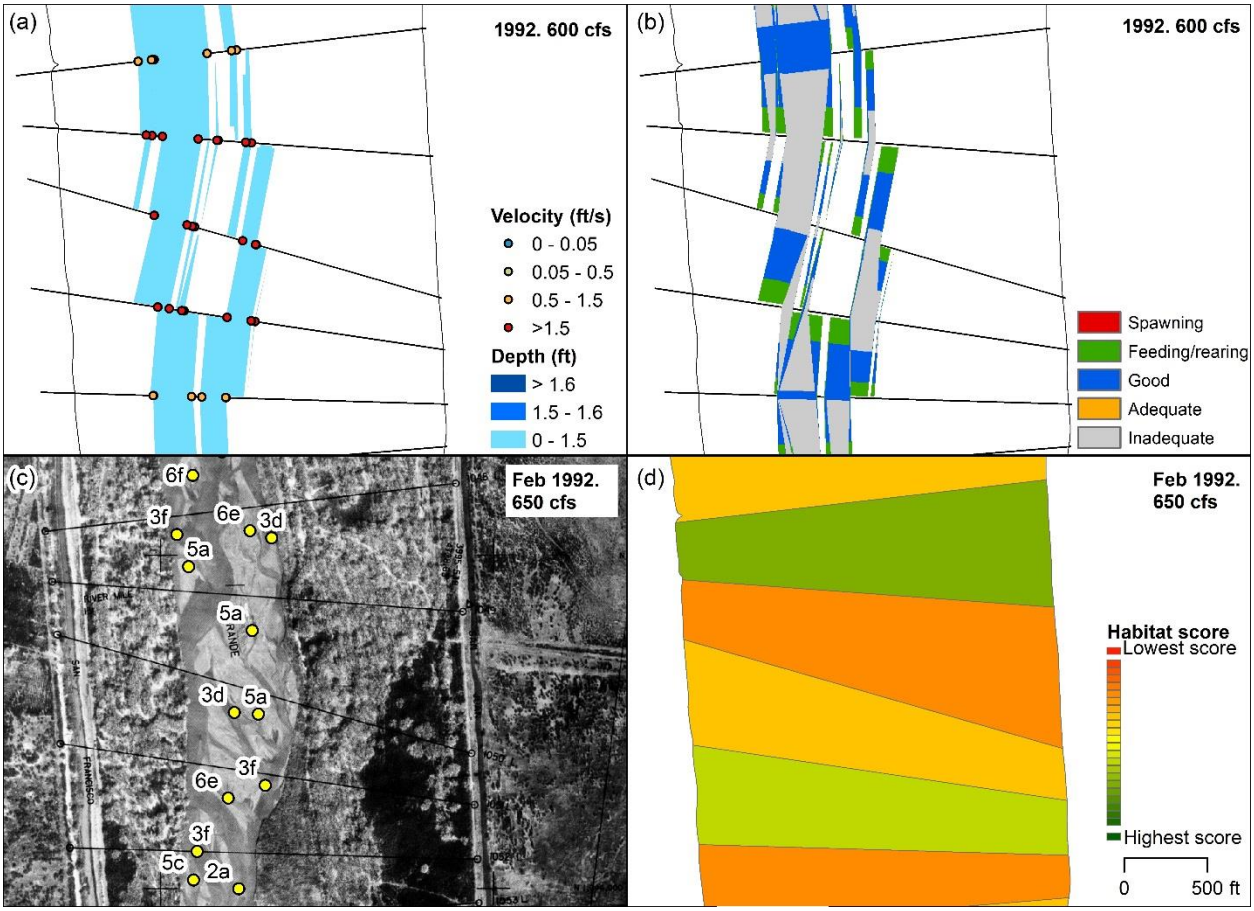

Summary of HEC-RAS and GIS habitat at subreach I5, agg/deg 1048 to 1053. (a) Velocity and depth of the simulation. (b) Habitat criteria mapped based on velocity and depth. (c) Habitat features mapped out by points and letters. (d) Habitat color scheme based on habitat features.

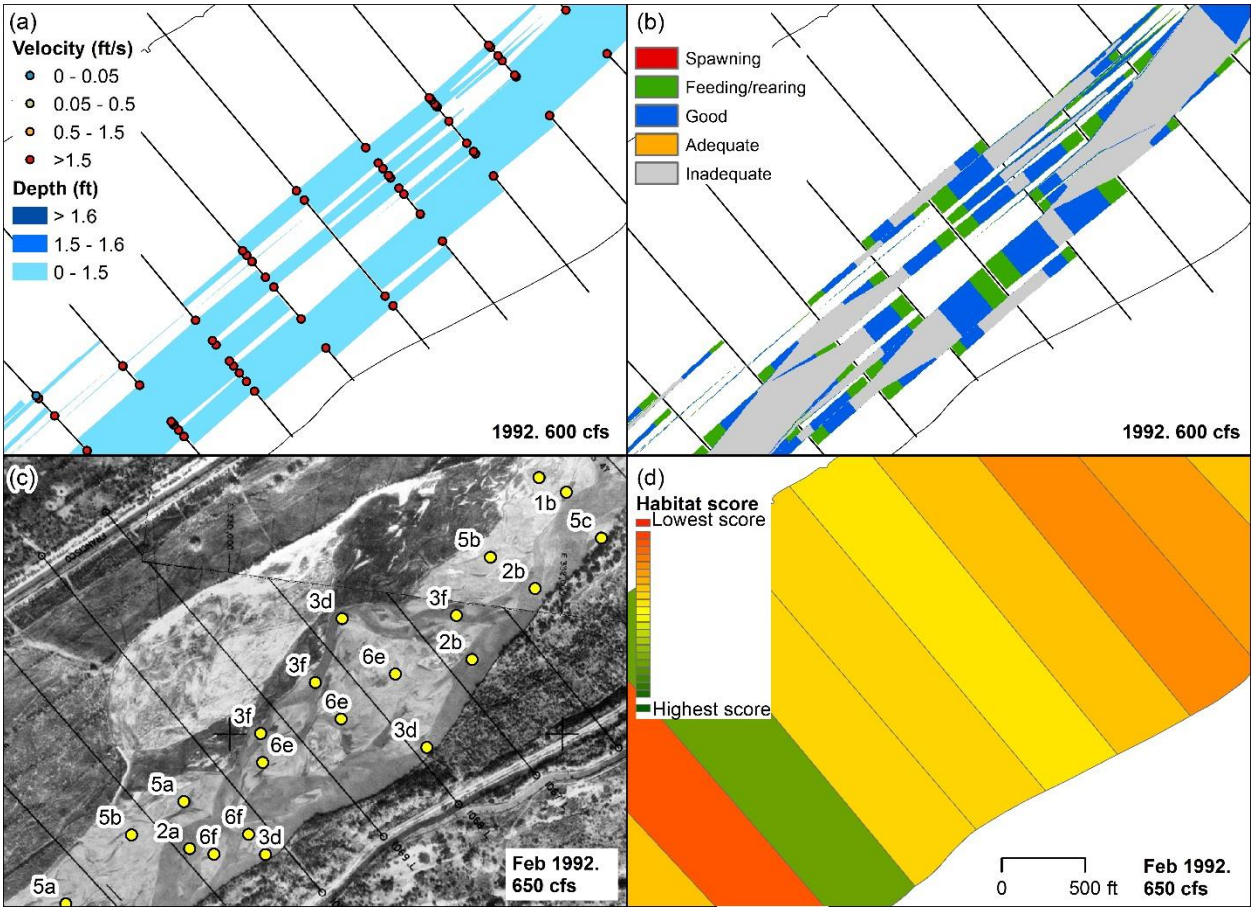

Summary of HEC-RAS and GIS habitat at subreach I6, agg/deg 1064 to 1072. (a) Velocity and depth of the simulation. (b) Habitat criteria mapped based on velocity and depth. (c) Habitat features mapped out by points and letters. (d) Habitat color scheme based on habitat features.